Targeting liposarcoma by various therapeutic approaches with concurrent exploitation of genetic aberrations

Inaugural-Dissertation

zur
Erlangung des Doktorgrades

Dr. rer. nat.

der Fakultät
für Biologie
an der
Universität Duisburg-Essen

vorgelegt von
Samayita Das
aus Santiniketan, Indien

April, 2018

Die der vorliegenden Arbeit zugrunde liegenden Experimente wurden am West German Cancer Center, Uniklinikum Essen, Universität Duisburg-Essen durchgeführt.

1. Gutachter: PD. Dr. Jürgen Thomale
2. Gutachter: Prof. Georg Iliakis

Vorsitzender des Prüfungsausschusses: Prof. Ralf Küppers

Tag der mündlichen Prüfung: 15.08.2018

DOI: 10.17185/duepublico/70104
URN: urn:nbn:de:hbz:464-20211012-084400-5

1 Contents

2 Introduction:

2.1 Classification of Liposarcoma:

Soft tissue sarcomas (STS) are a heterogeneous group of malignancies consisting of over 50 different histological subgroups with a mesenchymal origin [2]. Liposarcoma (LPS), as the name suggests, is a malignancy of the adipocyte-derived cells [2].

According to the World Health Organization (WHO) classification, liposarcomas are categorized into three distinct subtypes based on their unique characteristics and molecular genetic aberrations: (1) Well-differentiated / de-differentiated liposarcoma, (2) Myxoid / round cell liposarcoma, and (3) Pleomorphic liposarcoma [1-3].

Well-differentiated/de-differentiated liposarcoma (WDLP/DDLPS) is the most prevalent histological subtype, accounting for ~ 65 % of all LPS; myxoid / round cell LPS account for ~ 30 %; and pleomorphic LPS accounts for < 5 % of all liposarcomas. Histologically, all subtypes simulate normal adipose tissue to certain extent along with the presence of the malignant “lipoblast.” Lipoblasts have been described as the primitive, neoplastic cells descendant from a stem cell progenitor [4, 5].

WDLP/DDLPS

Well-differentiated / de-differentiated liposarcoma are grouped together based on the shared molecular genetic abnormality. However, they are different in their tumorigenic property, certain pathological characters and clinical courses.

Well-differentiated liposarcoma:

WDLPSs are also known as Atypical lipomatous tumor (ALT) local low-grade neoplasms, which rarely metastasize unless they dedifferentiate [6]. It has a low recurrence rate (10 %) occurring most often in the retroperitoneum and limbs [2]. The World Health Organization (WHO) classifies WDLPS into three main subtypes: adipocytic, sclerosing, and inflammatory [2].

De-differentiated liposarcoma:

DDLPS is a high grade, biphasic neoplasm with a component of WDLPS which is demarcated from a highly cellular, spindle cell-rich portion [2]. DDLPS is more

aggressive and has a metastatic rate of 10 % to 20 % and overall mortality of 50 % to 75 % [7-9].

2.2 Molecular genetic aberration in liposarcoma:

WDLPS tumors are characterized by the presence of one or more cancer-associated neochromosomes (CaNCs) on the background of a relatively normal and predominantly diploid karyotype [10]. Despite the neochromosome predominantly displayed a ring topology, rod shaped giant forms are also observed [11, 12]. In the case of WDLPS, the neochromosomes have a complex structure made up of interspersed amplifications of regions donated from various chromosomes (the 'core sequence'). Neocentromeres are a common feature of WDLPS CaNCs [12] (Figure 2.1). The ring or giant, rod-shaped CaNCs incorporate interspersed high-level amplifications of several chromosomal regions. The most universally amplified regions is 12q13–15. This region contains oncogenes such as HDM2 at 12q15 and CDK4 at 12q14. Amplification and increased expression of these two genes has the potential to attenuate the function of two key tumor suppressors, p53 and Rb, respectively [13].

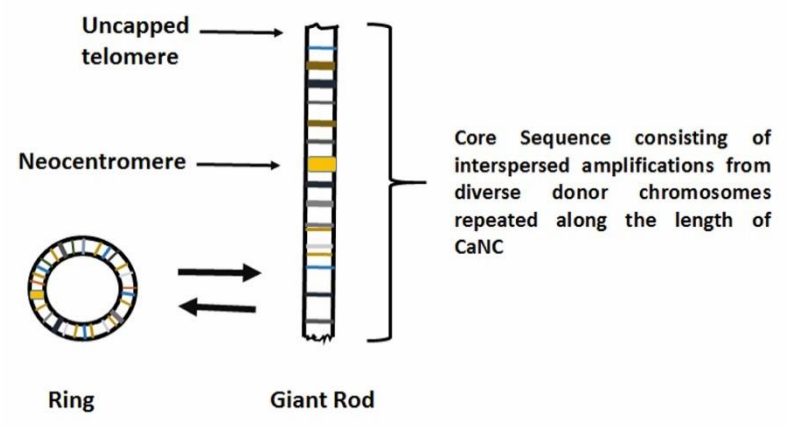

Cancer Associated Neochromosome (CaNC)

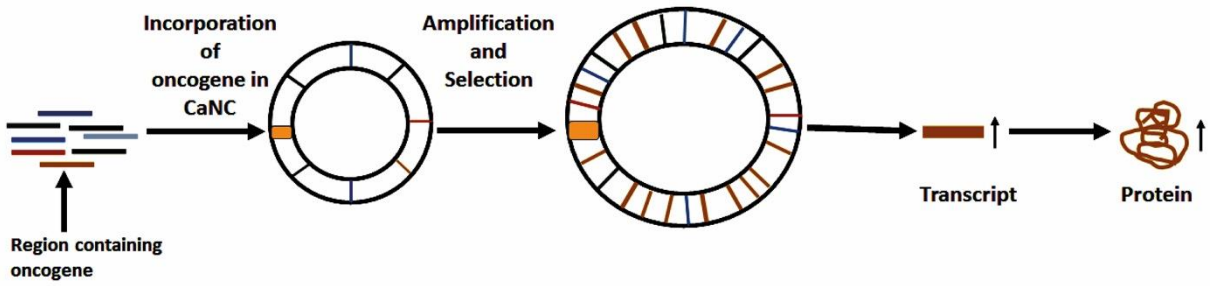

Figure 2.1: Potential mechanism of CaNC mediated oncogenesis. Amplification resulting in increased dosage of oncogenes contained within amplicon boundaries and subsequent increased expression of transcript and oncoproteins.

The progression from WDLPS to DDLPS is accompanied by certain genetic alterations. Crago et al (2012) identified the chromosomal/genomic changes in the process of liposarcoma pathogenesis by comparing WDLPS and DDLPS samples by genomic approaches. The most frequently observed alteration in the disease progression was the loss of 11q23~24 chromosomal region, which contains multiple tumor suppressor genes. The other chromosomal changes harboring diverse genes that have been identified to contribute in the oncogenesis of liposarcoma by different studies are summarized in Table 1.

Table 1: Genes contributing to the liposarcoma pathogenesis

Gene	Chromosome	Type of abberration	Biological Impact
MDM2	12q13~15	Amplification	Negative regulator of p53, E3 ubiquitin ligase, targets the tumor suppressor protein p53 for proteasomal degradation [14, 15]
CDK4		Amplification	Cyclin-dependent kinase that regulates cell cycle at the G1/S phase transition, can result in chromosomal instability and proliferation [16]
HMGA2		Amplification	Transcription factor that regulates cell cycle (G2/M) and role in adipogenesis and differentiation [17-19]
YEATS		Amplification	YEATS4 (transcription factor) along with MDM2 may cooperatively repress the p53 [20-22]

FRS2		Amplification	An adaptor protein and plays role in FGR signaling; enhances tumor formation, angiogenesis and tumor progression [23]
JUN	1p21~32	Amplification	Transcription factor, interferes with adipocytic differentiation and increases aggressiveness [24]
ASK1	6q23~24	Amplification	Kinase, inhibits adipocytic differentiation [25, 26]
	11q23~24	Loss	This region harbors key tumor suppressor genes that are lost during tumor progression from WDLPS to DDLPS (ZBTB16,PP2R1B, E124) [27]
C/EBPA	19q13	Loss	Regulates cell cycle at G2/M and involved in differentiation [24, 28]

Myxoid / Round cell liposarcoma:

Myxoid/round cell (MLPS/RCLPS), is the second most prevalent subtype. It is characterized by the molecular aberration of the recurrent translocation of chromosomes 12 and 16 t(12;16)(q13;p11) that results in the FUS-CHOP gene fusion present in over 95 % of cases [1, 2, 29]. Alternatively, translocation in t(12;22)(q13;q12) results in the formation of EWS-CHOP fusion gene. Both of the fusion gene events interfere with the process of adipocytic differentiation [29, 30].

Pleomorphic liposarcoma:

Pleomorphic liposarcoma (PLPS) is the rarest subtype of liposarcoma, accounting for only < 5 % of all liposarcomas and characterized by a high malignant potential with metastases in 30 % to 35 % of cases [2, 31]. The most common genetic aberration is

deletion of the 13q14.2~14.3 chromosomal region that occurs in over 60 % of PLS [1, 2].

Table 2: Classification of liposarcoma based on chromosomal abnormalities

Histological Subtype	**Cytogenetic Abberations**	**Molecular Genetics**	**Histological Features**
Well-Differentiated	Ring chromosomes and giant markers (12q13~15)	Amplification of *MDM2, CDK4, HMGA2*	Enriched with adipocytes with aberrant nuclei
De-differentiated	Ring chromosomes and giant markers (12q13~15)	Amplification of *MDM2, CDK4, HMGA2*	Rich in cellular content juxtaposed to a WD portion
Mixoid/Round cell	Translocation t(12;16) (q13;p11) t(12;22) (q13;q22)	FUS-CHOP/DDIT3 EWSCHOP/DDITS fusion protein	Immature lypoblasts and mature adipocytes, round cells with extracellular myxoid content
Pleomorphic	Complex karyotype	*TP53* mutations in 60%	Highly cellular portion; pleopmorphic lipoblasts

2.3 **Therapeutic interventions for dedifferentiated liposarcoma**

Surgery:

Surgical removal of tumors is the mainstay for localized disease. However, more than 80 % of DDLPS patients develop unresectable recurrences [32].

Chemotherapeutic interventions:

For advanced liposarcoma, the conventionally used first-line of chemotherapies are anthracyclines (Doxorubicin) or anthracycline-based compounds in combination. Non-anthracycline compounds such as a combination of gemcitabine and docetaxel are frequently used in the second-line setting for liposarcomas. While these chemotherapeutic compounds have been employed as the front-line treatment option when surgery is not an option, DDLPS has proven to be resistant to such conventional chemotherapy [33].

Radiation treatment:

Use of radiation treatment (RT) has been shown to have an effect on local control but no significant effect on the overall patient survival [34, 35]. For patients with deep seated lesions, RT in conjunction with surgery appears to improve local control [36].

Gamma-H2AX as a measure of radiosensitivity in cancer:

In response to DNA damage, when DNA double-strand break (DSB) lesions are formed, H2AX gets phosphorylated at Ser-139 [37, 38] which is also known as gamma-H2AX. H2AX is a variant form of H2A which is a component of histone octamer nucleosomes and phosphorylation of H2AX is an early step in recruiting the DNA repair components. The phosphorylation is mediated by the PIK family kinases such as ATM, ATR and DNA-PK [39-41]. In normal tissue, radiation-induced DSBs can lead to cancer. Vice versa, the induction of DSBs by application of anti-cancer therapeutics can activate cell death pathways and thus being used as a therapeutic approach [40, 42]. In recent years, gamma-H2AX has become a powerful tool to monitor DNA DSBs in translational cancer research [41, 42].The persistence of gamma-H2AX after radiotherapy is particularly significant since it can be used as a marker of radiosensitivity. Following treatment with ionizing radiation, gamma-H2AX foci are formed and over a predictable time in the presence of noromal physiological repair mechanisms, levels of gamma-H2AX are diminished. However, the persistence of gamma-H2AX indicates toward impairment of repair mechanisms. Thus, this is used as a marker of radiosensitivity [43-45].

Table 3: Systemic therapies for Liposarcoma

Therapy	Subtype	Mechanism of action	Trial Study
Trabectedin	MRC	Binding of DNA minor groove; direct interaction w/FUS-CHOP[46-48]	Phase II
Cabazitaxel + Prolonged infusional ifosfamide	Dediff.	Microtubule inhibitor (Hayward (2013 - NCT01913652)	Phase II
Eribulin	Dediff.	Microtubule inhibitor [49]	Phase II
Pazopanib, Sorafenib, Sunitinib	All subtypes	Tyrosine kinase receptor inhibitor [50-52]	Phase II
Troglitazone, Rosiglitazone, Efatutazone	All subtypes	PPAR-gamma agonist [53, 54]	Phase I, II
Nelfinavir	Well Diff/dediff.	SREBP-1 inhibitor [55]	Phase I
Flavopiridol	Well Diff/dediff	pan-CDK inhibitor, including CDK4 [56]	Phase I
PD 0332991	Well Diff/dediff	CDK4/6 inhibitor [57]	Phase I
Ribociclib	Well Diff/dediff	CDK4/6 inhibitor (NCT02571829)	Phase II

Systemic therapies for liposarcoma:

Based on tumor-specific biology, novel systemic therapies targeting the unique genetic aberrations specific to DDLPS have emerged in the past decades. In contrast to the non-specific chemotherapies, targeted therapies exert target specific actions sparing the normal tissues. The list of systemic therapies that are currently undergoing clinical trials are listed in Table 3.

2.4 The MDM2:P53 axis and its contribution in the liposarcomagenesis:

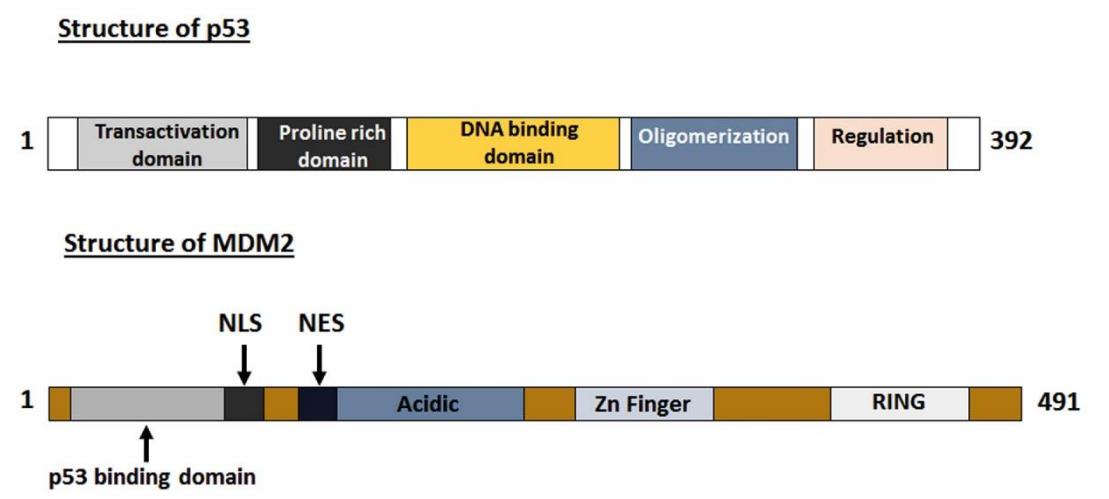

Figure 2.2: Schematic representation of structural domains of p53 and MDM2.

The p53 tumor suppressor is known as the 'guardian of genome' due to its ability to prevent accumulation of mutations. Consequently, in 50 % of all tumors harbor mutated or deleted *TP53* which lead to either complete or partial inactivation of p53 [58, 59]. The p53 protein is present at rather low concentrations in normal cells. In response to stress (hypoxia, DNA damage), p53 is accumulated in the nucleus and the choice of response depends on factors such as cell type, cell environment and other oncogenic alterations that are sustained by the cell [60, 61]. Thus, its activity is stringently controlled to maintain cellular homeostasis. One of the negative regulators of p53 is MDM2 which is associated with cellular homeostasis [62] and is part of an autoregulatory feedback loop [63]. MDM2 is transcriptionally activated by p53 [64] and MDM2, in turn, inhibits p53 activity in several ways: (1) MDM2 binds to the

transactivation domain of p53 [65] and inhibits p53-mediated transcription of downstream genes [14]. (2) MDM2 binds p53 *via* its signal sequence containing nuclear export signal [66] and transferring it from nucleus to cytoplasm [67]. Thus, MDM2 sequesters p53 in cytoplasm and the access to the DNA is inhibited. (3) MDM2 by its ubiquitin ligase [68] function, targets p53 for proteasomal degradation following ubiquitination [62, 69].

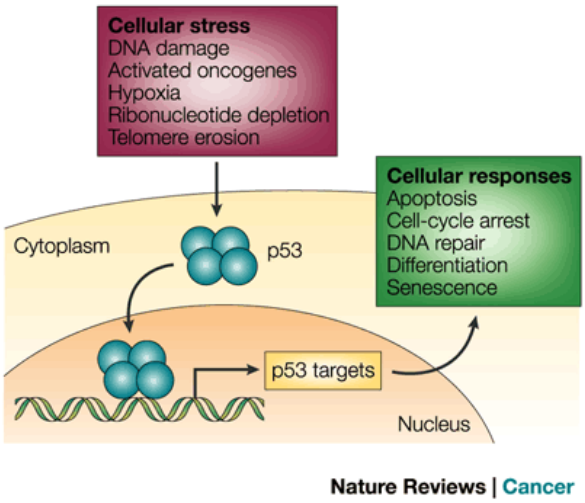

Figure 2.3: Diagram representing p53-mediated cellular response under normal and stress conditions. Image adapted from [70].

Approximately, 50 % of the human tumors are known to harbor mutations in *TP53* [71]. However, across a wide variety of cancers, *TP53* gene is intact and instead of mutations, the tumor suppressor activity is hindered by various other factors which regulate the level and activity of p53 [72] or by the expression of certain oncoviral proteins [73]. These could be overexpression of MDM2 [74], defects in the expression of p14ARF tumor suppressor [75], mutations in kinases such as ATM or Chk2 [76, 77], chromosome translocations and generation of fusion protein PML-RARα [78] or the nucleophosmin fusion protein NPM-RARα [78, 79] or the infection with certain viruses [80].

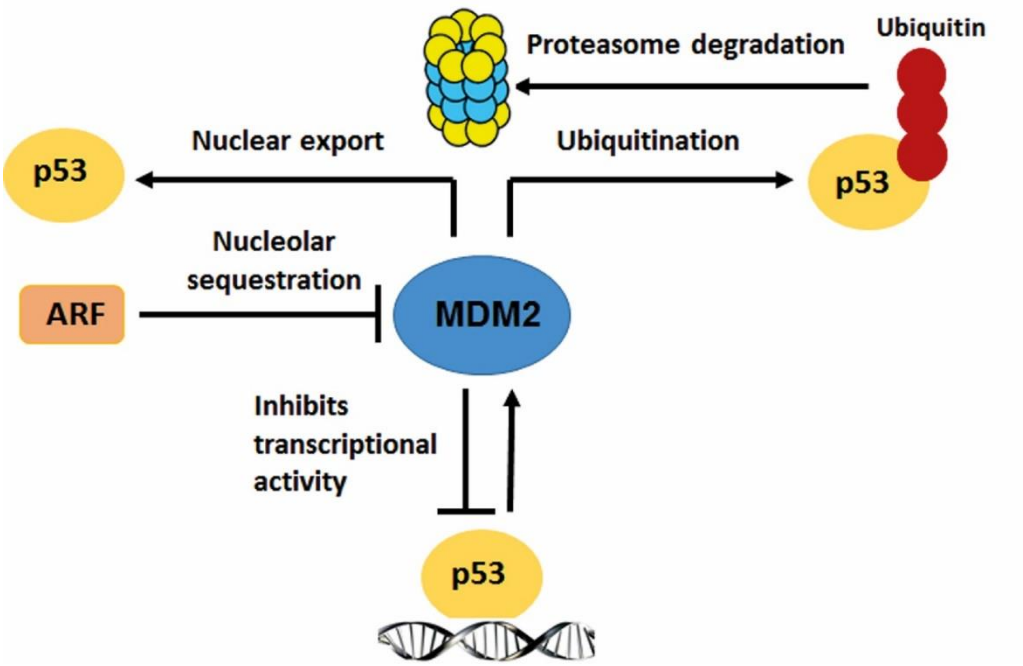

Figure 2.4: Diagram explaining regulation of p53 by MDM2: (1) Inhibition of transcription of p53, **(2)** nuclear export of p53 and **(3)** ubiquitination and degradation of p53.

In liposarcoma, overexpression of MDM2 inhibits p53 from executing its function and thus is considered one of the key oncogenic drivers of the disease [81, 82].

Genotoxic and non-genotoxic activation of p53

P53 harbors different sites for various post-translational modifications (phosphorylation, acetylation or sumoylation) in response to various cellular stress conditions. Stress-induced signaling pathways activate specific or groups of modifications on p53. Based on the modifications, activity of p53 is modulated and that in turn, subsequently, determines the cellular fate by inducing cell cycle arrest, apoptosis or cellular senescence.

Activation by genotoxic stress

Mammalian cells appear to have at least two largely independent signaling pathways for activating p53 in response to genotoxic stress; one is activated by the presence of DNA double-strand breaks, the other in response to bulky lesions such as pyrimidine dimers and base adducts.

Table 4: Genotoxic and non-genotoxic mediators [83]

Genotoxic Mediators	Non-genotoxic Mediators
Irradiation	**Anti-microtubule agents**
UV [84], Gamma [85], X-ray [86], alpha particles [87]	Taxol [88], Nocodazole [89]
Carcinogen	**Hypoxia/Anoxia** [90]
Polycyclic aromatic hydrocarbons [91], Mycotoxins [84], cadmium [92]	**Ribonucleotide depletion** [93]
Cytotoxic Drugs	**Oncogene activation**
Alkylating agent [94], Antimetabolites (5-FU [88], Methotrexate [95]), Anthracyclins [96]	Overexpression E1A [97]
Topoisomerase Inhibitors	**Cytokines** [98]
Camptothecin [88]	**Proteasome inhibitors** [99]

Table 5: Inhibitors in clinical trial [83]

Name of the compound	**Trial**	**Mechanism of action**
Nutlin-3	Phase I	Inhibits the p53 binding pocket of MDM2
RG7112	Phase I/II	
SAR405838	Phase I	
MI-63	Phase I	
RG7388	Phase I	
PXN-822	Pre-clinical	
NU8231	Pre-clinical	

CGM097	Phase I	Inhibits both p53 binding pocket of both MDM2 and MDMX
MK-8242	Phase I	
RO-5963	Pre-clinical	
RITA	Pre-clinical	Inhibits wild-type and mutant p53 and blocks the interaction with both MDM2 and MDMX

2.5 **CDK4-RB axis in cell cycle and its role in liposarcoma pathogenesis:**

Cellular proliferation and growth are tightly regulated processes and this regulation is executed by a biological phenomenon known as cell cycle [42]. Cell cycle constitutes of separate phases with possible checkpoints in between. The stringent control of every phases is mediated through a set of kinases known as cyclin-dependent kinases (CDKs). CDK activity requires binding of regulatory subunits known as cyclins. Cyclins are synthesized and destroyed at specific times during the cell cycle, thus regulating kinase activity in a timely and controlled manner. Human cells contain multiple loci encoding CDKs and cyclins (13 and 25 loci respectively) [43].

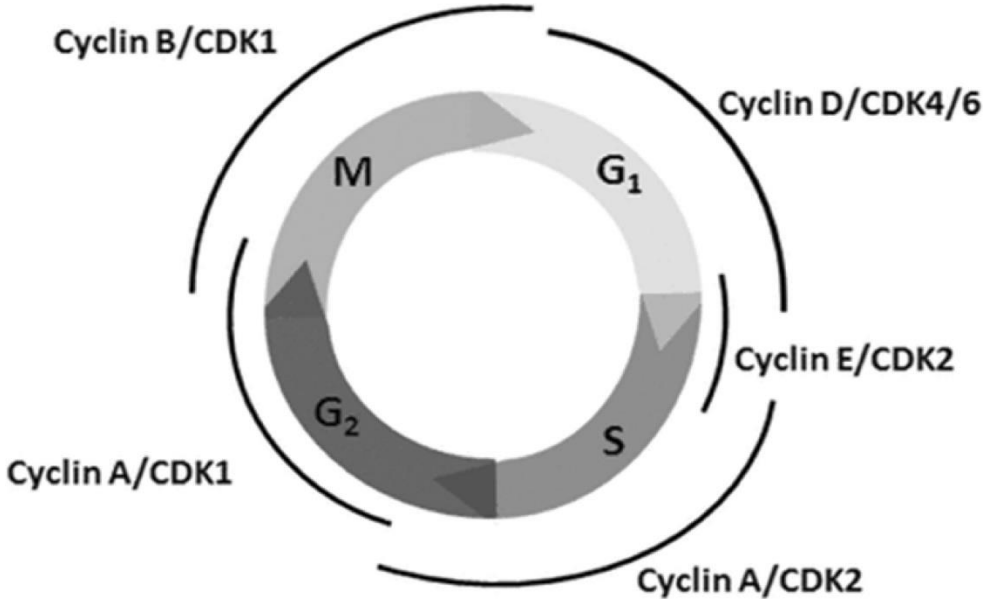

Figure 2.5 Control of cell cycle progression by phosphorylation of cyclin-dependent kinase (CDK) substrates. Image adapted from [100].

However, only a certain subset of CDK–cyclin complexes is directly involved in driving the cell cycle. They include three interphase CDKs (CDK2, CDK4 and CDK6), a mitotic CDK (CDK1, also known as cell division control protein 2 (CDC2)) and ten cyclins that belong to four different classes (the A-, B-, D- and E-type cyclins) [101]. Deregulation in certain CDK-cyclin complexes results in either continued proliferation or unscheduled re-entry into the cell cycle, two characteristics of most human tumor cells [101, 102].

According to the definition of 'classical model' of cell cycle control, the sequential activation and involvement of the CDK-cyclin complexes are as follows: in the G1 phase where the cells prepare to initiate DNA synthesis, mitogenic signals are first sensed by expression of the D-type cyclins (D1, D2 and D3) that preferentially bind and activate CDK4 and CDK6 [102]. Activation of these complexes leads to partial inactivation of the pocket proteins — RB, RBL1 (also known as p107) and RBL2 (also known as p130) by their phosphorylation. Rb in unphosphorylated state remains bound to E2F in G1 phase. In late G1, Rb is phosphorylated by Cyclin D-CDK4/6 complex and dissociates from E2F, allowing E2F-dependent transcription of genes necessary for S-phase progression [103]. This allows expression of E-type cyclins (E1 and E2), which bind and activate CDK2 [104]. CDK2–cyclin E complexes further phosphorylate these pocket proteins, leading to their complete inactivation [104-106] and this triggers the S phase. To ensure the transition from S phase to G2 phase, CDK2 is subsequently activated by Cyclin A2 at the late stages of DNA replication. Finally, CDK1 is identified to be activated by A-type cyclins at the end of interphase to facilitate the onset of mitosis. Following nuclear envelope breakdown, A-type cyclins are degraded, facilitating the formation of the CDK1–cyclin B complexes responsible for driving cells through mitosis [101, 107, 108].

The Rb protein is a tumor suppressor, which plays a pivotal role in the negative control of the cell cycle and in tumor progression. It has been shown that Rb protein (pRb) is responsible for a major G1 checkpoint, blocking S-phase entry and cell growth.

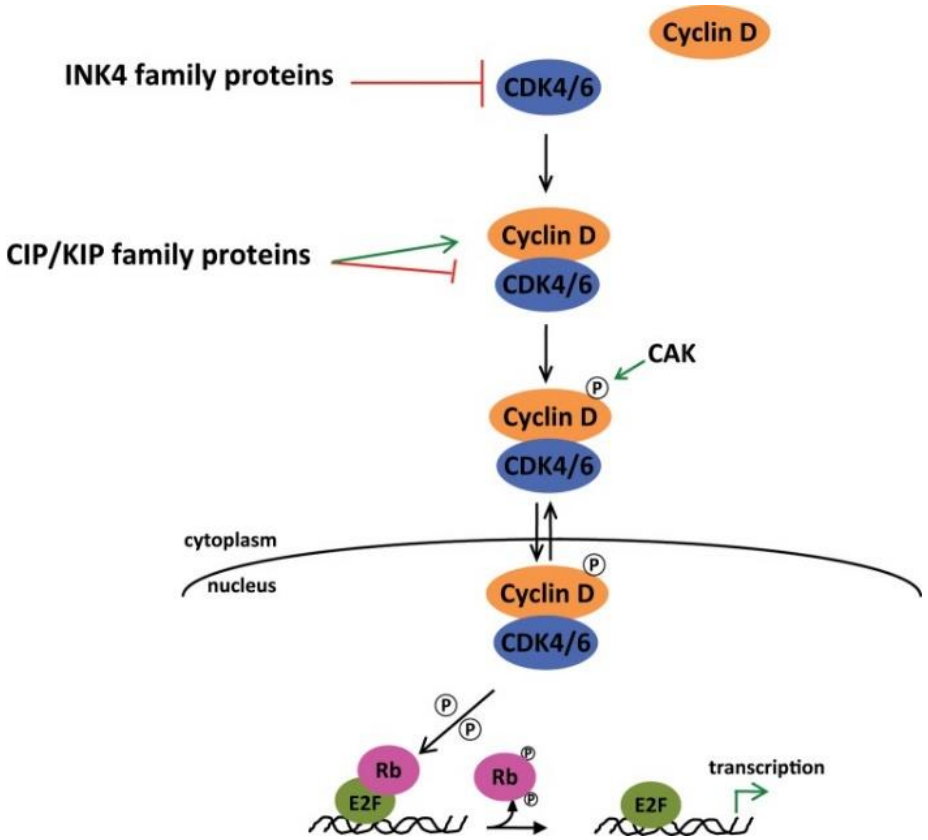

Figure 2.6: Scheme representing regulation and activation of CDK4 during cell cycle progression. Image adapted from [109].

Multiple mechanisms contribute to the deregulation of the G1-to-S checkpoint, which are known to play a pivotal role in the development of cancer [110]. These mechanisms include amplification or mutation of the CDK4 and CDK6 genes, amplification of the genes encoding D-type cyclins and deletion or silencing of the *CDKN2A/B* gene, which encodes for the INK4 inhibitors $p16^{ink4}$ [111-113].

In context of liposarcoma, existing reports suggest that amplification of *CDK4* confers a selection advantage to WD/DDLPS and may contribute to transformation as CDK4 negative WDLPS exhibit more favorable prognostic feature [114].

2.6 P53 mediated effects: cell cycle arrest, apoptosis and senescence

Cell cycle arrest:

Involvement of p53 has been demonstrated in several different aspects of the cell cycle. It transactivates or inhibits the expression of genes in order to mediate cell cycle progression [115]. Predominately, p53 influences the G1 phase of the cell cycle. For example, in response to DNA damage, p21 mediates p53-dependent cell cycle arrest

by binding to and inhibiting cyclin-CDK complexes [116]. Under the normal physiological conditions, pRB remains bound to the E2F protein. Upon reaching the end of the G1 phase, pRB is targeted for phosphorylation by Cyclin E-CDK2 and disrupts the pRB-E2F interaction, thus, ensuring the progression to S phase [117]. In contrast, under stress conditions, p53 induces p21 expression which inhibits the Cyclin E-CDK2 function and holds the cell in the G1 phase until the stress is overcome [118]. Arresting the cells at G1 phase restricts the cell from copying the unrepaired DNA damage in the S phase. However, if a cell has already progressed into S phase, p53-mediated activation of p21 employs the DNA polymerase machinery at the replication fork and inhibits further replication of DNA. P53 is also able to induce G2 arrest at G2/M checkpoint [115] by preventing the entry to mitosis by decreasing the transcription and synthesis of cyclin B1 [119].

Apoptosis:

Apoptosis or the programmed cell death is an evolutionarily conserved process that occurs during development, aging and as a homeostatic mechanism [120, 121]. The role of p53-mediated apoptosis has been studied widely. In response to cellular stress, p53 employs several critical transcriptional targets that are essential for cell death and can trigger apoptosis through extrinsic [122, 123] or intrinsic [124] signaling pathways [125].

Senescence:

Cellular senescence is defined as an essentially irreversible arrest of cell proliferation that occurs when cells experience potentially oncogenic stress. Existing physiological stimuli are unable to revert the arrest to proliferation. The causes of cellular senescence are: (1) telomere shortening [126], (2) genomic damage [127],(3) epigenomic damage [128], (4) activation of the tumor suppressors [129, 130] and (5) chronic and unbalanced mitogenic signals [131].

P53/p21 and $p16^{INK4a}$/pRB pathways are the two major tumor suppressor pathways that have been identified as regulators of senescence [129, 130] by widespread changes in gene expression [132]. Chronic activation of these proteins are capable of inducing senescent growth arrest [133].

2.7 **Immunotherapy in sarcoma:**

Immunotherapy has been considered as one of the most promising approaches in treatment of certain solid tumors (e.g., prostate cancer, melanoma), where significant progress and notable successes have been observed with the advanced disease [134].

Several rationales have been designed based on the existing features in STS for employment of immunotherapeutic approaches. For example, STS frequently have chromosomal translocations which result in unique fusion proteins and specific subtypes have been shown to express cancer testis antigens [134].

Existing immunotherapies can be divided into categories based on mechanism of action. These categories are (1) non-specific cytokine based therapies and innate cellular stimulation, (2) immune checkpoint inhibitors, (3) vaccine therapy (active immunization), and (4) adoptive T-cell therapy [134, 135].

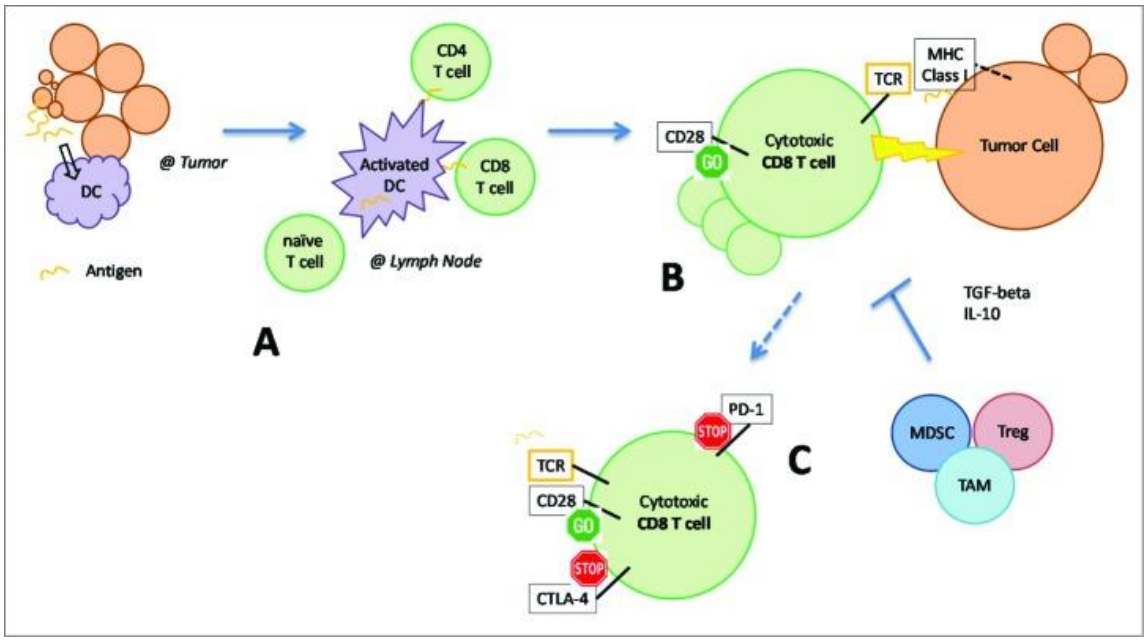

Figure 2.7 : Potential for immunotherapy in soft tissue sarcoma [134]: **(**A**)** Manipulation of DCs by cancer vaccines to enhance antigen presentation, **(**B**)** adoptive cell therapy utilizes expanded populations of cytotoxic T cells, **(**C**)** Blockade of immune checkpoint molecules (CTLA4, PD-1) on T cells to maintain their activation status and cytotoxic function. Image adapted from [134].

(1) Non-specific cytokine based therapies:

Non-specific immunomodulation refers to approaches of therapy aimed to induce antitumor immunity without exposing the patient to a target molecule [136].

Sarcoma context: Application of IFN-gamma in osteosarcoma have been reported in some studies [137].

(2) Immune checkpoint inhibitors:

Biology of Immune-checkpoint inhibitors:

T lymphocytes play essential roles as serving as effectors of the immune system [138]. Activation of naïve T cells occur following the recognition of an unique peptide presented by antigen-presenting cells (APCs), *via* interaction of major histocompatibility complex (MHC) molecules on antigen-presenting cells with the T-cell receptor, and a co-stimulatory signal [139, 140]. Activating signals are finely orchestrated by a complex array of inhibitory receptors, which are known as checkpoint molecules. Under the normal physiological conditions, immune checkpoints are crucial for the maintenance of self-tolerance (that is, the prevention of autoimmunity) and to protect tissues from damage when the immune system is responding to pathogenic infection. Tumor cells evade the immune-surveillance by over-expressing the ligands of the checkpoint inhibitors, bringing T cells to a state of non-responsiveness known as ‘exhaustion’ [141, 142]. T cell exhaustion is often associated with chronic infections and tumors. However, therapeutic manipulation of these pathways by revitalization of exhausted T cells can restore immunity [141]. Relatively recently, immunologic checkpoint blockade with antibodies that target cytotoxic T lymphocyte–associated antigen 4 (CTLA-4) and the programmed cell death protein 1 pathway (PD-1/PD-L1) have demonstrated promising results in a variety of malignancies [76-80].

Sarcoma context:

There has been one report with immune checkpoint blockade in STS patients. Maki et al., treated patients with synovial sarcoma with Ipilimumab (anti-CTLA4) in a pilot, phase II study designed to assess objective tumor response [143].

(3) Cancer vaccine

Cancer vaccines attempt to elicit an immune response against tumor cells through active manipulation of DCs.

Sarcoma context: Synovial sarcoma (due the presence of SYT-SSX fusion protein) patients were treated with autologous DCs pulsed with SYT-SSX derived peptide [144].

(4) Adoptive T-cell therapy

In contrast to cancer vaccines, in adoptive cell therapy, patients are given autologous T cells that typically have been expanded and enhanced *in vitro* with cytokines and other growth factors.

NK cell therapy:

Natural killer (NK) cells are lymphocytes derived from bone marrow. Unlike T and B cells, NK cells are controlled by a limited repertoire of germ line-encoded receptors that do not undergo somatic recombination and thus constitute part of the innate immune system [145]. There are the diverse set of NK cell receptors that have been identified and characterized.

NK cell activation is able to distinguish normal healthy cells from sensitive target cells by the ultimate balance between signals from activating and inhibitory receptors expressed on the surface [146, 147]. Activating receptors induce diverse signaling cascades, whereas inhibitory receptors are known to employ a common mechanism for inhibition. Among the different types of activating receptors, NKG2D is one type. Ligands for NKG2D, such as MHC class I chain-related gene A (MICA), MHC class I chain-related gene B (MICB), and UL16-binding protein (ULBP), is expressed on some tumor cells and on infected or stressed cells [148]. NKG2D ligands can be induced by genotoxic stress and stalled DNA replication, conditions that activate DNA damage checkpoint [149] .

The other type of receptors that are known to be modulating the activation of NK cells are DNAM-1 and NCR (natural cytotoxicity receptors) which have already been reported to participate in recognition and lysis in melanoma and myeloma by NK cells [150, 151] . Among the sarcoma subtypes, Ewing sarcoma cell lines have been experimentally shown to be responding or vulnerable to resting as well as cytokine activates NK cells [152] and dependent on the combined contribution of NKG2D and DNAM-1 ligands.

Table 6 : Different set of cell surface receptors of NK cells

Activation receptors	Inhibitory receptors	Adhesion receptors
NKp46, NKp30,NKp44 NKG2D CD16 KIR-S CRACC	MHC class I specific inhibitory receptors: CD94/NKG2A, KIR-L LILRB-1 KLRG-1 TIGIT CEACAM-1 LAIR-1	CD2 DNAM-1 β1 integrin β2 integrin

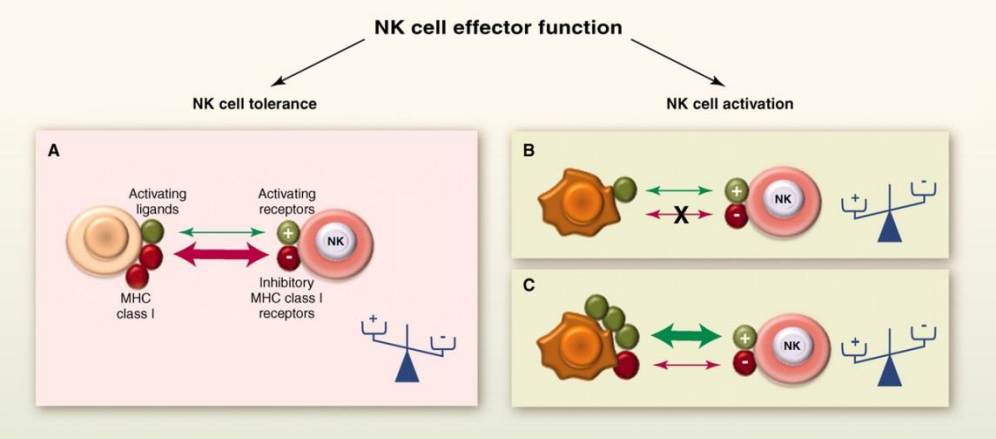

Figure 2.8 Regulation of effector function of NK cells. Image adapted from [153].

NK cell subsets:

Human NK cells can be divided into two subsets based on their cell-surface density of CD56: $CD56^{+bright}$ and $CD56^{+dim}$ each with distinct phenotypic properties. Functionally, the $CD56^{+dim}$ NK-cell subset is more naturally cytotoxic and expresses higher levels of Ig-like NK receptors and FCγ receptor III (CD16) than the $CD56^{+bright}$ NK-cell subset. By contrast, the $CD56^{+bright}$ subset has the capacity to produce abundant cytokines following activation of monocytes, but has low natural cytotoxicity and is either $CD16^{+dim}$ or $CD16^{-}$ [154].

2.8 **Translational perspective:**

Targeted therapies are currently in clinical trial and despite tumor shrinkage, relapse of tumors was evident with course of time. Combining targeted therapies and with simultaneous stimulation of patient's immune players to target tumor represents a promising and natural evolution in cancer treatment as this could exert specific and long-term antitumor efficacy. However, following targeted therapy, tumors and NK cells might display changes [155] in their phenotypic and functional property and autologous NK cells direct for tumors, that recognize self-cells are inhibited [156]. To overcome this limitation, concept of allogeneic NK cells emerged. For STS (soft-tissue sarcoma), diverse immunotherapeutic approaches have been employed and tested. Use of NK-cell based adoptive therapy has been reported in epithelioid sarcoma rendering long-term efficacies. Employment of adoptive NK cell therapy for targeting other cancer has been reported to be effective in both autologous [157] and allogeneic setting [158].

3 Aims:

1) Assessment of combined targeted therapy-mediated effect in liposarcoma
2) Radiotherapy and MDM2 inhibitor-mediated effect in liposarcoma
3) Targeting CDK4 in liposarcoma and assessment of susceptibility to radiotherapy
4) Elucidation of NK cell ligands for potential application of immunotherapy in treatment of liposarcoma

3.1 Rationale for targeting the CDK4 and MDM2 in liposarcoma

With consideration of the oncogenic genetic background of amplified *CDK4* and *MDM2* in well/dedifferentiated liposarcoma, which contributes to enhanced proliferation and blocking of apoptosis, respectively, it was hypothesized that dual targeting by CDK4i and MDM2i would exert an enhanced growth inhibition in liposarcoma cells.

3.2 Rationale for combining radiotherapy and MDM2 inhibitors in liposarcoma

The small-molecule MDM2 antagonist Nutlin-3 activates the p53 pathway and efficiently induces apoptosis in tumors with *MDM2* amplification and overexpression [160]. Nutlin-3 treatment radio-sensitizes lung cancer harboring wild-type *TP53* [161] and the combined treatment leads to increased apoptosis and cell cycle arrest. Additionally, it has been demonstrated that pharmacological activation of p53 by Nutlin-3 can sensitize lung cancer cells (NSCLC) to radiation therapy *via* promoting irradiation-induced premature senescence [162]. Based on its molecular genetic signature, it was aimed to evaluate the potential radio-sensitizing efficacies of MDM2 antagonist, Nutlin-3 in liposarcoma cells.

3.3 Targeting liposarcoma with CDK4 inhibitor and radiotherapy

Previous studies demonstrated CDK4 knockdown mediated radio-sensitization in breast cancer *via* activating the mode of apoptosis [163]. Inhibition of CDK4 activity by the CDK4/6 inhibitor PD033991 prevents RB phosphorylation, resulting in cytostasis and tumor regression in RB-positive carcinoma xenografts [164]. CDK4 is an important cell cycle regulator. However, the increased radiosensitivity in CDK4 knock-down cells

was not correlated with cell cycle alterations or impaired DNA repair [163], suggesting that CDK4 inhibition may confer its effects through inhibition of cell survival pathway of AKT/Cyclin D/CDK4 [165, 166]. The effect of CDK4/6 inhibition by PD033991 was similarly observed in liposarcoma cell lines [167], which provided the basis for the translation of CDK4 inhibition to STS patients achieved through a phase I trial by Flaherty et al.,[168]. Given the theoretical and preclinical association between CDK4 modulation and radio-sensitization, it was addressed whether CDK4 inhibition sensitize liposarcoma cells to radiation treatment.

3.4 **Exploring the potential for immunotherapy in treatment of liposarcoma**

- It was aimed to elucidate the therapy-driven expression pattern of the NKG2D ligands and DNAM-1 ligand in liposarcoma cells which might serve as predictive pharmacodynamic biomarker for subsequent NK cell-mediated lysis.
- Based on the phenotypic expression of the ligands, it was aimed to dissect the effect of NK-cell mediated cytotoxicity in liposarcoma cells and explore the feasibility of potential employment of NK-cell mediated immunotherapy for treatment of liposarcoma.

4 Materials

4.1 Chemicals and Reagents:

Table 7: Chemicals and reagents

Chemical	Company
Amphotericin B	Biochrom
Amersham ECL Prime Western Blotting Detection Reagent	GE Healthcare
Aprotinin	Sigma-Aldrich
Aqua Braun	B.Braun Meslungen AG
beta-Mercaptoethanol	Sigma-Aldrich
Bio-Rad DC Protein Assay	Bio-Rad Laboratories
BSA (Bovine Serum Albumin)	Sigma-Aldrich
Chloroquin	Sigma-Aldrich
Crystal Violet	Sigma-Aldrich
Dinatriumhydrogenphosphat (Na 2HPO4)	Applichem
DAPI	Thermo Fisher Scientific
Dithiothreitol (DTT)	Sigma-Aldrich
Dimethylsulfoxid(DMSO)	Merck
DPBS	Gibco
Ethanol, absolute	Sigma-Aldrich
Ethelendiaminetetraacetic Acid (EDTA)	Sigma-Aldrich
FBS (Fetal Bovine Serum)	Biochrom AG
Formalin	Sigma-Aldrich

Glycin	Carl Roth
Hepes	Sigma-Aldrich
Hoechst 33342	Sigma-Aldrich
Isopropanol	VWR
Leupeptin Trifluoroacetate salt	Sigma-Aldrich
L-Glutamine	Gibco
Magnessium Chloride	Sigma-Aldrich
Methanol	VWR
MOPS	Invitrogen
Paraformaldehyde	Sigma-Aldrich
Pen-Strep	Gibco
Potassium acetate	Sigma-Aldrich
PMSF (Phenylmethanesulfonyl Chloride)	Sigma-Aldrich
Ponceau S	Sigma-Aldrich
Propidium Iodide (DNA stain)	Beckman Coulter
Protein Ladder Spectra™ Multicolor Broad Range	Thermo Scientific
Skim milk powder	Fluka
Sodiumchloride (NaCl)	Carl Roth
Sodiumdodecylsulphate (SDS)	Sigma-Aldrich
Sodiumfluoride	Sigma-Aldrich
Sodiumhydrogencarbonate 8.4 %	B.Braun Melsungen AG
Sodium hydroxide (NaOH)	Sigma-Aldrich
Sodium molybdate (Na_2MoO_4)	Sigma-Aldrich

Sodium pyrophosphate	Sigma-Aldrich
Sodium vanadate	Sigma-Aldrich
NEA non-essential amino acids (100x)	Biochrom AG
Tergitol NP-40	Sigma-Aldrich
Tris (hydroxymethyl)aminomethane	Carl Roth
TripLE Express	Gibco
Tween 20	Sigma-Aldrich
WesternBright ECL	Biozym

4.2 Medium

Table 8:Media

Media	**Company**
Iscove's Modified Dulbecco's Medium (IMDM)	Gibco
RPMI 1640	Gibco

4.3 Antibodies

4.3.1 Primary Antibodies

Table 9: Primary antibodies

Antibody	**Dilution**	**Company**
Beta-actin	1:10000	Cell Signaling
Cyclin A	1:2000	Cell Signaling
Cyclin B	1:2000	Cell Signaling
Cyclin D1	1:1000	Cell Signaling

Gamma H2AX	1:500	Abcam
MDM2	1:2000	Zymed
PARP	1:1000	Cell Signaling
p16	1:1000	Cell Signaling
p21	1:1000	Cell Signaling
p53	1:2000	Cell Signaling
Phospho-Histone H3 (Ser-10)	1:500	Cell Signaling
Phospho-p53 (Ser-15)	1:500	Cell Signaling
Phospho-Rb (Ser-780)	1:1000	Santa Cruz
Rad51	1:1000	Abcam
Rb	1:1000	Cell Signaling

4.3.2 **Secondary Antibodies**

Table 10: Secondary antibodies

Antibody	**Dilution**	**Company**
ECL Anti-Rabbit IgG Horseradish peroxidase (HRP) linked	1:2000	GE Healthcare
ECL Anti-Mouse IgG Horseradish peroxidase (HRP) linked	1:4000	GE Healthcare
Anti-Rabbit IgG HRP Horseradish peroxidase (HRP) linked	1:2000	Cell Signaling

Anti-Mouse IgG Horseradish peroxidase (HRP) linked	1:4000	Cell Signaling

4.3.3 **Fluorochrome labelled antibodies**

Table 11: Fluorochrome labelled antibodies

Antibody	**Fluorochrome**	**Company**
Anti-human HLA-ABC	APC	eBioscience
Anti-hMICA	PE	R&D Systems
Anti-hMICB	Alexa 488	R&D Systems
Mouse Anti-Human CD155	FITC	Santa Cruz
Anti-ULBP-2	PE	R&D Systems
HLA-DR	PC7	Beckman Coulter
Anti-Melanoma	PE	MACS
Anti-CD3	FITC	Becton Dickinson
Anti-CD56	PE	Becton Dickinson
goat anti-mouse F(ab')2	PE	Dianova

4.4 **Equipments**

Table 12: Equipments

Equipment	**Company**
Incubator Forma 371	Thermo Electron Corp.
Countess® Automated Cell Counter	Life Technologies
Centrifuge (Rottina 46)	Hettich GmbH
Disperser T 10 Basic	IKA-Werke

FACS CXP 500	Beckman Coulter
FACS Celesta	BD Biosciences
Fluorescence Microscope BZ-9000	Keyence GmbH
Gel electrophoresis Chamber Sub-cell GT	Bio-Rad
Incubator 1000	Heidolph
137Cs irradiator	J.L Shepard and assoc.
Luminescent Image Analyzer LAS-3000	Fujifilm
Macs magnetic separator	Miltenyi Biotec
Microscope CKX41	Olympus
Microplate Reader GENios	Tecan
Microcentrifuge 5415 C	Eppendorf
Voltage source power pack base	Bio-Rad
Water bath 1000	GFL

4.5 Plastic materials and aid

Plastic materials for cell culture were from Greiner Bioscience, BD (Becton, Dickinson and Company) or TPP (Techno Plastic Products).

Table 13: Membranes and gels for immunoblotting

Nitrocellulosemembrane Hybond-ECL	Amersham Biosciences
Nu-PAGE 4-12 % Bis-Tris Gels	Invitrogen

4.6 Kits

Table 14: Kits

Kit	Company
Caspase-Glo®3/7 assay	Promega Corp.
Senescence beta-galactosidase staining kit	Cell Signaling
NK cell isolation kit	Miltenyi Biotec

4.7 FISH (Fluorescence *in situ* hybridization) probes

Table 15: FISH probes

Probe	Company
Green fluorochrome labelled MDM2	Zytovision
Orange fluorochrome labelled CEN 12	Zytovision

4.8 Cell culture medium

Table 16 : Composition of cell culture medium

Medium A	500 mL RPMI 1640 90 mL FBS 6 mL L-Glutamine 6 mL Penicillin/ Streptomycin/ Amphotericin B
Medium IMDM	500 mL IMDM 90 mL FBS 6 mL L-Glutamine 6 mL Penicillin/ Streptomycin/ Amphotericin B

4.9 Working solutions

Table 17 : Working solutions

IP Buffer (Protein Lysate Preparation)	10 mL 1 % Tergitol NP-40 50 mL 1M Tris HCL, pH 8 4.199g Na Flouride 13.38g Na Pyrophosphate 0.4839g Na Molybdate 0.3678g Na Vanadate 100 mL 0,05M EDTA
Lysis Buffer (Western Blot)	4 mL IP-Buffer 4 µL Aprotinin (10mg/mL) 4 µL 21mM Leupeptin 40 µL 100mM PMSF
Ladder Buffer (Western Blot)	2.812 mL 0,5M Tris, pH 6,7 6.75 mL 10 % SDS 450mg 87 % DTT 10 mL Glycin 10mg Bromphenolblue Filled up to 20 mL with Aqua.dest
Stripping Buffer (Western Blot)	6.25 mL 100 mM Tris,pH6,7 1 mL 20 % SDS 0,07 mL beta-Mercaptoethanol Filled up to 10 mL with Aqua.dest
Running Buffer (Western Blot)	21 mL MOPS 399 mL Aqua.dest.

Transfer Buffer (Western Blot)	200 mL Methanol 14.4g Glycin 3.03g Tris Filled up to 1000 mL with Aqua.dest
PBS-T (Western Blot)	80g NaCl 2g KCL 14.4g Na_2-$HPPO_4$ 2.4 KH_2PO_4 10 mL Tween 20 Filled up to 10L with Aqua.dest
Crystal violet (Clonogenic assay)	1L Fixing/Staining solution: 0.5 g Crystal Violet (0.05 % w/v) 27 mL 37 % Formaldehyde (1 %) 100 mL 10X PBS (1X) 10 mL Methanol (1 %) 863 dH20 to 1L
Facs Buffer (Flow cytometry)	450 mL 1X PBS 50 mL FCS
Hoechst 33342 solution	918.7 µL 1XPBS 81.3 µL Hoechst 33342 solution

4.10 **Inhibitors**

4.10.1 **MDM2 inhibitor**

Nutlins are potent and specific small molecule inhibitors of MDM2 protein developed in 2004 by scientists from Hoffmann-La Roche, Inc.[169]. Nutlin-3, Racemic, a cell-permeable *cis*-imidazoline compound. By occupying the same pockets in MDM2 where p53 binds, MDM2 inhibitors block the MDM2-p53 protein-protein interaction, and hence the MDM2-mediated p53 ubiquitination and degradation of p53, leading to p53

accumulation and transcriptional activation of p53 in cells with wild-type p53 but not in cells with mutated or deleted p53 [169]. Nutlin-3 is a candidate for neoadjuvant therapy in cancers with a functional p53 [170].

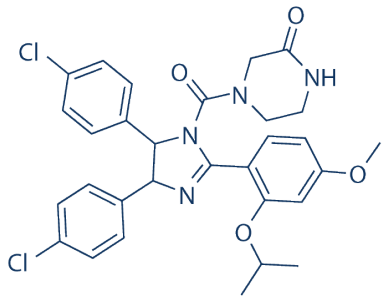

Structure of Nutlin-3

4.10.2 CDK4 inhibitors

CDKs are important modulators of cell cycle entry and progression in response to growth signals, and inhibition of these kinases with palbociclib/ribociclib could enhance the activity of other anticancer drugs in tolerable regimens.

4.10.3 Ribociclib:

Ribociclib (formerly known as LEE011) is an orally available, and highly specific CDK4/6 inhibitor designed and developed by Novartis. A phase II single arm study assessing efficacy & safety of ribociclib in patients with advanced well-differentiated or dedifferentiated liposarcoma has been initiated and ongoing (NCT02571829). Another phase Ib/II, open-label, multicenter study of oral HDM201 in combination with oral LEE011 in adult patients with liposarcoma (NCT02343172) is ongoing.

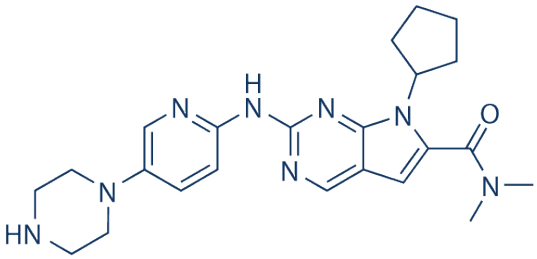

Chemical Structure of Ribociclib

4.10.4 **Palbociclib:**

Palbociclib (Ibrance®) is an oral, reversible, selective, small-molecule inhibitor of cyclin-dependent kinases (CDK) 4 and CDK6 developed by Pfizer for the treatment of cancer [171, 172]. Palbociclib is an investigational drug. An investigational drug is a medication that has not been approved for marketing by the Food and Drug Administration (FDA). Palbociclib (PD-0332991) has been purchased from Selleck Chemicals. Clinical trial (Phase II) study has been conducted with palbociclib (NCT01209598) in patients with advanced and metastatic liposarcoma.

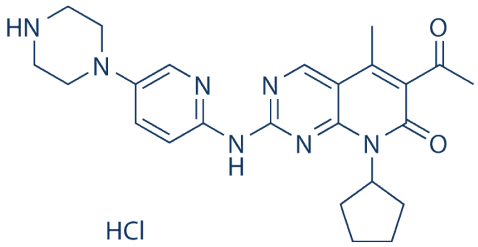

Chemical Structure of Palbociclib

4.10.5 **Proteasome inhibitor (Bortezomib):**

Bortezomib, a boronic acid dipeptide, is a highly selective, reversible inhibitor of the 26S proteasome which primarily functions in the degradation of mis-folded proteins and is essential for the regulation of the cell cycle. It was purchased from selleck chemicals and used as a biochemical tool to study certain pathways.

5 Methods

5.1 Cell lines:

Human WD/DDLPS liposarcoma cell lines (LPS141, LPS853) were kindly provided by Dr. Jonathan Fletcher (Brigham and Women's Hospital, Boston, MA), T449 and T778 kindly provided by Dr. Florence Pedeutour (Université de Nice-Sophia Antipolis, Nice, France). All four cell lines have been characterized for harboring amplified *MDM2* and *CDK4*. SW872 (undifferentiated liposarcoma) was purchased from ATCC. Cell lines were cultured in RPMI-1640/DMEM supplemented with 15 % FBS (Hyclone, Logan, UT), 1× penicillin–streptomycin–amphotericin B (Invitrogen, Carlsbad, CA), and 1× glutamax (Invitrogen) at 37°C in a humidified incubator with 95 % air and 5 % CO_2.

8 primary WD/DDLPs samples from patients were analysed for expression of certain proteins. The removal and processing of the tumor materials was always with the consent of all the patients and approved by the responsible ethical committee.

Table 18: Liposarcoma cell lines

Cell line	Origin	*TP53* status	*MDM2* status copy number	Colony-forming ability
T449	WDLPS	Wild-type	Amplified	Moderate
T778	WDLPS	Wild-type	Amplified	Moderate
LPS853	DDLPS	Wild-type	Amplified	Moderate
LPS141	DDLPS	Wild-type	Amplified	Very low
SW872	UDLPS	Mutated (I251N)	Wild-type	Moderate

5.2 Passaging of cells:

Liposarcoma cells are strongly adherent and were cultured in 25/75/150 cm2 flasks depending on the requirement of the experiments. Trypsin-EDTA was used for

detaching the cells from the plastic. The cells were first washed with 1XPBS for removal of excess FCS, which inhibits the action of trypsin. After the washing step, cells were incubated for 5-10 minutes with trypsin-EDTA at 37°C. Finally, cells were suspended with the complete medium in order to inhibit trypsin. The cell suspensions were further diluted 1:3 to 1.7 in fresh complete medium.

5.3 Freezing of cells:

Following trypsinization and centrifugation of the cells, the supernatants were removed and the cells were transferred to a cryo tube in 1.5mL freezing medium (FCS containing 10 % DMSO). The cryo tubes were transferred to a cooling container filled with isopropanol and kept at -80 °C overnight allowing a temperature drop gradually with approximately 1°C/min. The cells were transferred to liquid nitrogen the following day.

5.4 FISH (Flourescence *In Situ* Hybridization)

Flourescence *In Situ* Hybridization (FISH) is a robust cytogenetic method which allows the detection of various chromosomal or genetic abnormalities (gene fusion, amplification, aneuploidy, loss of part of a chromosome or whole chromosome) and thus important for diagnosis of a genetic disease or predicting prognostic outcomes [173-175]. In research, it has been widely used for gene mapping or the identification of novel oncogenes or genetic aberrations that contribute towards various cancers [174, 176, 177].

Liposarcoma cells were seeded in 6-well plate and grown for overnight. Following next day, cells were detached by gentle but repeated pipetting up and down. 300µL of medium containing the detached cell suspension was transferred to Cytospin plus slide for 10 min in order to lay the cells in the slide. The slide containing the cells was warmed in the Hybrite at 45 degree for 10 min. The slides were kept in KCL for 30 min and fixation was carried out by incubating it ice-cold Methanol/Acetic acid (-20 degree), for 30 min. For gradual drying, the slide was washed consecutively and increasing concentration of ethanol (70 %, 85 % and 100 %) each for 1 min and finally kept for 5 min at 37 degree.

Principle:

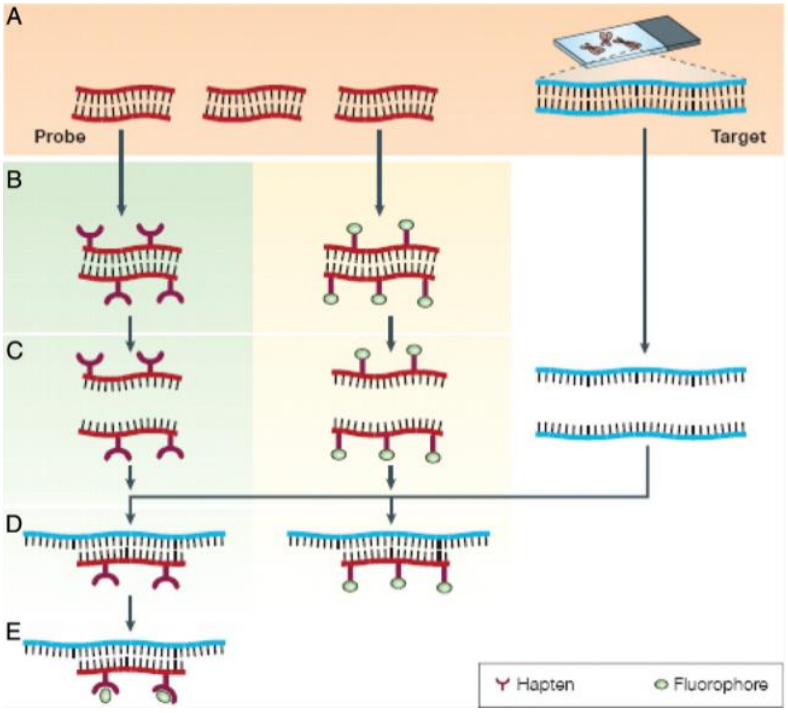

Figure 5.1: **The principles of fluorescence *in situ* hybridization (FISH). (A)** The basic and primary elements are a DNA probe and a target sequence. **(B)** Two methods of hybridization: the DNA probe is labelled indirectly with a hapten (left panel) or directly labelled *via* the incorporation of a fluorophore (right panel). **(C)** The labelled probe and the target DNA are denatured to yield single-stranded DNA. **(D)** Following denaturation, combination step is carried out which allows the annealing of complementary DNA sequences between the labelled probe and target sequence. **(E)** In case of indirect labelling, an additional step is required for visualization of the non-fluorescent hapten that employs an enzymatic or immunological detection system. Finally, the signals are evaluated by fluorescence microscopy. Adapted from Speicher and Carter [178].

To prevent the protein interference, the slide was incubated with protease buffer for 20 min. Following protein degradation, slide was washed with 1X PBS for 1 min and kept in a solution composed of 1 % formaldehyde, 1X PBS and 50mM MgCl. The slides were again washed with 1X PBS for 1 min and the series of dehydration steps carried out by increasing concentration of 70 %, 85 % and 100 % each for 1 min and kept at 37 degree for 5 min. The probe for *MDM2* and *CEN 12* was diluted in buffer and dH2O mixed, centrifuged and added to the slide containing the cells and coverslip was mounted over the slide. The slide was kept in Hybrite at 37 degree overnight. Next day, the slide was kept at 73 degree and 7.2 pH in 0.4 % SSC buffer for 2 min and again dehydrated with increasing concentration of alcohol each with 15s and kept in dark for 5 min. The cells were stained with DAPI for nuclei staining and mounted with coverslip. Fluorescence microscopy was carried out by Leica MZ10 F.

5.5 SNP (single-nucleotide polymorphism) arrays

SNP array method is based on high-density oligonucleotide-based arrays and employs millions of markers (probes comprise 25-mer oligonucleotides) across the entire human genome [178]. There are two types of probes: non-polymorphic probes, used for assessing copy number variations (CNV) (Figure 5.2A), and polymorphic probes, used to assess genotypes (Figure 5.2B) [179]. For copy number analysis, DNA from patients or cells are labeled with a fluorochrome provides signal intensity and are compared to a set of reference DNAs. This indicates whether there is a gain or loss of genetic material. For genotype analysis, a single nucleotide polymorphism (SNP) has a single base-pair substitution (A, T, C, or G) of one nucleotide to another, then, the alleles corresponding to the nucleotide base changes are arbitrarily given the designation allele A and allele B (polymorphic probes). The probe intensities that correspond to the two possible alleles of the SNP reveal which of the three expected genotypes (for example, AA, BB or AB) is present [180, 181].

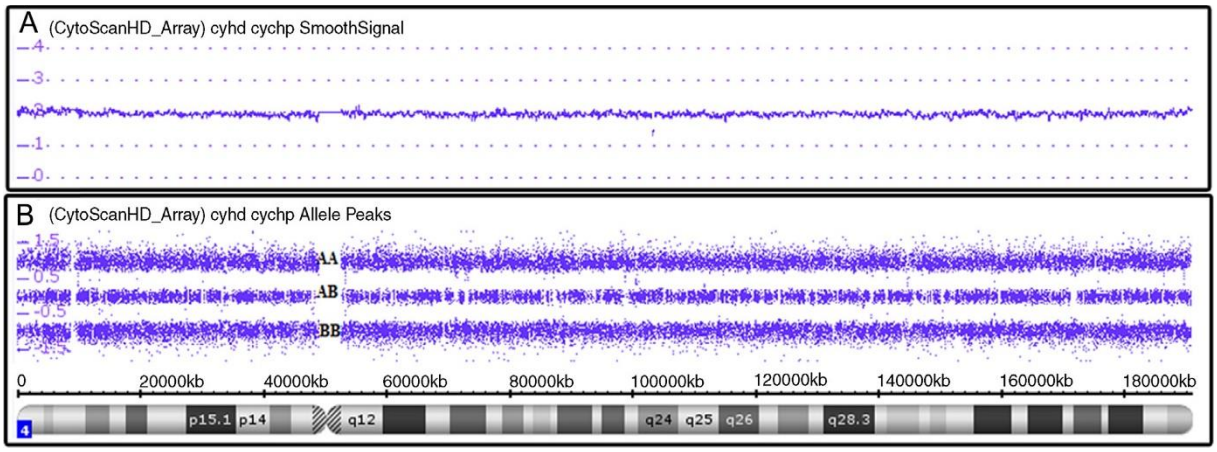

Figure 5.2: Image representing smooth signal and allele peaks of chromosome 4 following ChAS analysis. (A) Smooth signal with copy number = 2 denotes normal copy number. (B) Allele peaks with three purple lines denote a normal genotype with AA, AB and BB alleles. Image adapted from [181].

Implementation and evaluation of single nucleotide polymorphism (SNP) array analysis were carried out at the Institute for Cell Biology (Tumor Research) of the University of Duisburg-Essen by PD Dr. Ludger Klein-Hitpass. The isolation of genomic DNA from cells was carried out using the QIAamp DNA Mini Kit (Qiagen) according to the manufacturer's instruction. The DNA concentration was determined by the micro-volume spectrophotometer (NanoDrop 1000). DNA (250 ng) from cell was digested, amplified, purified, fragmented, labeled and hybridized using Affymetrix CytoScan® HD

Array GeneChip; CEL files were created using the GeneChip® System 3000 7G according to the manufacturer's instructions (Affymetrix). The CEL files were analyzed using Chromosome Analysis Suite v 2.0 (ChAS) software. To stabilize the calling of copy number gains or losses, the ChAS software implements a smoothing step. Smoothing will combine adjacent segments that are both gains, even if they are not the same Copy Number State. Smooth signal represents a normal copy number by CN = 2.00. CN > 2 denotes amplification of the specified gene.

5.6 **Clonogenic assay:**

Clonogenic assay or colony formation assay is a classical and robust *in vitro* cell survival assay based on the ability of a single cell to grow into a colony [182, 183]. This method employed to determine the ionizing radiation treatment driven reproductive death by cell, but can also be used to determine the effectiveness of other cytotoxic agents [184, 185].

To investigate the long-term effects of treatment with a biochemical inhibitor of MDM2 or CDK4 along with radiation treatment (RT) in liposarcoma cells, such as the eradication of clonogenic tumor forming cells, colony formation assay was conducted. Cells were diluted serially (400-2500) and plated into 6 well plates in 2 mL medium in triplicates. Cells were treated with the biochemical inhibitor and then within 20-30min irradiated with increasing doses of radiation (0, 2, 4 and 6 Gy). Cells were incubated for 24 hours before the inhibitor was washed off and fresh growth medium was added. Cells were irradiated using a 137Cs irradiator (J.L. Shepherd and Associates, San Fernando, CA) at room temperature. After treatment, cells were maintained for 12-18 days, depending on the growth rate of the cell lines, for colony formation. Cells were then fixed for 1h with 70 % (methanol/acetic acid) and stained for 15 minutes with Crystal violet in methanol. After staining, colonies were counted by naked eye, or under a microscope with a cut-off of 50 viable cells for scoring a colony.

The survival curves were established by plotting the log of the surviving fraction versus the treatment dose. Survival (*S*) data after a radiation dose (*D*) are fit by a weighted, stratified, linear regression according to the linear–quadratic formula given by: $S(D)/S(O) = \exp^{-(\alpha D+\beta D^{2})}$ [184, 186]. Survival fraction (SF) was estimated according to the formula: SF = number of colonies formed in test condition / (number of cells

seeded × plating efficiency of the control group).The radiation dose enhancement ratio (DER) or sensitization enhancement ratio (SER) was calculated as the dose (Gy) for radiation alone divided by the dose (Gy) for radiation plus drugs (normalized for drug toxicity) as determined at a surviving fraction of 0.5.

5.7 **SRB Assay:**

The sulforhodamine B (SRB) assay is employed for cell density determination, based on the measurement of cellular protein content and frequently used The method for the toxicity screening of compounds to adherent cells in a 96-well format [187].
For Sulforhodamine B (SRB) assays cells were plated at 1,000-5,000 cells/well in a 96-well flat bottom plate and cultured for 24 hours. Cells were then incubated with media containing inhibitors or solvent control (dimethyl sulfoxide, DMSO). If the treatment duration exceeded 72 hours, media with solvent control and inhibitors was changed. After 24-144 hours medium was removed and surviving cells were fixed at the bottom of the plate using 50µl of TCA 10 % (Trichloroacetic acid) for 1-2 hours at 4°C. Plates were then washed with Dulbecco's phosphate buffered saline (DPBS) or Aqua dest. for at least 3 times. To stain the protein of adherent cells 50µl of Sulforhodamine B (SRB, Sigma-Aldrich, MO, USA) 0, 4 % was added into the bottom of each well. Cells were incubated for 15 min to 1h at room temperature. Then, SRB solution was removed and the plates were washed with acetic acid 1 % to remove residual stain for at least 3 times. Afterwards, 150µl of Tris-Buffer solution (10mM, pH10.5) was added to each well to solve the SRB stain. At the plate shaker, plates were shaked for 5 minutes and absorption was measured at 560nm with a Genion luminometer (Tecan, Crailsheim, Germany). All measurements were carried out in triplicate/quadruplicate wells for at least two times and a representative example is shown.

5.8 **MTT Assay:**

Among the enzyme-based assays, MTT (3-(4, 5-dimethylthiazol-2-yl)-2, 5-diphenyl-2H-tetrazolium bromide) assay is considered one of the robust methods for determination of cytotoxicity assessment. In this method, viable cells contain NADPH-dependent oxidoreductase enzymes which reduce the MTT reagent to formazan. MTT

formazan is water-insoluble, and it forms purple needle shaped crystals in the cells [188]. The crystals are dissolved in an organic solvent for the subsequent colorimetric analysis.

For each experiment, the appropriate number of cells was plated (decided empirically) in order to be in their log phase of growth 24 hours later. Following treatment and irradiation in the next day, they were kept for 6 days. Prior to the assay, media was removed and MTT reagent was prepared (0.5 mg/mL) and 100µl added to the cells and kept at 37 degrees for 4-5 hour until the time crystals are formed. The crystal is solubilized thoroughly by adding organic solvent. At the plate shaker, plates were shaked for 5 minutes and absorption was measured at 560nm with a Genion luminometer (Tecan, Crailsheim, Germany).

Calculation of TGI (Total Growth Inhibition):

The 50 % growth inhibition parameter (GI_{50}) is the concentration of test drug where 100 x (T_i-T_O) / (C-T_O) = 50 which is the 50 % reduction in the net protein increase in control cells during the drug incubation. The optical density of the test well after the certain hour drug exposure is $T_{i;}$ the optical density at time zero is T_O; and, the control optical density is C. GI_{50} is defined as a growth-inhibitory level of effect, the TGI signifies a "total growth inhibition" or cytostatic level of effect. The TGI is the drug concentration where 100 x (T_i-T_O)/ (C-T) = 0. The LC_{50} is the lethal concentration, "net cell killing" or cytotoxicity parameter. It is the concentration where 100 x (T_i-T_O) / T_O = -50. This is the concentration of drug resulting in a 50 % reduction in the measured protein at the end of the drug treatment as compared to that at the beginning. The control optical density is not used in the calculation of LC_{50} [189].

5.9 Caspase 3/7 assay:

The Luminiscent Caspase Glo® assay (Promega, Madison, Wisconsin, USA) was employed to detect cellular apoptosis, as represented by activation of caspase 3/7, according to the manufacturer's protocol.

Principle of caspase assay: Caspases (cysteinyl-directed aspartate-specific proteases) are a family of enzymes that play a pivotal role in the apoptotic process. Once activated in response to extrinsic or intrinsic stimuli, these enzymes cause

degradation of key cellular proteins. Among the series of caspases, caspase 3 and caspase 7 are known as “executioner caspases”. Activation of caspase-3/7 is thus a hallmark and confirmation of the apoptotic process. The Caspase-Glo® 3/7 assay provides a pro-luminescent caspase-3/7 substrate, which contains the tetrapeptide sequence DEVD. When, caspase - 3 and - 7 are activated in cell suspension or adherent cells, this substrate is cleaved to release aminoluciferin. Aminoluciferin, in turn, is substrate of luciferase, resulting in luciferase reaction and production of light. Luminescence was measured with a Genion luminometer (Tecan, Crailsheim, Germany). All measurements were carried out in triplicate wells. Average and standard deviation were calculated from the technical replicates.

5.10 **Senescence Assay:**

Principle of senescence assay: Senescent cells were identified based on the increased levels of lysosomal β-galactosidase activity. Under normal growth condition, cells produce acid lysosomal β-galactosidase, which is localized in the lysosomes. Using the chromogenic substrate 5-bromo-4chlor-3-indolyl β D-galactopyranoside (X-gal), the enzymatic activity can be detected at pH 4.0. In comparison, upon senescence, the lysosomal mass is increased, leading to production of a higher level of β-galactosidase, termed senescence-associated β-galactosidase (SA-β-gal). The abundant senescence-associated enzyme is detectable over background despite the less favorable pH conditions (pH 6.0).

Cytochemical staining for SA-β-galactosidase (β-gal) was performed using a Senescence β-Galactosidase Staining Kit (Cell Signaling Technology) at pH 6.0 following the manufacturer’s protocol and images were taken by bright field light microscope at 40X magnification.

5.11 **Statistical Analysis:**

For evaluating the significance between the groups, Student’s t-test was employed. A p-value ≤ 0.05 was considered significant. Data represent mean ± standard deviation (SD) if not otherwise indicated.

5.12 **Immunofluorescence:**

Cells were fixed with 4 % PFA for 15 min at room temperature and permeabilized and blocked with 1 % BSA, 0.5 % Triton-X, 0.02 % sodium azide for 30 min at RT. DAPI stain was added at 5µg/mL and images were taken by Carl Zeiss fluorescent microscope and Zen software were employed.

5.13 **Western Blot:**

5.13.1 **Preparation of cell lysates**

Cells were seeded into 6-well flat bottom plates/T25 flasks and grown to confluence and then incubated with inhibitors or solvent control for the stipulated length of time depending on the experimental requirement. Following that protein lysate preparation was conducted. This step was carried out on ice to minimize protein degradation. The medium was removed and cells were washed with 1mL 1X DPBS per well. In case of the higher cell death, medium was also collected. Lysis step was carried out by adding 80-100µl of IP-buffer with protease inhibitors aprotinin, sodium vanadate, leupeptin and PMSF to each well. The lysis buffer ruptures the cell membrane and protease inhibitors prevent cleavage of proteins. After an incubation time of 1-3 minutes, cells were scrapped and collected in Eppendorf tubes. Lysates were rotated for at least 1 hour or overnight at 4 degree to completely extract the proteins from the cells. Afterwards, cells were centrifuged at 4°C for 30 minutes at 18626 RCF. The supernatant, containing proteins, was collected in new Eppendorf tubes.

To measure the protein concentration using the Bradford's method [190], BioRad solution (BioRad laboratories, Munich, Germany) was prepared according to manufacturer's protocol and the standard curve was established.

For experimental sample protein measurement, 2 µL of sample lysates were added to 1mL of BioRad solution and mixed by votexing. 2 µL of lysis buffer was used for solvent control or blank. From the diluted samples, 200µL per well were added to a flat bottom 96 well plate in quadruplicates and absorption was measured at 565nm using the Genion luminometer. According to measurements, lysates were diluted to a uniform protein concentration of 2µg/µl.

For the denaturation step, loading buffer was added at an amount of one third of the lysate's volume to charge the proteins. The mixture was heated up to 95°C for 5 minutes to denature the proteins.

5.13.2 Sodium Dodecyl Sulfate PolyAcrylamide Gel Electrophoresis (SDS-PAGE) and Western Blotting

Construction of the gel chambers were carried out by incorporating the commercially available gels (NuPAGE® 4-12 % Bis-Tris-Gels, novex by life technologies, Carlsbad, CA, USA) in electrophoretic chamber and filling up the chamber with (N-morpholino) propanesulfonic acid (MOPS)-SDS-running buffer (novex by life technologies, Carlsbad, CA, USA). The combs of the gels were gently removed and the exposed wells were washed with MOPS buffer using a 200µl pipette prior to loading of the proteins. 8µl of Spectra multicolour broad range protein ladder (Thermo Scientific Fermentas, Rockford, IL, USA) was loaded into the first well and lysates (30µg protein) were loaded into the following wells. PAGE was done at 170V for approx. 55 minutes as a standard. For smaller protein assessment, the voltage was lowered and time was lengthened.

Following the SDS-PAGE, gels were uncased and equilibrated in transfer buffer for 10 min along with the Hybond P nitrocellulose membranes (Amersham Pharmacia Biotech, Uppsala, Sweden). Employing the sandwich western blot setting (Sponge **-** whatmann filter paper **-** gel **-** nitrocellulose membrane **-** whatmann filter paper**-** sponge), the protein transfer step was conducted at 25V for 100 min.

Ponceaue staining (Sigma-Aldrich, Steinheim, Germany) of the membranes was carried out following the protein transfer to confirm equal concentration of protein transfer in the membrane.

Prior to the staining of specific protein, the membranes were washed with NET-G buffer for 30 min to block the non-specific binding of the antibodies. Following the blocking step, primary antibody (see Table 9 for antibodies and used dilutions) was added to the membrane and incubated overnight at 4 degree. Next day, the primary antibody was removed and washed by NET-G buffer with sequential washing steps. Secondary HRP linked antibody (see Table 10 for antibodies and used dilutions) was added and membranes were incubated at room temperature for 2h. Following this step,

membranes were washed by NET-G buffer and ECL substrate was added to the blots for enzymatic reaction of HRP. Chemiluminescence was measured and quantified using a FUJI LAS3000 system with Science Lab 2001 ImageGauge 4.0 software (Fujifilm Medial Systems, Stanford, CT, USA). The staining of Beta-actin was used as a loading control.

5.14 **Flow cytometry:**

5.14.1 **Cell cycle distribution by PI stain:**

Propidium iodide is a DNA binding dye, which intercalates between the bases with little or no sequence preference and with a stoichiometry of one dye per 4–5 base pairs of DNA [191]. It is frequently employed to measure cell cycle distribution as the cells in different cell cycle phases harbor different DNA content (G1 cells with diploid, G2 cells tetraploid and S-phase is clustered between diploid and tetraploid cells).

Two protocols have been used for the cell cycle distribution analysis.

For the first method of cell cycle analysis, cells were trypsinized, centrifuged and the supernatant was removed. Fixation was carried out by addition of ice-cold ethanol 70% to the pellet, re-suspended by vortexing and kept for 1 hour at 4 degree. Afterwards, cells were washed in DPBS (room temperature), centrifuged, 1X PBS was removed, and cells were re-suspended in 500µl propidium iodide-containing DNA PREP stain (Beckman Coulter, Brea, CA, USA). After 20 min of incubation, cell cycle was measured using the Cytomic FC 500 flow cytometer (Beckman Coulter), FL2-diode (585nm). ModFit LT® software was used for data analysis.

For the second method, cells were seeded, treated (with RT, inhibitor and vehicle) for stipulated time and cells were harvested at different time points depending on the experimental set up. Following that trypsinized, centrifuged and the pellets were fixed by ice-cold 70 % ethanol for 1h at -20 degree. Following that cell pellet was obtained by centrifugation and washing by 1X PBS. 500µL DNA extraction buffer was added and incubated for 15 min. Following, centrifugation and washing with 1X PBS propidium iodide PI stain was added and samples are incubated for 30 min at room temperature in dark. Cell cycle analysis was performed by BD Biosciences Celesta and analyzed by the BD Biosciences Diva software.

5.14.2 **Hoechst 33342 staining and live cell sorting:**

Hoechst 33342 is a fluorescent dye with lipophilic property, used for DNA-labelling in fluorescence microscopy and stains both live and dead cells even after fixation. Due to its cell permeability, it is routinely used to label intact or early apoptotic nuclei. The excitation wavelength of Hoechst 33342 is UV approximately at 380 nm and emission wavelength is around 461 nm.

10^6 cells were placed into a 12 x 15 mm test tube after trypsinization and centrifuged for 5 min at 300 x g.). Staining of cells with Hoechst 33342 (Sigma –Aldrich) was carried out by removing the supernatant and adding 500 µl of the medium that was used for growing the cells to be studied. 5µl of Hoechst 33342 was added to stock solution and mixed again and incubated at 37°C for 45 min. Doublets were gated out by FSC-A vs FSC-W plotting. Cell sorting was performed based on DNA content using a BD Biosciences (FACSvantage SE DIVA) cytometer equipped with a UV excitation laser. The sorted cells with different DNA content were plated at low density and kept for 15-17 days for clonogenic growth.

5.14.3 **Analysis of cell surface markers expression by multicolor flow cytometry:**

Preceding the staining of cell surface markers, tumor cells were seeded, treated and harvested according the experimental requirement. For each marker analysis, 5 $x10^5$ cells were collected in each Eppendorf tube suspended into 100µL of Facs Buffer. Fluorochrome-conjugated specific antibody (Table 11) is diluted according to the optimum titrated dilution and added to the cell suspension. Following homogeneous mixing, cells were incubated for 30 min in dark with gently shaking. 3mL of Facs buffer was added to each tube and centrifuged at 1500 rpm for 5 min. The supernatant was removed and 500µL of 4 % paraformaldehyde was added. Unstained cells or cells stained with anti-melanoma antibody (Miltenyi Biotec, Bergisch Gladbach, Germany) were taken as negative control. Cells stained with the phyco-erythrin (PE)-conjugated goat anti-mouse F(ab′)2 fragment (Dianova) were taken as isotype control. Measurement of the markers was carried out Beckman Coulter Flow cytometry instrument.

5.15 **Isolation of primary polyclonal NK cells:**

Polyclonal $CD3^{-}CD56^{+}$ NK cells were purified from peripheral blood mononuclear cells (PBMCs) of healthy donors. Briefly, PBMCs were depleted from monocytes by a 2h plastic adherence step. The remaining fraction of non-adherent cells was depleted from $CD3^{+}$ cells using anti-CD3-mAb-conjugated microbeads (Miltenyi Biotec, Bergisch Gladbach, Germany). In second step, CD3-depleted cells were employed as a source for positive selection of NK cells with anti-CD56-conjugated microbeads (Miltenyi Biotec). Depletion and positive selection were performed according to the instructions of the manufacturer. The purity of freshly isolated $CD3^{-}CD56^{+}$ NK cells was determined by flow cytometry, using the mAbs anti-CD3-FITC (Becton Dickinson Pharmingen, Heidelberg) and anti-CD56-PE (Becton Dickinson).

6 Results:

6.1 Cell line characterization

Primary WDLPS/DDLPS are known for harboring certain genetic abnormalities (amplification of 12q13~15). In order to confirm or validate the retention of the key oncogenes (*MDM2* and *CDK4*) in the patient-derived liposarcoma cell lines (LPS141, LPS853, T778, T449), genome-wide DNA copy number analysis was performed by HD cytoscan array. For copy number analysis, genomic DNA was isolated from the cell lines, processed (section 5.5) and hybridized to non-polymorphic probes. Signal intensities and SNP (Single-nucleotide polymorphism) calls in the samples were compared against a collection of >300 normal references in the database in order to determine loss and gain. Additionally, FISH (Fluorescence *in situ* hybridization) was carried out in order to determine *MDM2* amplification with *CEN 12* as an internal control.

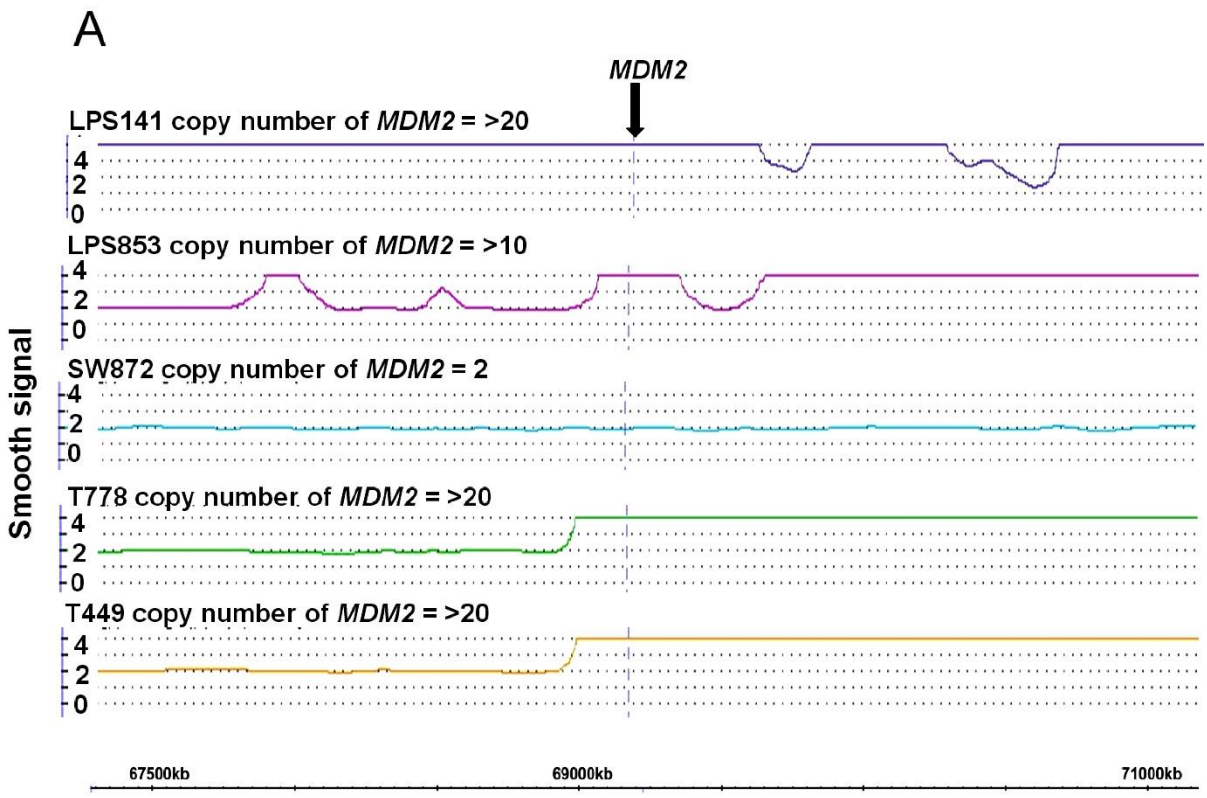

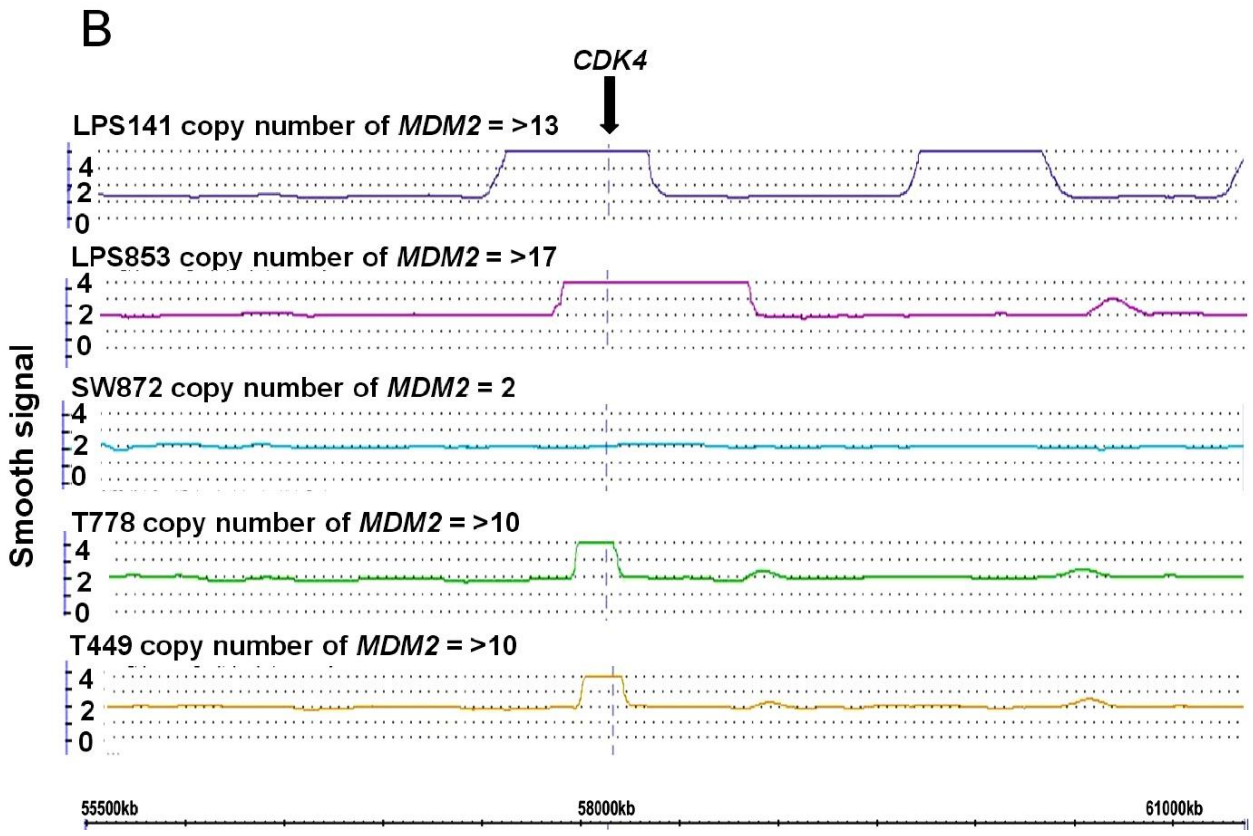
B
CDK4
LPS141 copy number of MDM2 = >13
LPS853 copy number of MDM2 = >17
SW872 copy number of MDM2 = 2
T778 copy number of MDM2 = >10
T449 copy number of MDM2 = >10
Smooth signal
4
2
0
55500kb
58000kb
61000kb

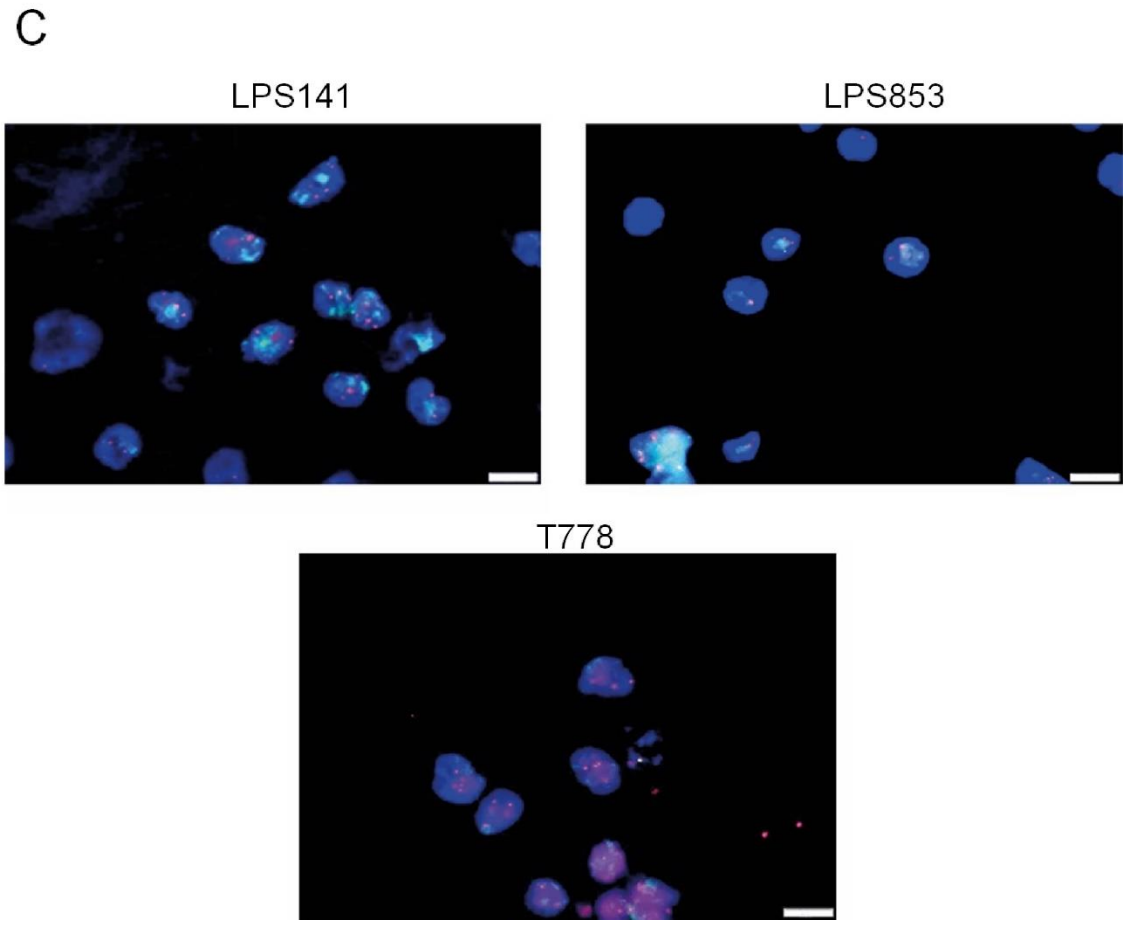
C
LPS141
LPS853
T778

Figure 6.1: Detection of amplification of *MDM2* and *CDK4* by SNP array and FISH in the liposarcoma cell lines. Smooth signal displaying copy numbers of **(A)** *MDM2* amplification and **(B)** *CDK4* amplification in LPS141, LPS853, T778, T449 and SW872. Copy number >2 indicates amplification and copy number = 2 implies normal status. **(C)** Interphase FISH images for *MDM2* amplification in LPS141, LPS853 and T778. For FISH staining, two fluorochromes were used: an orange fluorochrome directly labeled CEN 12 probe specific for the alpha satellite centromeric region of chromosome 12 (D12Z3) and a green fluorochrome directly labeled SPEC MDM2 probe specific for the MDM2 gene at 12q15.

For all the 4 WD/DDLPs cell lines (LPS141, LPS853, T778 and T449), the copy numbers of *MDM2* and *CDK4* genes were >10 which confirmed the amplifications of these genes. As expected, no amplification of *MDM2* (CN = 2) and *CDK4* (CN = 2) were detected in the UDLP, SW872.

Interphase FISH staining (Figure 6.1 C) was conducted in the 4 cell lines with Zytolite Spec MDM2/CEN 12 dual color probe. The MDM2/CEN 12 dual color probe is a mixture of an orange fluorochrome directly labeled CEN 12 probe specific for the alpha satellite centromeric region of chromosome 12 (D12Z3) and a green fluorochrome directly labeled SPEC MDM2 probe specific for the *MDM2* gene at 12q15. In a normal interphase nucleus, two orange and two green signals are expected to represent a single copy of *MDM2* per chromosome. In a cell with amplification of the *MDM2* gene locus, multiple copies of the green signal or green signal clusters are expected to be observed. *MDM2* amplification was defined as a ratio of MDM2/CEN 12 ≥ 2.1 per 100 tumor cells. *MDM2* amplification was detected prominently in LPS141, moderately in LPS853. In T778, a slight amplification was detected. In T449, no signal was detected (data not shown).

6.2 Determination of anti-proliferative effect exerted by combinatorial targeting of the oncogenic drivers (*MDM2* and *CDK4*) in liposarcoma cell lines

In order to accomplish this goal, growth inhibition, cell cycle distribution and apoptosis were measured following treatment with MDM2 inhibitor (Nutlin-3) and CDK4 inhibitors (Palbociclib or LEE011) in liposarcoma cell lines (LPS853 *MDM2* Amp/*CDK4* Amp, LPS141 *MDM2* Amp/*CDK4* Amp, T778 *MDM2* Amp/*CDK4* Amp and T449 *MDM2* Amp/*CDK4* Amp) *in vitro*.

6.2.1 Combination treatment exerted no significant additive effect in liposarcoma cells by SRB assay

For measurement of growth inhibition in response to combination treatment, Sulforhodamine B (SRB) assays (Figure 6.2) were carried out following 6 days of treatment with MDM2 inhibitor alone and in combination with CDK4 inhibitors.

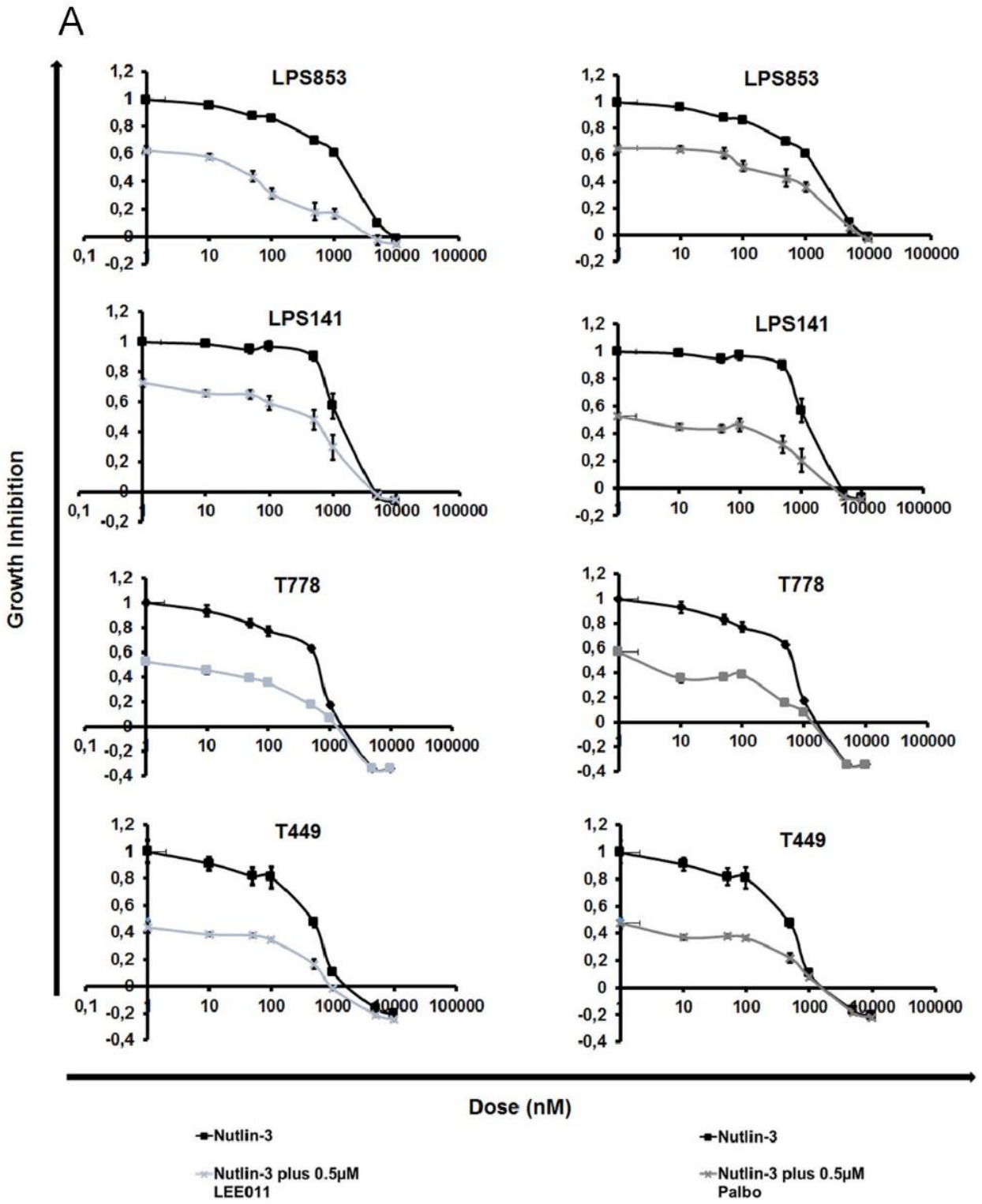

B

Cell Line	GI50 (μM)			TGI (μM)		
	Nutlin-3	Nutlin-3 + 0.5μM Palbociclib	Nutlin-3 + 0.5μM LEE011	Nutlin-3	Nutlin-3 + 0.5μM Palbociclib	Nutlin-3 + 0.5μM LEE011
LPS141	1.2	0.1	0.4	3.2	1.8	2.4
LPS853	1.5	0.13	0.03	4.8	3.7	1.7
T778	0.65	0.002	0.003	0.9	0.23	0.23
T449	0.48	0.001	0.001	0.8	0.3	0.2

Figure 6.2: **Combined targeting of CDK4 and MDM2 exerted no additive growth inhibition in liposarcoma cell lines. (A)** SRB assay graphs displaying growth inhibition in response to combination treatment to a concentration starting from 1nM to 10μM of MDM2 inhibitor (Nutlin-3) and a fixed concentration (0.5μM) of CDK4 inhibitors (Palbociclib or LEE011). **(B)** Table representing GI50 and total growth inhibition (TGI) in response to combined targeting. Experiments were conducted in triplicate or quadruplicate.

GI50 value and TGI (Total growth inhibition) were determined (for calculation see section 5.8) for MDM2i alone or in combination (fixed dose of 0.5μM of CDK4i) for the liposarcoma cell lines. The differences of GI50 values for monotherapy versus combination were higher. However, the differences in TGI values between monotherapy and combination were comparable. The convergence of the TGI values and shape of the graph indicated toward non-additivity or a narrow therapeutic window of additive effects in liposarcoma cells in response to the combination treatment. Application of CDK4i alone or in combination (fixed dose of 0.5μM of MDM2i) displayed equivalent or similar growth pattern (Figure S 11.1).

In summary, these results demonstrated no significant additive growth inhibition by blockade of functional CDK4 and MDM2 in liposarcoma cells.

6.2.2 Reduction of G1 arrested cells upon treatment with combination treatment in liposarcoma cells

In order to examine the effect of co-targeting in cell cycle distributions, cell cycle analysis by PI stain (Figure 6.3) was carried out in the liposarcoma cell lines following treatment with CDK4 inhibitor (0.5μM) and MDM2 inhibitor (1μM, 5μM). As, expected,

an enhanced G1 arrest (LPS853 ~75 %, T778 ~74 %, LPS141 ~82 % and T449 ~80 %) was observed in response to the CDK4 inhibitors alone. Addition of MDM2 inhibitors with increasing dose led to a dose-dependent decrease of G1 arrest in the cell lines. Apoptotic population (sub-G1) remained comparable or undetectable in all the treatment groups.

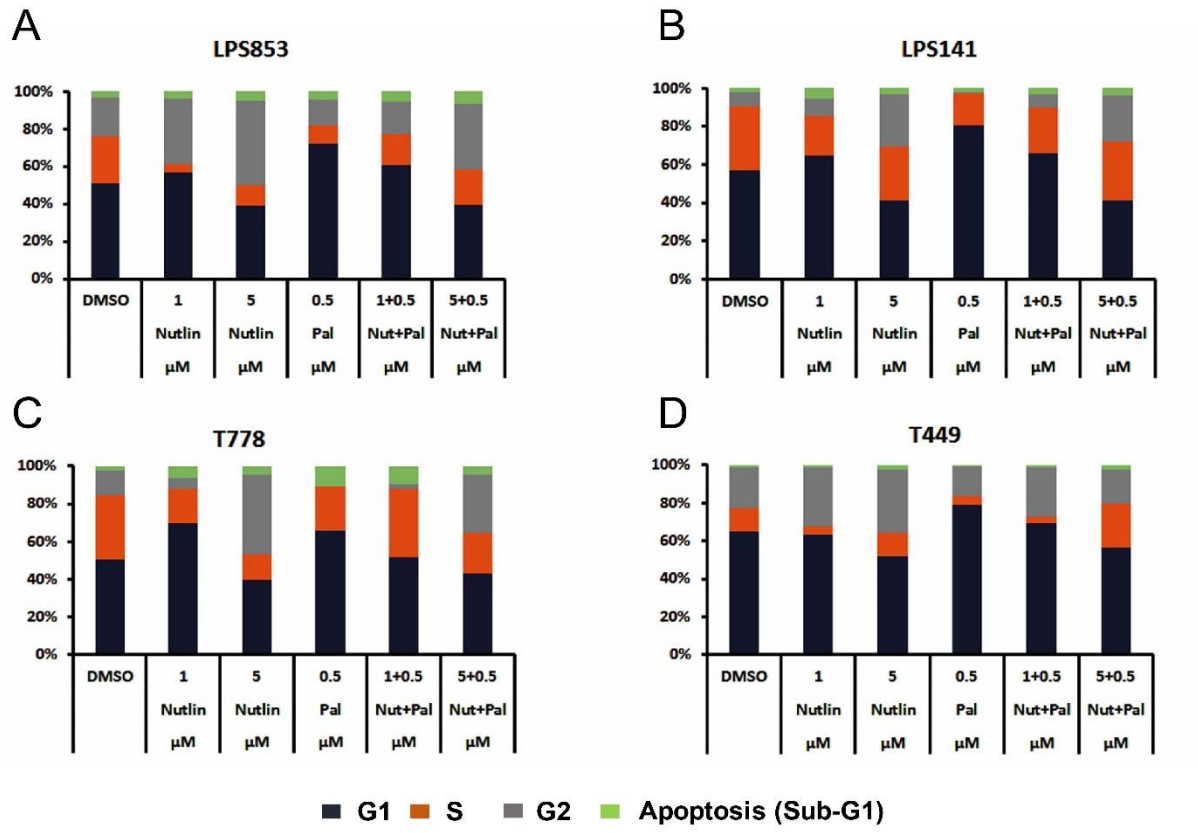

Figure 6.3: **Analysis of cell cycle distribution following combined treatment in liposarcoma cells.** Cell cycle distribution analysis by PI stain in **(A)** LPS853, **(B)** LPS141, **(C)** T778 and **(D)** T449 in response to MDM2i alone (increasing doses of 1µM, 5µM Nutlin-3) and CDK4i (0.5µM) and in combination after 48h. Bar graphs represent the percentage of distribution of cells in different phases (G1, S, G2 and Sub-G1) of the cell cycle.

In summary, these data implied that co-inhibition of CDK4 and MDM2 reduced G1 arrest than CDK4 inhibitor alone in liposarcoma cells.

6.2.3 No significant enhancement of apoptosis upon combined targeting of MDM2 and CDK4 in liposarcoma cells

For measurement of apoptosis, caspase 3/7 assay (Figure 6.4) was performed following treatment with CDK4 and MDM2 inhibitors after 24h and 48h. CDK4 inhibitor alone did not induce apoptosis in any of the cell lines. Apoptotic population was

unchanged or comparable among all of the treated (single or combined) and untreated groups for LPS853 at 24h and 48h. For LPS141, T778 and T449, MDM2 inhibitor alone induced apoptosis (~2 fold). However, the addition of CDK4 inhibitor did not show significant increase of apoptosis in LPS141, T449 and T778 at 24h. For T778, an additive effect was observed at 48h with 5μM MDM2i and 0.5μM CDK4i. However, increasing the dose of CDK4i to 1μM did not enhance the level of apoptosis.

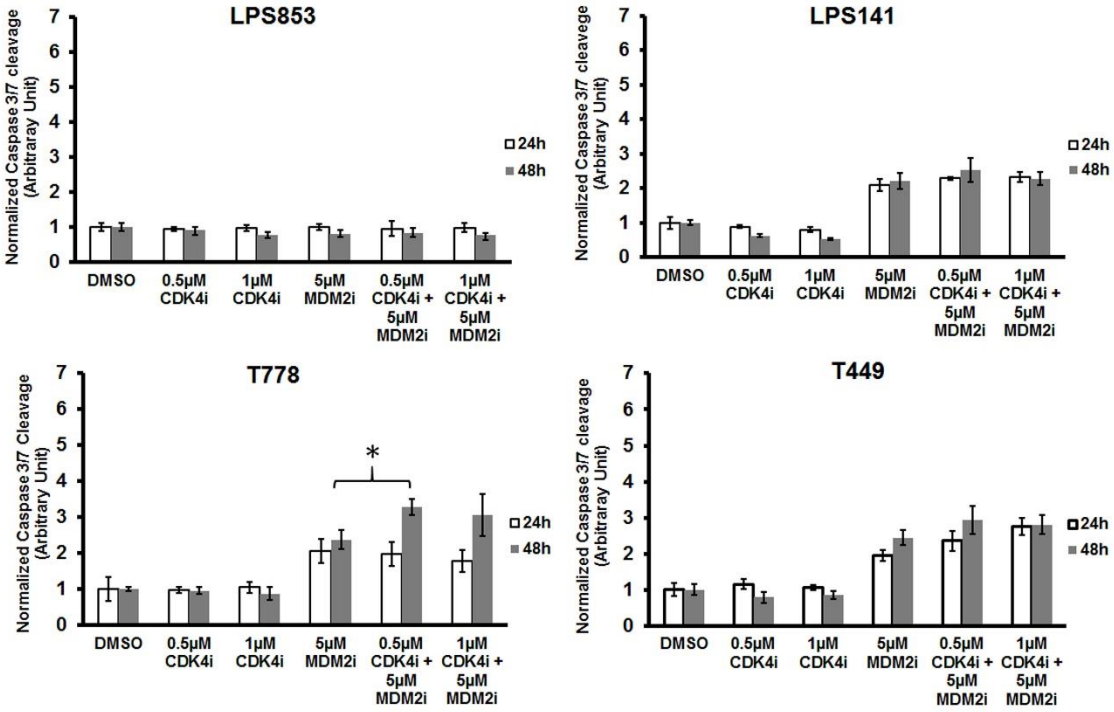

Figure 6.4: **No significant enhancement in apoptosis was observed in response to combined targeting.** Liposarcoma cells (LPS853, LPS141, T778 and T449) were treated with monotherapy (either with CDK4i or with MDM2i) and combined therapy for 24h and 48h. Caspase 3/7 assay was performed to detect apoptosis. Bar graphs represent mean ± SD. * $p \leq 0.05$.

In summary, combined blockade of CDK4 and MDM2 did not augment the level of apoptosis in liposarcoma cells.

6.2.4 Intracellular signaling pathway perturbation in response to combined targeted therapy in liposarcoma cells

Immunoblotting studies were carried out in order to detect the modulation of intracellular signaling pathways in response to dual targeted therapy (Figure 6.5). Cell lysates were prepared following treatment with CDK4 inhibitor, MDM2 inhibitor and combination of both for 48h. In LPS853 and in T449, a dose-dependent upregulation

of p53 was observed in response to MDM2i alone. An induction of MDM2 and p21 was detected. However, the addition of CDK4i did not alter the expression. Total Rb levels were reduced or inconsistent in the treatment groups. Phospho-Rb (Ser-780) was not observed to be changed in T449.

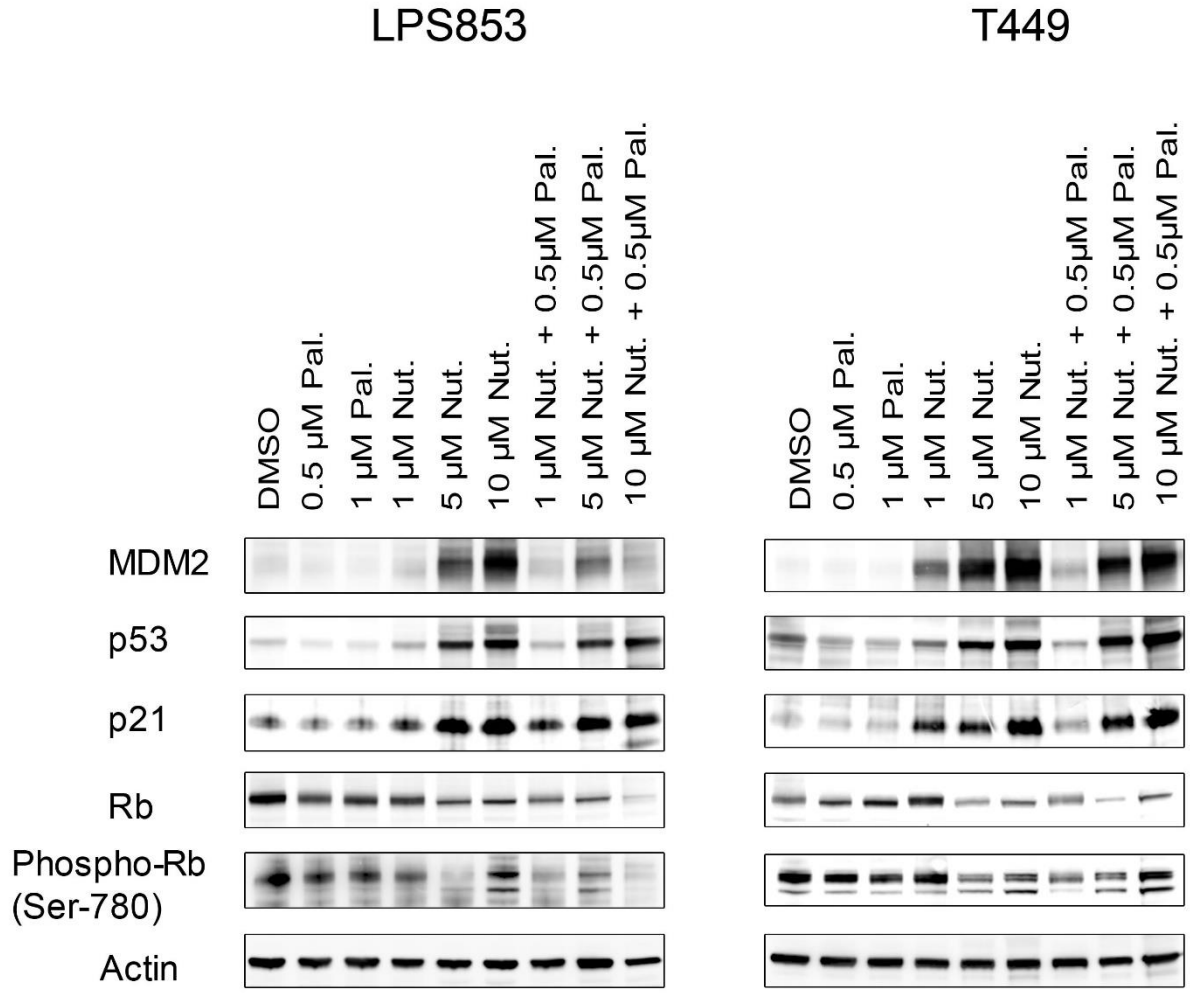

Figure 6.5: **Effect of combination treatment in signaling pathway.** Immunoblotting of signaling axis of MDM2-p53-p21 and Rb, phospho-Rb (Ser-780) in response to combined therapy following 48h in LPS853 and T449. Beta-actin was taken as a loading control.

In summary, these results indicated co-targeting of CDK4 and MDM2 in liposarcoma cells did not make significant modulation of the p53-p21 signaling pathway compared to the single agent treatment of Nutlin-3. Total Rb levels were reduced in response to the treatment of Nutlin-3 (± CDK4i).

6.2.5 **Effect of Nutlin-3 in Rb regulation in liposarcoma cells**

In order to observe the effect of Nutlin-3 on the level of total Rb, a cell line with deleted *TP53* and T449 (wild-type *TP53*) cells were treated with Nutlin-3 for 24 hours. By western blot analysis, total Rb level was detected to be reduced and unaffected in T449 and *TP53* negative cells, respectively (Figure 6.6).

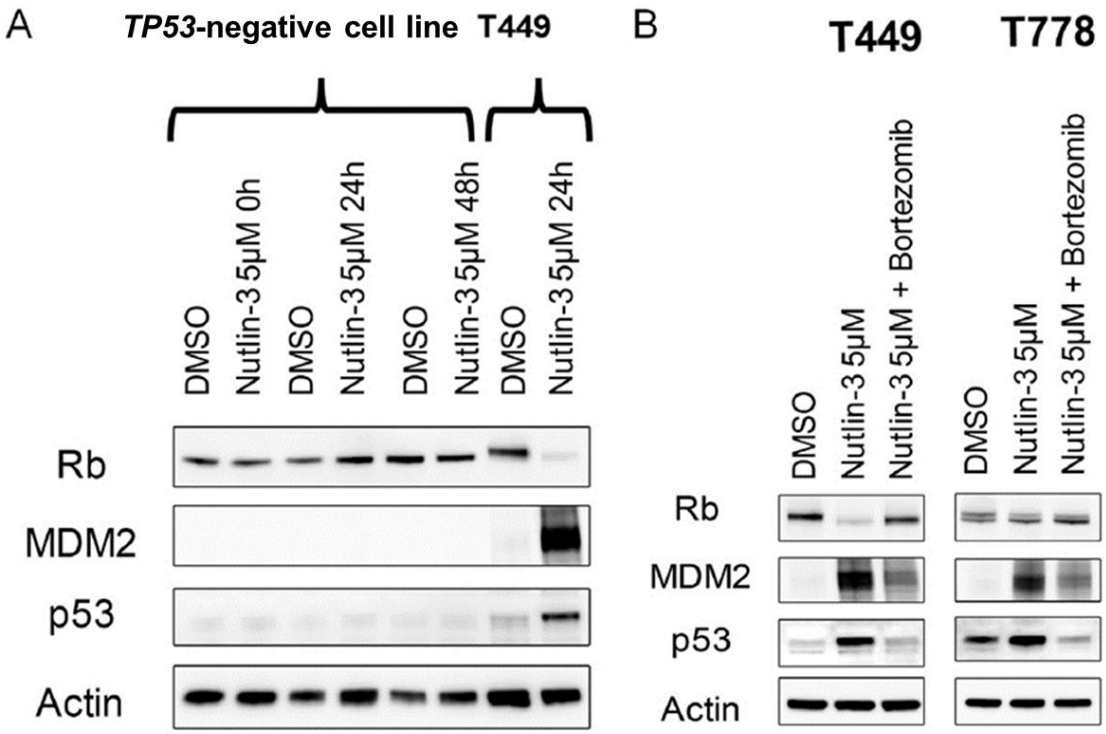

Figure 6.6: Nutlin-3 mediated Rb degradation in liposarcoma cells. (A) Western blot image representing Rb status in response to Nutlin-3. Following treatment of *TP53*-negative cell line for 24h and 48h and T449 for 24h with Nutlin-3, western blot was carried out with stains of MDM2, p53 and Rb. Beta-actin was probed to show equal amount of loading extracts. **(B)** Western blot images of T449 and T778 cells co-treated with 5μM Nutlin-3 and 10μM of Bortezomib for 18h**.**

The plausible explanation for the reduced level of Rb could be the induction of p53 by Nutlin-3 that is being otherwise inhibited by MDM2. Following p53 induction, there is an upregulation of MDM2 by p53 *via* feedback autoregulatory loop [15, 192] as observed in other tumors with wild-type *TP53*. Overexpression of MDM2 and destabilization of Rb *via* proteasome-mediated pathway has been previously demonstrated to be a cause of development of cancer [193, 194]. Thus, Rb might be degraded by upregulated MDM2 in liposarcoma (T449) with functional p53 while the *TP53*-negative cell line harbor intact Rb due to the non-functional p53 pathway.

To further explore whether the reduction in the levels of the total Rb in liposarcoma cells is *via* MDM2 directed proteasome-mediated degradation pathway, T778 and T449 cells (Figure 6.6), were co-treated with 10μM of Bortezomib (proteasome inhibitor) and Nutlin-3 for 18h. Following this, cells were harvested and lysates were prepared and Rb status was determined by western blot analysis.

Upon treatment with Nutlin-3 alone, as observed previously, level of total Rb was significantly diminished in T449. Addition of the proteasome inhibitor along with the MDM2 inhibitor, rescued total Rb level. However, in T778 the level of reduction of Rb upon treatment with MDM2 inhibitor was less than T449. Addition of proteasome inhibitor rescued the diminished level of Rb again.

In summary of these experiments, it is conceivable that as Rb is the substrate of CDK4, degradation of Rb might be a cause of insensitivity to co-treatment.

6.2.6 **Evaluation of growth inhibition by sequence alteration of CDK4 and MDM2 inhibitors.**

Following the observation of co-treatment of CDK4i and MDM2i in liposarcoma cells did not exert an additive effect; it was aimed to investigate the effects by changing the treatment sequence of the inhibitors.

The different sequences include:

- Continuous treatment with either CDK4i or MDM2i as a single agent
- Continuous co-treatment with CDK4i plus MDM2i
- Pre-treatment with CDK4i and post-treatment with MDM2i
- Pre-treatment with CDK4i and post-treatment with combined MDM2i plus CDK4i
- Pre-treatment with MDM2i and post-treatment with CDK4i
- Pre-treatment with MDM2i and post-treatment with combined MDM2i plus CDK4i
- Pre-treatment with combined MDM2i plus CDK4i and post-treatment with MDM2i
- Pre-treatment with combined MDM2i plus CDK4i and post-treatment with CDK4i

Cells were seeded in 96 well plates and were treated the next day. For continuous treatment (with CDK4i, MDM2i or combination of both), cells were treated for 6 days without changing the treatment. For treatment sequence alteration study, following three days of pre-treatment, a different combination of inhibitors was applied to the cells for another three days (post-treatment) as mentioned above. Lower and equal doses of MDM2i (2µM of Nutlin-3) and CDK4i (2µM of Palbociclib or LEE011) were chosen for the sequence alteration study as 5µM MDM2i was displayed a dominant effect alone in the earlier experiments. Upon application of CDK4i and MDM2i with all the possible permutation of treatment schedules (Figure 6.7) in T449 and T778, a reduced cell viability was observed in the treatment groups. CDK4i as a single agent reduced cellular growth to ~ 40 % to 80 % as compared to the untreated group. A dominant effect of MDM2i was noted (avg. cell viability ~ 19 % ± 2). In combination with CDK4i in any sequence exerted comparable effect (avg. cell viability ~ 19 % to 27 %).

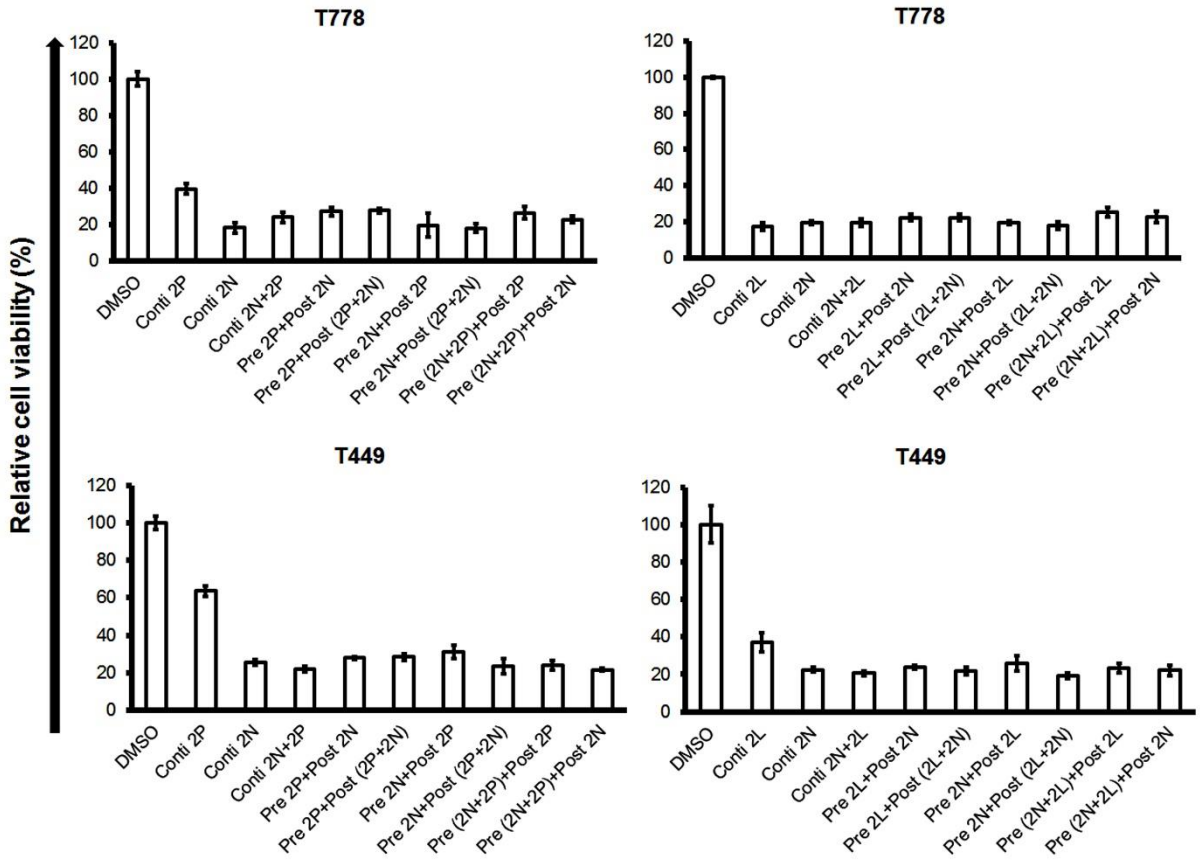

Figure 6.7: **Alteration of the treatment schedule of MDM2i and CDK4i did not enhance growth inhibition.** Cell viability was measured by MTT assay in response to different treatment schedules of CDK4 and MDM2 inhibitors in liposarcoma cell lines (T778 and T449). Bar graphs (mean ± SD) represent the percentage of viable cells relative to the untreated control. 2L= 2µM of LEE011, 2P = 2µM of Palbociclib, 2N = 2µM of Nutlin-3. Pre = pre-treatment, post = post-treatment.

In summary, these results suggested that altering the sequence of the inhibitors did not exert an additive growth inhibition in liposarcoma cells. Thus, these data indicated toward RB-independent compensatory pathways for evading the effects of the inhibitors.

6.3 Radiation treatment (RT) and MDM2 inhibitor mediated effect in liposarcoma cells

6.3.1 Nutlin-3 induced moderate radio-sensitization of liposarcoma cells with highly amplified *MDM2 in vitro*

In order to assess whether MDM2 inhibition leads to radio-sensitization of liposarcoma cells *in vitro*, liposarcoma cell lines (Table 18: LPS853 *MDM2* Amp/*TP53* WT, T778 *MDM2* Amp/*TP53* WT, T449 *MDM2* Amp/*TP53* WT and SW872 *TP53* Mut) were seeded as single cells, co-treated with Nutlin-3 and irradiated with increasing doses of gamma-radiation (Figure 6.8). Following 24h, Nutlin-3 containing medium was replaced by fresh medium and kept for 12-14 days until the colonies grew. For LPS853 and T778, three different doses of Nutlin-3 (1µM, 2.5µM and 5µM) were tested for clonogenic assays. For T449 and SW872, 5µM Nutlin-3 was used for assessing radio-sensitization.

Clonogenic cell growth was measured and compared for radiation treatment alone and the combination treatment group. Surviving fraction (SF) of cells was plotted on a logarithmic scale against dose on a linear scale and fit to a linear-quadratic (LQ) model. Sensitization enhancement ratio (SER) is defined as the ratio of radiation doses in absence and presence of inhibitor required to obtain the same biological effect (here survival fraction of 10 %). Thus, a value of SER greater than one means that presence of the inhibitor reduces the radiation dose to achieve the isoeffect.

With increasing doses of Nutlin-3, a dose-dependent increase in the radio-sensitization effect was observed in two of the liposarcoma cell lines (T778 *MDM2* Amp/*TP53* WT and LPS853 *MDM2* Amp/*TP53* WT) as indicated by the increasing SER_{10} values at a survival fraction of 10 % (Figure 6.8 A). The highest SER_{10} values at survival fraction of 10 %

were 1.42 and 1.39 for T778 and LPS853, respectively, as observed following the treatment with 5μM of Nutlin-3. In contrast, T449 harboring amplified *MDM2* and wild-type *TP53* did not show sensitization to x-rays by Nutlin-3 (SER_{10} = 0.79).

As expected, UDLPS cells (SW872) harboring non-functional p53 did not show radio-sensitization by MDM2 inhibition (SER_{10} = 1.06).

A

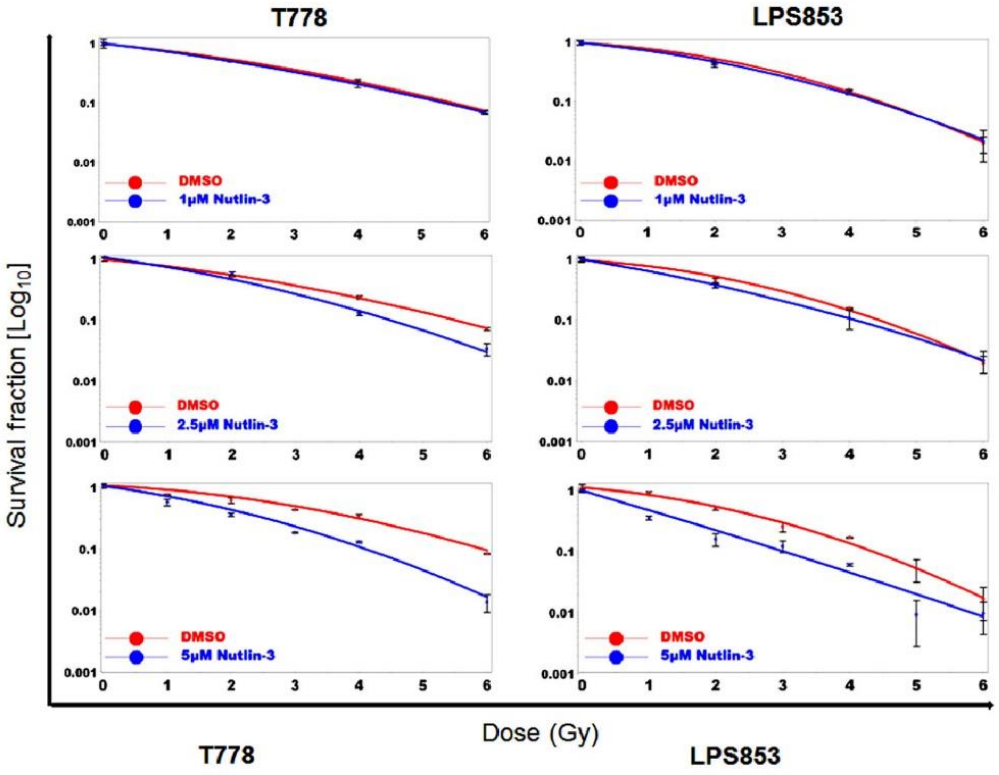

T778

Dose of Nutlin-3	SER at 0.1 survival level
1μM	1.03
2.5μM	1.25
5μM	1.43

LPS853

Dose of Nutlin-3	SER at 0.1 survival level
1μM	1.01
2.5μM	1.09
5μM	1.30

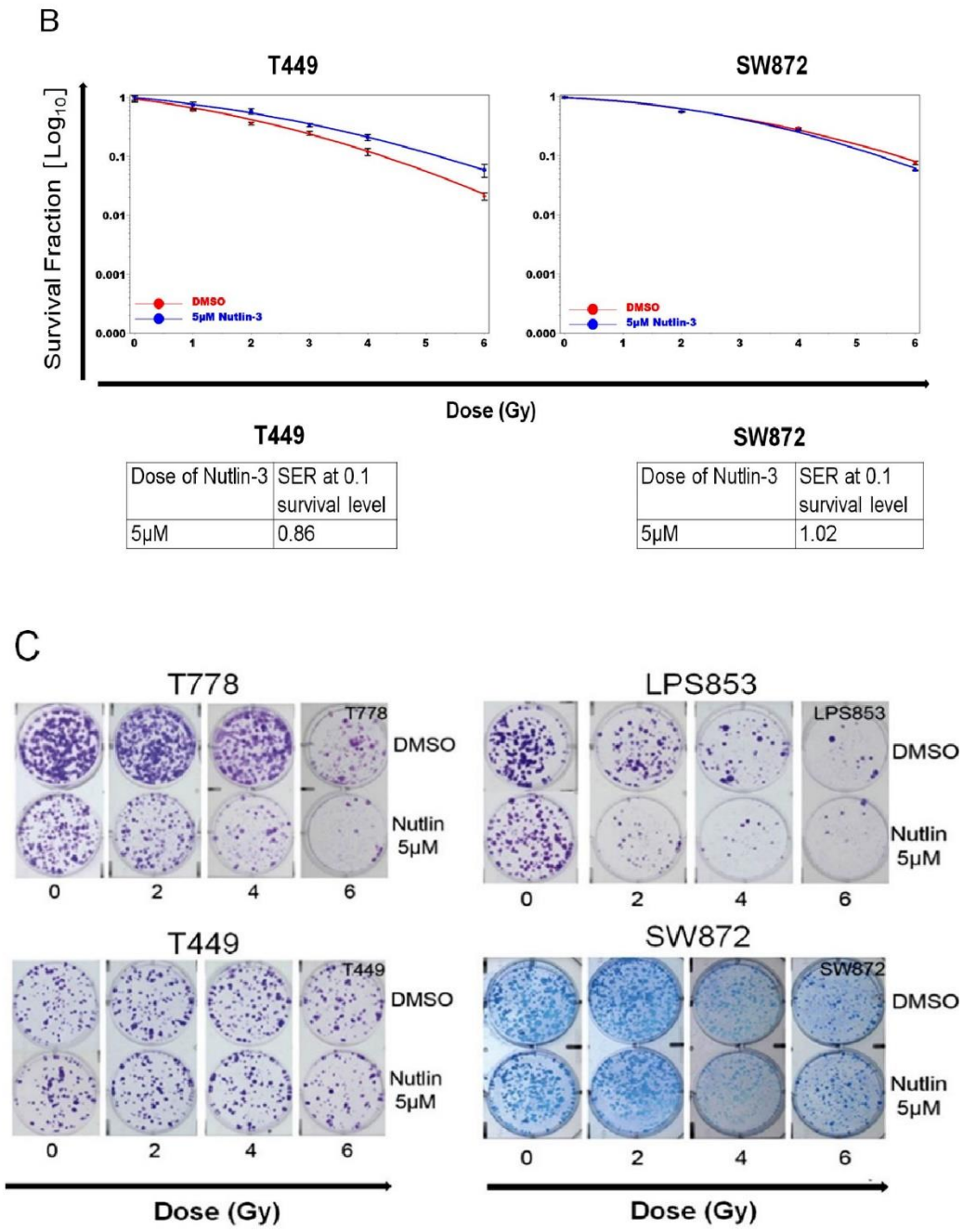

T449

Dose of Nutlin-3	SER at 0.1 survival level
5μM	0.86

SW872

Dose of Nutlin-3	SER at 0.1 survival level
5μM	1.02

Figure 6.8: ***In vitro*** **radio-sensitization by MDM2 inhibition in liposarcoma cells.** Liposarcoma cells were plated and treated with Nutlin-3 (1μM, 2.5μM and 5μM for LPS853 *MDM2* Amp/*TP53* WT and T778 *MDM2* Amp/*TP53* WT, 5μM for T449 *MDM2* Amp/*TP53* WT and SW872 *TP53* Mut) for 24h. Following drug removal, cells were kept for 10-12 days for colony formation.The surviving fraction (SF) was calculated from counted colonies (>50 cells) divided with plated number of cells. Values were normalized by plating efficiency. Sensitization enhancement ratio (SER) was calculated by the ratio of radiation dose alone to radiation dose in combination with Nutlin-3 at 10 % survival level. **(A)** Cell survival curves derived from clonogenic assay of 2 liposarcoma cells (T778 *MDM2* Amp/*TP53* WT and LPS853 *MDM2* Amp/*TP53* WT) and corresponding tables represented SER (sensitization enhancement ratio) at 0.1 survival fraction. **(B)** Survival curve of one WDLP (T449 *MDM2* Amp/*TP53* WT) and one UDLP (SW872 *TP53* Mut) cell lines with corresponding tables representing SER at 0.1 survival fraction. **(C)** Representative images from the colony formation assay**.**

In summary, this set of results suggested MDM2 inhibition led to radio-sensitization in two of the liposarcoma cell lines with wild-type *TP53*. Liposarcoma cell line with *TP53* mutation did not display sensitivity to radiation following Nutlin-3 treatment which indicated the importance of wild-type *TP53* status for responsiveness of liposarcoma cells to the combination treatment. However, radiosensitvity was not evident in the other liposarcoma cell line with wild-type *TP53*.

6.3.2 Nutlin-3 mediated radio-sensitization by enhanced cell cycle arrest and induction of senescence

Next, the possible phenotypic cell fates of liposarcoma cell lines in response to the treatments were determined by assessing apoptosis, cell cycle distribution and senescence. Cells were treated with 5μM Nutlin-3 or with ionizing radiation (4 Gy) or in combination. Activation of caspases 3/7 was examined as a marker of apoptosis. Following 24h of treatment, no significant change in the apoptotic response was observed among the untreated and treated groups (Figure 6.9 A) in LPS853, T778, T449 and SW872. Thus, the mechanism of sensitization to x-rays by Nutlin-3 might not be by the induction of apoptosis in liposarcoma cell lines. However, in response to Nutlin-3 treatment alone, a significantly higher ($p < 0.05$) apoptotic cell population was observed in T449. Addition of the RT led to a reduced level of apoptosis. In parallel, immunoblotting of total PARP (116 Kd) and cleaved PARP (89 Kd) was carried out in all the treatments (Figure 6.9 E) as a measurement of caspase-3 activation and apoptosis after 48h. Total PARP levels were slightly reduced indicating PARP cleavage. However, cleaved PARP (89 Kd) was not detected. One plausible explanation could be the degradation of the cleaved fragments after 48h of treatment. Total PARP levels were comparable in 5μM Nutlin-3 and combination treatment treated groups in T778 *MDM2* Amp/*TP53* WT and LPS853 *MDM2* Amp/*TP53* WT. In contrast, for T449 *MDM2* Amp/*TP53* WT total PARP was higher in combination than Nutlin-3 treatment alone (Figure 6.9 E). In SW872*TP53* Mut, total PARP remained unperturbed.

Cell cycle distribution (Figure 6.9 D) was assessed by PI stain following 48h of treatment in liposarcoma cell lines. A strong G2 arrest (by 4N DNA content) was detected by treatment with combination treatment in LPS853 (G2 ~ 57 %), T778 (G2 ~ 60 %) and in T449 (G2 ~ 42 %). Cell cycle distribution was unperturbed in SW872 in response to the treatments.

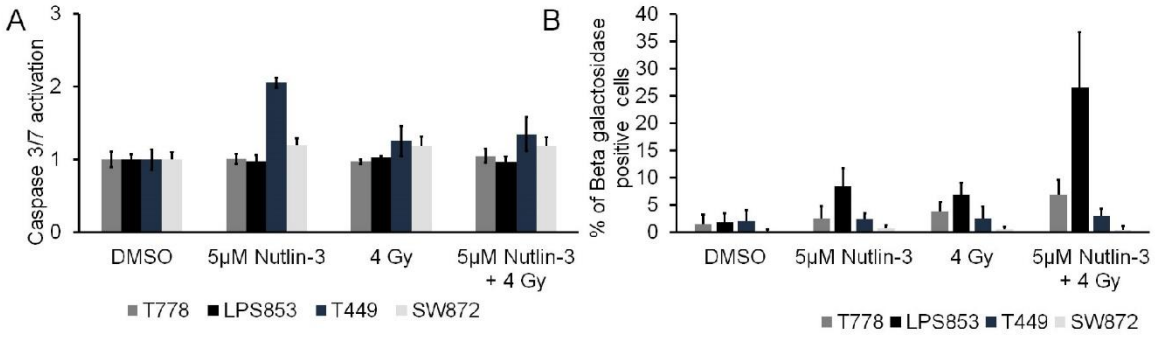
A
Caspase 3/7 activation
3
2
1
0
DMSO
5μM Nutlin-3
4 Gy
5μM Nutlin-3 + 4 Gy
T778 LPS853 T449 SW872
B
% of Beta galactosidase positive cells
40
35
30
25
20
15
10
5
0
DMSO
5μM Nutlin-3
4 Gy
5μM Nutlin-3 + 4 Gy
T778 LPS853 T449 SW872

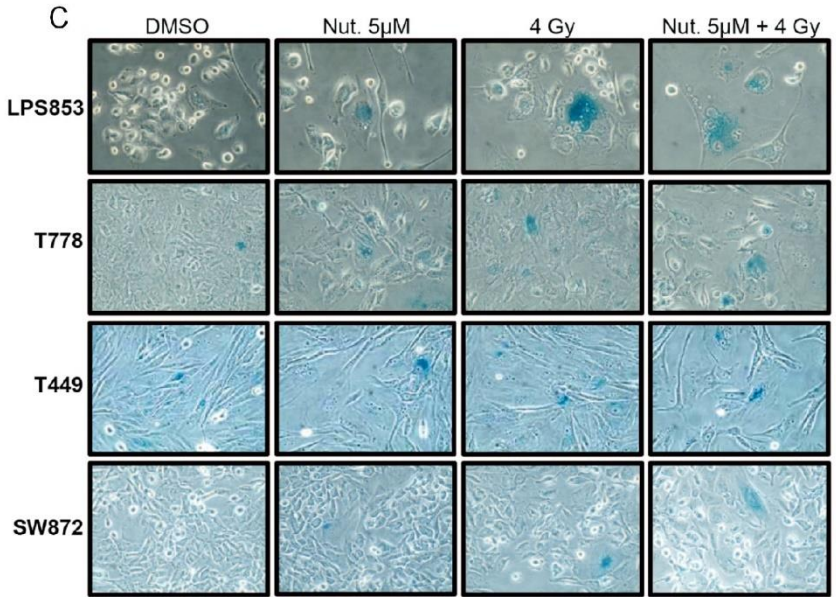
C
DMSO
Nut. 5μM
4 Gy
Nut. 5μM + 4 Gy
LPS853
T778
T449
SW872

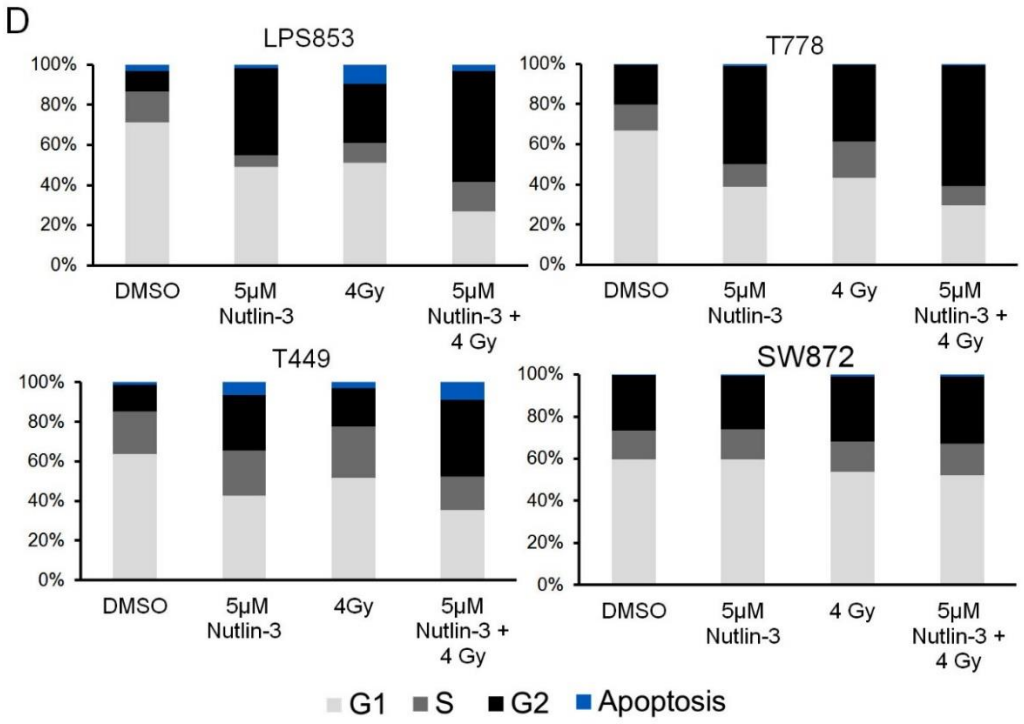
D
LPS853
T778
T449
SW872
100%
80%
60%
40%
20%
0%
DMSO
5μM Nutlin-3
4Gy
4 Gy
5μM Nutlin-3 + 4 Gy
G1 S G2 Apoptosis

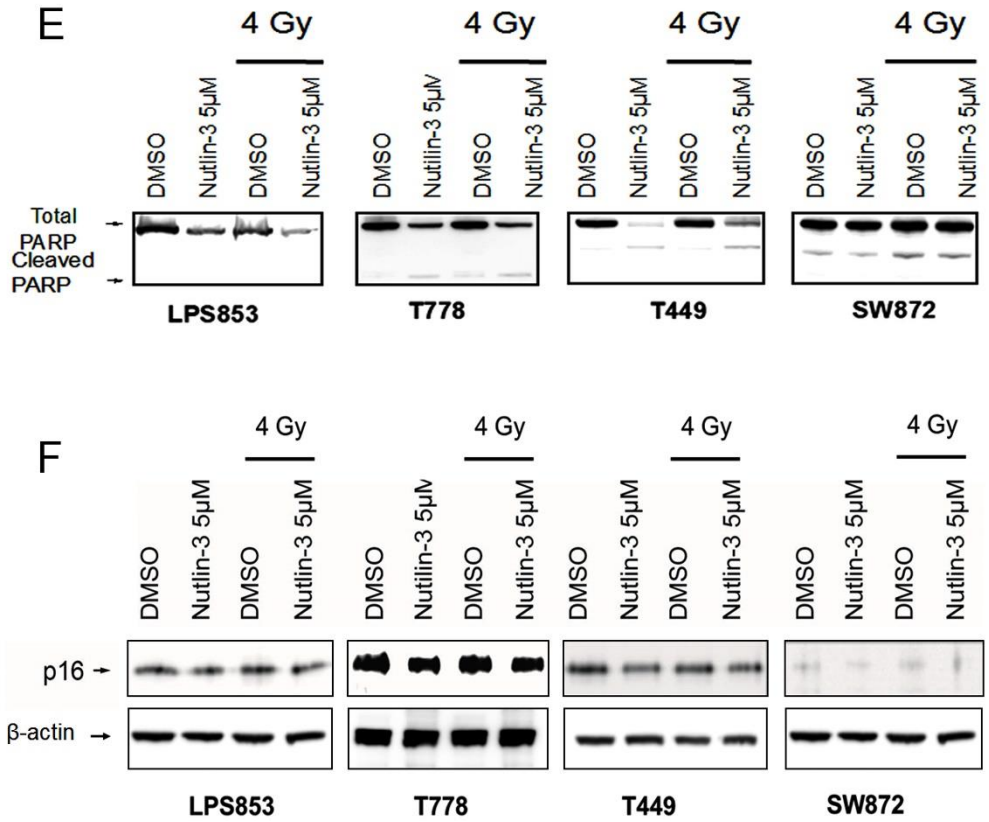

Figure 6.9: Measurement of apoptosis, senescence and cell cycle. (A) Apoptotic response as measured by caspase 3/7 activation following treatment with either DMSO, Nutlin-3 (5μM), ionizing radiation (4 Gy) or combination of both. Cells were treated for 24 hours. Bar graphs represent averages (n = 3) normalized by the untreated group. Error bars indicate SD. **(B)** Senescence-associated beta-galactosidase staining of liposarcoma cells. Bar graphs represent quantification of an average of the percentage of beta-galactosidase positive cells, n = 5, error bars indicate SD. **(C)** Corresponding bright field microscopy images. **(D)** Cell cycle distribution analysis of liposarcoma cells following 48h of treatment. Western blots of **(E)** total PARP, cleaved PARP and **(F)** p16 in all the cell lines following 48h of treatment**.** Beta-actin was taken as a loading control.

For detection of senescence, beta-galactosidase staining and quantification were carried out after 48h of treatment. Nutlin-3 alone moderately induced senescence (~10% of beta-gal positive cells) only in LPS853, which was increased ~3-fold by addition of RT. In contrast, no significant induction of senescence was observed in T778, T449 and SW872 (Figure 6.9 B and Figure 6.9 C). Treatment-driven expression of p16 levels was determined by western blot (Figure 6.9 F) which is one of the markers for senescence. P16 levels were observed at the basal level (untreated) and remained unchanged in response to the treatments in LPS853, T778 and T449. In SW872, p16 was not detected by western blot.

In summary, all the liposarcoma cell lines with wild-type *TP53* displayed an enhanced G2 arrest irrespective of their radiosensitivity to Nutlin-3. Apoptosis remained unperturbed and an increased number of beta-galactosidase positive cells (in LPS853 and T778) was observed as a short term-effect following the combined treatment.

6.3.3 Combining Nutlin-3 with RT led to upregulation of the p53-p21 signaling axis and additive stabilization of p53 by Ser-15 phosphorylation

To further ascertain how the intracellular signaling was modulated in response to MDM2 inhibition and RT, liposarcoma cells were treated with 5µM Nutlin-3, a radiation dose of 4 Gy and a combination of both for 48h. Cells were harvested and lysates were prepared. Following that, western blot analysis of p53, MDM2, p21 (Figure 6.10) were carried out. As expected, p53, MDM2 and p21 were upregulated in response to Nutlin-3 treatment in all the liposarcoma cell lines (with *MDM2* ^{Amp}/*TP53* ^{WT}) and the addition of ionizing radiation further enhanced the p53 and downstream p21 protein expression. In contrast, in the cell line SW872 (with *TP53* mutation), no induction of MDM2 by the autoregulatory feedback loop and no downstream p21 expression were detected due to its non-functional p53.

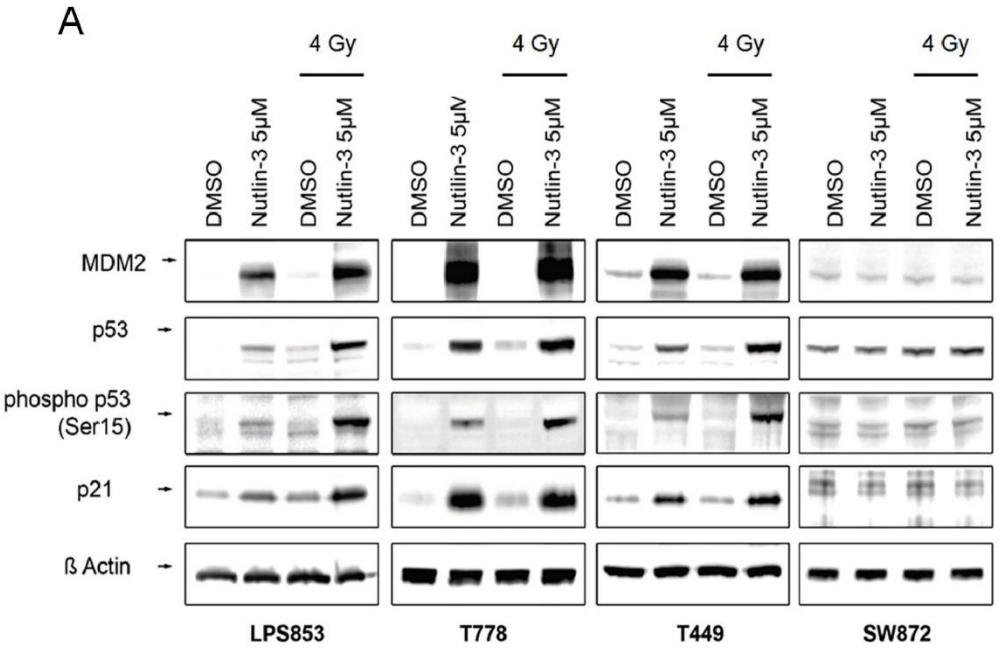

Figure 6.10: **Modulation of intracellular signaling of the p53-MDM2-p21 axis by the treatment with MDM2 inhibitor and RT in liposarcoma cells.** Liposarcoma cells with wild-type *TP53* (LPS853,

T778 and T449) and with mutant *TP53* (SW872) were seeded and treated. Cells were harvested following 48h of treatment. **(A)** Immunoblot studies showing effects of Nutlin-3 (5µM) alone, ionizing radiation of 4 Gy or a combination of both on expression of MDM2, p53, phospho-p53 (Ser-15), p21 in LPS cells 48h post-treatment. Beta-actin was taken as a loading control.

The status of phospho-p53 (Ser-15) in response to Nutlin-3 and RT was assessed as p53-mediated downstream effects are determined by how it is stabilized or post-translationally modified by phosphorylation [195]. Interestingly, enhanced phospho-p53 (Ser-15) levels in the combination treatment groups in all the cell lines with wild-type *TP53* were detected which further indicated toward cytostasis [196].

In summary, this data displayed an additive activation of the MDM2-p53-p21 axis in response to the combination treatment in all the liposarcoma cells lines with wild-type *TP53* confirming the enhanced reactivation of functional p53.

6.3.4 MDM2 inhibition and RT response was varied and not consistent for all DDLPS

LPS141 (with amplified *MDM2* / wild-type *TP53*) is another DDLP (Table 18) which did not develop into colonies when seeded as single cells. Thus, it was not considered for clonogenic assays. However, other assays were carried out in order to determine the therapy-driven fate. Apoptosis measurement (Figure 6.11 C) displayed an increased apoptosis (~5 fold) in Nutlin-3 treatment alone. Addition of RT (4 Gy) to Nutlin-3 significantly ($p \leq 0.05$) reduced the level of apoptosis (~2 fold). Total PARP (Figure 6.11 E) was significantly cleaved by Nutlin-3 (± RT) treatment. However, cleaved fragments were not detected due to degradation. Senescence assay (Figure 6.11 A and Figure 6.11 B) revealed higher but non-significant number of beta-galactosidase positive cells (~20 %) in combination treatment group than the monotherapies (5µM Nutlin-3; ~7 %, RT; ~9 %, $p \geq 0.5$). P16 basal expression was higher as evident form the untreated groups. Treatment with Nutlin-3 and the combination slightly reduced the levels (Figure 6.11 F). Immunoblotting of the MDM2-p53-p21 axis revealed an augmented induction of p53 with concomitant induction of MDM2 and p21 in the combined therapy-treated group. Phospho-p53 (Ser-15) was detected to be higher in response to the combination treatment. By cell cycle analysis (Figure 6.11 G), a G2 arrest (~46 %) was observed in response to Nutlin-3 alone group. Addition of RT did not significantly change the G2-arrested cells (G2 ~41 %). Apoptosis (by sub G1

population) levels were comparable among the treated groups (5μM Nutlin-3 ~6 %, RT ~4 %, Nutlin-3 plus RT ~5 %).

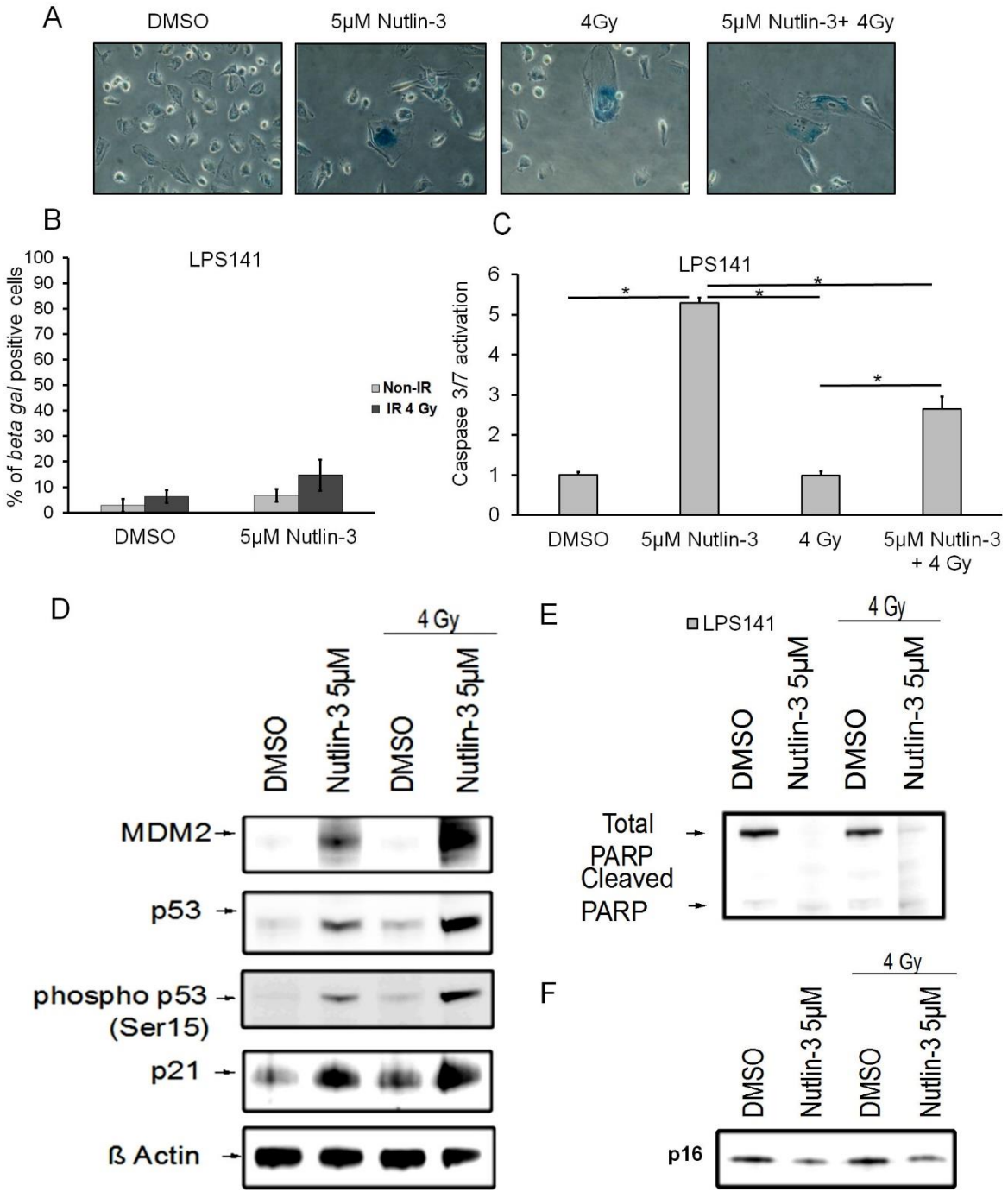

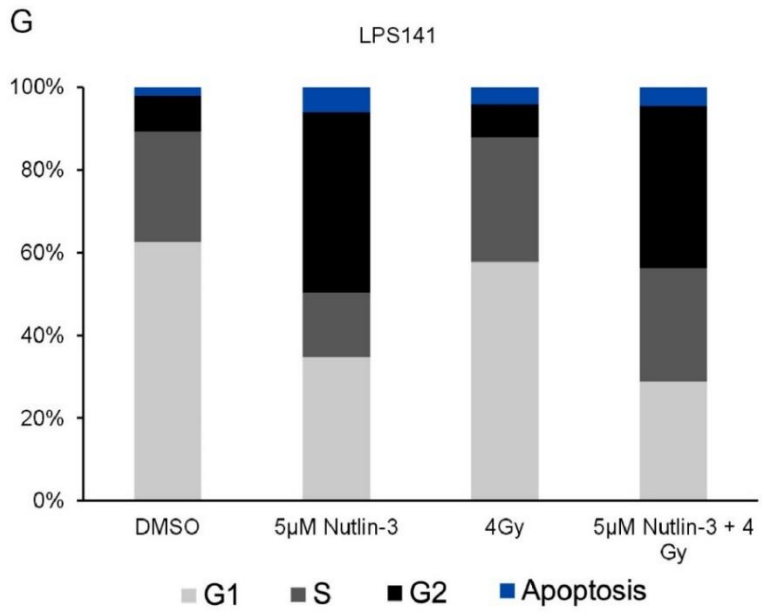

Figure 6.11: **Assessment of senescence, apoptosis, cell cycle and intracellular signaling in LPS141 (DDLP with *MDM2*^{Amp}/*TP53* ^{WT}).** **(A)** Bright field microscopy showing senescence-associated beta-galactosidase staining of liposarcoma cells with either DMSO, Nutlin-3, ionizing radiation or a combination of both **(B)** and corresponding bar graphs of quantified cells. Bar graphs represent quantification of an average of the percentage of beta-galactosidase positive cells, n = 5, error bars indicate SD. **(C)** Apoptotic response as measured by caspase 3/7 activation following treatment after 24h. Bar graphs represent averages (n = 3) normalized by the untreated group. Error bars indicate SD. **(D)** Immunoblot representing effects of Nutlin-3 alone or in combination with RT on the of MDM2, p53, phospho-p53 (Ser-15), p21 in LPS141 48h post-treatment. **(E)** Immunoblot of total and cleaved PARP. **(F)** Western blots images of p16. **(G)** Cell cycle analysis by PI (propidium iodide) stain. * p ≤ 0.05**.**

In summary, for DDLP (LPS141), the MDM2-p53-p21 signaling axis was modulated in the same pattern as of the other WD/DDLPS in this specific setting of treatment. However, Nutlin-3 displayed a dominant effect and addition of RT led to a diminished effect in terms of apoptosis and G2-arrest.

6.3.5 Nutlin-3 in combination with RT executed an activation of the MDM2-p53-p21 axis in other sarcoma with amplified *MDM2* and wild-type *TP53*

In order to determine the effect in other sarcoma with amplified *MDM2* and wild-type *TP53* status, GIST430 (gastrointestinal stromal tumors) and U2OS (osteosarcoma) cells were treated with ionizing radiation and MDM2 inhibitor for 48h and tested for the activation of the MDM2-p53-p21 signaling axis (Figure 6.12 A). An additive activation of MDM2, p53, phospho-p53 (Ser-15) and p21 were observed in response to combined treatment in both of the cell lines GIST430 and U2OS.

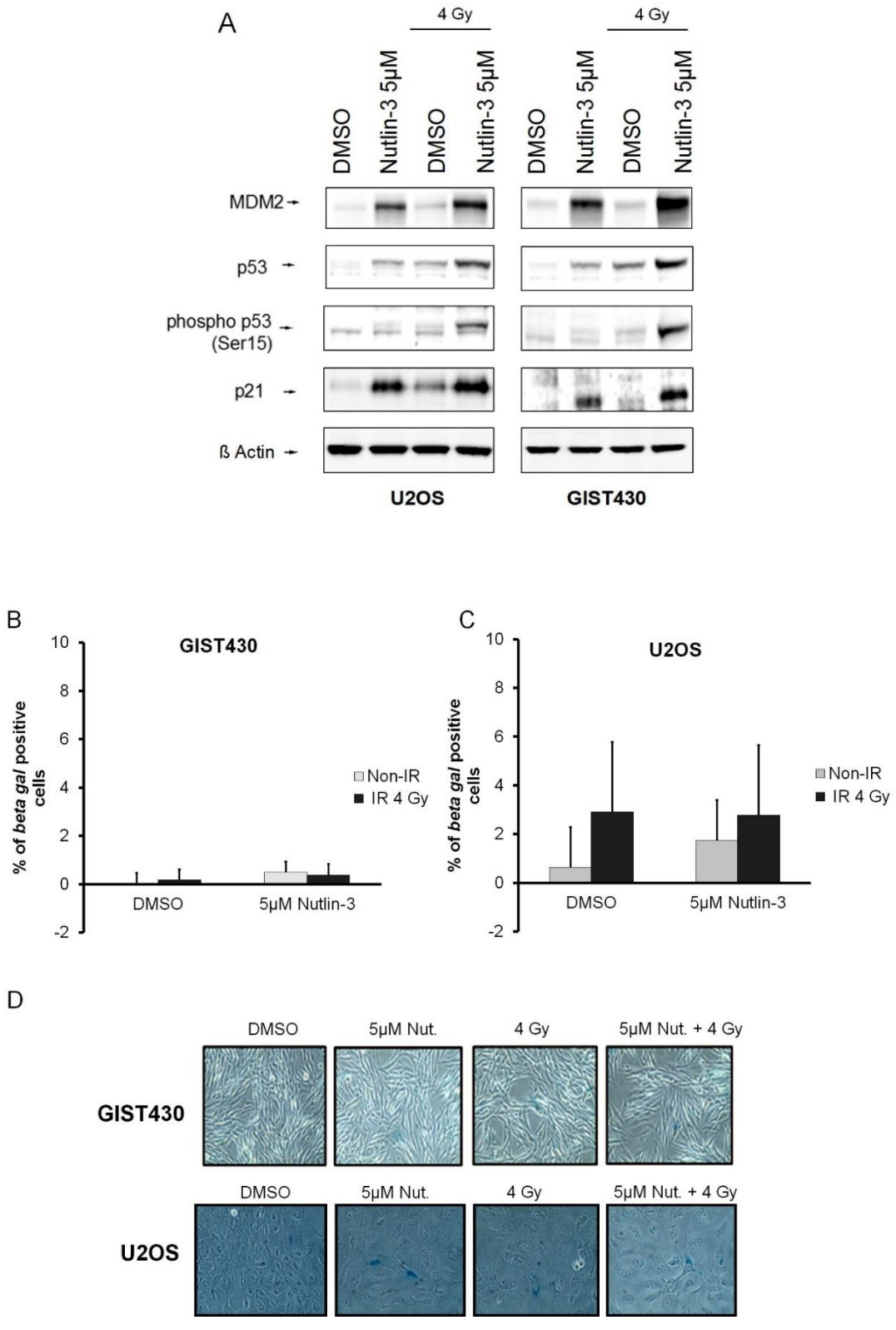

Figure 6.12: Assessment of senescence and intracellular signaling in other sarcoma with *MDM2*^{Amp} and *TP53*^{WT}. (A) Immunoblot representing effects of Nutlin-3 alone or in combination with ionizing radiation on the expression of MDM2, p53, phospho-p53 (Ser-15), p21 in other sarcoma (GIST430, U2OS) 48h post treatment. Beta-actin was taken as a loading control. Bar graphs indicate percentage of beta-galactosidase positive cells in response to treatments in **(B)** GIST430 and in **(C)** U2OS. Error bars indicate SD. **(D)** Corresponding bright field images of senescence assay.

For senescence measurement (Figure 6.12 B-D), beta-galactosidase staining was carried out following 48h of treatment in GIST430 and U2OS. Senescence induction was not observed in response to the treatment in GIST430 (5µM Nutlin-3 ~0.17 % ± 0.2, 4 Gy ~0.5 % ± 0.45, 4 Gy + 5µM Nutlin-3~ 0.4 % ± 0.44) and minimal in U2OS (DMSO ~0.63 % ± 0.87, 5µM Nutlin-3 ~2.91 ± 2.81, 4 Gy ~1.7 % ± 1.65, 4 Gy + 5µM Nutlin-3 ~2.8 % ± 2.8).

In summary, these data implied that activation of the p53-MDM2-p21 axis was not the exclusive pathway to determine the cellular phenotypic fate by the treatment with Nutlin-3 and RT. Other genetic lesions might govern the ultimate fate and treatment response in the setting of MDM2 inhibition and RT.

6.3.6 Determination of reversibility of cell cycle arrest by washout kinetics after treatment with Nutlin-3, RT and Nutlin-3 plus RT

In order to assess the reversibility of the growth inhibitory effect exerted by the combination of MDM2i and RT, washout experiments were conducted by treating the cells for 96h with Nutlin-3, RT and RT plus Nutlin-3 and drug-containing medium was replaced with fresh medium for another 96h. Following this schedule, resumption of proliferation was assessed by MTT assay (Figure 6.13).

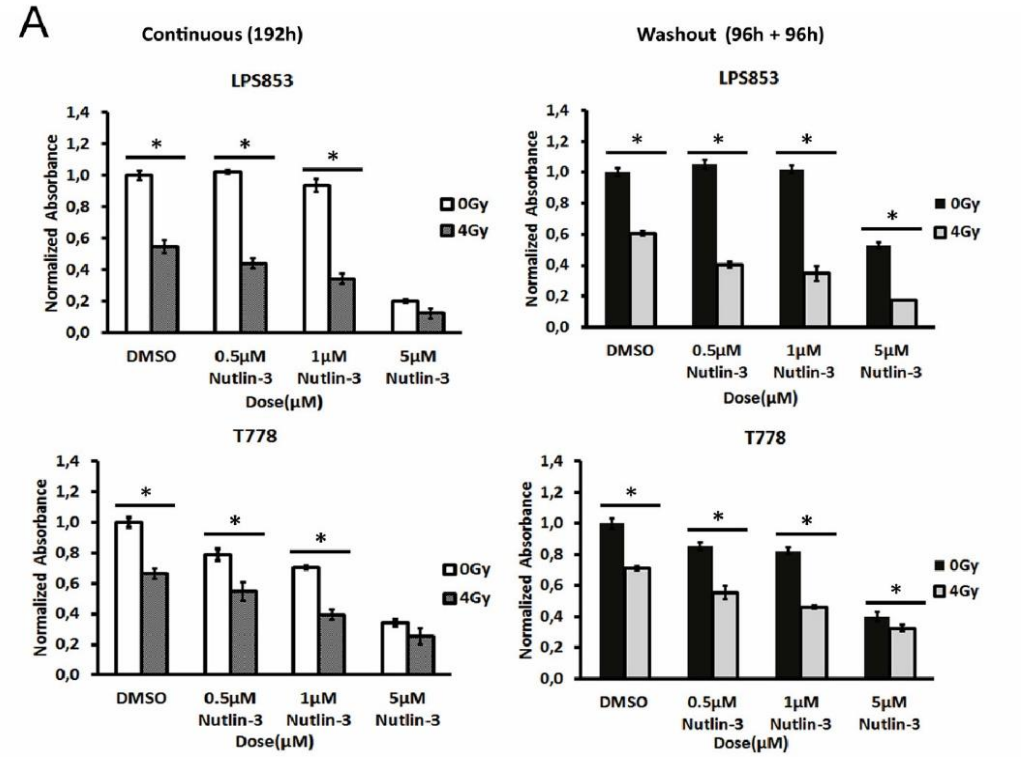

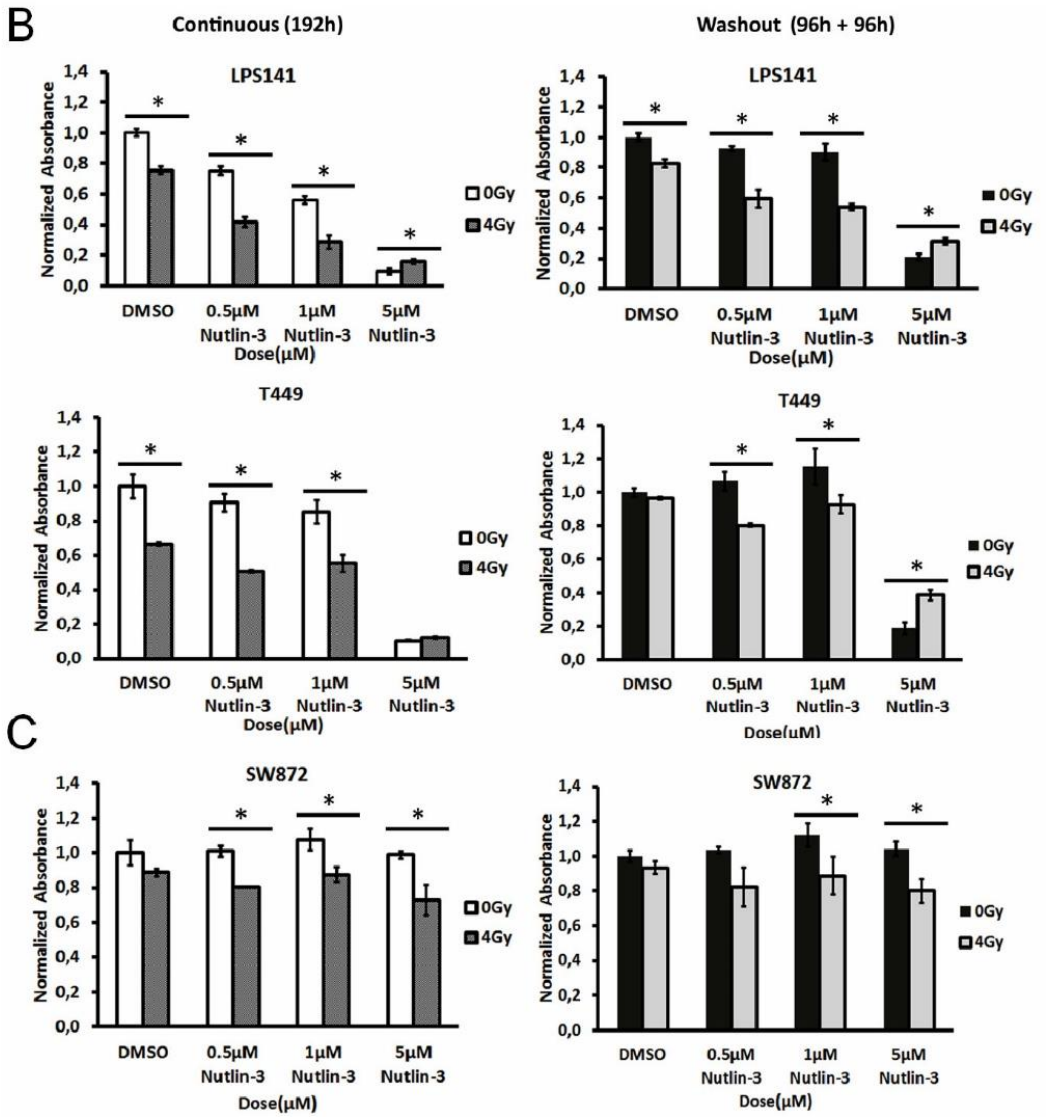

Figure 6.13: **Assessment of short-term washout kinetics of liposarcoma cell following treatment removal.** Bar graphs represent normalized absorbance of the liposarcoma cells **(A)** LPS853, T778 **(B)** LPS141, T449 and **(C)** SW872 in response to increasing doses (0.5µM, 1µM, 5µM) of Nutlin-3, RT (4Gy) and Nutlin-3 plus RT treated either for 192h (continuous treatment) or treated for 96h followed by 96h in drug-free medium (washout studies). * $p \leq 0.05$.

In cell lines (LPS853, T778) with wild-type *TP53*, growth inhibitory effect was enhanced with increasing doses (0.5µM, 1µM and 5µM) of Nutlin-3 plus RT (4 Gy) with continuous treatment for 192h. For LPS853 and T778, the growth inhibition effects in response to 5µM Nutlin-3, RT (4Gy) and 5µM Nutlin-3 plus RT are 80 %, 55 %, 90 % and 70 %, 30 %, 80 %, respectively. The effect or trend was persistent in washout studies. However, reversibility was observed to a lesser extent when the drug-containing medium was withdrawn in each treatment groups (Figure 6.13).

In the other two cell lines with wild-type *TP53* (T449 and LPS141), for continuous treatment of Nutlin-3 alone, a dose-dependent growth inhibition was observed. However, the addition of RT did not exert an additive effect at the dose of 5μM of Nutlin-3. Increased cell viability was observed upon removal of drug-containing medium following the same trend as with the continuous treatment. Increased cell viability denoted resumption of cellular proliferation. In addition, this data also indicated that the increased senescence phenotype following treatment with combination treatment in LPS141, which was evident in earlier experiments (Figure 6.11 A-B) was a senescence-like phenotype (SLP) than an irreversible arrest which retained proliferative potential.

In *TP53* mutated cell line (SW872), the growth inhibitory effect was less (10 % - 30 %) in the treatment groups. In contrast to the *TP53* wild-type cells, with increasing doses of Nutlin-3 and 4Gy of RT, no increase in the growth inhibitory effect was observed in SW872.

In summary, these set of experiments indicated toward the existence of heterogeneous populations of cells after each of the treatment that had the potential to revert back to proliferation to a certain extent as a short-term effect.

6.3.7 Generation of G1 tetraploid (4N) cells by Nutlin-3 (± RT) and emergence of >4N cells by treatment withdrawal

Cell cycle distribution analysis by PI stain displayed augmented G2/M arrest (by 4N DNA content) following 48h of treatment with Nutlin-3 plus RT compared to the respective monotherapies (RT, Nutlin-3) in LPS853 (G2/M with 4N DNA content; 75.7 % in Nutlin-3 plus RT, 39.8 % in Nutlin-3, 32.1 % in RT alone, 8.1 % in vehicle control) and T778 (G2/M with 4N DNA content 57.3 % in Nutlin-3 plus RT, 45.3 % in Nutlin-3, 32.9 % in RT alone, 16.6 % in vehicle control). In contrast, cell cycle distribution (G2/M with 4N DNA content 26.8 % in Nutlin-3 plus RT, 21.6 % in Nutlin-3, 26.1 % in RT alone, 21.7 % in vehicle control) was unperturbed in SW872 (Figure 6.14 A-C).

In parallel, for analyzing the changes of the cellular progression markers, immunoblotting was carried out following 48h of treatment. Cyclin B, cyclin A and phospho-histone H3 ser-10 levels were reduced in response to Nutlin-3 and combination treatment in LPS853, T778 and T449. Cyclin D1 was induced in Nutlin-3

and combined therapy treated groups in LPS853 and T778. However, for T449, the basal level of cyclin D1 was detected to be higher in the untreated group compared to the other cell lines and remained unchanged following treatment. Rb and phospho-Rb (Ser-780) levels were reduced in response to the treatments in LPS853, T778 and T449. For LPS141, the cell cycle proteins were modulated in the same way as T449. For SW872, all the progression markers were uniformly expressed and unperturbed following treatment (Figure 6.14 D).

In contrast to the cell cycle distribution measurement by DNA content which indicated toward an enhanced G2/M (by 4N DNA) arrest, immunoblotting of the cell cycle progression markers (Figure 6.14 B) in LPS853 and T778 after 48h displayed an upregulation of G1 (cyclin D1) marker and downregulation of the G2/M markers (Cyclin A, cyclin B, phospho-histone H3 Ser-10) in Nutlin-3 treated alone and in combination with RT treated cells. This indicated toward generation of G1 tetraploid (4N G1) cells. Furthermore, when the drug-containing medium was removed after 48h of treatment and replaced by drug-free medium for 24h and 48h, cell cycle distribution measurement revealed cells with >4N content population in all the treatment groups of LPS853 (After 24h, 5µM Nutlin-3 >4N 23.6 %, 4 Gy RT >4N 12.1 %, Nutlin-3 plus RT > 4N 46.6 % and after 48h vehicle treated >4N 2.8 %, 5µM Nutlin-3 >4N 12.4 %, 4 Gy RT >4N 12.8 %, Nutlin-3 plus RT 42.2 %).

For T778, following the drug removal, the distribution changed after 24h (5µM Nutlin-3 >4N 4.9 %, 4 Gy RT >4N 8.1 %, Nutlin-3 plus RT > 4N 5.1 %) and after 48h (vehicle treated >4N 6.2 %, 5µM Nutlin-5 >4N 17.6 %, 4 Gy RT >4N 9.5 %, Nutlin-3 plus RT 25.9 %). The visibility or accumulation of >4N cells was more after 48h than 24h as captured by PI staining in T778 was due to relatively slower growth or longer doubling time of T778 than LPS853.

A lower percentage of >4N population was detected in the untreated LPS853 (DMSO or vehicle treated >4N 4.4 %) and T778 (DMSO or vehicle treated 5.1%). This finding was indicative of pre-existing set of dividing tetraploid cells.

In contrast, with SW872, the percentage of >4N population remained unchanged (DMSO or vehicle treated >4N 5.7 %, 5µM Nutlin-3 >4N 5.6 %, 4 Gy RT >4N 4 %, Nutlin-3 plus RT > 4N) by the treatment groups after 24h washout studies (Figure 6.14).

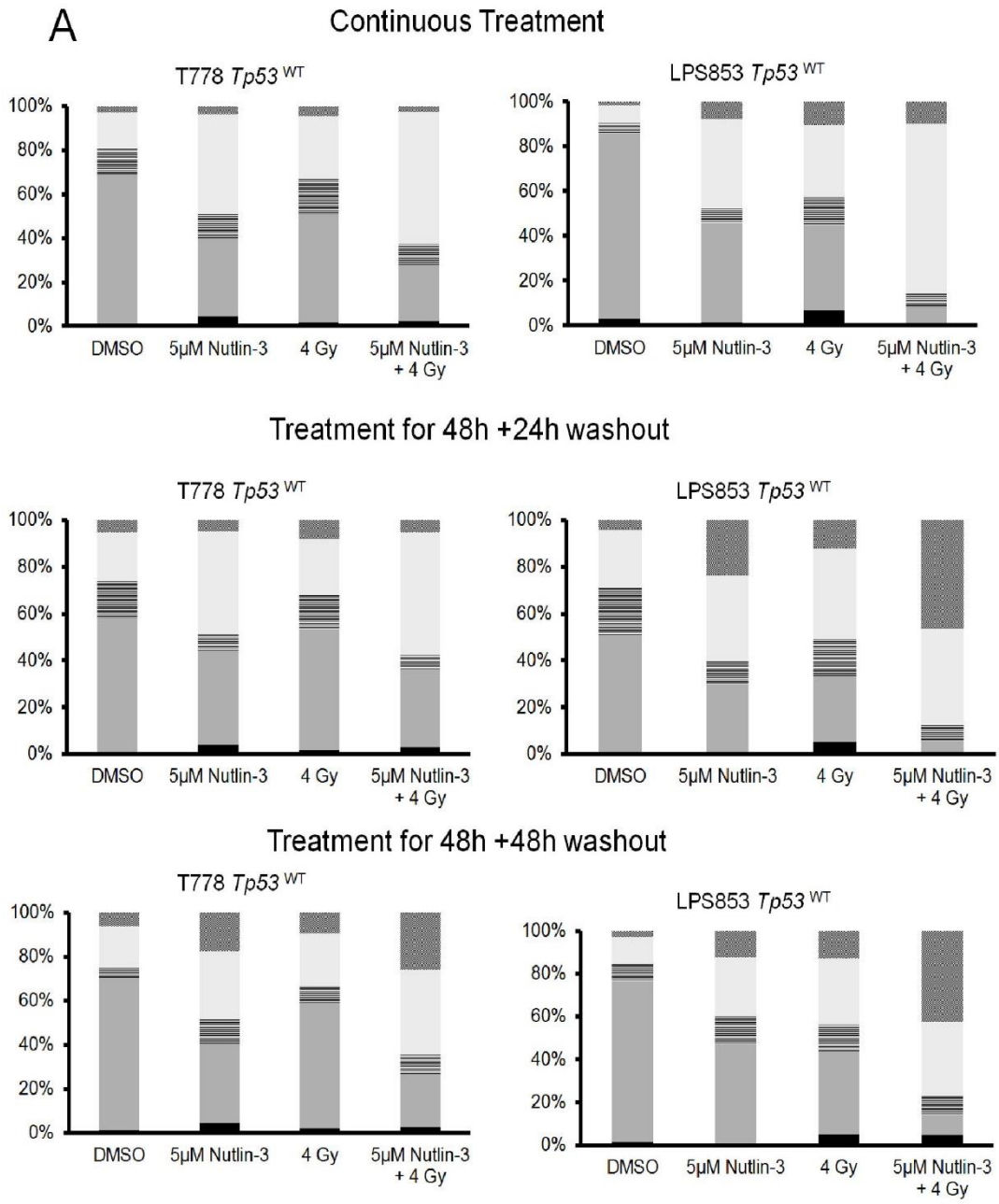
A
Continuous Treatment
T778 Tp53 WT
LPS853 Tp53 WT
100%
80%
60%
40%
20%
0%
DMSO
5μM Nutlin-3
4 Gy
5μM Nutlin-3 + 4 Gy
Treatment for 48h +24h washout
T778 Tp53 WT
LPS853 Tp53 WT
Treatment for 48h +48h washout
T778 Tp53 WT
LPS853 Tp53 WT

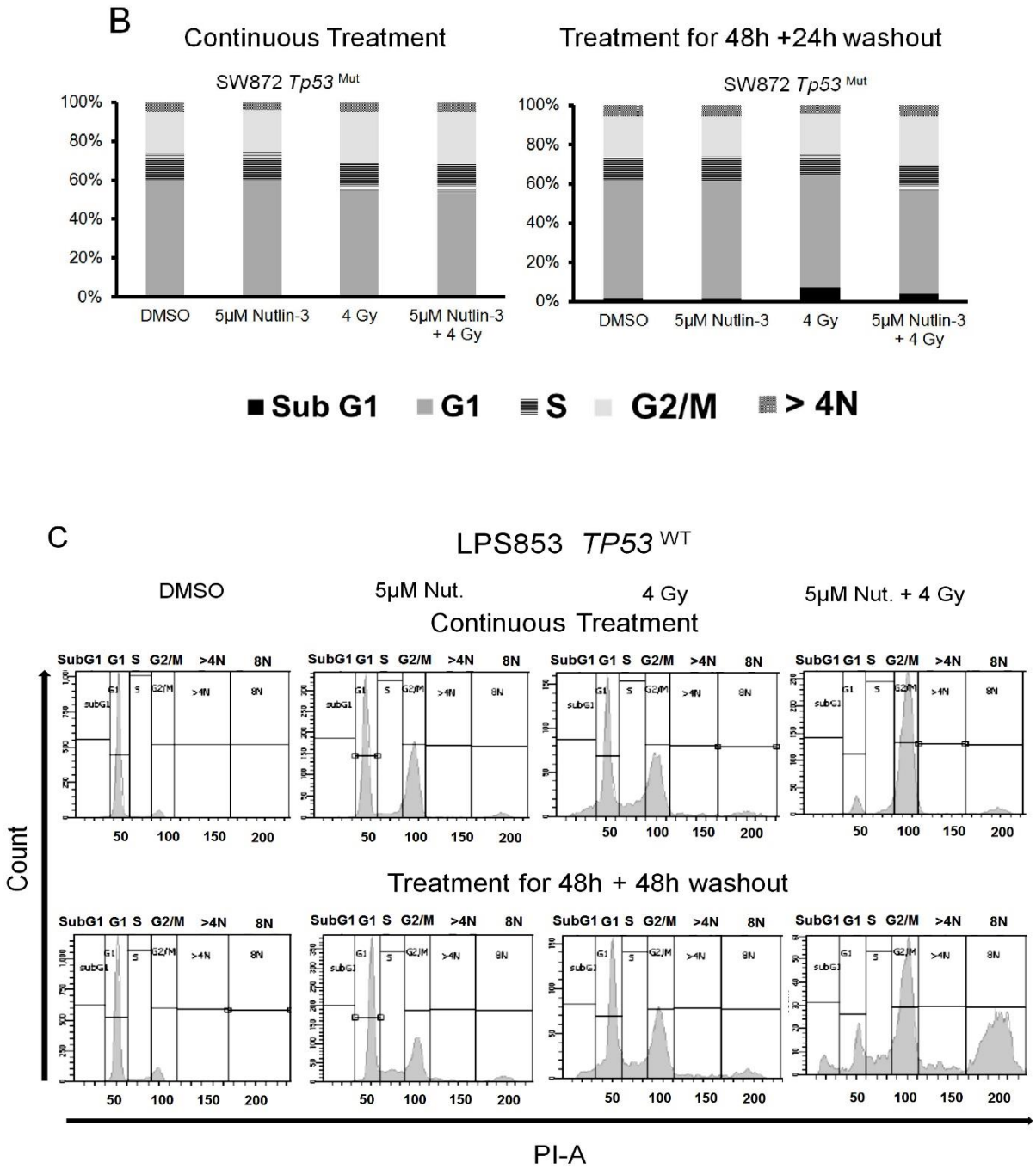
B
Continuous Treatment
Treatment for 48h +24h washout
SW872 Tp53 Mut
SW872 Tp53 Mut
100%
80%
60%
40%
20%
0%
DMSO
5μM Nutlin-3
4 Gy
5μM Nutlin-3 + 4 Gy
Sub G1
G1
S
G2/M
> 4N
C
LPS853 TP53 WT
DMSO
5μM Nut.
4 Gy
5μM Nut. + 4 Gy
Continuous Treatment
Treatment for 48h + 48h washout
SubG1 G1 S G2/M >4N 8N
Count
PI-A

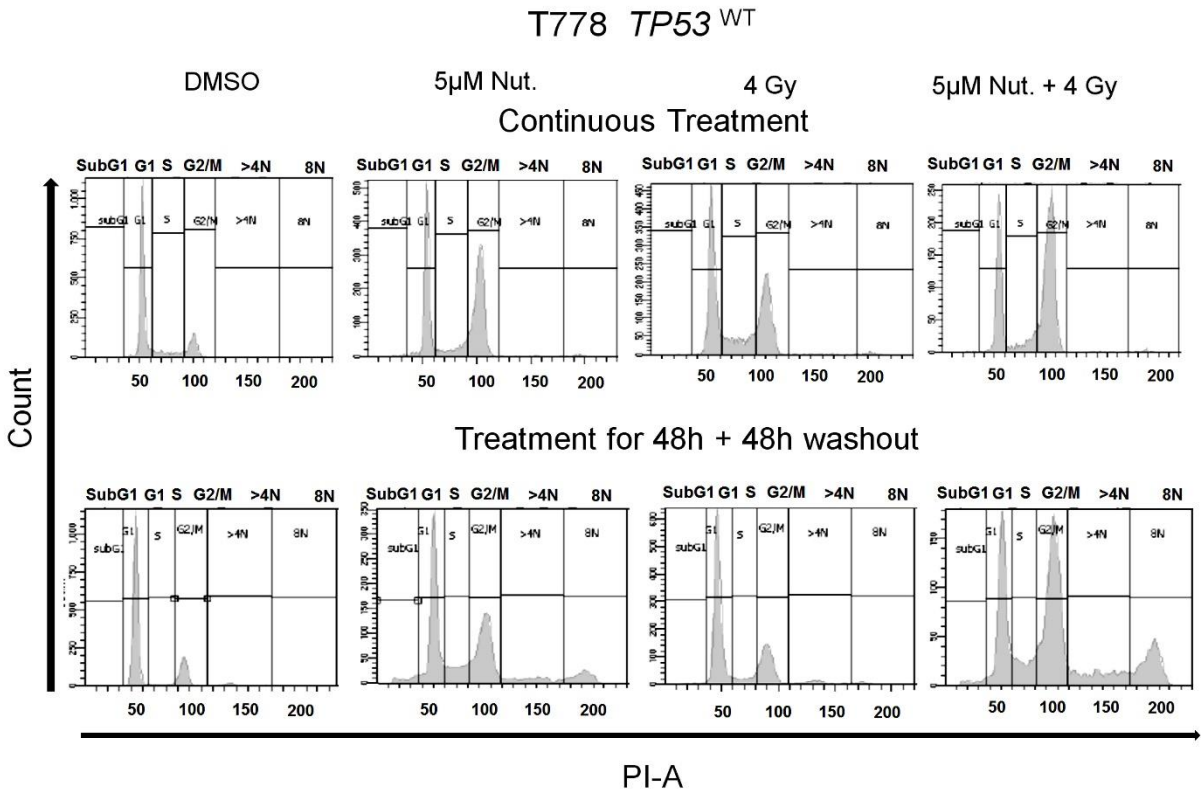
T778 TP53 WT
DMSO
5μM Nut.
4 Gy
5μM Nut. + 4 Gy
Continuous Treatment
Treatment for 48h + 48h washout
SubG1 G1 S G2/M >4N 8N
Count
PI-A

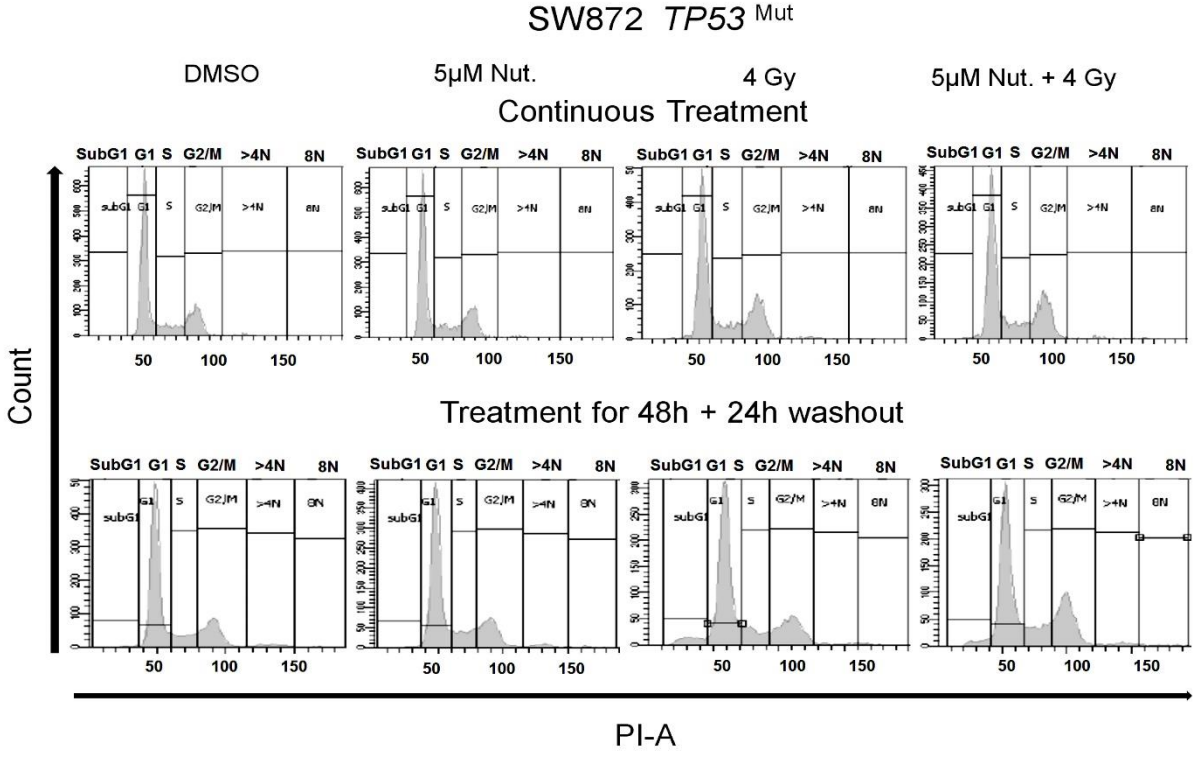
SW872 TP53 Mut
DMSO
5μM Nut.
4 Gy
5μM Nut. + 4 Gy
Continuous Treatment
Treatment for 48h + 24h washout
SubG1 G1 S G2/M >4N 8N
Count
PI-A

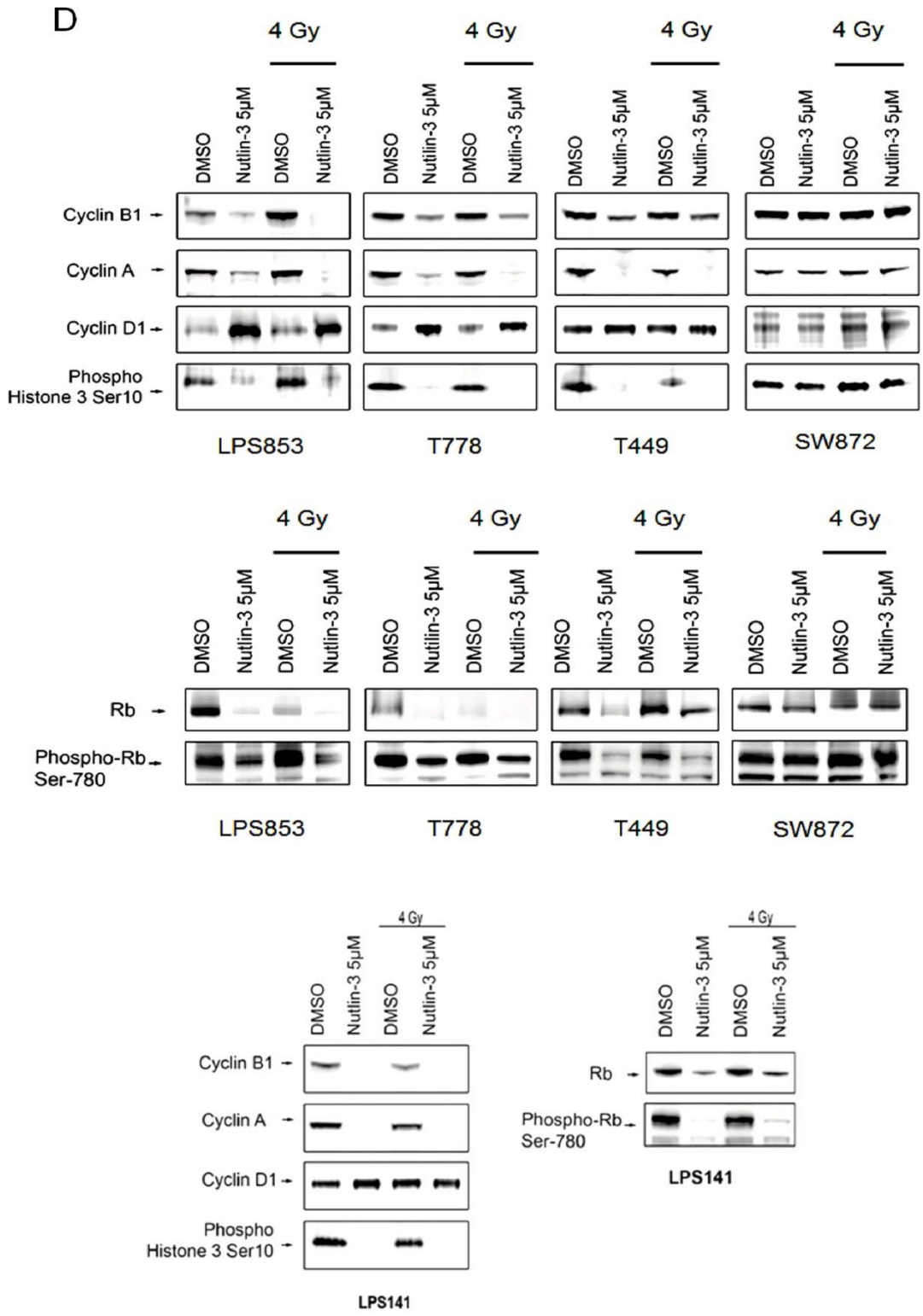

Figure 6.14: **Emergence of polyploid subpopulation in response to Nutlin-3 (± RT) in liposarcoma cells. (A)** Cell cycle distribution measurement by PI stain after continuous treatment of 48h, following 24h and 48h washout in LPS853 and T778. **(B)** For SW872 cell cycle distributions were measured at 48h with 24h washout. **(C)** Corresponding histograms representing the DNA content based populations.

(D) Western blot measurement of Cyclin B1, Cyclin A and Cyclin D1, phospho-histone H3 Ser-10, Rb, phospho-Rb (Ser-780) in all the cell lines after 48h of treatment. Beta-actin (refer to Figure 6.10) was used as a loading control.

In summary, this data suggested treatment with Nutlin-3 (± RT) led to generation of enhanced 4N G1 population and treatment withdrawal led to emergence of >4N population. This response was dependent on the *TP53* status of the liposarcoma cell lines.

6.3.8 Assessment of therapy-driven cell cycle progression markers in other sarcoma with amplified *MDM2* and wild-type *TP53*

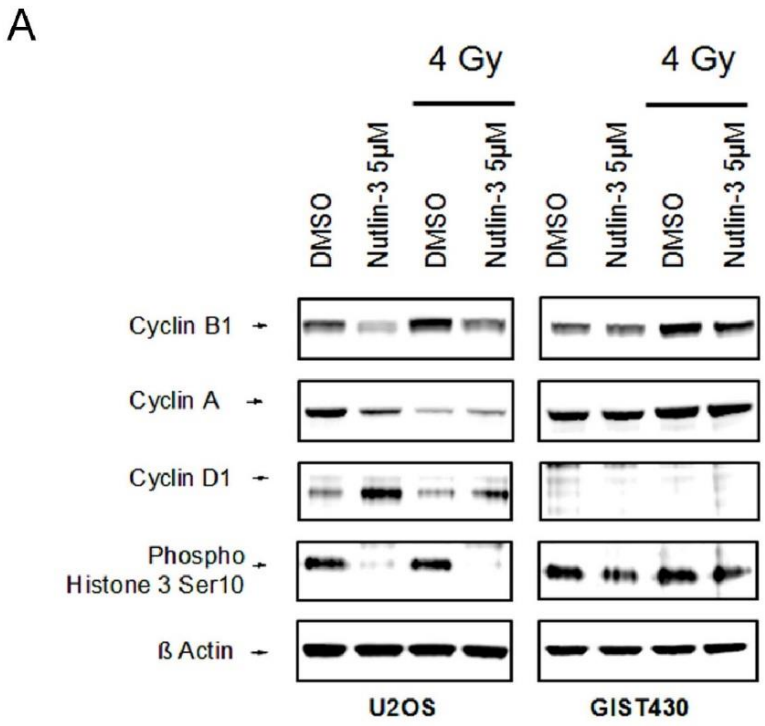

Figure 6.15: **Treatment-driven modulation of cell cycle progression markers in other sarcoma with amplified *MDM2* and wild-type *TP53***. GIST430 and U2OS cells were plated and treated with Nutlin-3, RT (4 Gy) and combination of both for 48h. Cells were harvested and lysates were prepared for immunoblotting. **(A)** Immunoblots representing Cyclin B1, Cyclin A and Cyclin D1, phospho-histone H3 Ser-10 in GIST430 and U2OS cell lines after**.** Beta-actin was used as a loading control**.**

For U2OS and GIST430, cell cycle proteins were differently regulated (Figure 6.15) in response to the treatment. For U2OS, cyclin D1 displayed a shift in response to treatment with Nutlin-3 and combination treatment while GIST430 lacked cyclin D1 expression. Cyclin A was unperturbed in case of GIST430 while U2OS displayed reduced expression in response to the treatment with 4Gy and combination treatment. Cyclin B1 was induced in response to RT and combination treatment and phospho-

histone H3 Ser-10 was unchanged by treatment in GIST430. U2OS displayed shift in expression of cyclin B1 and phospho-histone H3 Ser-10 in response to Nutlin-3 and combination treatment.

In summary, these results demonstrated the variance in the cell cycle proteins upon treatment with MDM2 inhibition, RT and combined treatment. Despite the activation of the MDM2-p53-p21 axis, the varied expression (intrinsic or treatment-driven) of the cell cycle proteins might play role in determining different cellular fates.

6.3.9 Evaluation of the senescence-inducing potential of the multiple subpopulation fractions with various DNA content in response to the treatment with MDM2 antagonist and RT

An induction of enhanced senescence or senescence-like phenotype (SLP) in LPS853 cells was detected after 48h of treatment with Nutlin-3 and RT (Figure 6.9 B). In order to elucidate the contributing population in senescence induction at 48h, LPS853 cells were stained by Hoechst 33342. Subsequently, different populations of 2N and 4N were sorted for different treatment groups (Figure 6.16 A Scheme 1). Following that, senescence was measured by beta-galactosidase staining in diverse populations isolated (Figure 6.16 C). Quantification of beta-galactosidase positive cells displayed enhanced level of senescence induction in both 2N (44 % ± 2.9 in Nutlin-3 alone, 46.7 % ± 4.2 in Nutlin-3 plus RT) and 4N (56.75 % ± 4.2 in Nutlin-3 alone, 55.24 % ± 4.3 in Nutlin-3 plus RT) populations in Nutlin-3 and combination treatment groups as compared to non-treated (2N 2.15 % ±1.28, 4N 5.90 % ± 1.09) or RT alone (2N 16.3 % ± 3.9, 4N 14.09 % ± 10.25) treatment groups.

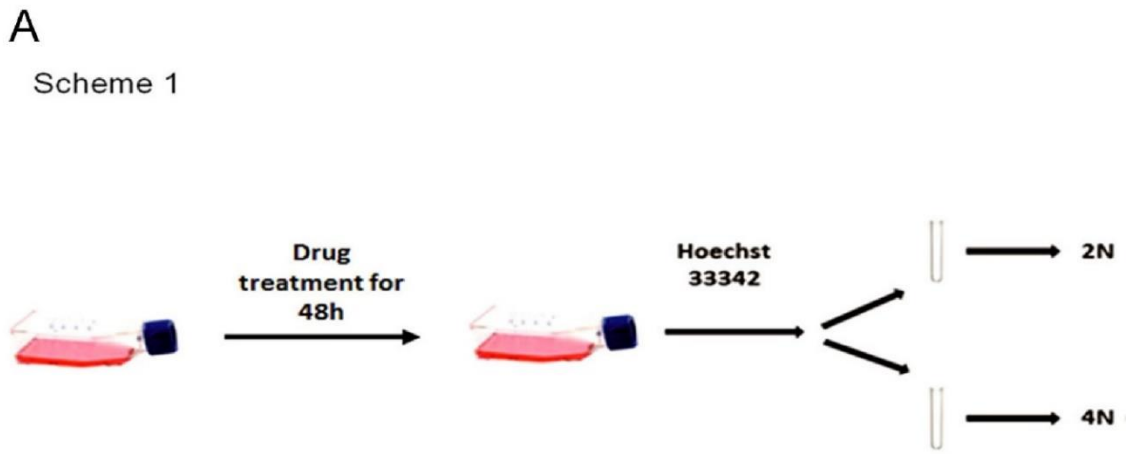

B

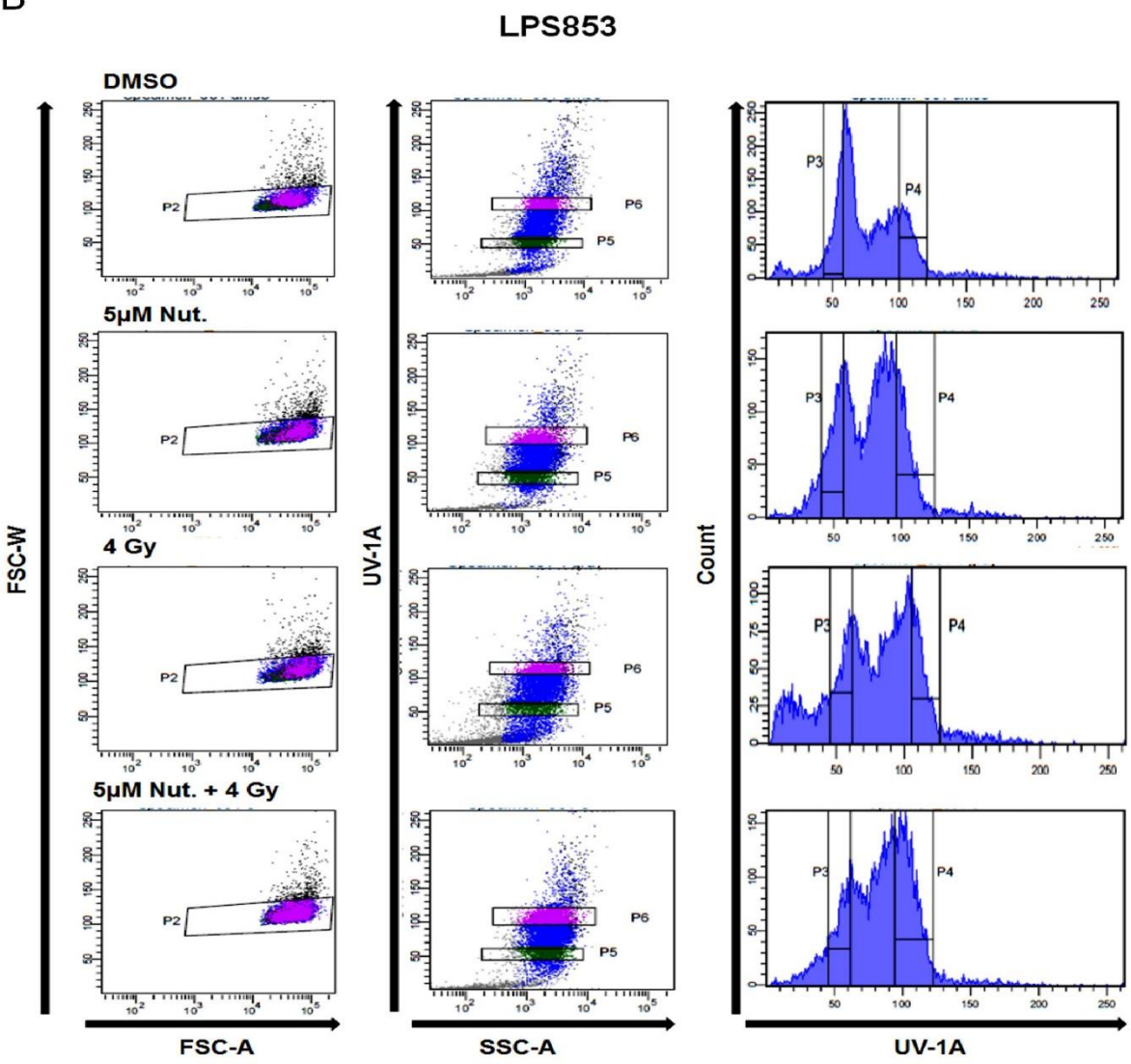
LPS853
DMSO
5μM Nut.
4 Gy
5μM Nut. + 4 Gy
FSC-W
FSC-A
UV-1A
SSC-A
Count
UV-1A
P2
P3
P4
P5
P6

C

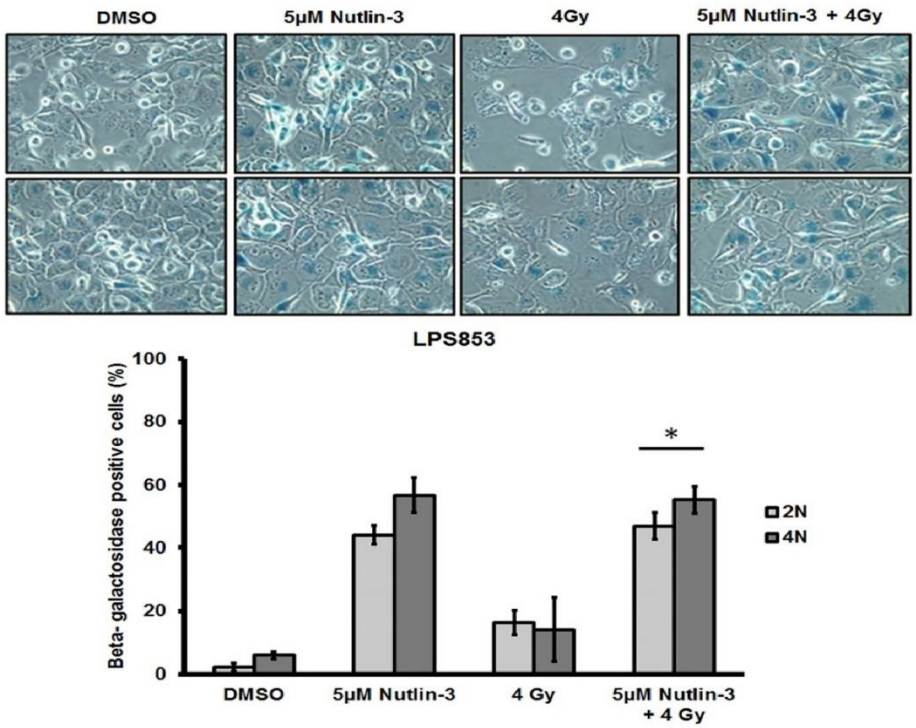
DMSO
5μM Nutlin-3
4Gy
5μM Nutlin-3 + 4Gy
LPS853
Beta- galactosidase positive cells (%)
100
80
60
40
20
0
*
2N
4N
DMSO
5μM Nutlin-3
4 Gy
5μM Nutlin-3
+ 4 Gy

Figure 6.16: **Measurement of senescence in treatment-generated diploid and polyploid fractions after short-term (48h). (A)** Scheme representing treatment and time point for sorting. **(B)** Histograms representing sorting of live Hoechst 33342 stained cells based on DNA content (2N and 4N populations) after 48h in vehicle treated, 5μM Nutlin-3, 4 Gy or 5μM Nutlin-3 plus 4Gy in LPS853. **(C)** Beta-galactosidase staining images and bar graphs (average of percentage of beta-galactosidase positive cells, n = 5, error bars indicate SD) of sorted 2N and 4N populations after 48h in vehicle treated, 5μM Nutlin-3, 4 Gy and 5μM Nutlin-3 plus 4Gy. * $p \leq 0.05$.

This confirmed a dominating effect of Nutlin-3 in senescence induction. The difference in the capacity of senescence in 2N population of Nutlin-3 versus 2N population of Nutlin-3 plus RT was not significant ($p \geq 0.3$). Similar trend was observed with 4N population ($p \geq 0.8$ in Nutlin-3 *vs* Nutlin-3 plus RT) when statistically analyzed.

However, the extent of senescence induction in 2N and 4N populations within the Nutlin-3 plus RT was significantly varied ($p \leq 0.04$) while in Nutlin-3 alone treatment, the difference was non-significant ($p \geq 0.07$).

In summary, this data suggested that 4N population displayed higher senescence-inducing potential than the 2N population in Nutlin-3 (± RT). As the cell cycle data (of the entire population) displayed 4N (G2/M) population to be the major one (77.6%) in response to the combination treatment after 48h (Figure 6.9 D), it could be stated that relative majority and enhanced senescence-inducing potential of the 4N population contributed to the observed enhanced senescence or senescence-like phenotype (SLP) post combined treatment.

6.3.10 Attenuated clone-forming potential of the treatment-induced tetraploid cells and polyploid cells in LPS853

To further confirm the effect of Nutlin-3 and RT, the sorted 2N and 4N populations (sorted according to Figure 6.16 A scheme 1) were seeded as single cells and allowed for the colony growth. Following 12-14 days of growth, colonies were stained and counted. The intrinsic ability of clonogenic growth of 2N population was observed to be higher (Figure 6.17 A) than respective 4N population in all the treatment groups (5μM Nutlin-3 $p < 0.05$ and 5μM Nutlin-3 plus RT $p < 0.05$) except in RT alone group ($p = 0.22$). The 2N cells of vehicle treated and Nutlin-3 treated have enhanced proliferative potential or clonogenicity than the RT alone and Nutlin-3 plus RT treatment groups. The clonogenic growth of 4N population was highest in vehicle treated

(average 19.5 % ± 0.48), low in Nutlin-3 treated (average 3 % ± 0.42), in RT exposed (average 1.6 % ± 1.64) and combination treatment (average 0.6 % ± 0.69). However, no significant difference was observed among the clone forming ability of the 4N cells generated by any of the treatments.

A

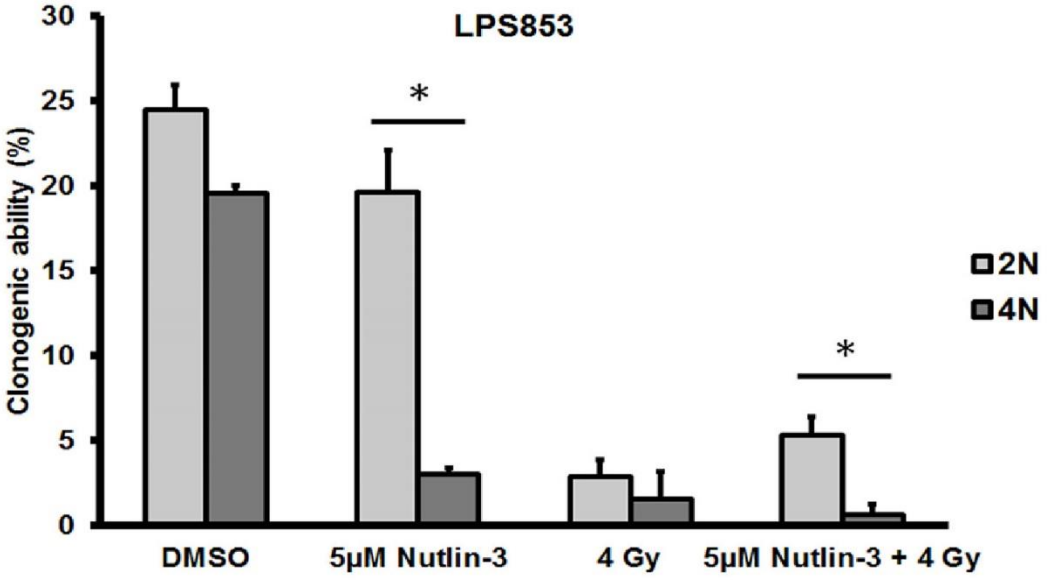

B

Scheme 2

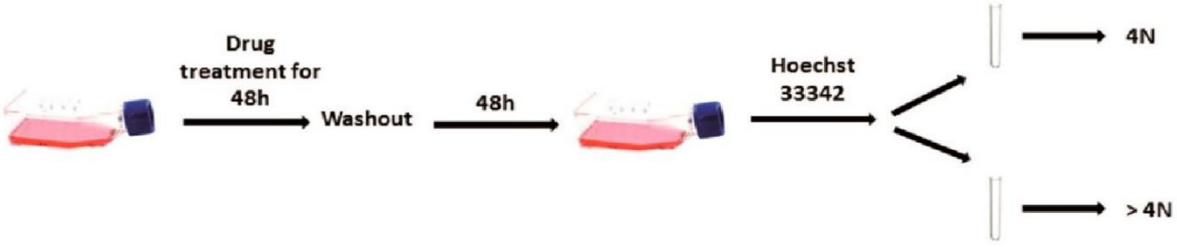

C

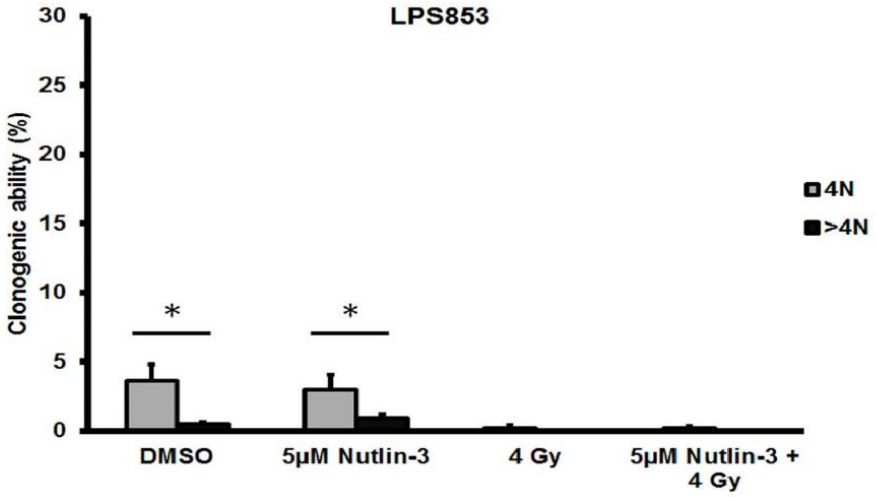
LPS853
Clonogenic ability (%)
30
25
20
15
10
5
0
*
*
4N
>4N
DMSO
5μM Nutlin-3
4 Gy
5μM Nutlin-3 + 4 Gy

D

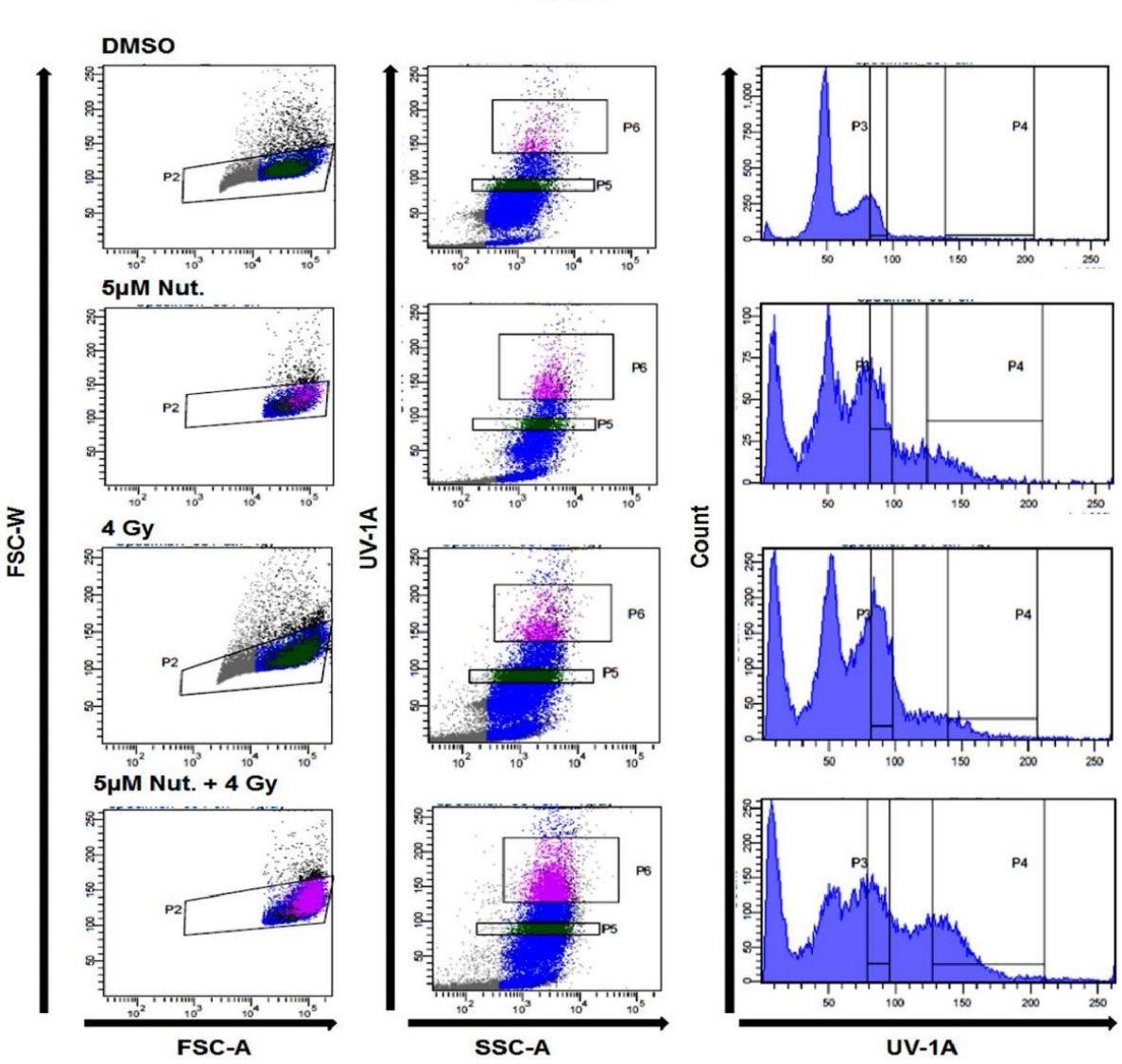
LPS853
DMSO
5μM Nut.
4 Gy
5μM Nut. + 4 Gy
FSC-W
FSC-A
UV-1A
SSC-A
Count
UV-1A
P2
P3
P4
P5
P6

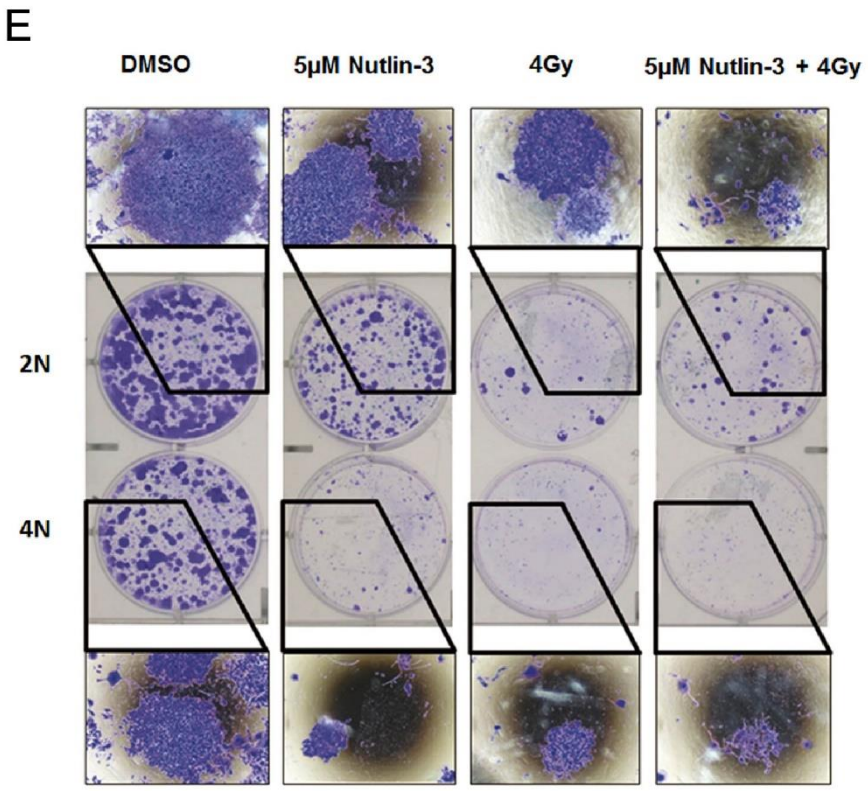

Figure 6.17: **Measurement of long-term fate of diverse ploidy based subpopulations by colony assay.** LPS853 cells were plated and treated with DMSO, 5μM Nutlin-3, 4 Gy and 5μM Nutlin-3 plus 4Gy for 48h and following that kept for 48h in drug-free medium. Cells were stained with Hoechst 33342 and different populations were sorted. 2N and 4N populations were sorted (**Figure** 6.16 A scheme 1) after 48h of treatment while 4N and >4N are sorted (Figure 6.17 B scheme 2) following 48h of drug removal. **(A)** Colony assay presented as bar graphs (percentage of cells developed into a colony following therapy withdrawal among the cells seeded, n = 2, error bars represent SD) for sorted 2N and 4N populations in each of the treatment groups in LPS853. **(B)** Scheme representing the treatment, washout and sorting for 4N and >4N populations in different treatment groups. **(C)** Colony assay presented as bar graphs (percentage of cells developed into a colony following therapy withdrawal among the cells seeded, n = 3, error bars represent SD) for sorted 4N and >4N populations in each of the treatment groups in LPS853. **(D)** Histogram representing sorting of live Hoechst 33342 stained cells based on DNA content (4N and >4N populations). **(E)** Microscopic images from colony assay following stain with crystal violet of 2N and 4N subpopulations. * $p \leq 0.05$.

The comparison of clonogenic potential of 4N and >4N populations (sorted according to the Figure 6.17 B scheme 2) showed higher ability of the 4N than the >4N in vehicle treated (4N 3.7 % ± 1.1, >4N 0.3 % ± 0.2, $p \leq 0.05$) and Nutlin-3 (4N 3 % ± 1, >4N 0.6 % ± 0.3, $p \leq 0.05$) treated. There was no visible significant difference between the clonogenic ability of 4N and >4N populations generated by RT alone and combination treatment. The overall potential of the >4N cells were significantly low (vehicle treated and Nutlin-3 treated) or almost undetectable (RT, Nutlin-3 plus RT) as measured by colony assay.

In summary, by short-term anti-proliferative or cell viability assays like MTT or caspase 3/7, it was difficult to predict the long-term therapy effects especially if the death mode was not mediated exclusively by apoptosis. Thus, it was conceivable that as the majority of the cells were distributed to 4N and >4N stage post combination treatment, they were the contributing population in exerting the radio-sensitization effect in LPS853 by their attenuated clone forming ability.

6.3.11 Morphologically variant cellular phenotype and shift in population dynamics in response to the treatments in liposarcoma cell lines

Tetraploidy/polyploidy generation has different modes: endo-reduplication [197], mitotic slippage, cytokinesis failure, and cell fusion [198]. The number of nuclei in the tetraploid/polyploid cells is the result of the mode adopted by the cell [199, 200]. In order to detect the mode of generation of polyploid cells (4N and >4N) in liposarcoma cell lines by the MDM2 inhibition (± RT), cells were sorted and stained with DAPI.

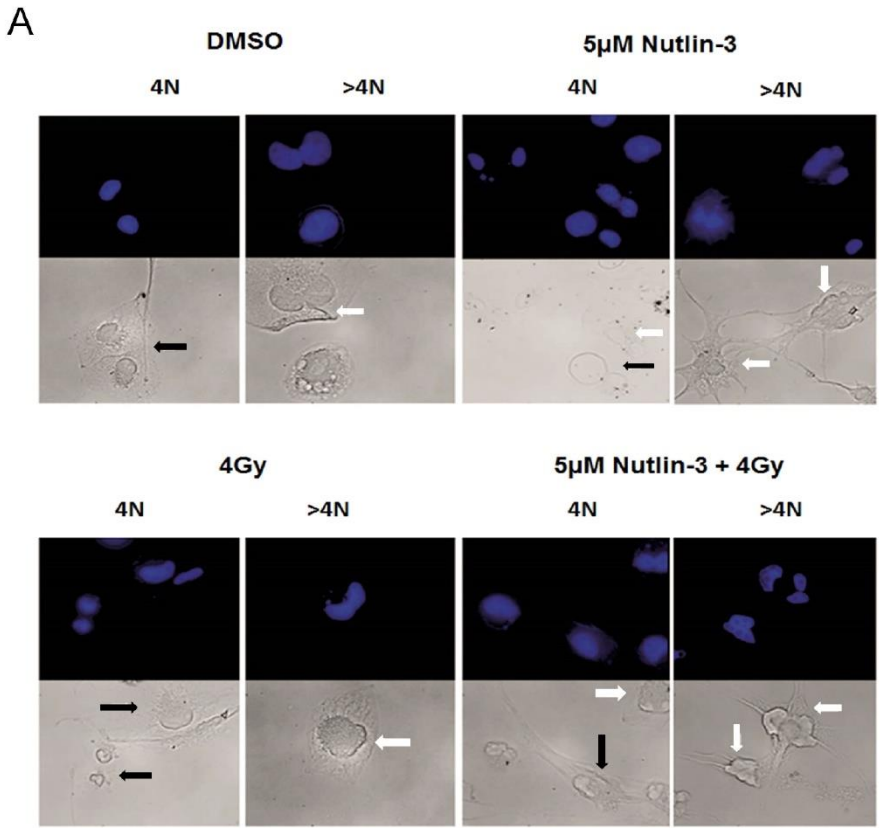

Figure 6.18: **Assessment of the status of nuclei in therapy-generated polyploid populations. (A)** DAPI stain of the nuclei and phase-contrast images of sorted 4N and >4N cells following treatment of 48h and withdrawal of 120h in LPS853.

As evident from the DAPI stain (Figure 6.18 A) of the nuclei in the sorted 4N population (after 48h of treatment and 120h of washout), there was existence of mixture of mono-nucleated (black arrow) cells and bi/multi-nucleated (white arrow) cells. More number of polyploid/multi-nucleated cells (white arrow) cells with 'giant' phenotype were detected in the >4N populations of Nutlin-3 and combination therapy-treated groups. The contribution of these multi-nucleated cells >4N cells was verified by subsequent clonogenic assays of the sorted populations. The existence of multi-nucleated cells possibly indicated toward polploidy generation either through cytokinesis failure or by cell fusion rather than mitotic slippage [201] in response to Nutlin-3 and combination treatment.

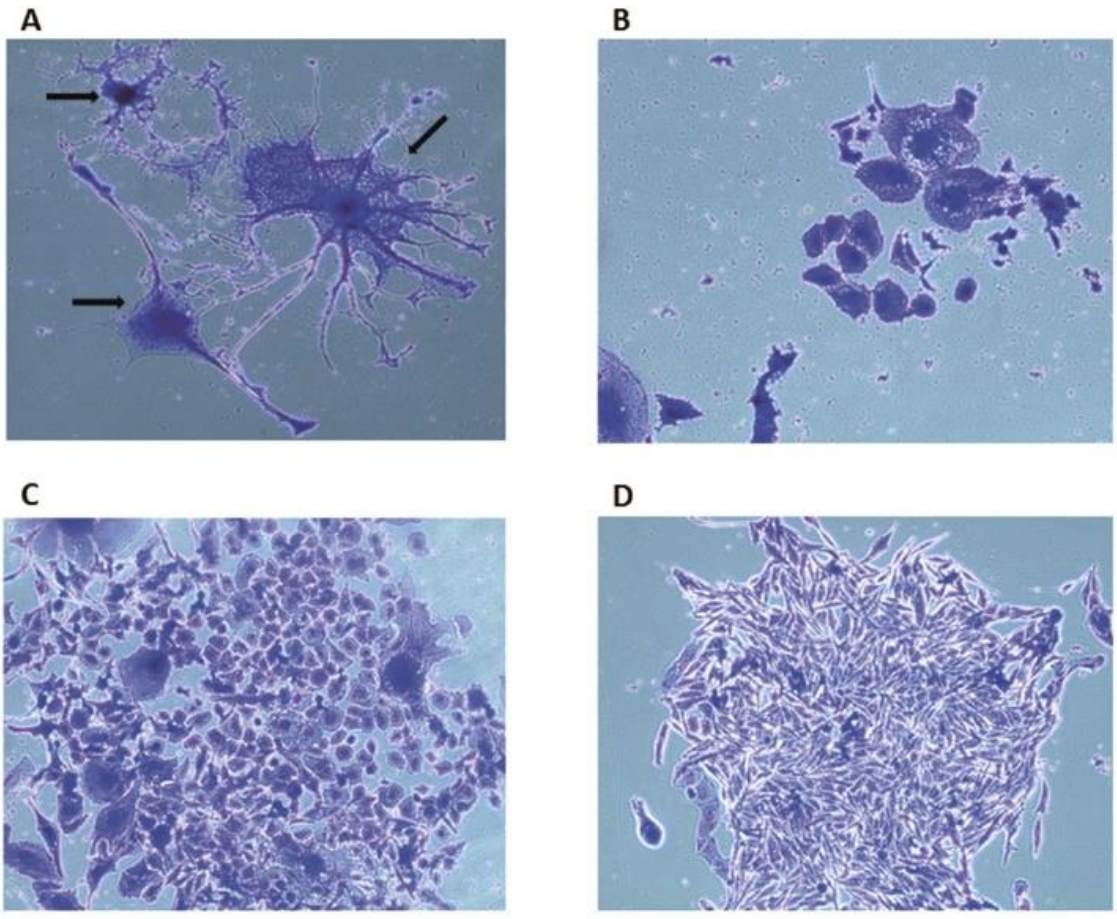

Figure 6.19: **Detection of giant cells generated through treatment. (A)** The giant cells with extended filopodia. **(B)** Colonies < 50 cells which were dispersed and cells had gone through some cycle and were unable to proliferate and develop as proper colony. **(C)** Colonies (> 50 cells) in between extended cells at 10x. **(D)** Colonies from untreated cells (> 50 cells) at 4x magnification.

Microscopic observation following crystal violet staining of the colonies revealed the morphology of >4N cells extending their filopodia for cell–cell paracrine interaction (Figure 6.19 A). These cells were deficient in clone-forming ability. In addition, morphologically, within the 4N population, solitary, extended and flattened cells were present (Figure 6.19 B-C). These set of elongated and flattened cells ultimately contributed (as they failed to develop as colonies) to the radio-sensitizing effect in LPS853 by Nutlin-3 and increased the SER values obtained from the clonogenic survival assay.In summary, these results confirmed the formation of morphologically variant polyploid cells in response to MDM2 inhibition (± RT) in liposarcoma cell lines. Detection of the multinuclei status of the tetraploid/polyploid cells indicated that the mode of generation of these cells was either by cytokinesis failure or *via* cell fusion.

6.3.12 **Elucidation of clone-forming potential of the diverse subpopulations 2N, 4N, > 4N in T778 and T449**

To investigate and differentiate the short-term and long-term fates of the treatment-generated ploidy-based different subpopulations in the other two liposarcoma cells lines (T778 and T449), sorting experiments were conducted based on the Hoechst 33342 stain by following the schemes (Figure 6.16 A scheme 1 and Figure 6.17 B scheme 2).

Earlier data (Figure 6.14 D) of western blot analysis of the cell cycle markers revealed the generation of 4N G1 cells in Nutlin-3 and Nutlin-3 plus RT treated cells in both T449 and T778. Furthermore, the generation of >4N population following the withdrawal of treatment was observed for both T449 and T778.

To elucidate the relative clone-forming ability of the diverse subpopulations, the sorted cells (T449 and T778) were seeded as single cells and allowed for the colony growth. Following 14-20 days of growth, colonies were stained and counted.

A

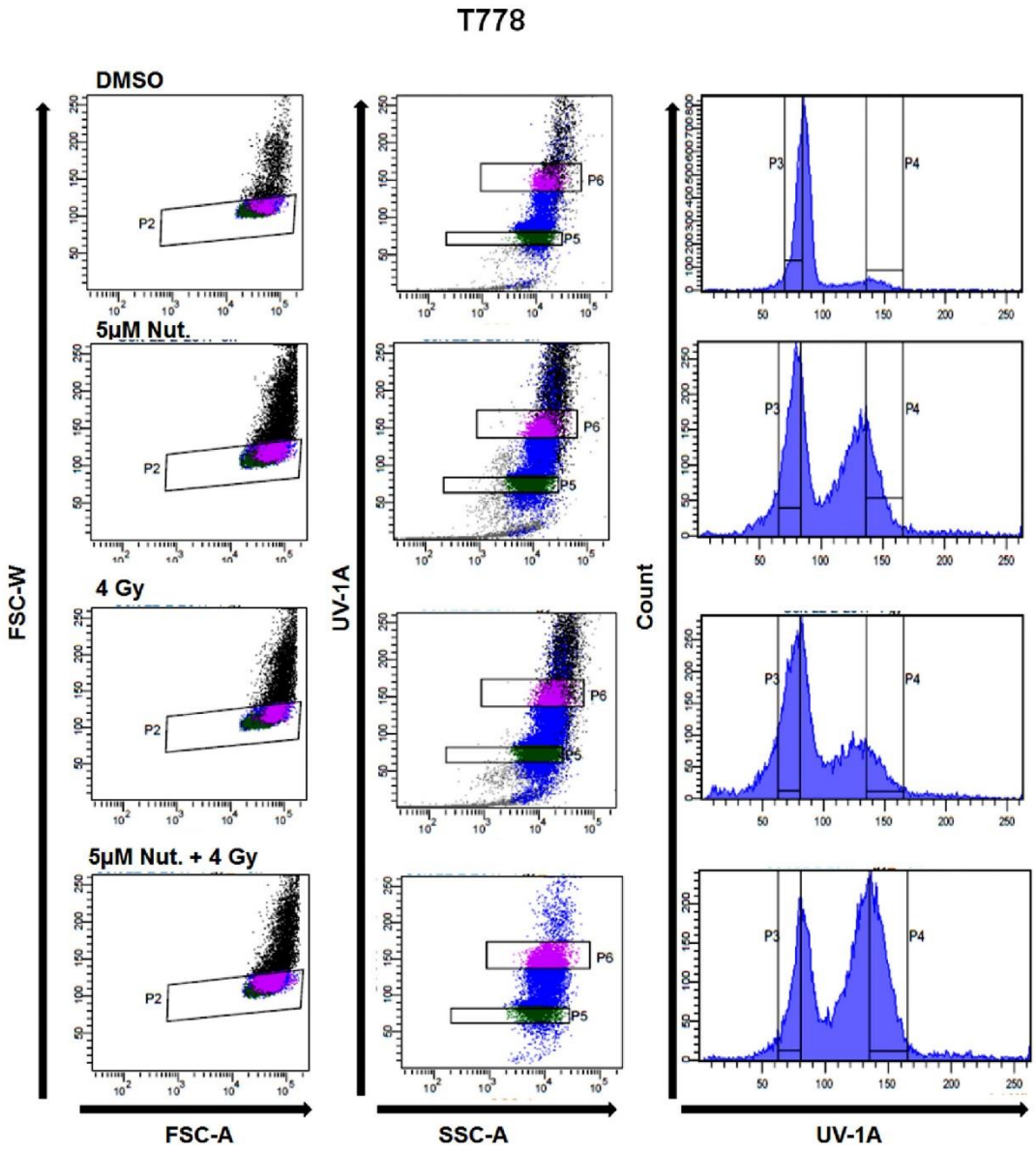
T778
DMSO
5μM Nut.
4 Gy
5μM Nut. + 4 Gy
P2
P3
P4
P5
P6
FSC-W
FSC-A
UV-1A
SSC-A
Count
UV-1A

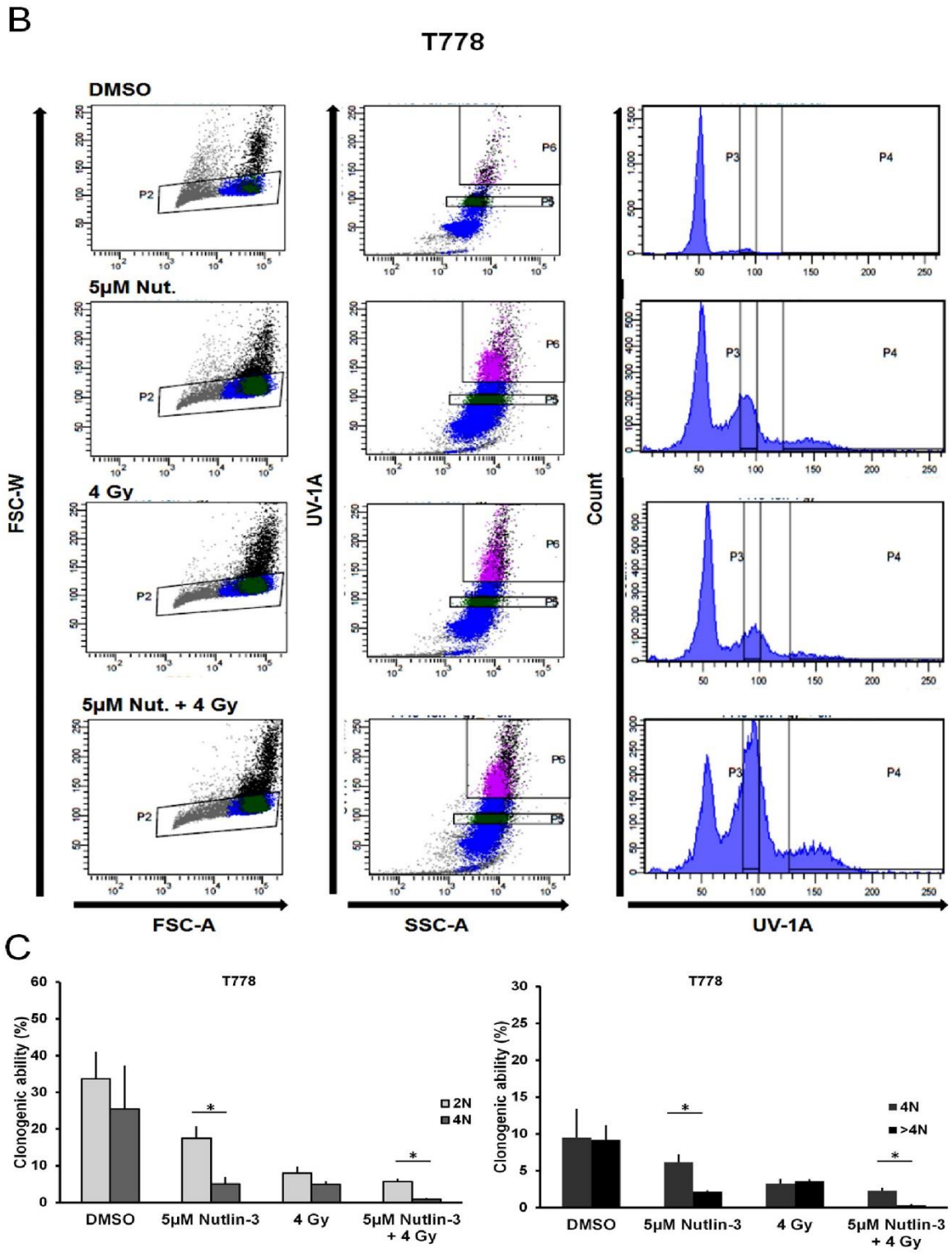

Figure 6.20: **Measurement of long-term fate of diverse ploidy based subpopulations by colony assay.** T778 cells were plated and treated with DMSO, 5μM Nutlin-3, 4 Gy and 5μM Nutlin-3 plus 4Gy for 48h and following that kept for 48h in drug-free medium. Cells were stained with Hoechst 33342 and different populations were sorted. 2N and 4N populations were sorted (**Figure** 6.16 A scheme 1) after 48h of treatment while 4N and >4N are sorted (Figure 6.17 B scheme 2) following 48h of drug removal. **(A)** Histograms representing sorting of live Hoechst 33342 stained cells based on DNA content (2N and 4N populations) in T778. **(B)** Histograms representing sorting of live Hoechst 33342 stained cells based on DNA content (4N and >4N populations) in T778. **(C)** Colony assay presented as bar graphs

(percentage of cells developed into a colony following therapy withdrawal among the cells seeded, n = 3, error bars represent SD) for sorted 2N and 4N and 4N and >4N populations in each of the treatment groups in T778. * $p \leq 0.05$.

A

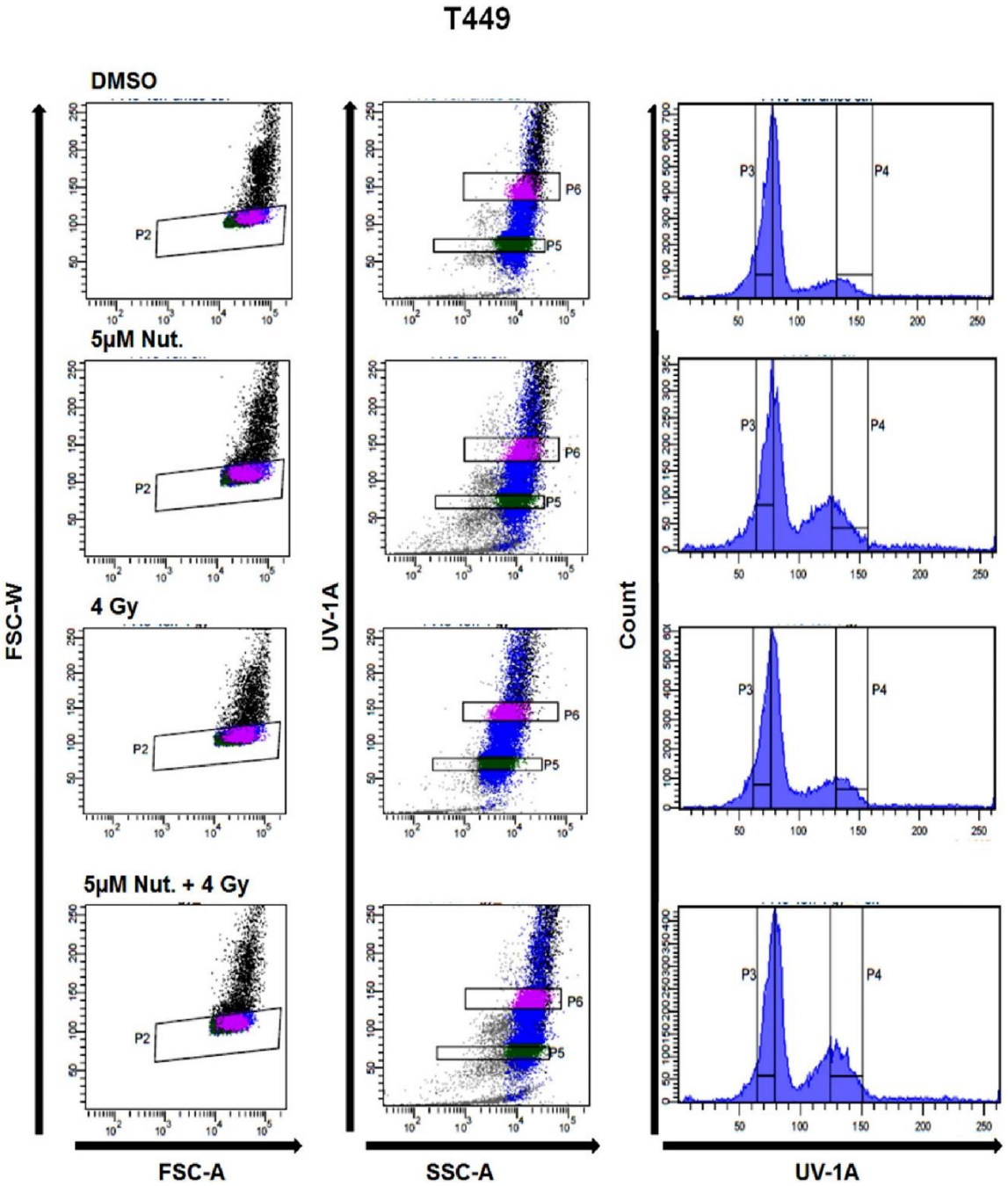

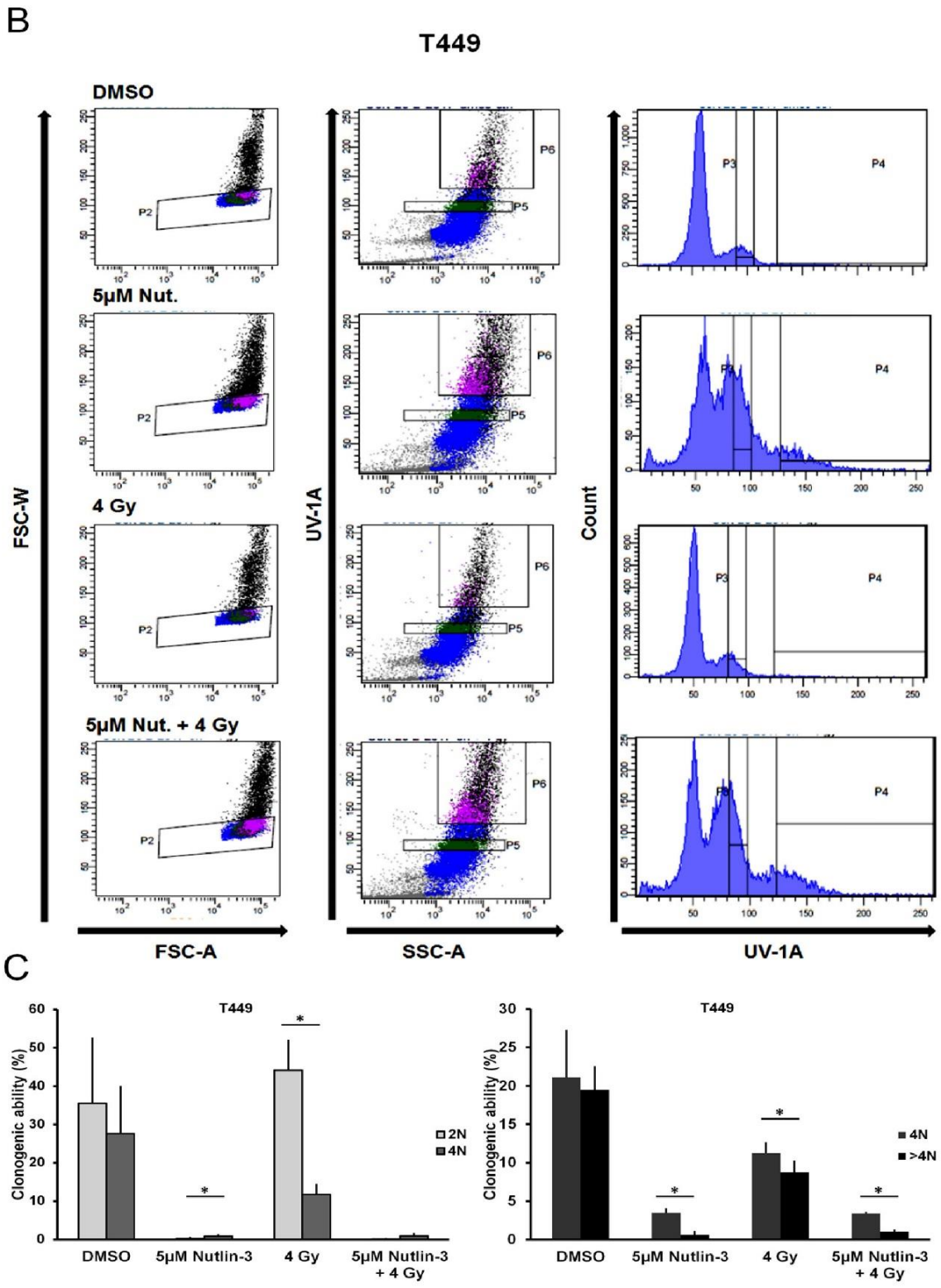

Figure 6.21: **Measurement of long-term fate of diverse ploidy based subpopulations by colony assay.** T449 cells were plated and treated with DMSO, 5μM Nutlin-3, 4 Gy and 5μM Nutlin-3 plus 4Gy for 48h and following that kept for 48h in drug-free medium. Cells were stained with Hoechst 33342 and different populations were sorted. 2N and 4N populations were sorted (**Figure** 6.16 A scheme 1) after 48h of treatment while 4N and >4N are sorted (Figure 6.17 B scheme 2) following 48h of drug removal. **(A)** Histograms representing sorting of live Hoechst 33342 stained cells based on DNA content (2N and 4N populations) in T449. **(B)** Histograms representing sorting of live Hoechst 33342 stained cells based

on DNA content (4N and >4N populations) in T449. **(C)** Colony assay presented as bar graphs (percentage of cells developed into a colony following therapy withdrawal among the cells seeded, n = 3, error bars represent SD) for sorted 2N and 4N and 4N and >4N populations in each of the treatment groups in T449. * $p \leq 0.05$**.**

The intrinsic ability of clonogenic growth of 2N populations was observed (Figure 6.20 C) to be higher than respective 4N populations in all the treatment groups (5μM Nutlin-3; $p < 0.05$ and 5μM Nutlin-3 plus RT; ≤ 0.05) except in RT alone group ($p \geq 0.05$) in T778. The 2N cells of vehicle treated (highest 33.6 % ± 7.2) have enhanced proliferative potential or clonogenicity than the Nutlin-3 alone (17.5 % ± 3), RT alone (8 % ± 1.6) and Nutlin-3 plus RT treatment groups (5.6 % ± 0.6).

The clonogenic growth of 4N population was highest in vehicle treated (average 25 % ± 11.6), comparable in Nutlin-3 treated (average 5.1 % ± 1.7) and in RT exposed (average 5 % ± 0.54) and significantly lower ($p \geq 0.05$ for Nutlin-3 vs combination, $p \leq 0.001$ for RT vs combination) in combination treatment (average 0.9 % ± 0.18) than the vehicle treated and monotherapies.

Assessment of clonogenic potential of 4N and >4N populations (sorted according to the Figure 6.17 B scheme 2) showed higher ability of the 4N than the >4N in Nutlin-3 (4N 6.2 % ± 1, >4N 2.3 % ± 0.1; $p \leq 0.05$) treated and in Nutlin-3 plus RT (4N 2.3 % ± 0.3, >4N 0.3 % ± 0.1). There was no visible significant difference between the clonogenic ability of 4N and >4N populations generated by RT alone (4N 3.3 % ± 0.5, >4N 3.6 % ± 0.1) and the vehicle treated. The overall potential of the >4N cells was significantly low in all the treatment groups than the vehicle treated for T778 (Figure 6.20 C).

In summary, for T778, combined therapy elicited an additive effect *via* enhanced attenuation of proliferation of the 4N and >4N populations.

For T449, 2N and 4N populations (sorted according to Figure 6.16 A scheme 1), showed enhanced clone-forming ability of the 2N populations than 4N populations in vehicle treated (2N 35.5 % ± 16.9, 4N 41 % ± 27.6) and RT alone (2N 44.2 % ± 7.7, 4N 11.8 % ± 2.47) group. In contrast, in Nutlin-3 and combination group, an inverse effect was observed in terms of clonogenic ability i.e. 4N populations had a slightly higher ability than 2N populations. 5μM Nutlin-3 alone displayed enhanced lethality and addition of RT did not show any additional effect. The clone-forming abilities of the

4N populations generated by of the Nutlin-3 (4N 0.8 % ± 0.32) and the combination treatment (4N 0.9 % ± 0.6) were comparable (Figure 6.21 C).

For T449, analysis of clonogenic potential of 4N and >4N populations (sorted according to the Figure 6.17 B scheme 2) showed higher ability of the 4N than the >4N in vehicle treated (4N 21.1 % ± 6.1, >4N 16.8 % ± 2.9), Nutlin-3 treated (4N 3.5 % ± 0.5, >4N 0.9 % ± 0.4; $p \leq 0.05$) and in RT alone (4N 11.2 % ± 1.4, >4N 7.5 % ± 1.4; $p \leq 0.05$) and Nutlin-3 plus RT (4N 3.4 % ± 0.2, >4N 1.2 % ± 0.2; $p \leq 0.05$) treated (Figure 6.21 C).

In summary, for T449, an overall reduction in the colony forming potential of the 4N and >4N populations was observed. However, Nutlin-3 displayed a dominant effect on the colony forming ability and combination treatment did not further diminish the proliferative potential of these populations. In contrast to T778, 2N populations in T449 had reduced clone-forming ability than 4N which indicated the participation of multiple governing factors other than ploidy in determining the proliferative capacity of the subpopulations.

6.3.13 Long-term fate analysis revealed augmented senescence mediated clone- forming ability of the 4N and >4N subpopulations in T778 and T449

For long-term fate analysis, senescence assay was carried out (after 18 days of treatment removal) for T449 and T778. An enhanced number of senescent cells were observed in 4N and >4N populations generated by the combination treatment in T778 (Figure 6.22 A-B). Induction of senescence in 2N and 4N were comparable in the RT alone (2N 11.6 % ± 2.34 vs 4N 11.98 % ± 7.16) and Nutlin-3 alone (2N 5.5 % ± 1.9 vs 4N 13.34 % ± 11.66) and significantly higher ($p \leq 0.01$) in the 4N population than 2N in Nutlin-3 plus RT treated group (2N 6.6 % ± 3.1 vs 4N 53.93 % ± 28.71) in T778.

A

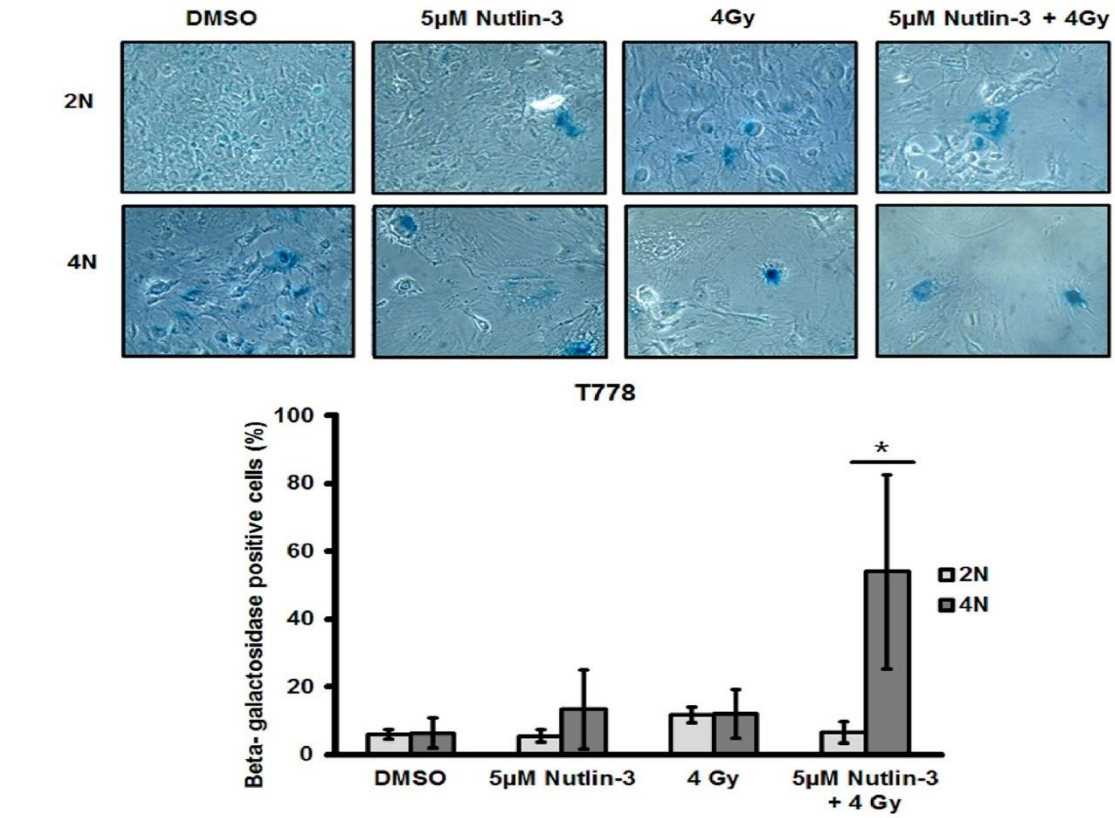
DMSO
5μM Nutlin-3
4Gy
5μM Nutlin-3 + 4Gy
2N
4N
T778
Beta- galactosidase positive cells (%)
100
80
60
40
20
0
*
2N
4N
DMSO
5μM Nutlin-3
4 Gy
5μM Nutlin-3
+ 4 Gy

B

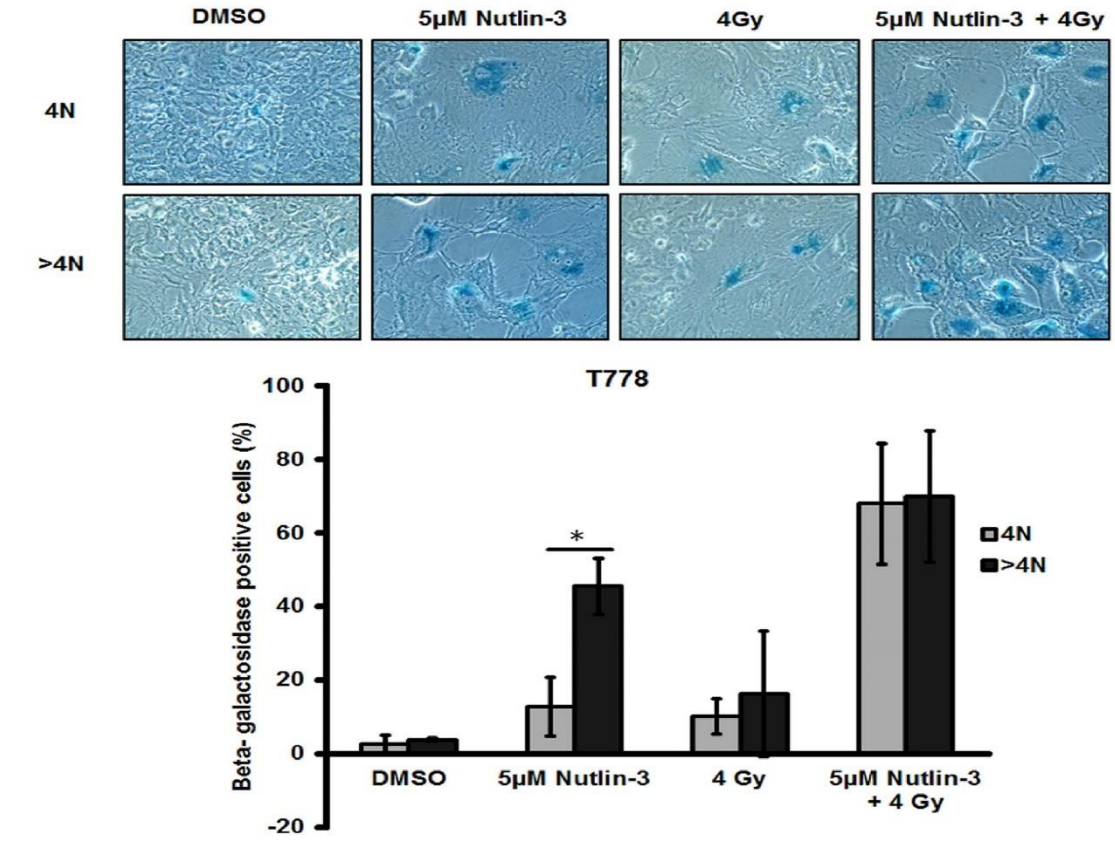
DMSO
5μM Nutlin-3
4Gy
5μM Nutlin-3 + 4Gy
4N
>4N
T778
Beta- galactosidase positive cells (%)
100
80
60
40
20
0
-20
*
4N
>4N
DMSO
5μM Nutlin-3
4 Gy
5μM Nutlin-3
+ 4 Gy

C

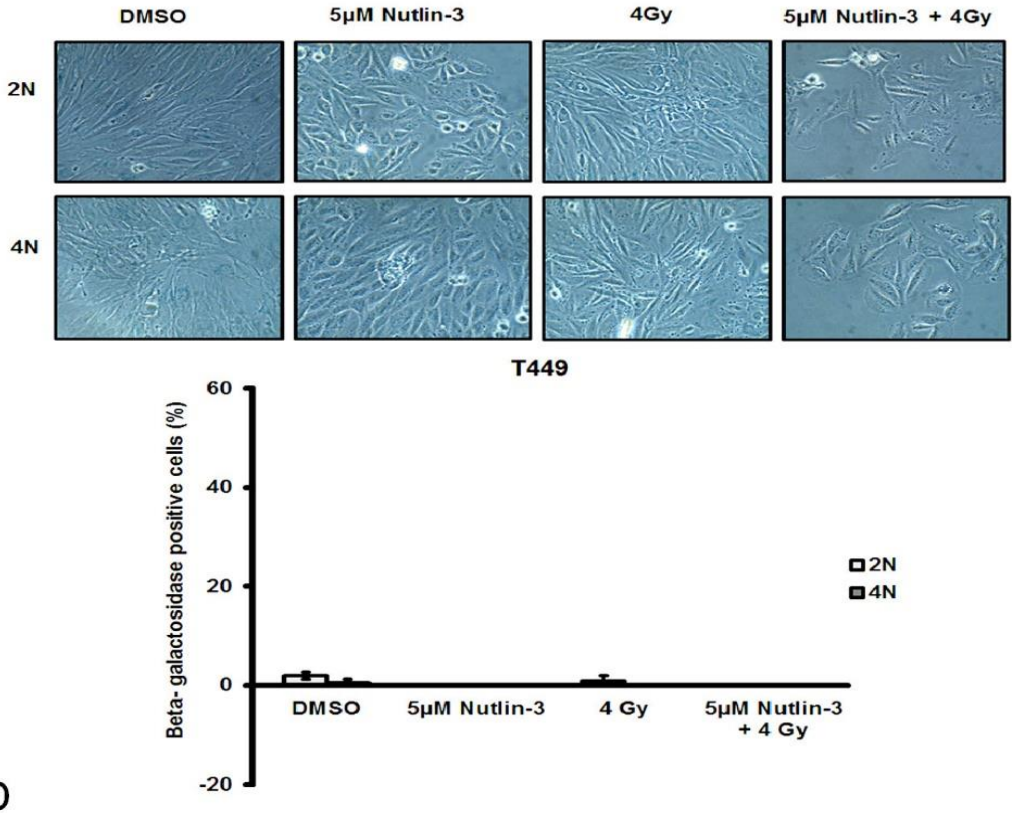
DMSO
5μM Nutlin-3
4Gy
5μM Nutlin-3 + 4Gy
2N
4N
T449
Beta- galactosidase positive cells (%)
60
40
20
0
-20
2N
4N
DMSO
5μM Nutlin-3
4 Gy
5μM Nutlin-3 + 4 Gy

D

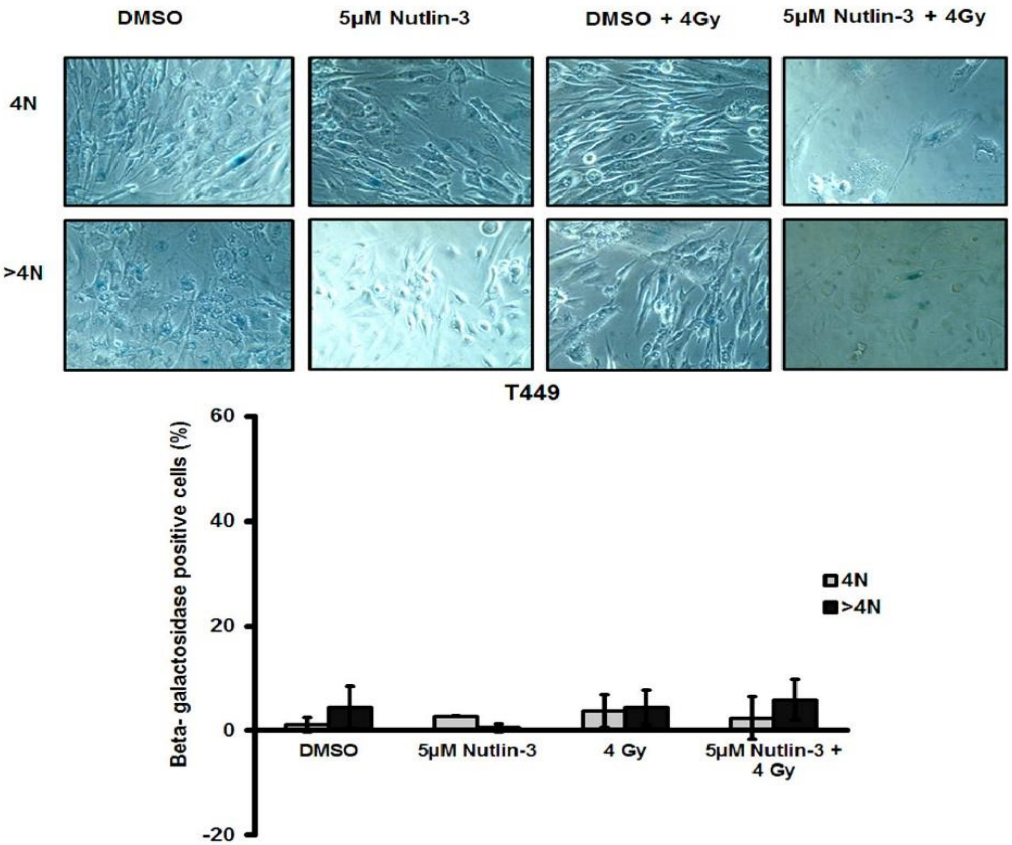
DMSO
5μM Nutlin-3
DMSO + 4Gy
5μM Nutlin-3 + 4Gy
4N
>4N
T449
Beta- galactosidase positive cells (%)
60
40
20
0
-20
4N
>4N
DMSO
5μM Nutlin-3
4 Gy
5μM Nutlin-3 + 4 Gy

Figure 6.22: **Analysis of long-term fate in liposarcoma in response to MDM2 inhibition and RT. (A)** Beta-galactosidase staining images and bar graphs (average of percentage of beta-galactosidase positive cells, n = 5, error bars indicate SD) of sorted 2N and 4N populations after 48h in vehicle treated, 5µM Nutlin-3, 4Gy and 5µM Nutlin-3 plus 4Gy in T778 after 18 days. **(B)** Beta-galactosidase staining images and bar graphs of sorted 4N and >4N populations in T778 after 18 days. **(C)** Beta-galactosidase staining images and bar graphs of sorted 2N and 4N populations in T449 after 20 days. (D) Beta-galactosidase staining images and bar graphs of sorted 4N and >4N populations in T449 after 20 days. * $p \leq 0.05$.

Comparison of level of senescence in 4N and >4N cells (for T778 cell line) isolated following scheme 2 (Figure 6.17 B) revealed significantly elevated level of beta-galactosidase positive cells in 4N (68 % ± 16.4) and >4N (69.82 % ± 17.91) in Nutlin-3 plus RT groups than all the treatment groups and vehicle treated one. However, extent of senescence was not significant ($p \geq 0.05$) between the 4N and >4N cells in combination treatment group. In Nutlin-3 treated group, >4N (45.53 % ± 7.58) cells displayed higher level of senescence traits than 4N (12.71 % ± 8) which is significant ($p \leq 0.01$).

By senescence assay for T449, it has been observed that for 2N and 4N populations (Figure 6.22 C), there are undetectable beta-galactosidase positive cells when analyzed after a prolonged period (20 days). The 4N and >4N populations have negligible amount of senescence (Figure 6.22 D) in response to different treatment groups for T449.

In summary, the radio-sensitizing effect observed in T778 as a long-term fate was mediated through enhanced senescence of the combination treatment-generated polyploid (4N and >4N) cells. However, therapy-generated polyploid cells might not lead to senescence in all liposarcoma cell lines (e.g.,T449). Thus, generation of polyploid cells in response to MDM2 inhibition (± RT) was a p53-dependent phenomenon in liposarcoma cell lines (with wild-type *TP53*) with diverse fates i.e. leading to either senescence or survival depending on other p53-independent factors and accordingly determined the therapy response.

6.3.14 Assessment of gamma-H2AX in response to treatment with MDM2i and RT

Chemotherapeutic approaches or radiotherapeutic modalities are known to induce p53 by genotoxic activity i.e. by inducing DNA damage leading to cellular death. However,

due to wild-type *TP53* status, normal tissues are susceptible to the activation of signaling pathways mediated by DNA damage. Nutlin-3 has emerged as one of the non-genotoxic activators of p53 in cells with wild-type *TP53*. However, conflicting views were reported for Nutlin-3 as an inducer of genotoxic activation of p53 [202]. In order to address the questions 1) whether Nutlin-3 (± RT) induced the genotoxic or non-genotoxic activation of p53 in liposarcoma cells, level of gamma-H2AX was measured in LPS853 (*TP53* WT) and SW872 (*TP53* Mut) following 48h of treatment. In addition, it was aimed 2) to correlate the levels of gamma-H2AX with the observed treatment-driven senescence.

In LPS853 and SW872, an induction of gamma-H2AX (Figure 6.23) was observed in RT and Nutlin-3 plus RT groups after 48h of treatment. Levels of gamma-H2AX were comparable in RT and Nutlin-3 plus RT in both the cell lines.

However, treatment-driven senescence induction (Figure 6.9) did not correlate with gamma-H2AX induction in LPS853.

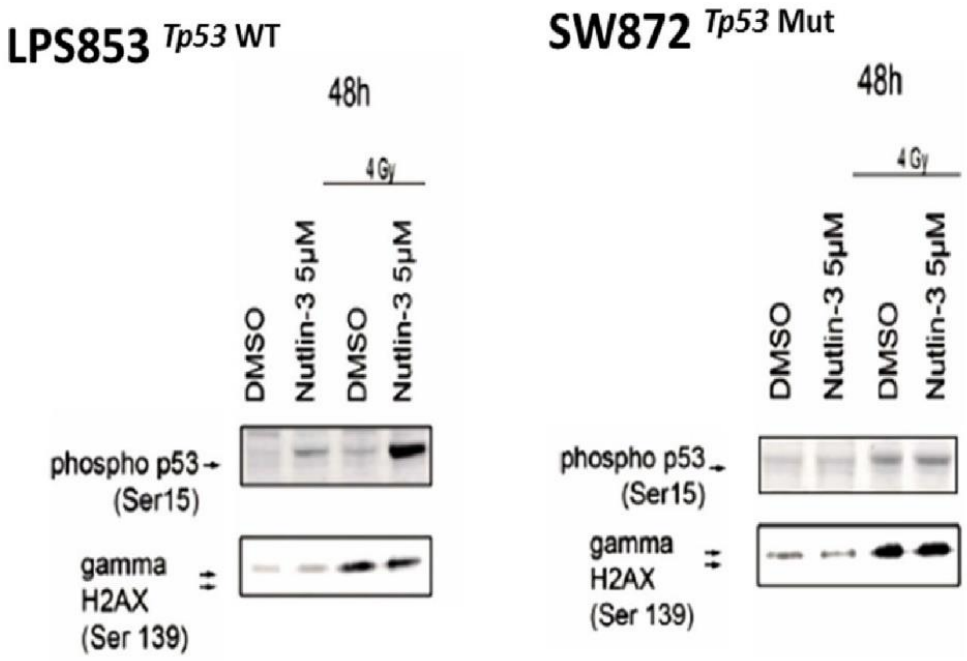

Figure 6.23: **Assessment of genotoxicity by MDM2 inhibition and combined therapy in liposarcoma cells**. **(A)** Western blot images of DNA damage activation pathway proteins (p53, phospho-p53 (Ser-15), gamma-H2AX) in LPS853 (with wild-type *TP53*) and SW872 (with mutant *TP53*) in response to Nutlin-3, RT, Nutlin-3 + RT after 48h of treatment. For beta-actin, refer to Figure 6.10.

In summary, levels of the induced gamma-H2AX were comparable in response to RT and Nutlin-3 plus RT. RT was contributing to the gamma-H2AX formation and addition

of Nutlin-3 did not enhance the levels of gamma-H2AX. This indicated Nutlin-3 to be non-genotoxic in LPS853. The levels of beta-galactosidase positive cells (Figure 6.9) in the treatment groups did not correlate with observed levels of gamma-H2AX.

As gamma-H2AX was detected at 48h after RT alone and after combination treatment in both with wild-type *TP53* and with mutant *TP53* cell lines, in the next step, it was aimed to identify whether any repair gene associated with NHEJ or HRR was overexpressed or deleted in DDLPS. By the existing data set of SNP array [203], the status of *RAD51*, *BRCA2* and other genes (e.g. *XRCC6BP1*) was determined. Among those genes, *RAD51* was observed to be deleted. In order to validate the finding, certain set of patient DDLPS samples obtained from WTZ (West German Cancer Center, Essen, Germany) and sarcoma cell lines were tested for Rad51 expression by western blot (Figure 6.24).

Rad51 was found to be expressed comparatively higher in SW872 and SKLMS01 among the sarcoma cell lines. In contrast, in all the DDLPS and WDLPS, Rad51 was expressed relatively low. In none of the patient samples (3 out of 8), Rad51 was detected. 5 patient samples were not considered as beta-actin levels were not equal.

Rad51 is an interaction partner of BRCA2 and assists in homologous recombination repair [204]. Poly(ADP-ribose) polymerase (PARP), is an enzyme that detects single-strand breaks and recruits DNA repair molecules. Inhibition of PARP results in accumulation of DNA breaks, which are recognized and repaired by the DNA double-strand break pathway. Thus, cells with HR pathway deficiency (e.g., BRCA2) are susceptible to cell death due to excessive DNA damage upon blockade with PARP inhibitors. This is known as synthetic lethal interaction between PARP and BRCA2 [205]. To exploit the Rad51 status of the cell lines, PARP inhibitor was employed alone or in combination with RT (analogous to the concept of ‘synthetic lethality’). In order to investigate, the two cell lines LPS853 (wild-type *TP53*, low Rad51 expression) and SW872 (mutant *TP53,* high Rad51 overexpression) were tested. Cells were seeded as single cells in low density and the following day treated with 5µM of ABT-888 (PARP inhibitor) for 6h prior to RT. Following irradiation with increasing doses of radiation, cells were washed off and new medium was added without ABT-888. The clonogenic

assays are represented in Figure 6.24 C. In parallel, MTT assay was conducted to measure growth inhibition.

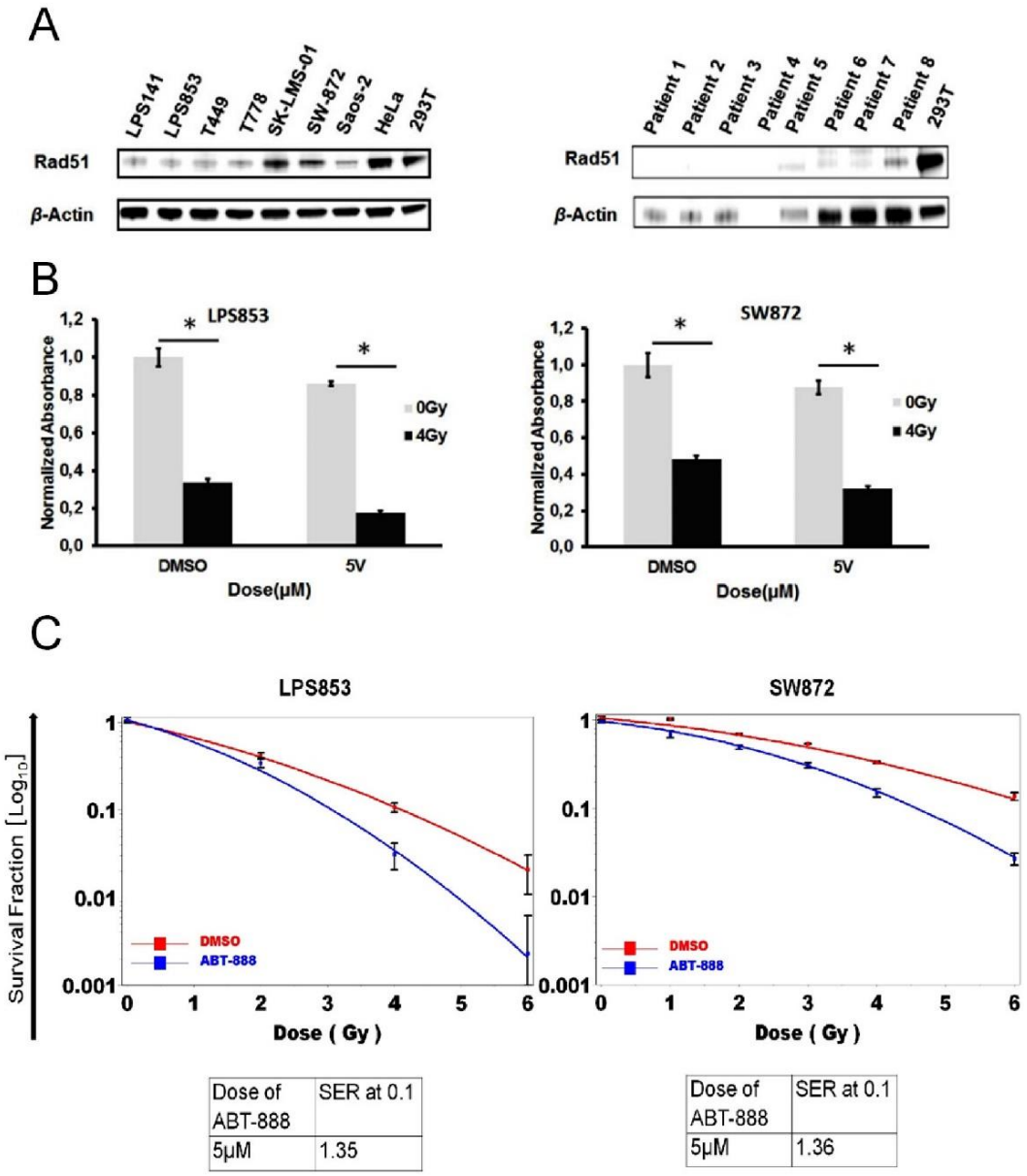

Figure 6.24: **PARP inhibition in combination with the RT in liposarcoma cell lines LPS853 (*TP53*^{WT}) and in SW872 (*TP53*^{Mut}).** (A) Western blot of Rad51 in sarcoma cell lines (WD/ DDLP; T449, T778, LPS853, LPS141, UDLP; SW872, Leiomyosarcoma; SKLMS01, Osteosarcoma; Saos-2, adenocarcinoma; HeLa and patient samples. 293T cells were used as positive control. (B) MTT assay following 6 days of treatment (ABT-888 and RT). (C) Cell survival curves (mean ± SD, n = 3) with RT ± PARP-1 inhibitor (ABT-888) in LPS853 (with wild-type *TP53* and low expression of Rad51) and SW872 (with mutant *TP53* and high expression of Rad51) and determination of SER at 0.1 survival fraction. * $p \leq 0.05$.

By clonogenic assay, it was observed that the two cell lines had comparable SER (LPS853 SER_{10} = 1.35 and SW872 SER_{10} = 1.36 at 0.1 survival level). MTT assay

displayed an additive growth inhibition by combination treatment in both LPS853 and SW872. For LPS853 and SW872, the growth inhibition by PARP-1 inhibitor alone was ~ 62 % and ~ 52 %, respectively. Addition of RT led to ~ 82 % and ~ 68 % growth inhibition, respectively. Thus, the extent of growth inhibition was comparable in both the cell lines tested.

In synthesis, these results suggested that the existence of defect in either of the components i.e. low Rad51 expression or non-functional p53 might elicit the same response following PARP inhibition.

6.4 Targeting CDK4-RB axis by inhibitor and RT

The next objective was to delineate whether application of CDK4 inhibitors radio-sensitize liposarcoma cell lines *in vitro*. In order to address that, two liposarcoma cell lines (T778 and T449, with *CDK4* amplifications) were seeded as single cells and treated with CDK4 inhibitors (0.5 µM LEE011 or 0.5µM Palbociclib) and irradiated with increasing doses (2, 4, 6 Gy) of radiation. Following 48h treatment, drug-containing medium was washed off and replaced with new medium. Cells were kept for 12-14 days for colony formation.

SER values were determined from the cell survival curves. It was observed that SER_{10} values were ~ 1 for both the cell lines (T778 and T449) and for both the inhibitors (Palbociclib and LEE011). This indicated that these liposarcoma cells were not sensitized to RT by CDK4 inhibitors (Figure 6.25 A-B).

CDK4 inhibitors induce G1 arrest. In order to determine how cell cycle distribution was modulated by the combined treatment with CDK4i and ionizing radiation, cell cycle analysis was carried out. Cells were seeded in 6 well plates and co-treated with CDK4 inhibitor and ionizing radiation with a dose of 4 Gy for 48h. Cells were stained with propidium iodide and cell cycle distribution was measured by FACs.

Cell cycle distribution analysis by PI stain revealed an induction of G1 arrest (> 85 %) in all four cell lines by treatment with CDK4 inhibitor alone. However, addition of RT led to a reduction of G1 arrested cells. Comparable fractions of G2 arrested cells were observed in RT alone and in combined therapy treated groups (Figure 6.25 C).

A

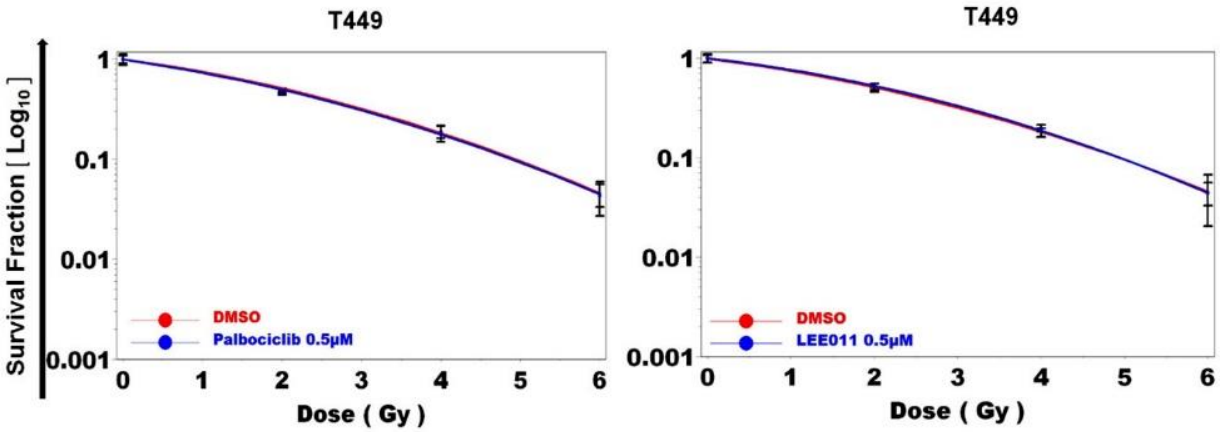

Dose of Palbociclib	SER at 0.1
0.5μM	1.008

Dose of LEE011	SER at 0.1
0.5μM	1.0004

B

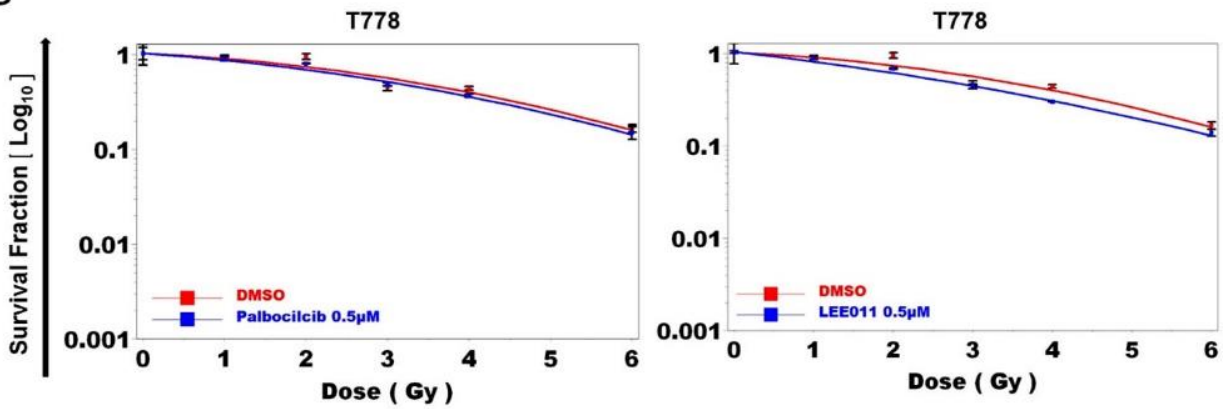

Dose of Palbociclib	SER at 0.1
0.5μM	1.027

Dose of LEE011	SER at 0.1
0.5μM	1.05

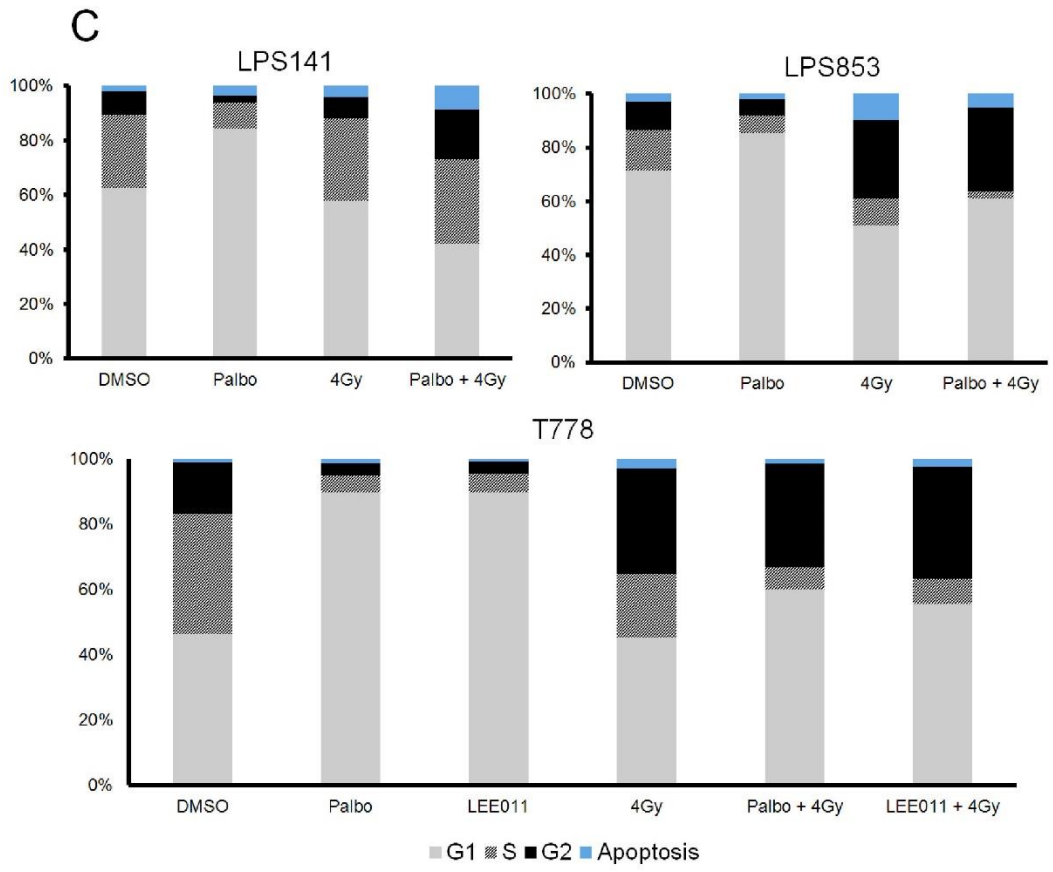

Figure 6.25: **Radiation response by functional inhibition of CDK4 in liposarcoma cells.** T778 and T449 cells were plated, treated with 0.5µM CDK4 inhibitor (either Palbociclib or LEE011) and increasing doses of ionizing radiations. Following 48h, fresh medium was added and kept for 12-14 days for colony growth. The surviving fraction (SF) was calculated from counted colonies (>50 cells) divided with plated number of cells. Values were normalized by plating efficiency. Sensitization enhancement ratio (SER) was calculated by the ratio of radiation dose alone to radiation dose in combination with CDK4i at 10 % survival level. **(A)** Cell survival curves (mean ± SD, n = 3) with RT ± CDK4i (LEE011 or Palbociclib) in T449 and determination of SER at 0.1 survival fraction. **(B)** Cell survival curves (mean ± SD, n = 3) with RT ± CDK4i (LEE011 or Palbociclib) in T778 and determination of SER at 0.1 survival fraction. **(C)** Analysis of cell cycle distribution by PI stain in liposarcoma cells in response to the RT (4Gy) and CDK4i (0.5µM or 2µM) were carried out following 48h of treatment. For T778, 0.5 µM of each inhibitors were tested while for LPS141 and LPS853, 2µM of palbociclib was used.

In summary, this study demonstrated CDK4 inhibitors were unable to act as radio-sensitizers for liposarcoma cell lines.

6.5 Exploring the potential for immunotherapy in the treatment of liposarcoma

6.5.1 Expression of NKG2D ligands and DNAM-1 ligands in liposarcoma cell lines in response to targeted therapy

In order to analyze the treatment-driven expression of NKG2D activating cell ligands (MICA, MICB, ULBP-2), DNAM-1 ligand (CD155), HLA-DR and the inhibitory HLA

class I molecules (A, B, C), the liposarcoma cell lines (T449, T778, LPS141) were seeded and treated with the targeted therapies (CDK4 inhibitor and the MDM2 antagonist alone and in combination) for 72h. Following treatment, cells were stained (see section 5.14.3) with primary antibodies (directly labelled to fluorochromes) specific for the NK cell ligands and then tested by multicolor flow cytometry. These ligands belong to the set of ligands that are known to be key molecules that can trigger the cytolytic activity of innate effector cells and are often modulated in tumor cells [151]. Goat-anti-mouse (GAM)-PE was used as a control. Melanoma antigen was used as negative control (Figure S 11.5)**.** LEE011 and Palbociclib have been used for the treatment of T449 and T778, respectively due to their efficacy as measured by the SRB assay in the previous study. Nutlin-3 was used for both of the cell lines as the MDM2 antagonist.

For the cell line T449 (derived from primary tumor), among the NKG2D ligands, as a baseline expression, MICA and ULBP2 were detected to be expressed low while inhibitory ligand HLA-ABC was observed to be expressed higher. However, in response to treatment, NKG2D ligands (for MICA; MFI for DMSO ~1.4, LEE011 ~1.65, Nutlin-3 ~4.6, for combination 4.9, for ULBP2; DMSO ~6.2, LEE011 ~7.8, Nutlin-3 ~9.8, combination ~10) were upregulated. In contrast, HLA-ABC molecules (MFI for DMSO ~60.6, LEE011 ~42, Nutlin-3 ~45, combination treatment ~32.4) were downregulated (Figure 6.26).

T778, the cell line derived from a recurrent tumor was also examined after 72h (Figure 6.26) for baseline and therapy-driven expression of the ligands. Enhanced levels of MICA were detected in response to Nutlin-3 and the combination treatment at 72h of treatment while other markers (MICB, ULBP2) remained unperturbed. HLA-ABC (MFI of DMSO ~17, Nutlin-3 ~18.6, Palbociclib ~14.75, combination ~19) was slightly upregulated in the treatment groups with Nutlin-3 and combination treatment.

For LPS141, therapy-driven expression of MICA and MICB were comparable to the untreated group while ULBP2 was slightly upregulated in response to the treatments (MFI of DMSO ~2.7, Nutlin-3 ~3.5, Palbociclib ~4.4 and combination of both ~4.2). Basal level of HLA-ABC was high and slightly perturbed in response to the treatments (MFI of DMSO ~94.9, Nutlin-3 ~87.4, Palbociclib ~109 and combined therapy ~87).

Consequently, the feasibility of recognition of the LPS141 by NK cells was less. For LPS853 (Figure S 11.6), the NK cell ligands were not modulated by targeted therapy.

For the DNAM-1 ligand, CD155 (Figure 6.26) was measured in both cell lines (T449 and T778) following 72h of treatment. A low expression of CD155 was detected at the basal level and remained unchanged following treatment. HLA-II (HLA-DR) molecules were unchanged in the cell lines.

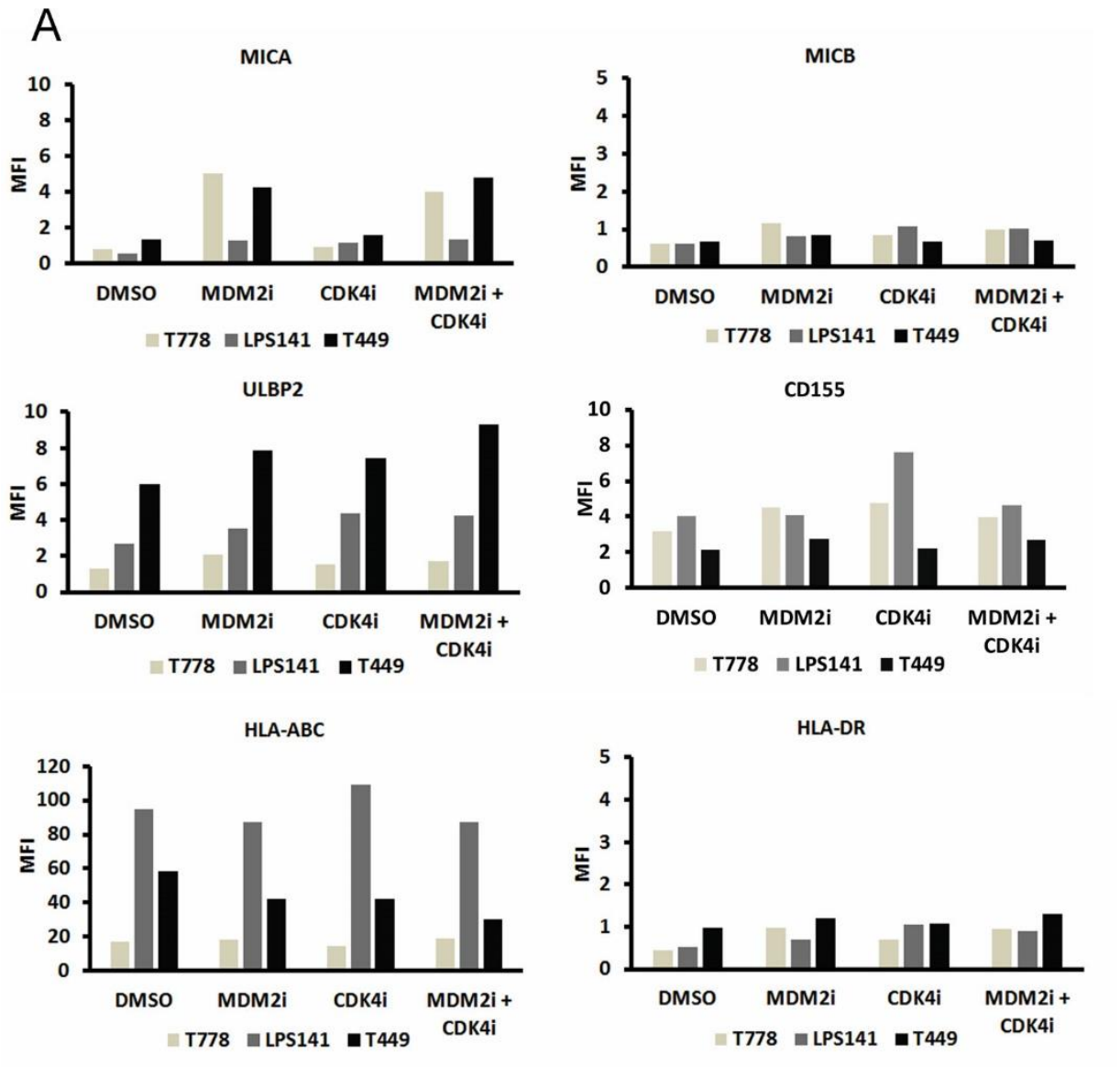

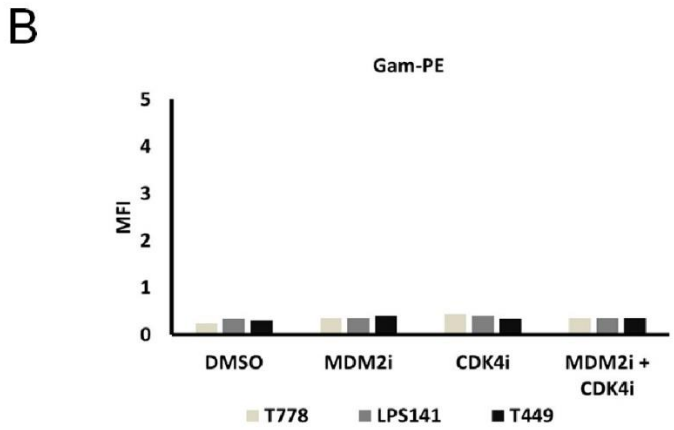

Figure 6.26: Delineation of NKG2D and DNAM-1 ligands in liposarcoma cells in response to functional block of CDK4 and MDM2. (A) Bar graphs represent the MFI (mean fluorescent intensity) of different ligands of NK cell receptors expressed as cell surface markers (MICA, MICB, ULBP2, CD155, HLA-ABC, HLA-DR) in T778, LPS141 and T449 as measured by multicolor flow cytometry in response to different treatment and combinations after 72h. **(B)** Goat-anti-mouse (GAM)-PE was used as control.

In summary, out of the four liposarcoma cell lines, T449 displayed modulation of NKG2D ligands (with activation ligands to be expressed higher and inhibitory ligands to be reduced) by functional block of CDK4, MDM2 and co-inhibition. Thus, this cell line was selected for the next functional experiments for primary NK cell recognition and lysis.

6.5.2 *In vitro* assessment of NK cell lysis targeting the NK cell ligands expressed in response to targeted therapy

Based on the analysis of the expression of the ligands, T449 cell line was selected for exposing and testing for NK cell cytotoxicity. Blood sample was collected from a healthy donor for primary NK cell isolation and for subsequent lysis experiment. From blood, peripheral mononuclear cells were isolated and MACs technology was employed to isolate $CD56^{+}CD3^{-}$ cells (Figure 6.27 scheme 1). $CD56^{+}CD3^{-}$ cells were consisting of $CD56^{+bright}$ and $CD56^{+dim}$ subpopulations.

A

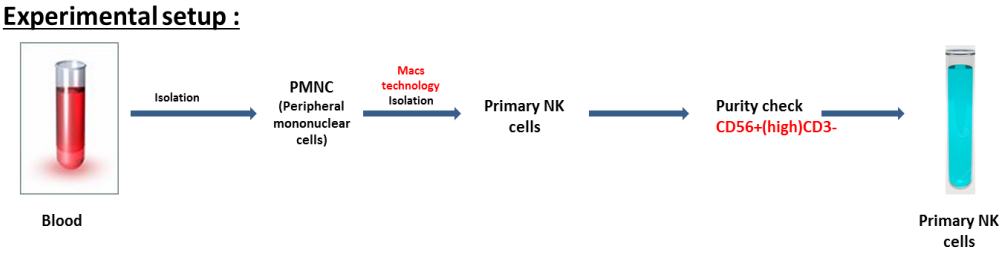

Scheme 1: Experimental set up describing the procedure of isolation of primary NK cells from blood.

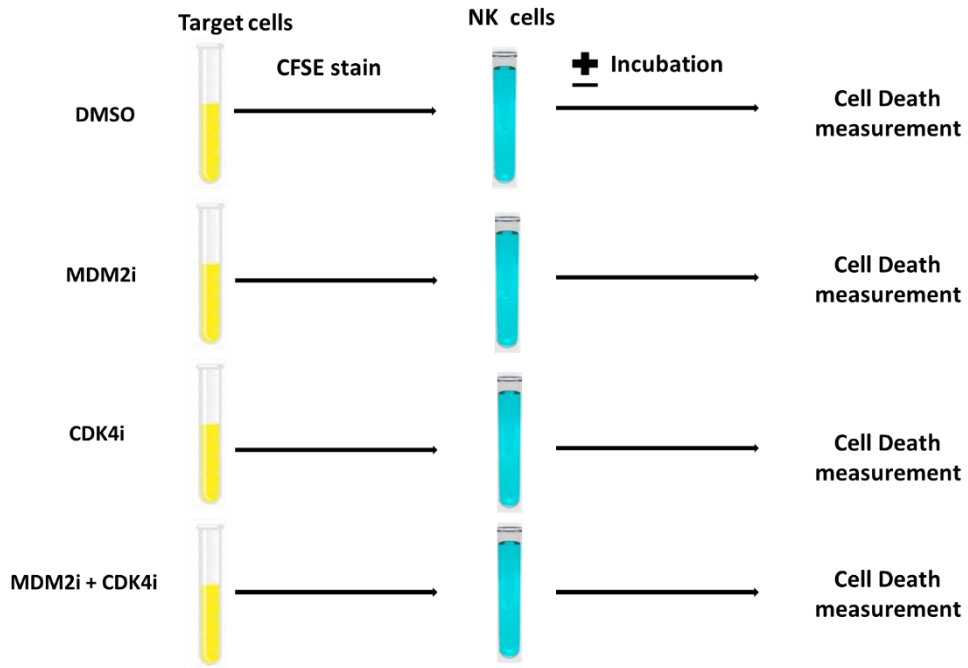

Scheme 2: Flowchart explaining the experimental design of NK cell lysis with target tumor cells expressing the ligands.

B

CFSE stained Tumor cells co-incubated with NK cells

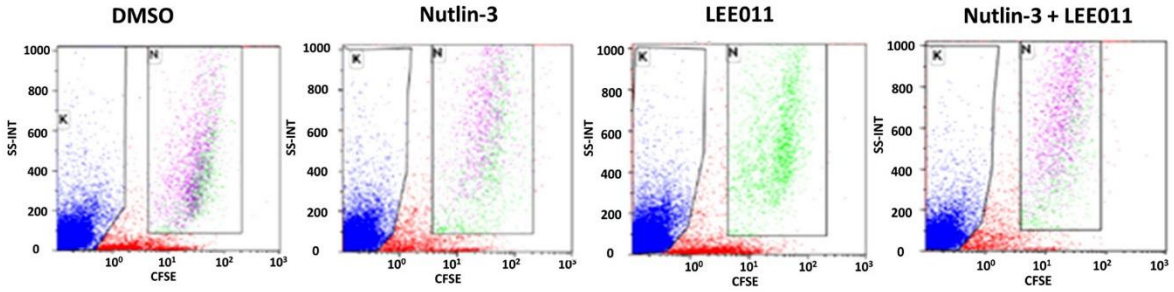

CFSE stained Tumor cells without NK cells

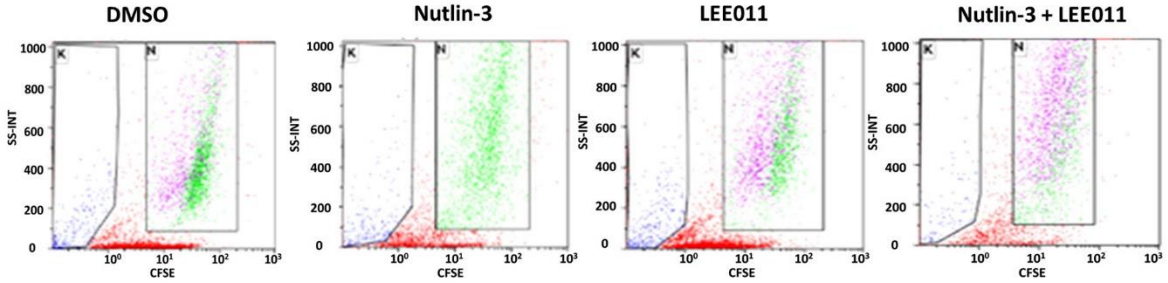

C

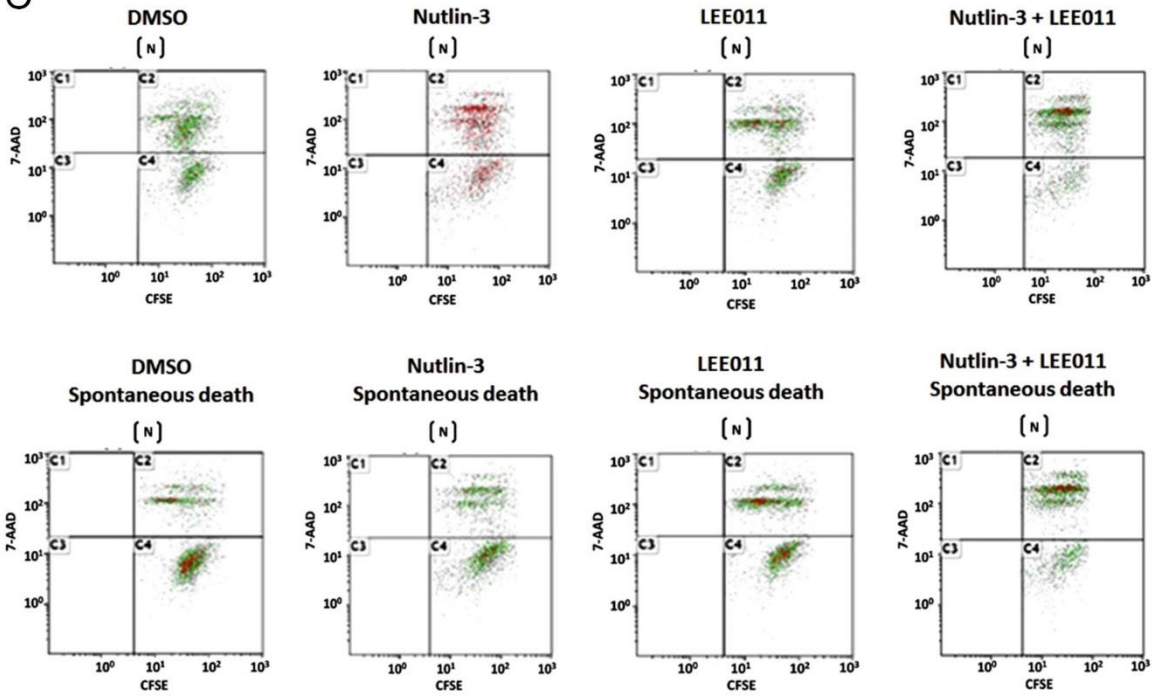

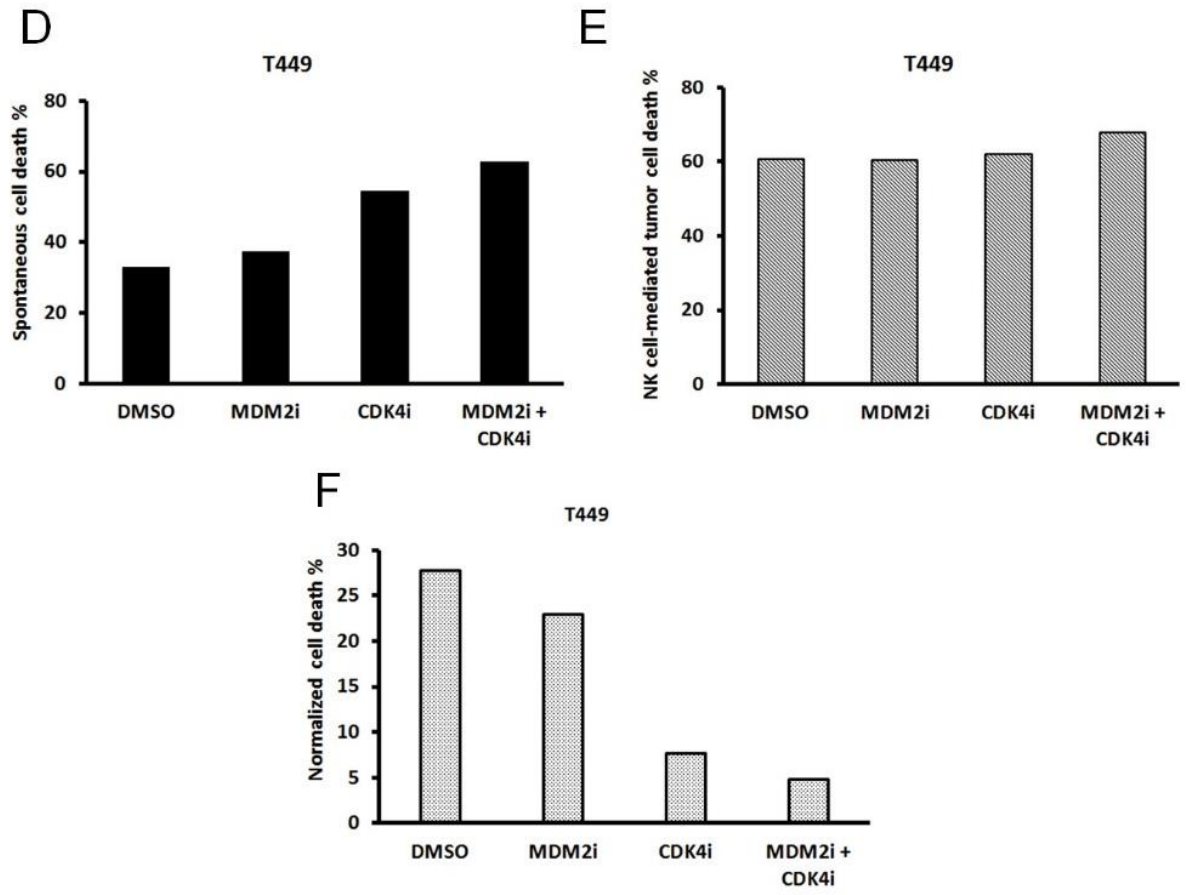

Figure 6.27: **Primary NK cell isolation and assessment of tumor cell lysis by NK cells**. **(A)** Scheme 1 and scheme 2 delineates the experimental design**. (B)** Scatter plot representing the CFSE stained tumor cells with or without NK cells. **(C)** Scatter plot representing the death of the CFSE stained liposarcoma cells with or without NK cells. Cell death was measured by 7-AAD. Bar graphs represent **(D)** spontaneous death (death of tumors cell without NK cells) **(E)** the extent of death of tumor cells by NK cells and **(F)** normalized death that implied death of tumor cells by the NK cells.

Target cells (liposarcoma cells) were plated and treated with targeted therapy (CDK4i, MDM2i or both) for 72h (Figure 6.27 scheme 2) and the drug-containing medium was washed off. Thereafter, the liposarcoma cells ($5x10^6$ cells/ml) were labeled with 2 nM CFSE for 10 min. Then NK cells were added to $5x10^4$ of CFSE-labeled liposarcoma cells at various effector to target ratios for 3 h. Following co-incubation of the effector cells (NK cells) and target cells, loss of vitality/integrity of the liposarcoma cells was measured by $7AAD^+$ staining.

$CFSE^+/7AAD^+$ cells were the readout for the death of liposarcoma cells in the mixed populations of liposarcoma and NK cells. The liposarcoma cells were treated with inhibitors prior to the NK cell-mediated lysis. Thus, the liposarcoma cells were vulnerable to spontaneous death. Spontaneous death of the target cells was measured without NK cell incubation (Figure 6.27 D). Measurement of NK cell-mediated lysis of

liposarcoma cells (Figure 6.27 F) were assessed by subtracting the spontaneous death (Figure 6.27 D) from the death (apoptosis) mediated by NK cell lysis (Figure 6.27 E). By the measurement of $CFSE^{+}/7AAD^{+}$, an enhanced level of liposarcoma cell death (by NK cells) was observed following treatment with combination of the inhibitors (Figure 6.27 E). However, spontaneous death was concomitantly high in combination treatment. This suggested that the liposarcoma cell death mediated by NK cells was not enhanced following treatment with targeted therapy. In this set of experiments, the selected dose used for inhibiting CDK4 and MDM2, was 2µM of the each inhibitors for treating T449 and the targeted therapy-mediated death (spontaneous death) was observed to be higher. In order to reduce the targeted therapy-mediated death, lower doses of the CDK4 (0.5µM) and MDM2 (0.5µM) inhibitors were employed for treating T449, followed by the measurement of the ligands. However, the expression of two (MICA and MICB) out three of the activation ligands tested, remained unperturbed by lowering the doses (Figure S 11.7). This excluded the possibility to use that set of lower doses for treating T449 and further targeting T449 with NK cell lysis.

In summary, this data implied that targeted therapy-driven upregulation of NKG2D ligands in tumor cells did not augment the vulnerability of the tumor cells to primary NK cell lysis.

7 Discussion:

For any anti-cancer modality, the ultimate goal is long-term eradication of the tumors. Chemotherapy and radiotherapy are integral components of therapeutic modalities. However, employment of these modalities is less tumor-specific and normal tissues are susceptible to cytotoxicity. Targeted therapies emerged to spare the normal tissue and treatment to be more tumor-specific. Targeted therapies were developed by exploiting the genetic aberrations present in tumor cells. Nevertheless, it is a prerequisite to further understand the genetic abnormalities involved in disease pathogenesis and employ concurrently the existing modalities to target cancer.

Liposarcoma harbors amplified *MDM2* (12q13~15) which is the known oncogenic driver of the pathogenesis of liposarcoma. Reactivating the tumor-suppressor activity of p53 has been demonstrated earlier to eradicate tumor cells and thus *TP53* has been an attractive target for drug development. Inhibition of the MDM2-p53 interaction with synthetic molecules might therefore, lead to the accumulation of active p53, followed by the apoptosis of tumor cells, as shown *in vitro* [206]. Along with *MDM2* amplification, *CDK4* has been detected to be invariably amplified (90%) of the cases of WDLPS/DDLPS. Recently, novel inhibitors of MDM2 (MDM2i; e.g. RG7112, RO-5503781, CGM097, HDM126) and CDK4 (CDK4i; Palbociclib, LEE011) have entered early clinical trials.

Single-agent trials have resulted in encouraging *proof-of-concept* findings, such as on-target effects within the therapeutic window. However, despite their clinical success by regressing the tumor growth, complete remission has not been rendered by these targeted therapies as single agents. The progressive and metastatic phases of LPS exhibit refractoriness to single agent treatments and are often fatal. Hence, it is conceivable that there is an urgent need for selection and application of multimodal approaches exploiting the genetic aberrations or dysregulated proteins in the tumor that could lead to an improved response.

In the current study, dysregulated pathways or genetic abnormalities in liposarcoma have been inhibited by the targeted therapies (as single agent and in combination) with concurrent employment of other existing modalities (radiotherapy and immunotherapy)

to observe the therapeutic response in terms of cellular phenotypic fates and perturbation of the signaling pathways.

7.1 Co-targeting the key oncogenic drivers (*MDM2* and *CDK4*) of liposarcoma cells did not lead to an additive effect

This study demonstrated no significant additive growth inhibitory effect in response to the combined targeting of the key oncogenes (*MDM2* and *CDK4*) in liposarcoma cell lines. SRB assay analysis revealed convergence of the curves (treated with MDM2i alone and in combination with CDK4i), which indicated a non-additive effect of the inhibitors in terms of growth inhibition (Figure 6.2). A narrow zone of additive effect was observed. However, it is questionable whether that narrow zone of additivity would translate to a clinical benefit. Cell cycle distribution demonstrated a reduction in G1 arrest with combination treatment (Figure 6.3). Apoptosis assay revealed no additive apoptotic fraction in response to the combination treatment (Figure 6.4). Senescence assay displayed no significant additive induction of senescence by the combined therapy (Figure S 11.2). Signaling pathway analysis by immunoblotting displayed a dose-dependent induction of the p53-p21 axis in the cell lines upon treatment with MDM2 inhibitor. Addition of CDK4 inhibitor to the MDM2i treated cells did not perturb the expression of p53 and p21. Immunoblotting of total RB in the cell lines was not constant (Figure 6.5).

Previous studies reported that MDM2 overexpression mediates RB degradation by proteasome-dependent and ubiquitin-independent manner [207]. Another study reported Nutlin-3 as a regulator of Rb protein level and Rb phosphorylation in which MDM2 plays a significant role [208].

Under the physiological situation, in response to any stress, MDM2-p53 interaction is disrupted [192]. Consequently, p53 is released, stabilized and executes its function *via* apoptosis and/or cell cycle arrest. Due to the existence of the cellular homeostasis, p53 for its own inhibition, transcriptionally upregulates MDM2 *via* autoregulatory feedback loop [209]. Upon upregulation, MDM2 negatively regulates p53 by inhibiting transactivation [14], ubiquitination and proteasomal degradation [15], or by sequestering p53 [67]. In contrast to the physiological situation, upon Nutlin-3 treatment, MDM2-p53 interaction is disrupted due to binding of Nutlin-3 in the N-

terminal region of MDM2 [210]. Consequently, p53 is alleviated from MDM2 interaction and reactivated. After executing its function, p53 promotes the upregulation of MDM2. Due to the presence of Nutlin-3, p53 binding site is inhibited and MDM2 is unable to exert its negative regulation over p53. However, Rb binds to the central acidic domain of MDM2 [211, 212] and as reported by the studies from Sdek et al., Rb is degraded *via* ubiquitin-independent and proteasome-dependent pathway [207]. As evident from the western blot (Figure 6.6), Rb was degraded by single-treatment of Nutlin-3 while Rb was restored upon co-treatment with Bortezomib (a proteasome inhibitor) in T449 and in T778. This study further supported the finding of Nutlin-3 mediated MDM2 accumulation, which in turn led to degradation of total Rb levels *via* proteasomal pathway. Additionally, this finding corroborated the importance of p53-independent function of upregulated MDM2.

Based on the *in vitro* finding, it could be stated that MDM2 inhibitor might lead to Rb degradation in liposarcoma cells that consequently rendered the tumor cells insensitive to CDK4 inhibitors due to the absence of Rb since Rb is the critical substrate for CDK4/6 enzymes [103, 213]. Consequently, inactivation of RB dictated the therapy outcome of CDK4/6 inhibitors as evident by previous existing experimental results which demonstrated RB-negative tumors (diverse other malignancies [27]) were resistant to CDK4 inhibitors.

As Rb was degraded by co-treatment with Nutlin-3, it was aimed to alter the sequence of inhibitors (Figure 6.7) in order to observe whether permutation of treatment schedules enhanced the efficacy of co-targeting. MTT assay results showed a dominant effect of MDM2 inhibitors in exerting an anti-proliferative effect. Addition of CDK4i in any sequence combination (pre or post) did not lead to a significant additive growth inhibition. Thus, additional factors other than Rb might contribute to the non-additivity of the combination treatment that needs additional investigation.

There are considerable amount of experimental results that showed combining MDM2 inhibitor along with genotoxic/cytostatic agents exerted additive/synergistic anti-proliferative effect *in vitro* in cancer [214-216].

In the current study, two non-genotoxic inhibitors were employed to assess the effects. From this study, it was conceivable that co-targeting of the key oncogenic drivers

should be considered with caution for clinical perspective. Proper dose selection for the combination treatment is a prerequisite for achieving the optimum therapeutic benefit. In contradiction to the current study, Laroche et al., [217] reported about synergistic anti-tumor effect in DDLPS by combined targeting of CDK4 and MDM2. However, Laroche et al., employed a separate set of liposarcoma cell lines and used RG-7388 as the MDM2 inhibitor for their studies.

7.2 *In vitro* radio-sensitization of WD/DDLPS by inhibition of MDM2

TP53 has long been known as tumor-suppressor and 'guardian' of the genome and responds to diverse stress stimuli by orchestrating specific cellular responses such as transient cell cycle arrest and senescence [218]. Both activating and inactivating mutations are reportedly known to be among the most frequent genetic abnormalities in cancer [219, 220].

Radiotherapy is one of conventional treatment options for liposarcoma but has limited efficacy alone. Moreover, it is well-documented that tumor types that harbor mutated *TP*53 or dysfunctional p53 pathway often exhibit radio-resistance [221]. Thus, wild-type *TP53* status and functional p53 signaling pathway are prerequisites for radiotherapy to execute its anti-proliferative efficacies [222].

There has been extensive body of investigations that described successful reactivation of p53 by Nutlin-3 in different types of cancer (laryngeal [223], lung [161], prostate [224]) which increased the susceptibility to radiotherapy *via* variable p53-dependent cell fate mechanisms like cell cycle arrest, apoptosis and senescence.

In this study it was examined whether MDM2 inhibition increased the vulnerability of the liposarcoma cells with wild-type *TP53* to ionizing radiation. The rationale of the study was to reactivate functional p53 by employment of small molecule inhibitor of MDM2. Irradiation of the liposarcoma cells would further enhance the cellular levels of functional p53 and mediate a p53-dependent treatment response.

From these studies, an enhancement of radiation response by Nutlin-3 was observed by long-term clonogenic assay in LPS853 and T778 (Figure 6.8) with SER value of 1.39 and 1.42 at $SF_{10,}$ respectively. For short-term readout after 48h, cells were

detected to be arrested at G2 (by DNA content) with concomitant enhancement in beta-galactosidase positive fractions following treatment with Nutlin-3 and **RT**.

By the experimental results in this study, it was evident that Nutlin-3 as a single agent inhibited the interaction between MDM2 and p53 with upregulation and stabilization of p53. P53 in its turn, led to upregulation of MDM2 by the autoregulatory negative feedback loop and downstream activation of p21 and thus confirming its reactivation. Combination treatment led to an increased activation of p53 and p21 as compared to radiation alone or to single-agent treatment in all the liposarcoma cell lines with wild-type *TP53* (Figure 6.10).

Caspase 3/7 assay (Figure 6.9) further revealed there was no change in the apoptotic population in Nutlin-3 and combination treatment in the liposarcoma cell lines (T778 $^{TP53\,WT}$ and LPS853 $^{TP53\,WT}$) after 24h. Hence, the radio-sensitizing effect in liposarcoma cell lines was not modulated through the process of apoptosis. Interestingly, Nutlin-3 mediated radio-sensitization effect *via* trigger of senescence has been described in laryngeal carcinoma [223] and thus these data reinforced the previously reported concept of the role of apoptosis-independent pathways in radio-sensitization effect exerted by Nutlin-3. However, p16 which is considered as one of the markers of senescence [225, 226], remained unperturbed in treated and untreated groups in the current study (Figure 6.9). One likely possibility is that presence of amplified *CDK4* which is an inhibitor of p16 [227, 228], might hinder the function of p16 by binding to it. In response to the treatment, p16 might undergo separation from CDK4 and induced senescence with the levels intact. This, however, warrants further intensive and detailed experimental investigation.

In contrast and as expected, SW872 (UDLPS), which has a mutated *TP53*, displayed SER_{10} = 1.02, was unable to transcribe and express p21 and promote cell phenotypic downstream effects such as cell cycle arrest or senescence in the treatment groups. Thus, the requirement of the wild-type *TP53* status is important when considering the application of MDM2 inhibition and radiotherapy in liposarcoma. However, not all the WD/DDLPS cells (harboring *MDM2* ^{Amp}/*TP53* ^{WT}) responded equally to MDM2 inhibition and RT. T449 displayed a SER_{10} value of 0.79 despite the MDM2-p53-p21 axis activation was similar to the other two cell lines. LPS141 (another DDLP) was not

considered for colony assays due to its inefficiency to grow as clones from single cells. Apoptotic response was observed to be similar in T449 and LPS141.

In order to determine whether application of MDM2i radio-sensitizes other sarcomas with amplified *MDM2* and wild-type *TP53*, the effect of Nutlin-3 and ionizing radiation was tested in GIST430 (gastrointestinal stromal tumors) and U2OS (osteosarcoma). Due to the wild-type *TP53* status, an induction of p53, upregulation of MDM2 and activation of p21 were detected by immunoblotting in GIST430 and U2OS. Despite short-term inhibition in cellular growth (Figure S 11.3) and activation of the MDM2-p53-p21 axis, no senescence induction was observed in GIST430 and U2OS (Figure 6.12).

Thus, activation of the MDM2-p53-p21 axis might not lead to senescence and radio-sensitization. The final fate might depend on other factors or genetic lesions specific to a cancer type.

Modulation of the cell cycle progression markers was different in liposarcoma cell lines (Figure 6.14) and other sarcoma (Figure 6.15) tested for the current study. Therefore, aberrations in cell cycle proteins in the different cell lines harboring *MDM2* amplification and wild-type *TP53* might dictate the therapy-driven fate.

7.3 Shift in ploidy based heterogeneity by emergence of clonally variant subpopulations in response to MDM2 inhibition and RT in liposarcoma cell lines

Previous studies reported that transient treatment with Nutlin-3 led to generation of 2N and 4N G1 arrested cells in cells with wild-type *TP53* in lung cancer and breast cancer [229]. Among this mixed population, the 4N cells opted for the permanent growth arrest while 2N cells retained the potential to resume proliferation [229].

In the present study, by FACS analysis it was observed that the cells were arrested in the G2/M phase (by 4N DNA content) of the cell cycle in response to Nutlin-3 (± RT). However, western blot studies of the cell cycle markers revealed that despite their 4N DNA content, they lacked the expression of the G2/M markers (Cyclin B1, Cyclin A, and phospho-histone H3 Ser-10) [100, 230, 231]. Instead, they expressed the G1 marker (cyclin D1) [100, 103, 232, 233]. Thus, these cells were not the real G2/M cells

as detected by the FACS analysis. These cells were defined as 4N G1 cells and were reportedly known in cancer [234] (Figure 6.14).

Following treatment and removal of MDM2 inhibitors, polyploid cells (>4N cells) were generated as measured by PI stain and Hoechst 33342 stain in liposarcoma cell lines with wild-type *TP53*. On removal of Nutlin-3 by washout studies, functional p53 was again inactivated. Consequently, the cells overcame 4N G1 arrest and resumed proliferation with generation of polyploid (>4N) cells. For cells with *TP53* mutation presence or absence of Nutlin-3 did not affect the cell cycle due to p53-dependent functioning of Nutlin-3.

Evolution of ploidy based variant subpopulations in response to Nutlin-3 have been reported earlier in other type of cancers [229]. This is the first report of recapitulation of that finding in liposarcoma cell lines with wild-type *TP53*. The process of Nutlin-3 mediated formation of tetraploid/polyploid cells has been described as endo-reduplication and associated with therapy resistance [229, 232, 235]. However, there are several processes of tetraploidy/polyploidy generation such as cell fusion, abortive cell cycle (karyokinesis failure or cytokinesis failure) and endo-reduplication [199]. Tetraploid/polyploid cells generated through endo-reduplication and karyokinesis failure harbor a single nucleus while cells emerging *via* cell fusion or cytokinesis failure possess multi-nuclei [234]. As the polyploid cells displayed to be multinucleated by DAPI stain (Figure 6.18 A), it excludes the possibility of the processes like endo-reduplication and karyokinesis failure. Thus, it is conceivable that the cells were generated either by cell fusion or by cytokinesis failure.

The low percentage of >4N populations in the un-treated or vehicle treated groups of liposarcoma (LPS853 and T778) cells provided the hint of pre-existing set of 4N cells in the tumor population describing intrinsic intra-tumoral ploidy based heterogeneity of liposarcoma (Figure S 11.10). Thus, 4N population isolated based on DNA content in response to the treatments in liposarcoma cells was a heterogeneous mixture of populations harboring potential three subpopulations; normal 4N G2 derived from 2N diploid cells, pre-existing intrinsic stable tetraploid cells and treatment generated 4N G1. The existence of polyploid cells has been reported by the cytogenetic analysis of primary WDLP samples from patients [236]. Thus, the observation of cells with intrinsic polyploidy correlated with clinical finding.

Therefore, it was difficult to elucidate the origin of >4N population that was observed after Nutlin-3 (± RT) treatment and removal. This might be result of enhanced proliferation from the existing intrinsic 4N G1 population or from the proliferation of tetraploid 4N G1 cells generated by the treatment (Nutlin-3 alone and Nutlin-3 plus RT) or it was a joint contribution.

7.4 Relative abundance of polyploid cells and their clonogenic impairment *via* increased senescence contributed to radio-sensitization in liposarcoma

Upon removal of drug-containing media, the LPS853 cells underwent division (48h of treatment and 48h washout) as evident by the >4N populations in Nutlin-3 treated and in the combination treatment despite the senescence-like phenotype (SLP) as observed by the beta-galactosidase staining after 48h (Figure 6.9). Previous studies have shown similar effects of p53 activation accompanied by senescence-like phenotype (SLP) by Nutlin-3 without induction of proper senescence [237, 238].

It was aimed to investigate about the chronological and ultimate long-term fate of the 2N, 4N and >4N subpopulations following therapy withdrawal and their potential contribution in exerting the radio-sensitizing effect of Nutlin-3 in liposarcoma cell lines by clonogenic assays.

In line with that, the long-term fates of the 2N, 4N, >4N (following Figure 6.16 scheme 1 and Figure 6.17 scheme 2) cells were assessed after isolating and keeping them for a prolonged period in the culture (12-17 days). In comparison to their 2N counterpart, the 4N and >4N cells displayed a ‘reproductively dead’ phenotype or attenuated clone forming potential. The 4N or >4N populations underwent few cycles of growth after therapy withdrawal as evident by the disperse patches or clumps (with <50 cells) among the proper colonies (defined by ≥ 50 cells) by the microscopic observation (Figure 6.19). However, they lost eventually their proliferative potential despite initial few phases of proliferation and this cessation of proliferation by the therapy effect was only visible after several days or by long-term assays like colony assay. For T778, a diminished proliferative potential of the 4N and >4N populations in the different treatment groups was observed with highest attenuation in the combination treatment. Furthermore, the relative abundance of >4N populations upon drug removal (in the

combination treatment group) also contributed to the observed radio-sensitizing effect. By senescence assay in T778, an enhanced level of beta-galactosidase positive cells was detected in the combination group confirming the mode of death by senescence as a long-term fate.

In contrast to LPS853 and T778, Nutlin-3 did not improve the radiation response in T449 as observed by SER_{10} value < 1, although this cell line is assumed to be genomically similar to T778. While the latter cell line was derived from a recurrent well-differentiated liposarcoma, T449 cell line was established from the same patient but from the primary tumor [6]. However, cell line characterization studies showed, in contrast to the T449 cells, T778 cells lack the ability for spontaneous adipocytic differentiation [6]. Differentiation is inversely correlated with radiosensitivity [239]. Thus, the difference in the differentiation status could be one of the attributors to the observed difference in radiosensitivity of the two cell lines that needs to be investigated.

For T449, the treatment-generated 4N cells and >4N cells have diverse fates as evident by these studies. The clonogenic ability of 4N and >4N subpopulations generated by Nutlin-3 plus RT in T449 is comparable to the 4N and >4N subpopulations generated by Nutlin-3 treatment alone (Figure 6.21). Consequently, no additive effect of RT to Nutlin-3 has been observed in T449 despite the generation of polyploid cells on treatment and removal like the other two liposarcoma cells (LPS853 and T778). Moreover, 2N subpopulation generated by Nutlin-3 treatment alone and by the combination treatment have lesser clonogenic ability than the 4N and >4N subpopulations (Figure 6.21). The additional or unidentified factors that attribute to the dichotomous clone forming potential have not been investigated by these studies. Intrinsic cellular traits might be the governing factors for the long-term fates of the subpopulations.

In the present study, therapy-driven long-term fate of the cells was assessed and it was observed that the cells initially underwent initial few rounds of cycles but eventually lost the clone forming potential when seeded as single cells. The reproductive death was mediated by the cellular fate of senescence as observed by the beta-galactosidase stain. The relative abundance of the tetraploid cells and their reduced

clone-forming ability after the combination treatment (Figure 7.1) ultimately led to the treatment effect in T778 and LPS853.

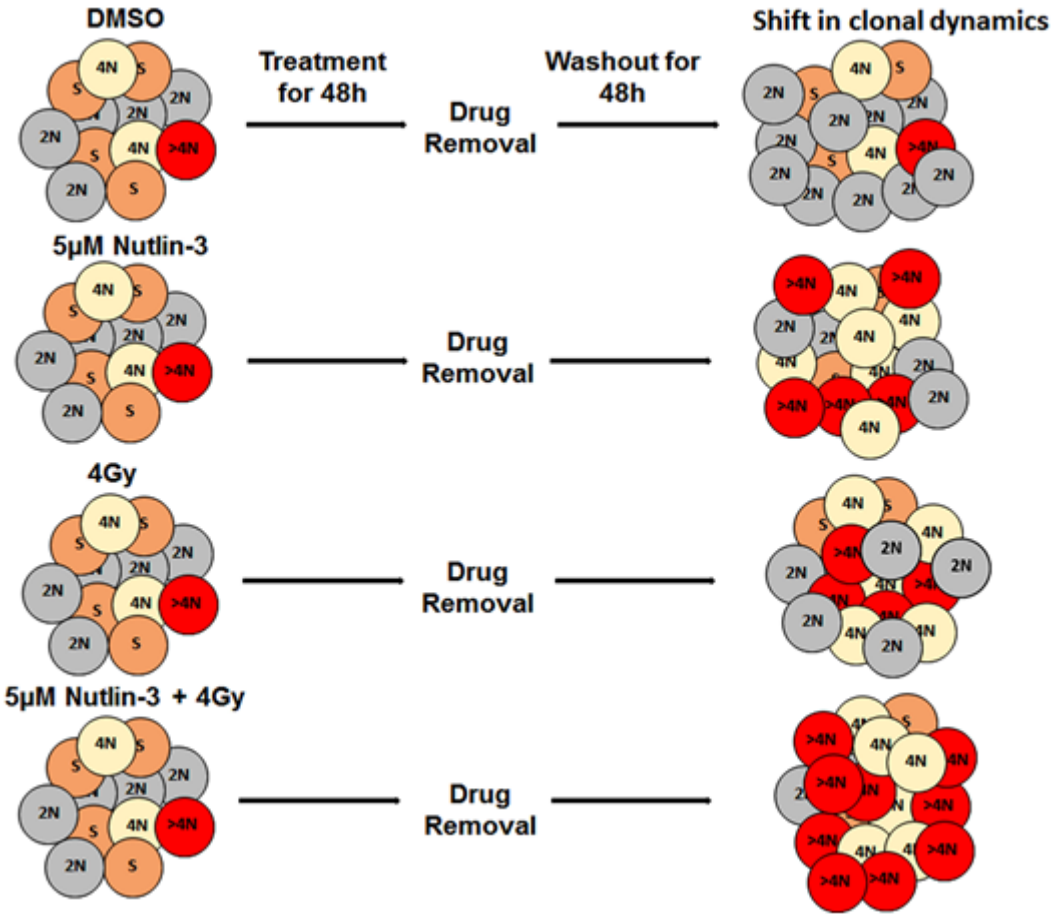

Figure 7.1: Schematic demonstrating the potential mechanism of treatment-driven ultimate fate in liposarcoma cell lines by shift of ploidy based heterogeneity and attenuation of clonal ability.

7.5 Wild-type *TP53* status is not the exclusive determinant of treatment (MDM2 inhibition and RT) driven fate in liposarcoma cell lines

By this current set of experiments, in context of liposarcoma cell lines, it could be stated that generation of polyploid cells in response to the treatment with MDM2 inhibition (± RT) is a p53-dependent phenomenon as it was evident in all the liposarcoma cell lines with wild-type *TP53* regardless of their susceptibility to RT. Conversely, in response to Nutlin-3 (± RT) treatment in the *TP53* mutated cell line, polyploid clones were not generated (Figure 6.14) which further reinforced the finding.

By existing research evidence in context of other tumors, it is reported that mitotic spindle agents, in contrast to MDM2 inhibitors, drives the cellular fate in a different way

by inducing polyploidy in the mutant *TP53* cells and preventing polyploidy in the wild-type *TP53* cells by inducing G1 tetraploid arrest. The cells with wild-type *TP53* status are able to halt themselves at G1 arrest following mitotic slippage by the virtue of their functional p53 while cells with non-functional p53 are unable to stop at G1 and enter the next S-phase with the generation of polyploid cells [176, 177]. Thus, formation of polyploid cells in a generalized context appears to be a biological event in response to a specific treatment independently of *TP53* status.

In the current study, for T449, tetraploid/polyploid cells did not display senescence. In contrast, for T778 and LPS853, tetraploid/polyploid cells displayed enhanced senescence. Thus, treatment-driven polyploid cells might lead to diverse fates depending on the additional traits of the cell type or concurrent trigger of the other pathways. This implied that for responsiveness to Nutlin-3 (± RT), p53-depedent polyploidy generation is essential but not the sole determinant of treatment-driven fate in liposarcoma (Figure 7.2).

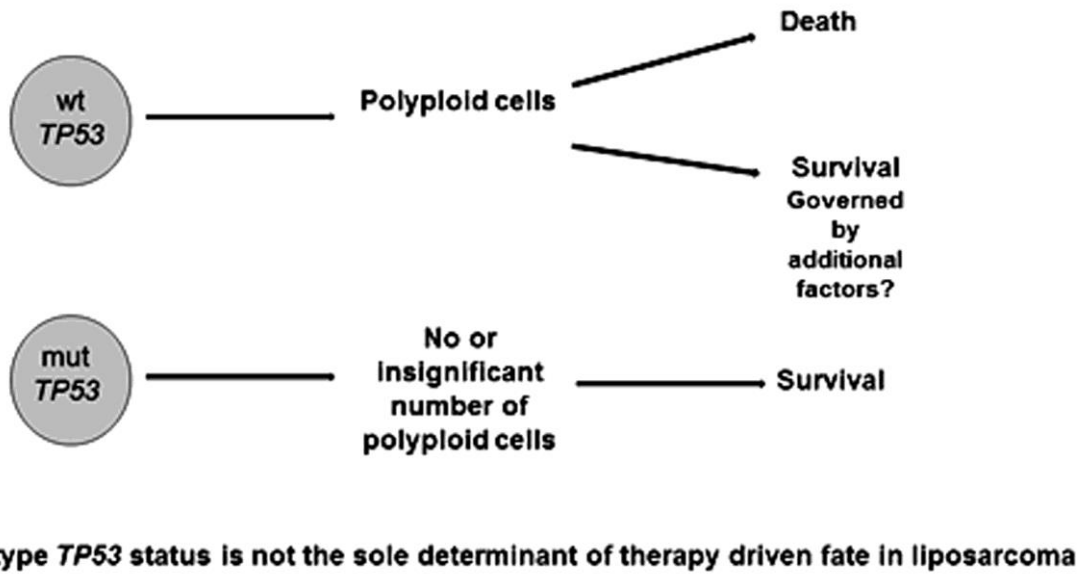

Figure 7.2: Scheme representing p53-dependent polyploidy generation and p53-independent cellular fate by MDM2 inhibition and RT in liposarcoma.

Tetraploid cells are mostly considered for contributors in therapy resistance and tumor development [240, 241]. Conversely, it has been demonstrated that tetraploid cells by the virtue of containing double the amount of p53-MDM2 complexes are more sensitive to Nutlin-3 treatment than their diploid counterparts [242]. In this study, the levels of

p53, MDM2 and p21 were not determined separately in diploid or tetraploid clones following treatment in liposarcoma cell lines. However, in the total population, p53 was induced and stabilized by Ser-15 phosphorylation in response to Nutlin-3 and Nutlin-3 plus RT, with an enhanced induction in the combination (Figure 6.10).

Restoration or reactivation of p53 in *TP53* deficient tumors has been reported to exert tumor suppressive effects by tumor regression and prolonged survival [243, 244]. However, the tumor suppressive effects were context dependent i.e. dependent on the type of genetic lesions driving carcinogenesis. For lymphomas, e.g., the tumor regression was mediated through apoptosis and for sarcomas; the mode of cessation of tumor growth was cellular senescence [245, 246]. The current set of experiments once again reinforced the finding of involvement of apoptosis-independent pathways in response to augmented p53 reactivation by co-treatment with MDM2 inhibition and RT in a subtype of sarcoma (i.e. liposarcoma). However, other sarcomas harboring *MDM2* ^{Amp}/*TP*53 ^{WT} did not respond to MDM2 inhibition and RT by induction of senescence despite upregulated expression of p53 and p21 (Figure 6.12). Thus, this study implies that treatment response not solely rely on the presence of wild-type *TP53* but other pathways or factors or tumor specific lesions might play a role in the responsiveness which warrants further investigation.

In synthesis, by this study, it could be demonstrated that combination treatment-induced enhanced tetraploid populations are adopting for senescence-like phenotype (SLP) or senescence-like growth arrest as detected by the senescence assay measured after short-term treatment (48h). However, the cells not entirely but partially were capable of reversing the senescence-like phenotype by resuming the cell proliferation and simultaneous generation of > 4N populations. Thus, there was a shift in clonal dynamics (See Figure 7.1) of the cells based on ploidy with > 4N being the most abundant. The 4N and >4N cells as separate subpopulations were ‘reproductively dead’ by the terminal fate following 15-17 days of culture after treatment removal. Consequently, the ultimate effect was displayed by the attenuated clonogenic ability of the polyploid cells which contributed to the radio-sensitizing effect in liposarcoma cell lines by the > 1 sensitizing enhancement ratio (SER).

Translational perspective:

Notably, the remnant solitary cells (Figure 6.19) with extended features ceased to proliferate or lack the clone forming ability. However, they were survivors of therapy. Therefore, it is a matter of investigation what they execute within the tumor or how they modulate the adjacent cells through paracrine effects by the secretory phenotype [247, 248]. Giant cells have been described to display senescence-like phenotypes and are potential cell populations to exhibit therapy resistance and escape [249, 250]. Moreover, the giant cells in the present study, due to their non-proliferative state contributed in lowering the denominator of SER and consequently increased the values of SER. Therefore, the generation of these set of 'giant polyploid cells' and their real effect within a tumor is debatable in context of clinical translation of MDM2 inhibition and RT in combination.

Theoretically, the use of MDM2 inhibitors in combination with radiotherapy predisposes the normal tissue to potential therapy-induced toxicity as those cells harbor wild-type *TP53* and all the components of p53 signalling axis intact. Conversely, it has been demonstrated that Nutlin-3 is being employed as part of 'cyclotherapy' [251] where it exerts a cytoprotective effect to the normal tissue from chemotherapy-induced toxicity by transiently arresting them in the cell cycle phases. The right representative (or cell lines) for normal tissue which has all the components of MDM2/p53/p21/p16 pathway intact or wild-type is still lacking. Liposarcoma cell lines retain tumorigenic potential for subcutaneous xenograft as demonstrated by some groups [6]. However, in our effort to develop subcutaneous xenograft models, two cell lines (LPS853 and T778) developed into palpable tumors following 4-6 weeks and regressed without any treatment (data not shown). Thus, those models were suboptimal for further evaluation of treatment modalities. Certain groups established patient-derived xenograft (PDX) subcutaneous models of well/de-differentiated liposarcoma [252]. Patient-derived orthotopic xenograft (PDOX) models of other soft-tissue sarcoma are established and reported to be more clinically relevant as they recapitulate the histology of original tumors [253]. However, PDOX models of liposarcoma have not been reported yet. Thus, it is difficult to predict the real consequences or side effects of combination treatment in a more clinically relevant setting.

Higher doses of Nutlin-3 (20µM) with concurrent application of RT (Figure S 11.8) in liposarcoma were also tested. A dose-dependent induction of p53 and downstream p21 with simultaneous upregulation of MDM2 were observed. However, apoptosis level remained unperturbed in combination with RT as measured by annexin V/7-AAD stain. Thus, increasing the doses of Nutlin-3 might not enhance radiosensitivity.

In liposarcoma cell lines with highly amplified *MDM2* and wild-type *TP53* (LPS141 and T449), Nutlin-3 protected the cells from radiation as observed by the apoptosis assay after 24h and with SER_{10} value < 1 for T449 (Figure 6.8). On a critical note, for executing a radio-sensitizing effect by Nutlin-3, an enhanced activation of $MDM2^{amp}$-p53-p21 signaling axis might not be the sole or exclusive axis that needs to be considered. MDM2-mediated p53-independent effects might play a compensatory role or exert a radio-protective effect by Nutlin-3 in liposarcoma cells with highly amplified *MDM2*. Overexpression of cyclin D1 has been reported to contribute to radio-resistance in several types of tumors [166, 254]. On the other hand, cyclin D1 is cell cycle regulatory protein and thus is temporally expressed depending on the cell cycle phase and serves as one of the G1 markers [213, 255, 256]. In the liposarcoma cells (LPS141 and T449) with high amplification of *MDM2*, basal levels of cyclin D1 were higher and in response to the treatments, levels remained unchanged. (Figure 6.14). On a speculative note, the intrinsic higher baseline expression could be the acting component in exerting the radio-protective effect in T449 and LPS141, which warrants further investigation. In the other two cell lines, LPS853 and T778, cyclin D1 was induced by Nutlin-3 and by combination treatment. This might be a consequence of shift in cell cycle distributions toward enhanced 4N G1 populations with acquired G1 cyclin markers. Thus, for the LPS853 and T778, cyclin D1 accumulation was the effect of augmented G1 population that might not contribute to any radio-protective effect. Prior to application of RT and Nutlin-3, it might be required to analyze the intrinsic cyclin D1 levels along with *MDM2* amplification and other MDM2-mediated, p53-independent effects that might exert a radio-protective effect, which warrants further investigation.

7.6 Inhibition of MDM2 in combination with ionizing radiation-induced enhanced senescence did not correlate with DNA damage

In the current study, an induction of gamma-H2AX was observed in the RT alone group and after combination treatment in LPS853 *TP53* WT and SW872 *TP53* Mut following 48h (Figure 6.23). The extent of induction of gamma-H2AX was comparable between RT and combination treatment groups independent of the *TP53* status of the cell lines. One of the implications could be that the addition of MDM2 inhibitor did not increase the levels of gamma-H2AX induced by ionizing radiation alone. This study once again indicated the role of Nutlin-3 as non-genotoxic. Thus, it could be stated that the enhanced senescence observed by the combined treatment was not mediated by DNA-damage. This indicated multiple contributing factors (e.g. MDM2-dependent cellular response to RT-induced DNA damage) which played role in the induction of senescence in LPS853 in response the combined treatment (Figure 7.3).

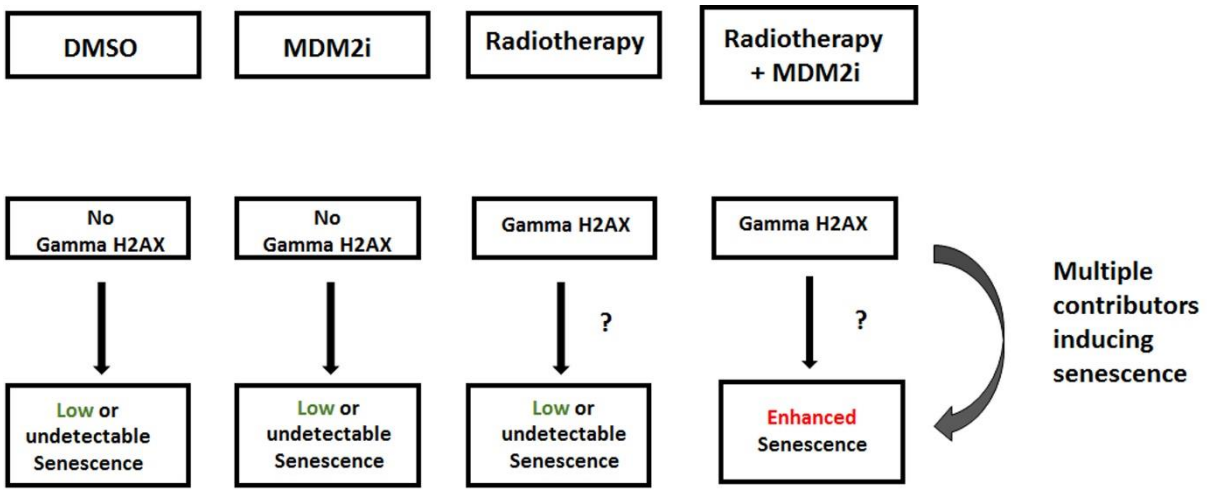

Figure 7.3 Scheme representing induction of senescence is not associated with DNA damage induction in liposarcoma in response to MDM2 inhibition and RT.

Paradoxically, increased levels of gamma-H2AX were observed in response to Nutlin-3 and combination treatment (Figure S 11.4) in T449 *TP53* WT and T778 *TP53* WT, which indicated toward Nutlin-3 as genotoxic in these cell lines. This remains unexplained why Nutlin-3 displayed two contrasting effects in LPS853 and in the other two cell lines (T449, T778). Certain experimental studies demonstrated that induction of gamma-H2AX was cell type-dependent [257]. In addition, some other studies reported that gamma-H2AX might appear without formation of DSBs. This was attributed to certain

stage of the cell cycle and activity of certain PIKK family kinase [258]. In this study, gamma-H2AX was measured in total lysates but not detected as gamma-H2AX foci. Thus, the observed gamma-H2AX in our study was whether due to DSB formation needs further investigation.

Furthermore, Nutlin-3 has been shown to delay double-strand break repair (homologous recombination) process that occurs during replication by activation of p53 [202]. Thus, the observed varied levels of gamma-H2AX (in T449 and T778) might be the consequence of presence and absence of the Nutlin-3 modifying the repair kinetics. However, T449 did not display senescence phenotype and the induction of senescence in T778 did not correlate with the observed gamma-H2AX. This once again indicated toward other contributing factors for the enhanced senescence independent of DNA damage induction in liposarcoma cells in this specific set of treatment.

It has been reported that cells with wild-type *TP53* status are faster in repairing the DSBs while cells with mutant *TP53* are less competent in repair [39]. Thus, it is expected that in cells with functional p53, the levels of residual gamma-H2AX should be lesser than in cells with mutant p53 following DNA damage e.g. application of RT. However, in the current pieces of experiments, the levels of gamma-H2AX in wild-type *TP53* and mutant *TP53* cell lines were comparable. The plausible explanation could be various genes involved in repair process might be upregulated or overexpressed in the cells with mutant *TP53* that might compensate for repair efficacy. On the other hand, cells with wild-type *TP53* might harbor defective repair genes. In the current experiments, the Rad51 protein (involved in HR repair pathway) was detected at a much higher level in the undifferentiated SW872 as compared to the liposarcoma cell lines (LPS853, T778 and T449). Based on this observation, by employing the concept analogous to ‘synthetic lethality’ [259], the PARP inhibitor (ABT-888) was used in combination with RT and clonogenic assays were performed in LPS853 and SW872. However, SER_{10} values for both of the cell lines were found to be comparable. This indicated that defect in either of the components i.e. low Rad51 expression or non-functional p53 might elicit the same response following PARP-1 inhibition (Figure 6.24). On a speculative note, it could be said that the ultimate balance of efficacy or

status of the repair genes and *TP53* status is the determinant of gamma-H2AX level in tumor cells that needs further investigation.

7.7 Targeting p53–independent pathway in liposarcoma cells did not show additive growth inhibition (Pilot study)

The MDM2 oncoprotein is a negative regulator of p53 [15] as it ubiquitinates and antagonizes p53. However, p53-independent effects of MDM2 [260] or a number of additional interaction partners and/or ubiquitination substrates for MDM2 have been reported [261, 262]. Little was known about the role of these interaction partners in the biological activities of MDM2, e.g., in MDM2-driven oncogenesis. By recent studies, several proteins of Polycomb Group (PcG) family have been identified which directly interact with MDM2. PcG proteins form polycomb repressive complexes PRC1 and PRC2. PRC2 (*via* EZH2) mediates histone 3 lysine 27 (H3K27) trimethylation, and PRC1 (*via* RING1B) mediates histone 2A lysine 119 (H2AK119) monoubiquitination which is often essential for stemness maintenance and cancer cell survival. Most of the MDM2-controlled genes also respond to the inactivation of the Polycomb Repressor Complex 2 (PRC2) and its catalyst component EZH2. MDM2 physically associated with EZH2 on chromatin, enhancing the trimethylation of histone 3 at lysine 27 and the ubiquitination of histone 2A at lysine 119 (H2AK119) at its target genes [260]. The p53-independent effects of MDM2 might contribute to oncogenesis of liposarcoma as it has amplified *MDM2* through the PRC2 and EZH2. MDM2 antagonists disrupt the function of p53 and MDM2 but do not interfere with the PcG family proteins which might contribute to oncogenesis as well. Based on these reports, it was addressed whether inhibiting both the p53-dependent and p53-independent pathways of the amplified/overexpressed MDM2 exert enhanced anti-proliferative effects in the liposarcoma cell lines. Growth inhibition in liposarcoma cell lines (LPS853, T778 and SW872) was measured following treatment with MDM2i, EZH2i and combination of both. Neither EZH2i alone nor in combination with MDM2i exerted an additive growth inhibition in the liposarcoma cell lines (Figure S 11.9). In liposarcoma cell lines, it is yet not validated whether EZH2 is expressed and contributes to the process of oncogenesis. This data indicates toward the possibility of EZH2 does not contribute to the disease pathogenesis of liposarcoma. However, it warrants further intensive investigation.

7.8 Targeting CDK4 did not sensitize liposarcoma cells to RT

CDK4 inhibitors, palbociclib and LEE011 have been in phase II clinical trial of liposarcoma [263, 264] and have shown compelling efficacies in breast cancer as well.

In this study, inhibition of CDK4 did not show radio-sensitization of liposarcoma cells. Earlier studies of the combination of CDK4 inhibitor and radiotherapy in a preclinical model of glioblastoma multiforme (GBM) demonstrated synergistic efficacy with prevention of cells entering to S-phase and inducing apoptosis [265]. Moreover, siRNA mediated silencing of CDK4 has been reported to radio-sensitize breast cancer cells *via* apoptosis without perturbing the cell cycle [163]. However, in this study, palbociclib as a single agent induced a strong G1 arrest and application of RT reduced the fraction arrested in G1. No significant change or increase in the apoptosis (sub G1) was noted in response to combination treatment. On a speculative note, CDK4 inhibition-driven cell cycle arrest in liposarcoma cells might provide an advantage for repairing RT-mediated DNA damage.

7.9 Targeted therapy-driven upregulation of NKG2D ligands in liposarcoma cells

The first part of the study demonstrated an upregulation of certain groups of NK cell ligands (corresponding to the NKG2D activation receptors) with concomitant downregulation of inhibitory ligands upon treatment with targeted therapy. This built up the rationale for exploring the susceptibility of tumor cells to NK cell lysis and potential employment of NK cell-based immunotherapy in an allogeneic setting for the treatment of liposarcoma following targeted therapy.

By this study, MICA, MICB and ULBP2 were found to be upregulated in response to the treatment with CDK4 inhibitor, MDM2 inhibitor and in combination in T449 cells (derived from the primary tumor). In contrast, T778 cells (derived from the recurrent tumor of the same patient) did not express NKG2D ligands (Figure 6.26). Those ligand molecules are expressed as response to stress such as infection, heat-shock, or DNA damage induction. On the other hand, p53 activation or ectopic expression has been shown to induce one of the NKG2D ligands like ULBP1 and ULBP2 [266, 267]. In this study, the MDM2 antagonist, Nutlin-3, which acts through activating p53 might be

contributing to the upregulation of ULBP2 in T449 cells when treated alone or in combination with CDK4 inhibitor. The ligands are responsible for activating the activation receptors present on NK cell surface. In addition, HLA-ABC, which is the ligand for inhibitory receptor was observed to be downregulated in response to the treatment when compared to vehicle treated cells. This further reinforced the rationale for examining the sensitization of liposarcoma cells to NK cell therapy

The cell line T778 lacked intrinsic expression as well as therapy-driven expression of NKG2D ligands as observed by the experiments. The expression of NKG2D ligands on tumor cells is observed early in the process of tumorigenesis [268, 269]. Tumors with metastatic potential often downregulate NKG2D ligands to escape immune surveillance [270]. Several mechanisms can be involved such as intracellular retention of NKG2D or shedding of the ligands. For cells of solid tumors like melanoma cells, intracellular retention of immature MICA molecules within the endoplasmic reticulum has been reported [271]. For the ligand shedding mechanism, it has been documented that tumor cells release MIC and ULBP molecules by proteolytic cleavage from the cell surface or as exosome bound molecules [270]. The intracellular expression of the NKG2D ligands or the secretory forms in the media of the cell line was not studied in these experiments to confirm the mode of losing the ligands.

NK cell-mediated lysis of neuroblastoma cells and ovarian carcinoma cells were reported to be dependent on the interaction of DNAM-1 with its ligands [272, 273]. CD155 (PVR) expression, which is the ligand for DNAM-1 activating adhesion receptors on NK cells, was also tested in the current study. The expression of CD155 in liposarcoma cell lines was measured to be low intrinsically and remained unperturbed in response to treatment.

7.10 Therapy-driven upregulation of NKG2D ligands in tumor cells did not sensitize them to primary NK cell lysis

Next, the potential recognition and lysis by resting allogeneic NK cells was investigated for the cell line T449 following inhibition of CDK4, MDM2 and both (Figure 6.27). The vehicle treated or untreated cells were lysed more frequently by the NK cells than the treated ones despite having high HLA-I expression and low NKG2D activation ligands expression.

As evident from the literature and by the previously reported experimental studies, NK cell-mediated lysis depends on the balance of activation or inhibitory ligands on the surface of tumor cells. Therefore, the susceptibility might depend on the activation of combined set of activation ligands or downregulation of inhibitory ligands which is a tumor-specific response [274]. The intrinsic expression of the other ligands (e.g. NCR ligands) might play role in modulating the response in untreated ones.

Another possible reason could be the primary NK cells ($CD56^{+}CD3^{-}$) isolated from healthy donor were heterogeneous as it consisted of $CD56^{+bright}$ and $CD56^{+dim}$ subpopulations. $CD56^{+dim}$ populations are the abundant one and with natural cytotoxicity. Thus, the mixed populations of NK cells derived from the healthy donors might exert varied cytotoxicity depending on the relative abundance of cytotoxic $CD56^{+dim}$ cells, which might in turn influence the results.

Based on these experiments, it could be stated that potential application of adoptive primary NK cell-based therapy following targeted therapy (CDK4i and MDM2i) treatment did not mediate recognition and lysis of tumor cells. Determination of expression and role of other inhibitory receptor ligands evading the tumor recognition and lysis remains to be explored.

In a pilot study, therapy-driven modulation of PDL-1 was determined in liposarcoma following targeted therapy. Experimental results displayed an enhanced expression of PDL-1 in one of the cell lines in response to MDM2 inhibition (Figure S 11.11). However, due to the reduced expression of HLA-ABC, it remained elusive whether tumor cells would be recognized with HLA-restricted T cells.

8 Zusammenfassung:

Nach den unbefriedigenden Erfolgen der Standardverfahren (Operation, Chemotherapie und Strahlentherapie) zur langfristigen Behandlung von Liposarkomen, wurden gezielt tumorspezifische Therapien für die Behandlung von Patienten mit Tumoren insbesondere des Subtyps gut differenziert / de-differenziert (WD / DDLPS) entwickelt. Therapeutische Ansätze mit Einzelwirkstoffen, die auf die Aktivität der wichtigsten krankheitsrelevanten Onkogenprodukte MDM2 oder CDK4 abzielten, zeigten vielversprechende Ergebnisse. Jedoch ist die klinische Wirksamkeit der eingesetzten pharmakologischen Inhibitoren noch sehr begrenzt. Deshalb wurden aufgrund der genetischen Anomalien in dieser Arbeit verschiedene Ansätze entwickelt, um solche Inhibitoren mit gleichzeitiger Anwendung bestehender Therapien (Strahlentherapie, Immuntherapie) zu kombinieren, um eine verbesserte Wirkung zu erzielen. Parallel dazu wurde die Therapie-gesteuerte Modulation von Signalwegen und der Phänotyp des induzierten Zelltods in einer Reihe von Liposarkom-abgeleiteten Zelllinien in vitro untersucht.

Basierend auf der Anwesenheit von Schlüssel-Onkogenen wurde untersucht, ob die Ko-Inhibierung von CDK4 und MDM2 zu einer verstärkten anti-proliferativen Wirkung bei Liposarkom-Zelllinien führte. Die Ergebnisse der Studie zeigten ungestörte Signalwege mit nicht-additiven Effekten durch die Ko-Inhibierung beider Proteine. Darüber hinaus deutet die Studie auch auf einen MDM2-vermittelten Abbau des Retinoblastom (RB) -Proteins hin, der die Zellen gegenüber CDK4-Inhibitoren unempfindlicher gemacht haben könnte. Die Sequenzveränderung der Inhibitoren zeigte jedoch keine signifikante Verstärkung der Wachstumshemmung, was darauf hinweist, dass der RB-Abbau nicht der Hauptgrund für die beobachtete Nichtadditivität ist. Somit kann gefolgert werden, dass ein “Co-Targeting“ von CDK4 und MDM2 keine synergistische Wachstumshemmung in Liposarkomzellen ausübt.

Als nächstes wurde untersucht, ob die MDM2-Hemmung in TP53-Wildtyp-Liposarkom-Zelllinien ihre Empfindlichkeit gegenüber der Behandlung mit ionisierender Strahlung erhöhte. Es wurde die Hypothese aufgestellt, dass die MDM2-Inhibierung die MDM2-p53-Interaktion unterbrechen und das Wildtyp-funktionelle p53 reaktivieren würde. Der Zusatz von Strahlentherapie würde diese Wiederherstellung von funktionellem p53 weiter verstärken, was zu einem verstärkten p53-vermittelten Zelltod führen könnte. Um diese Hypothese zu beweisen, wurden TP53-Wildtyp- und TP53-mutierte Liposarkom-Zelllinien untersucht. Die Ergebnisse dieser Studie zeigten eine durch MDM2-Hemmung herbeigeführte radiosensitivierung von zwei der Zelllinien mit Wildtyp-TP53. Die Apoptose blieb ungestört, jedoch wurde ein erhöhtes Seneszenz-vermitteltes terminales Schicksal als Reaktion auf eine Kombinationstherapie beobachtet. Gleichzeitig wurde eine verstärkte Hochregulation der MDM2-p53-p21-

Signalachse beobachtet. Im Gegensatz dazu waren Liposarkomzellen mit mutiertem TP53 nach MDM2-Inhibierung nicht erhöht Strahlungs-empfindlich. Darüber hinaus zeigten TP53-Mutantenzellen ungestörte Signalgebung, Apoptose und Seneszen, was bestätigt, dass für die Radio-Sensitivierung funktionelles TP53 erforderlich ist. Die Auswertung von Zellzyklusmarkern und die DNA-Gehaltsanalyse zeigten das Auftreten von p53-abhängiger Ploidie-basierter klonaler Heterogenität als Reaktion auf die MDM2-Inhibitoren in Abwesenheit oder Anwesenheit einer Strahlentherapie in allen Zelllinien mit Wildtyp-TP53. Die relative Häufigkeit von 4N- und >4N-Populationen war als Reaktion auf die Kombinationsbehandlung offensichtlich. Sortierung und Zelltodanalyse dieser polyploiden Subpopulationen zeigten jeweils abgeschwächte Klon-bildende Fähigkeit und erhöhte Seneszenz in den zwei Zelllinien mit Wildtyp-TP53, welche eine Radio-Sensitivierung zeigten. Die kombinierte therapiegetriebene relative Häufigkeit der polyploiden Populationen und ihre reduzierte Klonbildungsfähigkeit mit gleichzeitiger Seneszenz führten zu dem letztendlichen Effekt. In einer der Liposarkom-Zelllinien (mit Wildtyp-TP53), die nach Blockade von MDM2 nicht bestrahlungsempfindlicher war, zeigte die durch FACS-Sortierung isolierte polyploiden Zellfraktion ein Langzeit-Überleben und keine Seneszenz-Induktion. Diese Befunde weisen darauf hin, dass funktionelles p53 zwar eine Voraussetzung, aber nicht die alleinige Determinante für eine MDM2-abhängige Resistenz gegenüber ionisierender Strahlung ist, sondern weitere p53-unabhängige Faktoren das Zellschicksal bestimmen.

Als nächstes wurde die Empfindlichkeit der Liposarkom-Zelllinien gegenüber ionisierender Strahlung nach Behandlung mit CDK4-Inhibitoren getestet. Die Ergebnisse der Studie zeigten, dass die CDK4-Inhibierung nicht zu einer Radio-Sensitivierung der Zellen führte. Daher kann diese Kombination nicht als sinnvoller therapeutischer Ansatz angesehen werden.

Zuletzt wurden Behandlungs-induzierte Veränderungen im Expressionsmuster der NKG2D und DNAM-1-Liganden in Liposarkom-Zelllinien untersucht, um den möglichen Einfluss auf eine nachfolgende allogene NK-Zell-vermittelte Erkennung und Lyse zu analysieren. Die Ergebnisse der Studie zeigten nach dem funktionellen Block von CDK4 und MDM2 erhöhte und verringerte Expressionen von Aktivator-NKG2D-Liganden bzw. dem inhibitorischen NK-Zell-Liganden in einer der Zelllinien. Funktionelle Tests durch primäre NK-Zell-vermittelte Lyse der Tumorzellen zeigten jedoch einen verstärkten Zelltod lediglich in der unbehandelten Gruppe. Daher sind weitere Untersuchungen zur intrinsischen Modulation / Expression von NKG2D-unabhängigen Aktivierungsliganden und anderen inhibitorischen NK-Zell-Liganden in Liposarkom-Zellinien erforderlich.

Insgesamt erklären diese Daten 1) potentielle Wirksamkeiten oder Ausfälle, die durch Inhibitoren hervorgerufen werden, die auf den tumorspezifischen genetischen Hintergrund abzielen, und 2) wie eine gezielte Therapie-gesteuerte Modulation der

Signalwege in Liposarkom-Zelllinien diese für bestehende therapeutische Modalitäten anfällig macht. Die Ergebnisse dieser Studie tragen auch dazu bei, besser zu verstehen, wie neue Therapien gegenüber den bestehenden Therapien ausgewählt werden können oder welche möglichen Änderungen für eine verbesserte Reaktion erforderlich sind.

9 Summary

Following the failure of the standard modalities (surgery, chemotherapy, and radiotherapy) for long-term eradication of tumors, tumor-specific targeted therapies emerged for the treatment of patients with liposarcoma in particular of subtype well-differentiated/de-differentiated (WD/DDLPS). Therapeutic approaches with single agents targeting the activity of the key disease-related oncogene products *MDM2* or *CDK4* displayed encouraging results. However, the clinical efficacy of these pharmacological inhibitors is still quite limited. To this end, based on the presence of the genetic abnormalities, several rationales were designed to combine such inhibitors with concurrent application of existing therapies (radiotherapy, immunotherapy) in order to achieve an improved response. In parallel, the therapy-driven modulation of signaling pathways and phenotypic cellular fates were studied in a set of liposarcoma-derived cell lines *in vitro*.

Based on the presence of key oncogenes, it was examined whether co-inhibition of CDK4 and MDM2 led to an enhanced anti-proliferative efficacy in liposarcoma cell lines. The findings of the study demonstrated unperturbed signaling pathways with non-additive effects by co-inhibition. This study also indicated MDM2-mediated degradation of the retinoblastoma (RB) protein, which might have rendered the cells insensitive to CDK4 inhibitors. However, sequence alteration of inhibitors revealed no significant enhancement of growth inhibition, which indicated RB degradation not to be the primary cause of observed non-additivity. Thus, it could be stated that co-targeting of CDK4 and MDM2 might not exert a synergistic growth inhibition in liposarcoma cells.

Next, it was evaluated whether MDM2 inhibition in *TP53* wild-type liposarcoma cell lines enhanced the susceptibility of tumor cells to the treatment with ionizing radiation. It was hypothesized that MDM2 inhibition would disrupt the MDM2-p53 interaction and reactivate the wild-type functional p53. Addition of radiation treatment would further augment this restoration of functional p53 which might lead to enhanced p53-mediated cellular fates. To prove this, *TP53* wild-type and *TP53* mutant liposarcoma cell lines were tested. The results of this study demonstrated an *in vitro* radio-sensitization of two of the cell lines harboring wild-type *TP53* by MDM2 inhibition. Apoptosis remained unperturbed but increased senescence-mediated terminal fate was observed in response to combination treatment. An enhanced upregulation of MDM2-p53-p21

signaling axis was noted concomitantly. In contrast, cells with mutant *TP53* were not susceptible to radiation following MDM2 inhibition. Furthermore, *TP53* mutant cells displayed unperturbed signaling, apoptosis, and senescence confirming the requirement of functional *TP53* for radio-sensitization. Assessment of cell cycle markers and DNA content analysis revealed the emergence of p53-dependent ploidy based clonal heterogeneity in response to the MDM2 inhibitors in absence or presence of radiation in all cell lines with wild-type *TP53*. Relative abundance of 4N and >4N populations were evident in response to the combination treatment. Sorting and eventual fate analysis of these polyploid subpopulations displayed attenuated clone-forming ability and increased senescence in the two cell lines with wild-type *TP53* that displayed radio-sensitization. Thus, combined therapy-driven relative abundance of the polyploid populations and their attenuated clone -forming ability with concomitant senescence led to the ultimate effect. However, in one of the liposarcoma cell lines (with wild-type *TP53)* which was not susceptible to radiation following blockade of MDM2, sorting and long-term fate analysis of the polyploid cells displayed survival and no senescence induction. Thus, this study indicates functional p53 as a prerequisite for the response but not the sole determinant and p53-independent factors might govern the final fate.

Next, the vulnerability of the liposarcoma cell lines to ionizing radiation was tested following treatment with CDK4 inhibitors. The results of the study demonstrated CDK4 inhibition did not lead to radio-sensitization of liposarcoma cell lines. Thus, this combination might not be considered as a promising therapeutic approach.

Next, the therapy-driven expression pattern of the NKG2D ligands and DNAM-1 ligands in liposarcoma cell lines was elucidated for targeting them to subsequent allogeneic NK cell-mediated recognition and lysis. The findings of the study demonstrated increased and decreased expressions of activator NKG2D ligands and the inhibitory NK cell ligand, respectively, in one of the cell lines derived from primary liposarcoma tumors, following functional block of CDK4 and MDM2. However, functional assays by primary NK cell-mediated lysis of tumor cells demonstrated enhanced death of tumor cells in the untreated group. Thus, further investigation about the intrinsic modulation/expression of NKG2D-independent activation ligands and other inhibitory NK cell ligands in liposarcoma cell lines is mandatory.

Altogether, these data explain 1) toward potential efficacies or failures elicited by inhibitors targeting the tumor-specific genetic background and 2) how targeted therapy -driven modulation of the pathways in liposarcoma cell lines make them vulnerable to existing therapeutic modalities. The findings of this study also aid to better understand how new therapies could be selected over the existing ones or potential modifications that are pre-requisites for an improved response.

10 Reference

1. Coindre, J.M., *[New WHO classification of tumours of soft tissue and bone].* Ann Pathol, 2012. **32**(5 Suppl): p. S115-6.
2. Conyers, R., S. Young, and D.M. Thomas, *Liposarcoma: molecular genetics and therapeutics.* Sarcoma, 2011. **2011**: p. 483154.
3. Zambo, I. and K. Vesely, *[WHO classification of tumours of soft tissue and bone 2013: the main changes compared to the 3rd edition].* Cesk Patol, 2014. **50**(2): p. 64-70.
4. Matushansky, I., et al., *Derivation of sarcomas from mesenchymal stem cells via inactivation of the Wnt pathway.* J Clin Invest, 2007. **117**(11): p. 3248-57.
5. Dodd, L.G., *Update on liposarcoma: a review for cytopathologists.* Diagn Cytopathol, 2012. **40**(12): p. 1122-31.
6. Stratford, E.W., et al., *Characterization of liposarcoma cell lines for preclinical and biological studies.* Sarcoma, 2012. **2012**: p. 148614.
7. Henricks, W.H., et al., *Dedifferentiated liposarcoma: a clinicopathological analysis of 155 cases with a proposal for an expanded definition of dedifferentiation.* Am J Surg Pathol, 1997. **21**(3): p. 271-81.
8. McCormick, D., et al., *Dedifferentiated liposarcoma. Clinicopathologic analysis of 32 cases suggesting a better prognostic subgroup among pleomorphic sarcomas.* Am J Surg Pathol, 1994. **18**(12): p. 1213-23.
9. Hasegawa, T., et al., *Dedifferentiated liposarcoma of retroperitoneum and mesentery: varied growth patterns and histological grades--a clinicopathologic study of 32 cases.* Hum Pathol, 2000. **31**(6): p. 717-27.
10. Fletcher, C.D.M., et al., *Correlation between clinicopathological features and karyotype in lipomatous tumors - A report of 178 cases from the chromosomes and morphology (CHAMP) collaborative study group.* American Journal of Pathology, 1996. **148**(2): p. 623-630.
11. Iwasaki, H., et al., *Supernumerary ring chromosomes and nuclear blebs in some low-grade malignant soft tissue tumours: atypical lipomatous tumours and dermatofibrosarcoma protuberans.* Virchows Arch, 1998. **432**(6): p. 521-8.
12. Garsed, D.W., A.J. Holloway, and D.M. Thomas, *Cancer-associated neochromosomes: a novel mechanism of oncogenesis.* Bioessays, 2009. **31**(11): p. 1191-200.
13. Pedeutour, F., et al., *Structure of the supernumerary ring and giant rod chromosomes in adipose tissue tumors.* Genes Chromosomes & Cancer, 1999. **24**(1): p. 30-41.
14. Momand, J., et al., *The mdm-2 oncogene product forms a complex with the p53 protein and inhibits p53-mediated transactivation.* Cell, 1992. **69**(7): p. 1237-45.
15. Moll, U.M. and O. Petrenko, *The MDM2-p53 interaction.* Mol Cancer Res, 2003. **1**(14): p. 1001-8.
16. Segura-Sanchez, J., et al., *Chromosome-12 copy number alterations and MDM2, CDK4 and TP53 expression in soft tissue liposarcoma.* Anticancer Res, 2006. **26**(6C): p. 4937-42.
17. Arlotta, P., et al., *Transgenic mice expressing a truncated form of the high mobility group I-C protein develop adiposity and an abnormally high prevalence of lipomas.* J Biol Chem, 2000. **275**(19): p. 14394-400.
18. Italiano, A., et al., *HMGA2 is the partner of MDM2 in well-differentiated and dedifferentiated liposarcomas whereas CDK4 belongs to a distinct inconsistent amplicon.* International Journal of Cancer, 2008. **122**(10): p. 2233-2241.
19. Xi, Y., et al., *HMGA2 promotes adipogenesis by activating C/EBP beta-mediated expression of PPAR gamma.* Biochemical and Biophysical Research Communications, 2016. **472**(4): p. 617-623.
20. Barretina, J., et al., *Subtype-specific genomic alterations define new targets for soft-tissue sarcoma therapy.* Nat Genet, 2010. **42**(8): p. 715-21.

21. Santarius, T., et al., *A census of amplified and overexpressed human cancer genes.* Nat Rev Cancer, 2010. **10**(1): p. 59-64.
22. Park, J.H. and R.G. Roeder, *GAS41 is required for repression of the p53 tumor suppressor pathway during normal cellular proliferation.* Molecular and Cellular Biology, 2006. **26**(11): p. 4006-4016.
23. Zhang, K.Q., et al., *Amplification of FRS2 and Activation of FGFR/FRS2 Signaling Pathway in High-Grade Liposarcoma.* Cancer Research, 2013. **73**(4): p. 1298-1307.
24. Mariani, O., et al., *JUN oncogene amplification and overexpression block adipocytic differentiation in highly aggressive sarcomas.* Cancer Cell, 2007. **11**(4): p. 361-74.
25. Chibon, F., et al., *ASK1 (MAP3K5) as a potential therapeutic target in malignant fibrous histiocytomas with 12q14-q15 and 6q23 amplifications.* Genes Chromosomes & Cancer, 2004. **40**(1): p. 32-37.
26. Coindre, J.M., F. Pedeutour, and A. Aurias, *Well-differentiated and dedifferentiated liposarcomas.* Virchows Arch, 2010. **456**(2): p. 167-79.
27. Crago, A.M., et al., *Copy Number Losses Define Subgroups of Dedifferentiated Liposarcoma with Poor Prognosis and Genomic Instability.* Clinical Cancer Research, 2012. **18**(5): p. 1334-1340.
28. Wu, Y.V., et al., *Restoration of C/EBPalpha in dedifferentiated liposarcoma induces G2/M cell cycle arrest and apoptosis.* Genes Chromosomes Cancer, 2012. **51**(4): p. 313-27.
29. Rubin, B.P. and C.D. Fletcher, *The cytogenetics of lipomatous tumours.* Histopathology, 1997. **30**(6): p. 507-11.
30. Yang, S., et al., *Fused in sarcoma/translocated in liposarcoma: a multifunctional DNA/RNA binding protein.* Int J Biochem Cell Biol, 2010. **42**(9): p. 1408-11.
31. Rychly, B., H. Sidlova, and D. Danis, *[The 2007 World Health Organisation classification of tumours of the central nervous system, comparison with 2000 classification].* Cesk Patol, 2008. **44**(2): p. 35-6.
32. Park, J.O., et al., *Predicting outcome by growth rate of locally recurrent retroperitoneal liposarcoma: the one centimeter per month rule.* Ann Surg, 2009. **250**(6): p. 977-82.
33. Tseng, W.W., et al., *Novel systemic therapies in advanced liposarcoma: a review of recent clinical trial results.* Cancers (Basel), 2013. **5**(2): p. 529-49.
34. Harrison, L.B., et al., *Long-term results of a prospective randomized trial of adjuvant brachytherapy in the management of completely resected soft tissue sarcomas of the extremity and superficial trunk.* Int J Radiat Oncol Biol Phys, 1993. **27**(2): p. 259-65.
35. Pisters, P.W., et al., *Long-term results of a prospective randomized trial of adjuvant brachytherapy in soft tissue sarcoma.* J Clin Oncol, 1996. **14**(3): p. 859-68.
36. Lietman, S.A., *Soft-tissue sarcomas: Overview of management, with a focus on surgical treatment considerations.* Cleve Clin J Med, 2010. **77 Suppl 1**: p. S13-7.
37. Huang, X., H.D. Halicka, and Z. Darzynkiewicz, *Detection of histone H2AX phosphorylation on Ser-139 as an indicator of DNA damage (DNA double-strand breaks).* Curr Protoc Cytom, 2004. **Chapter 7**: p. Unit 7 27.
38. Rogakou, E.P., et al., *DNA double-stranded breaks induce histone H2AX phosphorylation on serine 139.* Journal of Biological Chemistry, 1998. **273**(10): p. 5858-5868.
39. Kuo, L.J. and L.X. Yang, *gamma-H2AX - A novel biomarker for DNA double-strand breaks.* In Vivo, 2008. **22**(3): p. 305-309.
40. Bonner, W.M., et al., *GammaH2AX and cancer.* Nat Rev Cancer, 2008. **8**(12): p. 957-67.
41. Burma, S., et al., *ATM phosphorylates histone H2AX in response to DNA double-strand breaks.* J Biol Chem, 2001. **276**(45): p. 42462-7.
42. Ivashkevich, A., et al., *Use of the gamma-H2AX assay to monitor DNA damage and repair in cancer research.* Cancer Letters, 2012. **327**(1-2): p. 123-133.
43. Taneja, N., et al., *Histone H2AX phosphorylation as a predictor of radiosensitivity and target for radiotherapy.* Journal of Biological Chemistry, 2004. **279**(3): p. 2273-2280.

44. Olive, P.L. and J.P. Banath, *Phosphorylation of histone H2AX as a measure of radiosensitivity.* International Journal of Radiation Oncology Biology Physics, 2004. **58**(2): p. 331-335.
45. Bourton, E.C., et al., *Prolonged expression of the gamma-H2AX DNA repair biomarker correlates with excess acute and chronic toxicity from radiotherapy treatment.* Int J Cancer, 2011. **129**(12): p. 2928-34.
46. Gronchi, A., et al., *Phase II clinical trial of neoadjuvant trabectedin in patients with advanced localized myxoid liposarcoma.* Ann Oncol, 2012. **23**(3): p. 771-6.
47. Casali, P.G., R. Sanfilippo, and M. D'Incalci, *Trabectedin therapy for sarcomas.* Curr Opin Oncol, 2010. **22**(4): p. 342-6.
48. Lopez-Guerrero, J.A., I. Romero, and A. Poveda, *Trabectedin therapy as an emerging treatment strategy for recurrent platinum-sensitive ovarian cancer.* Chin J Cancer, 2015. **34**(1): p. 41-9.
49. Schoffski, P., I.L. Ray-Coquard, and A. Cioffi, *Activity of eribulin mesylate in patients with soft-tissue sarcoma: a phase 2 study in four independent histological subtypes (vol 12, pg 1051, 2011).* Lancet Oncology, 2015. **16**(9): p. E427-E427.
50. Mahmood, S.T., et al., *Phase II study of sunitinib malate, a multitargeted tyrosine kinase inhibitor in patients with relapsed or refractory soft tissue sarcomas. focus on three prevalent histologies: leiomyosarcoma, liposarcoma and malignant fibrous histiocytoma.* International Journal of Cancer, 2011. **129**(8): p. 1963-1969.
51. Sleijfer, S., et al., *Pazopanib, a Multikinase Angiogenesis Inhibitor, in Patients With Relapsed or Refractory Advanced Soft Tissue Sarcoma: A Phase II Study From the European Organisation for Research and Treatment of Cancer-Soft Tissue and Bone Sarcoma Group (EORTC Study 62043).* Journal of Clinical Oncology, 2009. **27**(19): p. 3126-3132.
52. von Mehren, M., et al., *Phase 2 Southwest Oncology Group-directed intergroup trial (S0505) of sorafenib in advanced soft tissue sarcomas.* Cancer, 2012. **118**(3): p. 770-6.
53. Debrock, G., et al., *A phase II trial with rosiglitazone in liposarcoma patients.* Br J Cancer, 2003. **89**(8): p. 1409-12.
54. Pishvaian, M.J., et al., *A phase 1 study of efatutazone, an oral peroxisome proliferator-activated receptor gamma agonist, administered to patients with advanced malignancies.* Cancer, 2012. **118**(21): p. 5403-13.
55. Pan, J., et al., *Phase I study of nelfinavir in liposarcoma.* Cancer Chemother Pharmacol, 2012. **70**(6): p. 791-9.
56. Luke, J.J., et al., *The Cyclin-Dependent Kinase Inhibitor Flavopiridol Potentiates Doxorubicin Efficacy in Advanced Sarcomas: Preclinical Investigations and Results of a Phase I Dose-Escalation Clinical Trial.* Clinical Cancer Research, 2012. **18**(9): p. 2638-2647.
57. Schwartz, G.K., et al., *Phase I study of PD 0332991, a cyclin-dependent kinase inhibitor, administered in 3-week cycles (Schedule 2/1).* Br J Cancer, 2011. **104**(12): p. 1862-8.
58. Muller, P.A.J. and K.H. Vousden, *p53 mutations in cancer.* Nature Cell Biology, 2013. **15**(1): p. 2-8.
59. Goh, A.M., C.R. Coffill, and D.P. Lane, *The role of mutant p53 in human cancer.* J Pathol, 2011. **223**(2): p. 116-26.
60. Oren, M., *Regulation of the p53 tumor suppressor protein.* J Biol Chem, 1999. **274**(51): p. 36031-4.
61. Vousden, K.H. and X. Lu, *Live or let die: the cell's response to p53.* Nat Rev Cancer, 2002. **2**(8): p. 594-604.
62. Kubbutat, M.H., S.N. Jones, and K.H. Vousden, *Regulation of p53 stability by Mdm2.* Nature, 1997. **387**(6630): p. 299-303.
63. Picksley, S.M. and D.P. Lane, *The p53-mdm2 autoregulatory feedback loop: a paradigm for the regulation of growth control by p53?* Bioessays, 1993. **15**(10): p. 689-90.
64. Barak, Y., et al., *Mdm2 Expression Is Induced by Wild Type-P53 Activity.* Embo Journal, 1993. **12**(2): p. 461-468.

65. Chen, J., V. Marechal, and A.J. Levine, *Mapping of the p53 and mdm-2 interaction domains.* Mol Cell Biol, 1993. **13**(7): p. 4107-14.
66. Roth, J., et al., *Nucleo-cytoplasmic shuttling of the hdm2 oncoprotein regulates the levels of the p53 protein via a pathway used by the human immunodeficiency virus rev protein.* EMBO J, 1998. **17**(2): p. 554-64.
67. Tao, W.K. and A.J. Levine, *Nucleocytoplasmic shuttling of oncoprotein Hdm2 is required for Hdm2-mediated degradation of p53.* Proceedings of the National Academy of Sciences of the United States of America, 1999. **96**(6): p. 3077-3080.
68. Honda, R., H. Tanaka, and H. Yasuda, *Oncoprotein MDM2 is a ubiquitin ligase E3 for tumor suppressor p53.* Febs Letters, 1997. **420**(1): p. 25-27.
69. Haupt, Y., et al., *Mdm2 promotes the rapid degradation of p53.* Nature, 1997. **387**(6630): p. 296-9.
70. Chene, P., *Inhibiting the p53-MDM2 interaction: An important target for cancer therapy.* Nature Reviews Cancer, 2003. **3**(2): p. 102-109.
71. Soussi, T., K. Dehouche, and C. Beroud, *p53 website and analysis of p53 gene mutations in human cancer: Forging a link between epidemiology and carcinogenesis.* Human Mutation, 2000. **15**(1): p. 105-113.
72. Lain, S. and D. Lane, *Improving cancer therapy by non-genotoxic activation of p53.* European Journal of Cancer, 2003. **39**(8): p. 1053-1060.
73. Scheffner, M., *Ubiquitin, E6-AP, and their role in p53 inactivation.* Pharmacology & Therapeutics, 1998. **78**(3): p. 129-139.
74. Freedman, D.A., L. Wu, and A.J. Levine, *Functions of the MDM2 oncoprotein.* Cellular and Molecular Life Sciences, 1999. **55**(1): p. 96-107.
75. Sherr, C.J., *Tumor surveillance via the ARF-p53 pathway.* Genes Dev, 1998. **12**(19): p. 2984-91.
76. Dasika, G.K., et al., *DNA damage-induced cell cycle checkpoints and DNA strand break repair in development and tumorigenesis.* Oncogene, 1999. **18**(55): p. 7883-99.
77. Bartek, J. and J. Lukas, *Mammalian G1- and S-phase checkpoints in response to DNA damage.* Curr Opin Cell Biol, 2001. **13**(6): p. 738-47.
78. Salomoni, P. and P.P. Pandolfi, *The role of PML in tumor suppression.* Cell, 2002. **108**(2): p. 165-70.
79. Colombo, E., et al., *Nucleophosmin regulates the stability and transcriptional activity of p53.* Nat Cell Biol, 2002. **4**(7): p. 529-33.
80. zur Hausen, H., *Viruses in human cancers.* Eur J Cancer, 1999. **35**(14): p. 1878-85.
81. Tos, A.P.D., et al., *Molecular abnormalities of the p53 pathway in dedifferentiated liposarcoma.* Journal of Pathology, 1997. **181**(1): p. 8-13.
82. Pilotti, S., et al., *Molecular abnormalities in liposarcoma: Role of MDM2 and CDK4-containing amplicons at 12q13-22.* Journal of Pathology, 1998. **185**(2): p. 188-190.
83. Pluquet, O. and P. Hainaut, *Genotoxic and non-genotoxic pathways of p53 induction.* Cancer Lett, 2001. **174**(1): p. 1-15.
84. Yamaizumi, M. and T. Sugano, *Uv-Induced Nuclear Accumulation of P53 Is Evoked through DNA-Damage of Actively Transcribed Genes Independent of the Cell-Cycle.* Oncogene, 1994. **9**(10): p. 2775-2784.
85. Kastan, M.B., et al., *Participation of p53 protein in the cellular response to DNA damage.* Cancer Res, 1991. **51**(23 Pt 1): p. 6304-11.
86. Wang, X.J., et al., *p53 accumulation in various organs of rats after whole-body exposure to low-dose X-ray irradiation.* Anticancer Research, 1996. **16**(4a): p. 1671-1674.
87. Hickman, A.W., et al., *Alpha-Particle-Induced P53 Protein Expression in a Rat Lung Epithelial-Cell Strain.* Cancer Research, 1994. **54**(22): p. 5797-5800.
88. Tishler, R.B., et al., *Increases in sequence specific DNA binding by p53 following treatment with chemotherapeutic and DNA damaging agents.* Cancer Res, 1993. **53**(10 Suppl): p. 2212-6.

89. Yasui, W., et al., *Increased expression of p34cdc2 and its kinase activity in human gastric and colonic carcinomas.* Int J Cancer, 1993. **53**(1): p. 36-41.
90. Graeber, T.G., et al., *Hypoxia induces accumulation of p53 protein, but activation of a G1-phase checkpoint by low-oxygen conditions is independent of p53 status.* Mol Cell Biol, 1994. **14**(9): p. 6264-77.
91. Ramet, M., et al., *P53 Protein Expression Is Correlated with Benzo[Alpha]Pyrene-DNA Adducts in Carcinoma Cell-Lines.* Carcinogenesis, 1995. **16**(9): p. 2117-2124.
92. Meplan, C., K. Mann, and P. Hainaut, *Cadmium induces conformational modifications of wild-type p53 and suppresses p53 response to DNA damage in cultured cells.* J Biol Chem, 1999. **274**(44): p. 31663-70.
93. Linke, S.P., et al., *A reversible, p53-dependent G0/G1 cell cycle arrest induced by ribonucleotide depletion in the absence of detectable DNA damage.* Genes Dev, 1996. **10**(8): p. 934-47.
94. Huang, T.S., et al., *Distinct p53-mediated G1/S checkpoint responses in two NIH3T3 subclone cells following treatment with DNA-damaging agents.* Oncogene, 1996. **13**(3): p. 625-32.
95. Elledge, R.M., et al., *Accumulation of P53 Protein as a Possible Predictor of Response to Adjuvant Combination Chemotherapy with Cyclophosphamide, Methotrexate, Fluorouracil, and Prednisone for Breast-Cancer.* Journal of the National Cancer Institute, 1995. **87**(16): p. 1254-1256.
96. Magnelli, L., M. Cinelli, and V. Chiarugi, *Phorbol esters attenuate the expression of p53 in cells treated with doxorubicin and protect TS-P53/K562 from apoptosis.* Biochem Biophys Res Commun, 1995. **215**(2): p. 641-5.
97. Lowe, S.W. and H.E. Ruley, *Stabilization of the P53 Tumor Suppressor Is Induced by Adenovirus-5 E1a and Accompanies Apoptosis.* Genes & Development, 1993. **7**(4): p. 535-545.
98. Gotlieb, W.H., et al., *Cytokine-induced modulation of tumor suppressor gene expression in ovarian cancer cells: up-regulation of p53 gene expression and induction of apoptosis by tumor necrosis factor-alpha.* Am J Obstet Gynecol, 1994. **170**(4): p. 1121-8; discussion 1128-30.
99. Maki, C.G., J.M. Huibregtse, and P.M. Howley, *In vivo ubiquitination and proteasome-mediated degradation of p53(1).* Cancer Res, 1996. **56**(11): p. 2649-54.
100. Suryadinata, R., M. Sadowski, and B. Sarcevic, *Control of cell cycle progression by phosphorylation of cyclin-dependent kinase (CDK) substrates.* Biosci Rep, 2010. **30**(4): p. 243-55.
101. Malumbres, M. and M. Barbacid, *Cell cycle, CDKs and cancer: a changing paradigm.* Nat Rev Cancer, 2009. **9**(3): p. 153-66.
102. Malumbres, M. and M. Barbacid, *To cycle or not to cycle: A critical decision in cancer.* Nature Reviews Cancer, 2001. **1**(3): p. 222-231.
103. Giacinti, C. and A. Giordano, *RB and cell cycle progression.* Oncogene, 2006. **25**(38): p. 5220-7.
104. Harbour, J.W., et al., *Cdk phosphorylation triggers sequential intramolecular interactions that progressively block Rb functions as cells move through G1.* Cell, 1999. **98**(6): p. 859-869.
105. Lundberg, A.S. and R.A. Weinberg, *Functional inactivation of the retinoblastoma protein requires sequential modification by at least two distinct cyclin-cdk complexes.* Molecular and Cellular Biology, 1998. **18**(2): p. 753-761.
106. Hatakeyama, M., et al., *Collaboration of G(1) Cyclins in the Functional Inactivation of the Retinoblastoma Protein.* Genes & Development, 1994. **8**(15): p. 1759-1771.
107. Malumbres, M. and M. Barbacid, *Mammalian cyclin-dependent kinases.* Trends Biochem Sci, 2005. **30**(11): p. 630-41.
108. Hochegger, H., S. Takeda, and T. Hunt, *Cyclin-dependent kinases and cell-cycle transitions: does one fit all?* Nature Reviews Molecular Cell Biology, 2008. **9**(11): p. 910-U26.
109. Baker, S.J. and E.P. Reddy, *CDK4: A Key Player in the Cell Cycle, Development, and Cancer.* Genes Cancer, 2012. **3**(11-12): p. 658-69.
110. Hanahan, D. and R.A. Weinberg, *The hallmarks of cancer.* Cell, 2000. **100**(1): p. 57-70.

111. Gil, J. and G. Peters, *Regulation of the INK4b-ARF-INK4a tumour suppressor locus: all for one or one for all.* Nat Rev Mol Cell Biol, 2006. **7**(9): p. 667-77.
112. Hamilton, E. and J.R. Infante, *Targeting CDK4/6 in patients with cancer.* Cancer Treatment Reviews, 2016. **45**: p. 129-138.
113. Perez, M., et al., *Efficacy of CDK4 inhibition against sarcomas depends on their levels of CDK4 and p16ink4 mRNA.* Oncotarget, 2015. **6**(38): p. 40557-40574.
114. Italiano, A., et al., *Clinical and biological significance of CDK4 amplification in well-differentiated and dedifferentiated liposarcomas.* Clin Cancer Res, 2009. **15**(18): p. 5696-703.
115. Agarwal, M.L., et al., *p53 controls both the G2/M and the G1 cell cycle checkpoints and mediates reversible growth arrest in human fibroblasts.* Proc Natl Acad Sci U S A, 1995. **92**(18): p. 8493-7.
116. Ashcroft, M., Y. Taya, and K.H. Vousden, *Stress signals utilize multiple pathways to stabilize p53.* Mol Cell Biol, 2000. **20**(9): p. 3224-33.
117. Nevins, J.R., *The Rb/E2F pathway and cancer.* Human Molecular Genetics, 2001. **10**(7): p. 699-703.
118. Cazzalini, O., et al., *Multiple roles of the cell cycle inhibitor p21(CDKN1A) in the DNA damage response.* Mutat Res, 2010. **704**(1-3): p. 12-20.
119. Innocente, S.A., et al., *p53 regulates a G2 checkpoint through cyclin B1.* Proc Natl Acad Sci U S A, 1999. **96**(5): p. 2147-52.
120. Elmore, S., *Apoptosis: a review of programmed cell death.* Toxicol Pathol, 2007. **35**(4): p. 495-516.
121. Hengartner, M.O., *The biochemistry of apoptosis.* Nature, 2000. **407**(6805): p. 770-6.
122. Walczak, H. and P.H. Krammer, *The CD95 (APO-1/Fas) and the TRAIL (APO-2L) apoptosis systems.* Exp Cell Res, 2000. **256**(1): p. 58-66.
123. Krueger, A., et al., *FLICE-inhibitory proteins: regulators of death receptor-mediated apoptosis.* Mol Cell Biol, 2001. **21**(24): p. 8247-54.
124. Green, D.R. and G. Kroemer, *The pathophysiology of mitochondrial cell death.* Science, 2004. **305**(5684): p. 626-9.
125. Fulda, S. and K.M. Debatin, *Extrinsic versus intrinsic apoptosis pathways in anticancer chemotherapy.* Oncogene, 2006. **25**(34): p. 4798-811.
126. Levy, M.Z., et al., *Telomere end-replication problem and cell aging.* J Mol Biol, 1992. **225**(4): p. 951-60.
127. Wang, C., et al., *DNA damage response and cellular senescence in tissues of aging mice.* Aging Cell, 2009. **8**(3): p. 311-23.
128. Adams, P.D., *Healing and Hurting: Molecular Mechanisms, Functions, and Pathologies of Cellular Senescence.* Molecular Cell, 2009. **36**(1): p. 2-14.
129. Collins, C.J. and J.M. Sedivy, *Involvement of the INK4a/Arf gene locus in senescence.* Aging Cell, 2003. **2**(3): p. 145-50.
130. Campisi, J. and F.D. di Fagagna, *Cellular senescence: when bad things happen to good cells.* Nature Reviews Molecular Cell Biology, 2007. **8**(9): p. 729-740.
131. Blagosklonny, M.V., *Cell senescence and hypermitogenic arrest.* Embo Reports, 2003. **4**(4): p. 358-362.
132. Campisi, J., *Aging, Cellular Senescence, and Cancer.* Annual Review of Physiology, Vol 75, 2013. **75**: p. 685-705.
133. Beausejour, C.M., et al., *Reversal of human cellular senescence: roles of the p53 and p16 pathways.* Embo Journal, 2003. **22**(16): p. 4212-4222.
134. Tseng, W.W., N. Somaiah, and E.G. Engleman, *Potential for immunotherapy in soft tissue sarcoma.* Hum Vaccin Immunother, 2014. **10**(11): p. 3117-24.
135. Wilky, B.A. and J.M. Goldberg, *Immunotherapy in sarcoma: a new frontier.* Discov Med, 2014. **17**(94): p. 201-6.

136. Pedrazzoli, P., et al., *Immunotherapeutic Intervention against Sarcomas.* J Cancer, 2011. **2**: p. 350-6.
137. Muller, C.R., et al., *Interferon-alpha as the only adjuvant treatment in high-grade osteosarcoma: Long term results of the Karolinska Hospital series.* Acta Oncologica, 2005. **44**(5): p. 475-480.
138. Intlekofer, A.M. and C.B. Thompson, *At the Bench: Preclinical rationale for CTLA-4 and PD-1 blockade as cancer immunotherapy.* Journal of Leukocyte Biology, 2013. **94**(1): p. 25-39.
139. Hude, I., et al., *The emerging role of immune checkpoint inhibition in malignant lymphoma.* Haematologica, 2017. **102**(1): p. 30-42.
140. Chen, L.P. and D.B. Flies, *Molecular mechanisms of T cell co-stimulation and co-inhibition.* Nature Reviews Immunology, 2013. **13**(4): p. 227-242.
141. Wherry, E.J. and M. Kurachi, *Molecular and cellular insights into T cell exhaustion.* Nature Reviews Immunology, 2015. **15**(8): p. 486-499.
142. Dong, H., et al., *Tumor-associated B7-H1 promotes T-cell apoptosis: a potential mechanism of immune evasion.* Nat Med, 2002. **8**(8): p. 793-800.
143. Maki, R.G., et al., *A Pilot Study of Anti-CTLA4 Antibody Ipilimumab in Patients with Synovial Sarcoma.* Sarcoma, 2013. **2013**: p. 168145.
144. Matsuzaki, A., et al., *Immunotherapy with autologous dendritic cells and tumor-specific synthetic peptides for synovial sarcoma.* J Pediatr Hematol Oncol, 2002. **24**(3): p. 220-3.
145. Bryceson, Y.T., et al., *Activation, coactivation, and costimulation of resting human natural killer cells.* Immunol Rev, 2006. **214**: p. 73-91.
146. Vivier, E., J.A. Nunes, and F. Vely, *Natural killer cell signaling pathways.* Science, 2004. **306**(5701): p. 1517-9.
147. Billadeau, D.D. and P.J. Leibson, *ITAMs versus ITIMs: striking a balance during cell regulation.* Journal of Clinical Investigation, 2002. **109**(2): p. 161-168.
148. Cerwenka, A. and L.L. Lanier, *NKG2D ligands: unconventional MHC class I-like molecules exploited by viruses and cancer.* Tissue Antigens, 2003. **61**(5): p. 335-343.
149. Gasser, S., et al., *The DNA damage pathway regulates innate immune system ligands of the NKG2D receptor.* Nature, 2005. **436**(7054): p. 1186-1190.
150. Lakshmikanth, T., et al., *NCRs and DNAM-1 mediate NK cell recognition and lysis of human and mouse melanoma cell lines in vitro and in vivo.* Journal of Clinical Investigation, 2009. **119**(5): p. 1251-1263.
151. El-Sherbiny, Y.M., et al., *The requirement for DNAM-1, NKG2D, and NKp46 in the natural killer cell-mediated killing of myeloma cells.* Cancer Res, 2007. **67**(18): p. 8444-9.
152. Verhoeven, D.H.J., et al., *NK cells recognize and lyse Ewing sarcoma cells through NKG2D and DNAM-1 receptor dependent pathways.* Molecular Immunology, 2008. **45**(15): p. 3917-3925.
153. Vivier, E., et al., *Innate or Adaptive Immunity? The Example of Natural Killer Cells.* Science, 2011. **331**(6013).
154. Cooper, M.A., T.A. Fehniger, and M.A. Caligiuri, *The biology of human natural killer-cell subsets.* Trends Immunol, 2001. **22**(11): p. 633-40.
155. Messaoudene, M., et al., *Patient's Natural Killer Cells in the Era of Targeted Therapies: Role for Tumor Killers.* Front Immunol, 2017. **8**: p. 683.
156. Geller, M.A. and J.S. Miller, *Use of allogeneic NK cells for cancer immunotherapy.* Immunotherapy, 2011. **3**(12): p. 1445-1459.
157. Burns, L.J., et al., *IL-2-based immunotherapy after autologous transplantation for lymphoma and breast cancer induces immune activation and cytokine release: a phase I/II trial.* Bone Marrow Transplant, 2003. **32**(2): p. 177-86.
158. Geller, M.A., et al., *A phase II study of allogeneic natural killer cell therapy to treat patients with recurrent ovarian and breast cancer.* Cytotherapy, 2011. **13**(1): p. 98-107.
159. Muller, C.R., et al., *Potential for treatment of liposarcomas with the MDM2 antagonist Nutlin-3A.* International Journal of Cancer, 2007. **121**(1): p. 199-205.

160. Tovar, C., et al., *Small-molecule MDM2 antagonists reveal aberrant p53 signaling in cancer: implications for therapy.* Proc Natl Acad Sci U S A, 2006. **103**(6): p. 1888-93.
161. Cao, C., et al., *Radiosensitization of lung cancer by nutlin, an inhibitor of murine double minute 2.* Mol Cancer Ther, 2006. **5**(2): p. 411-7.
162. Luo, H.M., et al., *Activation of p53 with Nutlin-3a radiosensitizes lung cancer cells via enhancing radiation-induced premature senescence.* Lung Cancer, 2013. **81**(2): p. 167-173.
163. Hagen, K.R., et al., *Silencing CDK4 radiosensitizes breast cancer cells by promoting apoptosis.* Cell Div, 2013. **8**(1): p. 10.
164. Fry, D.W., et al., *Specific inhibition of cyclin-dependent kinase 4/6 by PD 0332991 and associated antitumor activity in human tumor xenografts.* Molecular Cancer Therapeutics, 2004. **3**(11): p. 1427-1437.
165. Shimura, T., et al., *Activation of the AKT/cyclin D1/Cdk4 survival signaling pathway in radioresistant cancer stem cells.* Oncogenesis, 2012. **1**.
166. Shimura, T., *Targeting the AKT/cyclin D1 pathway to overcome intrinsic and acquired radioresistance of tumors for effective radiotherapy.* Int J Radiat Biol, 2016: p. 1-5.
167. Barretina, J., et al., *Subtype-specific genomic alterations define new targets for soft-tissue sarcoma therapy.* Nature Genetics, 2010. **42**(8): p. 715-U103.
168. Flaherty, K.T., et al., *Phase I, dose-escalation trial of the oral cyclin-dependent kinase 4/6 inhibitor PD 0332991, administered using a 21-day schedule in patients with advanced cancer.* Clin Cancer Res, 2012. **18**(2): p. 568-76.
169. Vu, B., et al., *Discovery of RG7112: A Small-Molecule MDM2 Inhibitor in Clinical Development.* ACS Med Chem Lett, 2013. **4**(5): p. 466-9.
170. Kumamoto, K., et al., *Nutlin-3a activates p53 to both down-regulate inhibitor of growth 2 and up-regulate mir-34a, mir-34b, and mir-34c expression, and induce senescence.* Cancer Research, 2008. **68**(9): p. 3193-3203.
171. Dhillon, S., *Palbociclib: first global approval.* Drugs, 2015. **75**(5): p. 543-51.
172. Fry, D.W., et al., *Specific inhibition of cyclin-dependent kinase 4/6 by PD 0332991 and associated antitumor activity in human tumor xenografts.* Mol Cancer Ther, 2004. **3**(11): p. 1427-38.
173. Cui, C., W. Shu, and P. Li, *Fluorescence In situ Hybridization: Cell-Based Genetic Diagnostic and Research Applications.* Front Cell Dev Biol, 2016. **4**: p. 89.
174. Anastasi, J., *Fluorescence in situ hybridization in leukemia. Applications in diagnosis, subclassification, and monitoring the response to therapy.* Ann N Y Acad Sci, 1993. **677**: p. 214-24.
175. Cheng, L., et al., *Fluorescence in situ hybridization in surgical pathology: principles and applications.* J Pathol Clin Res, 2017. **3**(2): p. 73-99.
176. Roh, M.H., et al., *The Application of Cytogenetics and Fluorescence In Situ Hybridization to Fine-Needle Aspiration in the Diagnosis and Subclassification of Renal Neoplasms.* Cancer Cytopathology, 2010. **118**(3): p. 137-145.
177. Vorobiev, V., et al., *Identification of T(11;14)(Q13;Q32) in Various Hematopoietic Lineages of Mantle Cell Lymphoma Patients. Joint Application of Fluorescence-Activated Cell Sorting and Fluorescence in Situ Hybridization.* Haematologica-the Hematology Journal, 2010. **95**: p. 610-610.
178. Speicher, M.R. and N.P. Carter, *The new cytogenetics: blurring the boundaries with molecular biology.* Nat Rev Genet, 2005. **6**(10): p. 782-92.
179. Sato-Otsubo, A., M. Sanada, and S. Ogawa, *Single-nucleotide polymorphism array karyotyping in clinical practice: where, when, and how?* Semin Oncol, 2012. **39**(1): p. 13-25.
180. Schwartz, S., *Clinical Utility of Single Nucleotide Polymorphism Arrays.* Clinics in Laboratory Medicine, 2011. **31**(4): p. 581-+.
181. Noronha, T.R., S.S. Rohr, and L. Chauffaille Mde, *Identifying the similarities and differences between single nucleotide polymorphism array (SNPa) analysis and karyotyping in acute*

myeloid leukemia and myelodysplastic syndromes. Rev Bras Hematol Hemoter, 2015. **37**(1): p. 48-54.
182. Puck, T.T. and P.I. Marcus, *Action of x-rays on mammalian cells.* J Exp Med, 1956. **103**(5): p. 653-66.
183. Puck, T.T., et al., *Action of x-rays on mammalian cells. II. Survival curves of cells from normal human tissues.* J Exp Med, 1957. **106**(4): p. 485-500.
184. Franken, N.A., et al., *Clonogenic assay of cells in vitro.* Nat Protoc, 2006. **1**(5): p. 2315-9.
185. Tanigawa, N., et al., *In vitro growth ability and chemosensitivity of gastric and colorectal cancer cells assessed with the human tumour clonogenic assay and the thymidine incorporation assay.* Eur J Cancer, 1992. **28**(1): p. 31-4.
186. Franken, N.A., et al., *Importance of TP53 and RB in the repair of potentially lethal damage and induction of color junctions after exposure to ionizing radiation.* Radiat Res, 2002. **158**(6): p. 707-14.
187. Vichai, V. and K. Kirtikara, *Sulforhodamine B colorimetric assay for cytotoxicity screening.* Nat Protoc, 2006. **1**(3): p. 1112-6.
188. Riss, T.L., et al., *Cell Viability Assays*, in *Assay Guidance Manual*, G.S. Sittampalam, et al., Editors. 2004: Bethesda (MD).
189. Shoemaker, R.H., *The NCI 60 human tumor cell line screen: An information-rich screen informing on mechanisms of toxicity.* In Vitro Cellular & Developmental Biology-Animal, 2006. **42**: p. 5a-5a.
190. Bradford, M.M., *A rapid and sensitive method for the quantitation of microgram quantities of protein utilizing the principle of protein-dye binding.* Anal.Biochem., 1976. **72**: p. 248-254.
191. Suzuki, T., et al., *DNA staining for fluorescence and laser confocal microscopy.* J Histochem Cytochem, 1997. **45**(1): p. 49-53.
192. Chene, P., *Inhibiting the p53-MDM2 interaction: an important target for cancer therapy.* Nat Rev Cancer, 2003. **3**(2): p. 102-9.
193. Sdek, P., et al., *MDM2 promotes proteasome-dependent ubiquitin-independent degradation of retinoblastoma protein.* Molecular Cell, 2005. **20**(5): p. 699-708.
194. Du, W., et al., *Nutlin-3 Affects Expression and Function of Retinoblastoma Protein ROLE OF RETINOBLASTOMA PROTEIN IN CELLULAR RESPONSE TO NUTLIN-3.* Journal of Biological Chemistry, 2009. **284**(39): p. 26315-26321.
195. Oda, K., et al., *p53AIP1, a potential mediator of p53-dependent apoptosis, and its regulation by Ser-46-phosphorylated p53.* Cell, 2000. **102**(6): p. 849-62.
196. Banin, S., et al., *Enhanced phosphorylation of p53 by ATM in response to DNA damage.* Science, 1998. **281**(5383): p. 1674-7.
197. Edgar, B.A. and T.L. Orr-Weaver, *Endoreplication cell cycles: more for less.* Cell, 2001. **105**(3): p. 297-306.
198. Deaven, L.L. and J.D. Kreizinger, *Cell fusion as a mechanism for the origin of polyploid cells in vitro.* Experientia, 1971. **27**(3): p. 311-3.
199. Storchova, Z. and D. Pellman, *From polyploidy to aneuploidy, genome instability and cancer.* Nat Rev Mol Cell Biol, 2004. **5**(1): p. 45-54.
200. Storchova, Z. and C. Kuffer, *The consequences of tetraploidy and aneuploidy.* J Cell Sci, 2008. **121**(Pt 23): p. 3859-66.
201. Ganem, N.J., Z. Storchova, and D. Pellman, *Tetraploidy, aneuploidy and cancer.* Current Opinion in Genetics & Development, 2007. **17**(2): p. 157-162.
202. Verma, R., et al., *DNA damage response to the Mdm2 inhibitor nutlin-3.* Biochem Pharmacol, 2010. **79**(4): p. 565-74.
203. Crago, A.M., et al., *Copy number losses define subgroups of dedifferentiated liposarcoma with poor prognosis and genomic instability.* Clin Cancer Res, 2012. **18**(5): p. 1334-40.
204. Lord, C.J. and A. Ashworth, *RAD51, BRCA2 and DNA repair: a partial resolution.* Nat Struct Mol Biol, 2007. **14**(6): p. 461-2.

205. Lord, C.J. and A. Ashworth, *PARP inhibitors: Synthetic lethality in the clinic.* Science, 2017. **355**(6330): p. 1152-1158.
206. Chene, P., *Inhibition of the p53-MDM2 interaction: Targeting a protein-protein interface.* Molecular Cancer Research, 2004. **2**(1): p. 20-28.
207. Sdek, P., et al., *MDM2 promotes proteasome-dependent ubiquitin-independent degradation of retinoblastoma protein.* Mol Cell, 2005. **20**(5): p. 699-708.
208. Du, W., et al., *Nutlin-3 affects expression and function of retinoblastoma protein: role of retinoblastoma protein in cellular response to nutlin-3.* J Biol Chem, 2009. **284**(39): p. 26315-21.
209. Wu, X., et al., *The p53-mdm-2 autoregulatory feedback loop.* Genes Dev, 1993. **7**(7A): p. 1126-32.
210. Kussie, P.H., et al., *Structure of the MDM2 oncoprotein bound to the p53 tumor suppressor transactivation domain.* Science, 1996. **274**(5289): p. 948-53.
211. Sdek, P., et al., *The central acidic domain of MDM2 is critical in inhibition of retinoblastoma-mediated suppression of E2F and cell growth.* Journal of Biological Chemistry, 2004. **279**(51): p. 53317-53322.
212. Yap, D.B., et al., *mdm2: a bridge over the two tumour suppressors, p53 and Rb.* Oncogene, 1999. **18**(53): p. 7681-9.
213. Sherr, C.J. and J.M. Roberts, *Inhibitors of mammalian G1 cyclin-dependent kinases.* Genes Dev, 1995. **9**(10): p. 1149-63.
214. Coll-Mulet, L., et al., *MDM2 antagonists activate p53 and synergize with genotoxic drugs in B-cell chronic lymphocytic leukemia cells.* Blood, 2006. **107**(10): p. 4109-4114.
215. Ohnstad, H.O., et al., *MDM2 antagonist Nutlin-3a potentiates antitumour activity of cytotoxic drugs in sarcoma cell lines.* BMC Cancer, 2011. **11**: p. 211:1-11.
216. Cheok, C.F., A. Dey, and D.P. Lane, *Cyclin-dependent kinase inhibitors sensitize tumor cells to nutlin-induced apoptosis: a potent drug combination.* Mol Cancer Res, 2007. **5**(11): p. 1133-45.
217. Laroche-Clary, A., et al., *Combined targeting of MDM2 and CDK4 is synergistic in dedifferentiated liposarcomas.* Journal of Hematology & Oncology, 2017. **10**.
218. Bieging, K.T., S.S. Mello, and L.D. Attardi, *Unravelling mechanisms of p53-mediated tumour suppression.* Nat Rev Cancer, 2014. **14**(5): p. 359-70.
219. Muller, P.A. and K.H. Vousden, *Mutant p53 in cancer: new functions and therapeutic opportunities.* Cancer Cell, 2014. **25**(3): p. 304-17.
220. Oren, M. and V. Rotter, *Mutant p53 gain-of-function in cancer.* Cold Spring Harb Perspect Biol, 2010. **2**(2): p. a001107.
221. Lee, J.M. and A. Bernstein, *p53 mutations increase resistance to ionizing radiation.* Proc Natl Acad Sci U S A, 1993. **90**(12): p. 5742-6.
222. Fei, P. and W.S. El-Deiry, *P53 and radiation responses.* Oncogene, 2003. **22**(37): p. 5774-83.
223. Arya, A.K., et al., *Nutlin-3, the small-molecule inhibitor of MDM2, promotes senescence and radiosensitises laryngeal carcinoma cells harbouring wild-type p53.* Br J Cancer, 2010. **103**(2): p. 186-95.
224. Feng, F.Y., et al., *MDM2 Inhibition Sensitizes Prostate Cancer Cells to Androgen Ablation and Radiotherapy in a p53-Dependent Manner.* Neoplasia, 2016. **18**(4): p. 213-22.
225. Althubiti, M., et al., *Characterization of novel markers of senescence and their prognostic potential in cancer.* Cell Death Dis, 2014. **5**: p. e1528.
226. Rodier, F. and J. Campisi, *Four faces of cellular senescence.* J Cell Biol, 2011. **192**(4): p. 547-56.
227. McConnell, B.B., et al., *Induced expression of p16(INK4a) inhibits both CDK4- and CDK2-associated kinase activity by reassortment of cyclin-CDK-inhibitor complexes.* Mol Cell Biol, 1999. **19**(3): p. 1981-9.
228. Li, J., M.J. Poi, and M.D. Tsai, *Regulatory mechanisms of tumor suppressor P16(INK4A) and their relevance to cancer.* Biochemistry, 2011. **50**(25): p. 5566-82.

229. Shen, H. and C.G. Maki, *Persistent p21 expression after Nutlin-3a removal is associated with senescence-like arrest in 4N cells.* J Biol Chem, 2010. **285**(30): p. 23105-14.
230. Li, D.W., et al., *Dynamic distribution of Ser-10 phosphorylated histone H3 in cytoplasm of MCF-7 and CHO cells during mitosis.* Cell Res, 2005. **15**(2): p. 120-6.
231. Goto, H., et al., *Identification of a novel phosphorylation site on histone H3 coupled with mitotic chromosome condensation.* J Biol Chem, 1999. **274**(36): p. 25543-9.
232. Chang, B.D., et al., *p21Waf1/Cip1/Sdi1-induced growth arrest is associated with depletion of mitosis-control proteins and leads to abnormal mitosis and endoreduplication in recovering cells.* Oncogene, 2000. **19**(17): p. 2165-70.
233. Ganem, N.J. and D. Pellman, *Limiting the proliferation of polyploid cells.* Cell, 2007. **131**(3): p. 437-40.
234. Zhao, B. and K.L. Guan, *Hippo pathway key to ploidy checkpoint.* Cell, 2014. **158**(4): p. 695-696.
235. Shen, H., D.M. Moran, and C.G. Maki, *Transient nutlin-3a treatment promotes endoreduplication and the generation of therapy-resistant tetraploid cells.* Cancer Res, 2008. **68**(20): p. 8260-8.
236. Ware, P.L., et al., *MDM2 copy numbers in well-differentiated and dedifferentiated liposarcoma: characterizing progression to high-grade tumors.* Am J Clin Pathol, 2014. **141**(3): p. 334-41.
237. Huang, B.Y., et al., *Pharmacologic p53 Activation Blocks Cell Cycle Progression but Fails to Induce Senescence in Epithelial Cancer Cells.* Molecular Cancer Research, 2009. **7**(9): p. 1497-1509.
238. Korotchkina, L.G., et al., *Cellular quiescence caused by the Mdm2 inhibitor nutlin-3a.* Cell Cycle, 2009. **8**(22): p. 3777-3781.
239. Washington, C.M. and D.T. Leaver, *Principles and practice of radiation therapy*. 2017.
240. Davoli, T. and T. de Lange, *The causes and consequences of polyploidy in normal development and cancer.* Annu Rev Cell Dev Biol, 2011. **27**: p. 585-610.
241. Castedo, M., et al., *Selective resistance of tetraploid cancer cells against DNA damage-induced apoptosis.* Signal Transduction Pathways, Pt A, 2006. **1090**: p. 35-49.
242. Davaadelger, B., H. Shen, and C.G. Maki, *Novel Roles for P53 in the Genesis and Targeting of Tetraploid Cancer Cells.* Plos One, 2014. **9**(11).
243. Martins, C.P., L. Brown-Swigart, and G.I. Evan, *Modeling the therapeutic efficacy of p53 restoration in tumors.* Cell, 2006. **127**(7): p. 1323-34.
244. Ventura, A., et al., *Restoration of p53 function leads to tumour regression in vivo.* Nature, 2007. **445**(7128): p. 661-5.
245. Junttila, M.R., et al., *Selective activation of p53-mediated tumour suppression in high-grade tumours.* Nature, 2010. **468**(7323): p. 567-71.
246. Aubrey, B.J., A. Strasser, and G.L. Kelly, *Tumor-Suppressor Functions of the TP53 Pathway.* Cold Spring Harb Perspect Med, 2016. **6**(5).
247. Davalos, A.R., et al., *Senescent cells as a source of inflammatory factors for tumor progression.* Cancer and Metastasis Reviews, 2010. **29**(2): p. 273-283.
248. Coppe, J.P., et al., *The Senescence-Associated Secretory Phenotype: The Dark Side of Tumor Suppression.* Annual Review of Pathology-Mechanisms of Disease, 2010. **5**: p. 99-118.
249. Wang, Q., et al., *Polyploidy road to therapy-induced cellular senescence and escape.* Int J Cancer, 2013. **132**(7): p. 1505-15.
250. Mosieniak, G. and E. Sikora, *Polyploidy: The Link Between Senescence and Cancer.* Current Pharmaceutical Design, 2010. **16**(6): p. 734-740.
251. Rao, B., S. Lain, and A.M. Thompson, *p53-Based cyclotherapy: exploiting the 'guardian of the genome' to protect normal cells from cytotoxic therapy.* Br J Cancer, 2013. **109**(12): p. 2954-8.
252. Zhang, Y.X., et al., *Antiproliferative effects of CDK4/6 inhibition in CDK4-amplified human liposarcoma in vitro and in vivo.* Mol Cancer Ther, 2014. **13**(9): p. 2184-93.

253. Hiroshima, Y., et al., *Patient-derived orthotopic xenograft (PDOX) nude mouse model of soft-tissue sarcoma more closely mimics the patient behavior in contrast to the subcutaneous ectopic model.* Anticancer Res, 2015. **35**(2): p. 697-701.
254. Shimura, T., et al., *Acquired radioresistance of human tumor cells by DNA-PK/AKT/GSK3 beta-mediated cyclin D1 overexpression.* Oncogene, 2010. **29**(34): p. 4826-4837.
255. ConnellCrowley, L., J.W. Harper, and D.W. Goodrich, *Cyclin D1/Cdk4 regulates retinoblastoma protein-mediated cell cycle arrest by site-specific phosphorylation.* Molecular Biology of the Cell, 1997. **8**(2): p. 287-301.
256. Baldin, V., et al., *Cyclin D1 Is a Nuclear-Protein Required for Cell-Cycle Progression in G(1).* Genes & Development, 1993. **7**(5): p. 812-821.
257. Banath, J.P., S.H. Macphail, and P.L. Olive, *Radiation sensitivity, H2AX phosphorylation, and kinetics of repair of DNA strand breaks in irradiated cervical cancer cell lines.* Cancer Res, 2004. **64**(19): p. 7144-9.
258. Tu, W.Z., et al., *gamma H2AX foci formation in the absence of DNA damage: Mitotic H2AX phosphorylation is mediated by the DNA-PKcs/CHK2 pathway.* Febs Letters, 2013. **587**(21): p. 3437-3443.
259. Kaelin, W.G., *The concept of synthetic lethality in the context of anticancer therapy.* Nature Reviews Cancer, 2005. **5**(9): p. 689-698.
260. Wienken, M., et al., *MDM2 Associates with Polycomb Repressor Complex 2 and Enhances Stemness-Promoting Chromatin Modifications Independent of p53.* Mol Cell, 2016. **61**(1): p. 68-83.
261. Bohlman, S. and J.J. Manfredi, *p53-independent effects of Mdm2.* Subcell Biochem, 2014. **85**: p. 235-46.
262. Marine, J.C. and G. Lozano, *Mdm2-mediated ubiquitylation: p53 and beyond.* Cell Death Differ, 2010. **17**(1): p. 93-102.
263. Dickson, M.A., et al., *Progression-Free Survival Among Patients With Well-Differentiated or Dedifferentiated Liposarcoma Treated With CDK4 Inhibitor Palbociclib: A Phase 2 Clinical Trial.* JAMA Oncol, 2016. **2**(7): p. 937-40.
264. Dickson, M.A., et al., *Phase II trial of the CDK4 inhibitor PD0332991 in patients with advanced CDK4-amplified well-differentiated or dedifferentiated liposarcoma.* J Clin Oncol, 2013. **31**(16): p. 2024-8.
265. Whittaker, S., et al., *Combination of palbociclib and radiotherapy for glioblastoma.* Cell Death Discov, 2017. **3**: p. 17033.
266. Li, H., et al., *Pharmacological activation of p53 triggers anticancer innate immune response through induction of ULBP2.* Cell Cycle, 2011. **10**(19): p. 3346-3358.
267. Textor, S., et al., *Human NK Cells Are Alerted to Induction of p53 in Cancer Cells by Upregulation of the NKG2D Ligands ULBP1 and ULBP2.* Cancer Research, 2011. **71**(18): p. 5998-6009.
268. Pende, D., et al., *Major histocompatibility complex class I-related chain a and UL16-binding protein expression on tumor cell lines of different histotypes: Analysis of tumor susceptibility to NKG2D-dependent natural killer cell cytotoxicity.* Cancer Research, 2002. **62**(21): p. 6178-6186.
269. Paschen, A., J. Baingo, and D. Schaciendorf, *Expression of stress ligands of the immunoreceptor NKG2D in melanoma: Regulation and clinical significance.* European Journal of Cell Biology, 2014. **93**(1-2): p. 49-54.
270. Groh, V., et al., *Tumour-derived soluble MIC ligands impair expression of NKG2D and T-cell activation.* Nature, 2002. **419**(6908): p. 734-738.
271. Fuertes, M.B., et al., *Intracellular retention of the NKG2D ligand MHC class I chain-related gene A in human melanomas confers immune privilege and prevents NK cell-mediated cytotoxicity.* J Immunol, 2008. **180**(7): p. 4606-14.
272. Carlsten, M., et al., *DNAX accessory molecule-1 mediated recognition of freshly isolated ovarian carcinoma by resting natural killer cells.* Cancer Res, 2007. **67**(3): p. 1317-25.

273. Castriconi, R., et al., *Natural killer cell-mediated killing of freshly isolated neuroblastoma cells: critical role of DNAX accessory molecule-1-poliovirus receptor interaction.* Cancer Res, 2004. **64**(24): p. 9180-4.
274. Stewart, C.A. and E. Vivier, *Strategies of Natural Killer (NK) Cell Recognition and Their Roles in Tumor Immunosurveillance.* 2008.

11 Appendix

11.1 **Supplement data:**

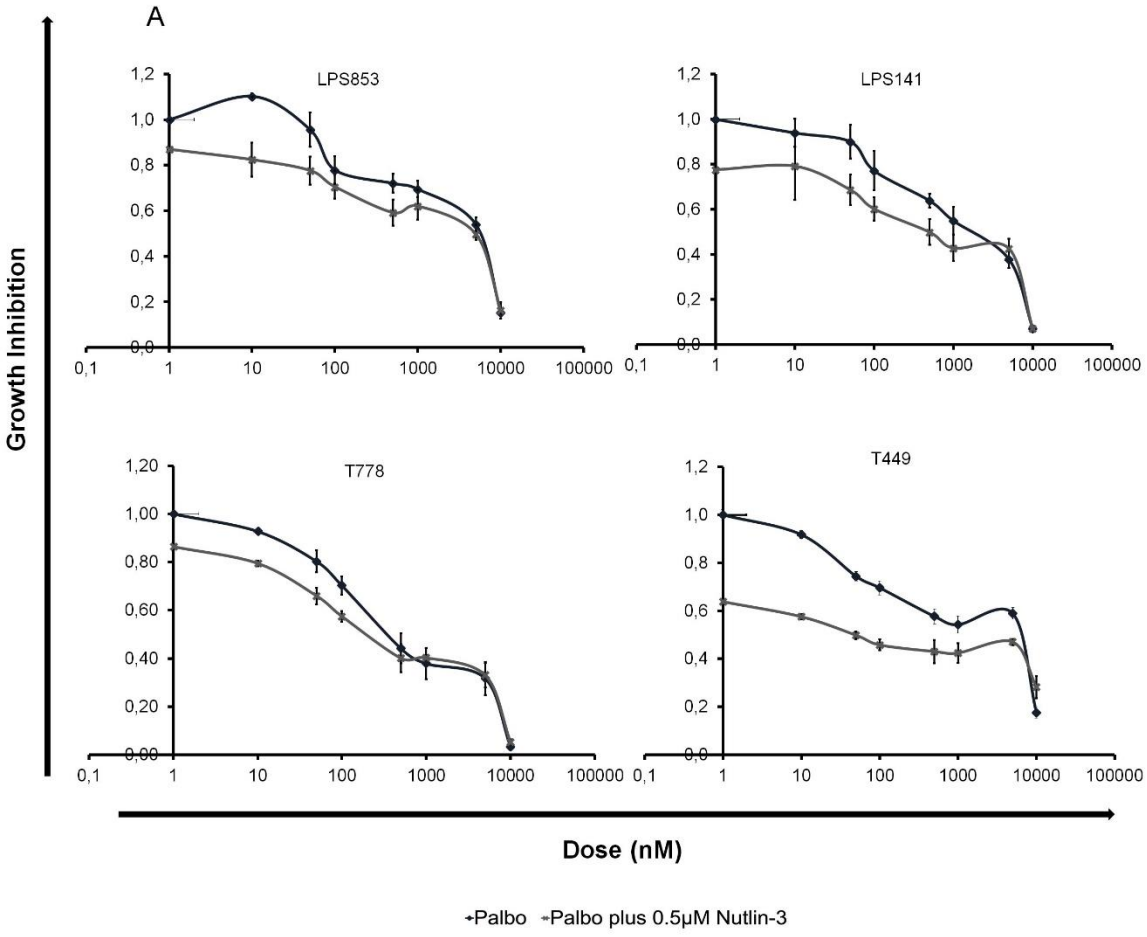

Figure S 11.1 Co-targeting of CDK4 and MDM2 in liposarcoma. (A) SRB assay graphs displaying growth inhibition in response to combination treatment to a concentration starting from 1nM to 10µM of CDK4 inhibitor (Palbociclib) and fixed concentration (0.5µM) of MDM2 inhibitor (Nutlin-3).

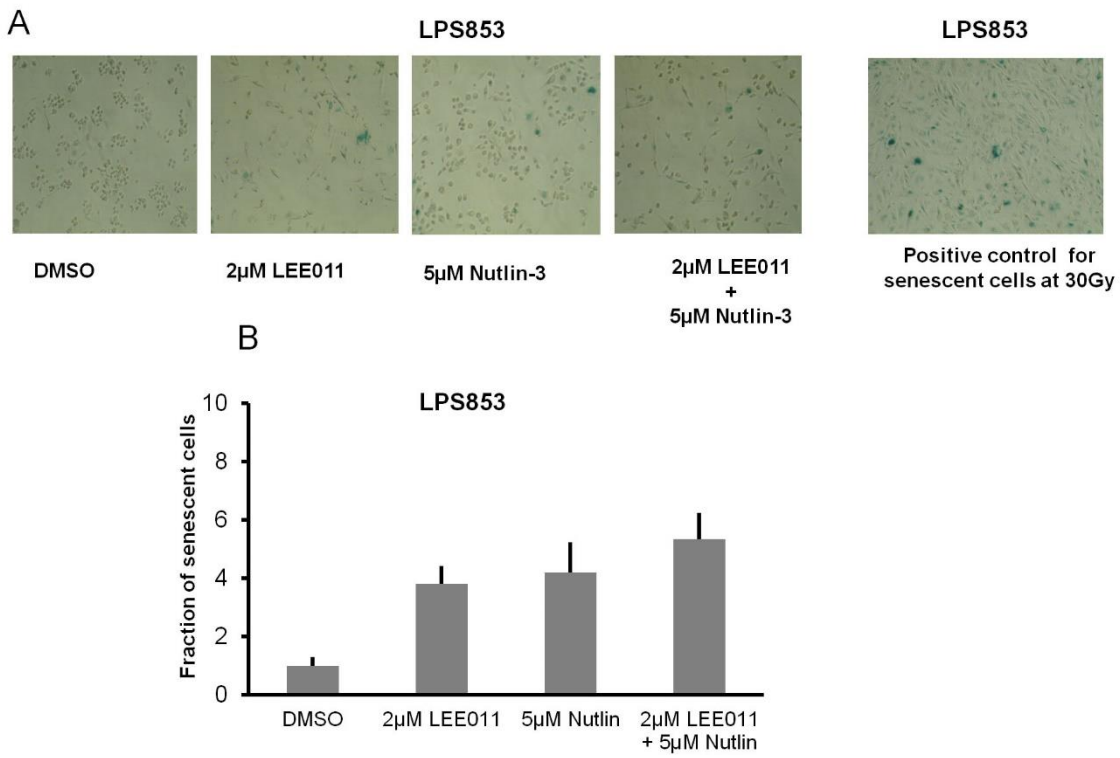

Figure S 11.2: **Measurement of senescence in response to co-inhibition of CDK4 and MDM2. (A)** Staining of beta-gal positive cells in LPS853 following 48h of treatment with CDK4i, MDM2i and combination of both the inhibitors. **(B)** Quantification of senescent positive cells. Bar graphs represent average of percentage of beta-galactosidase positive cells, n = 5, error bars indicate SD. * p ≥ 0.05.

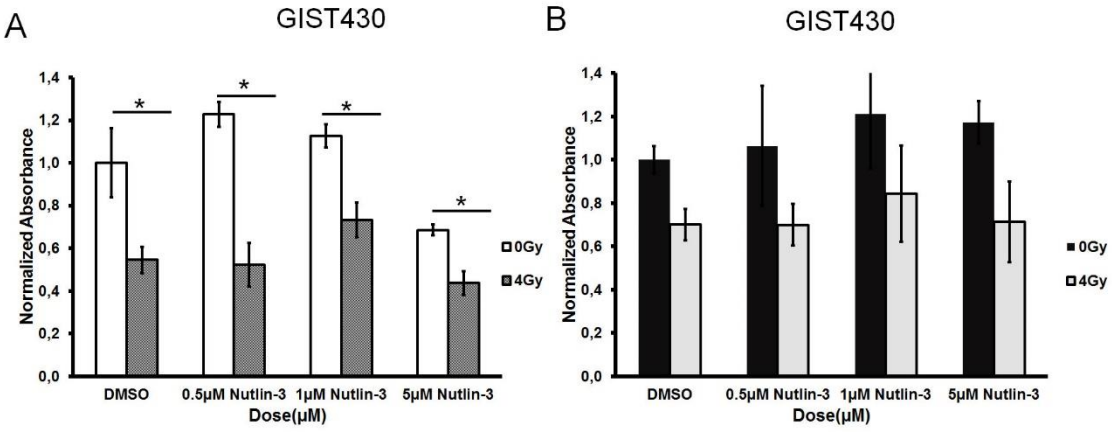

Figure S 11.3: **Assessment of short-term washout kinetics of GIST430 cell following treatment removal. (A)** Bar graphs represent normalized absorbance of liposarcoma cells in response to increasing doses (0.5μM, 1μM, 5μM) of Nutlin-3, RT and Nutlin-3 plus RT treated for continuous 192h and **(B)** 96h continuous followed by 96h drug free medium. * p ≤ 0.05.

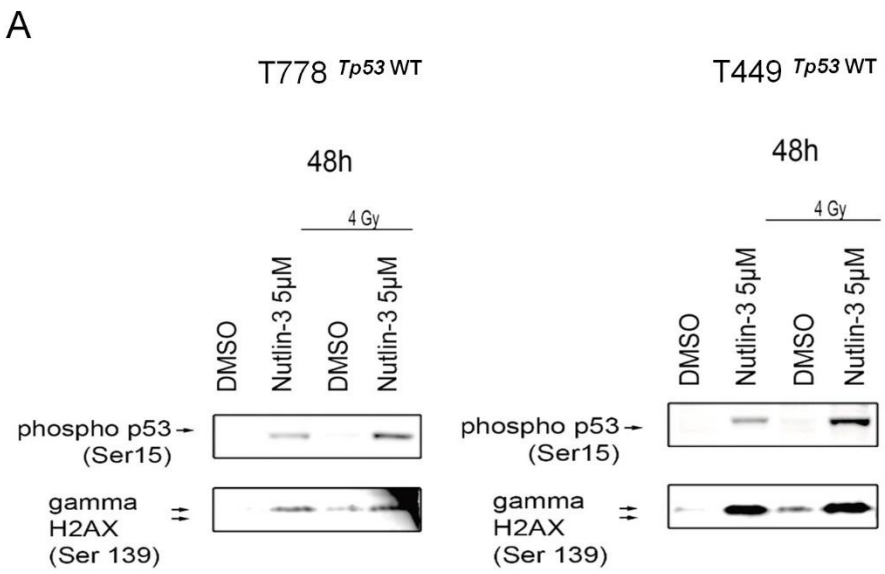

Figure S 11.4: **Assessment of induction of gamma-H2AX in response to MDM2 inhibition and RT in T778 and T449. (A)** Immunoblots of phospho-p53 (Ser-15) and gamma-H2AX in T778 and T449 following 48h of treatment with DMSO, 5µM Nutlin-3, 4 Gy and combination of both. For beta-actin, refer to **Figure 6.10**.

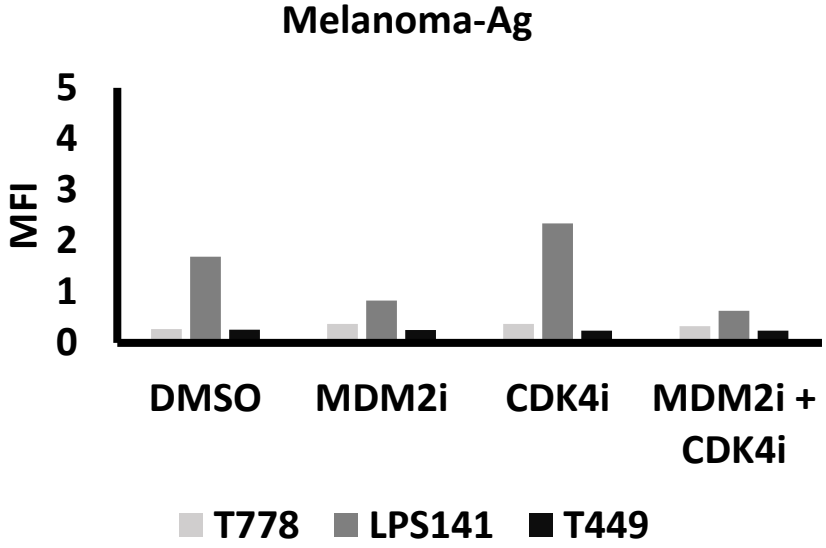

Figure S 11.5: **Negative control for liposarcoma: (A)** MFI representing melanoma antigen as negative control in liposarcoma (T778, LPS141, T449) during assessment of NKG2D ligands and DNAM-1 ligands by treatment with targeted therapy.

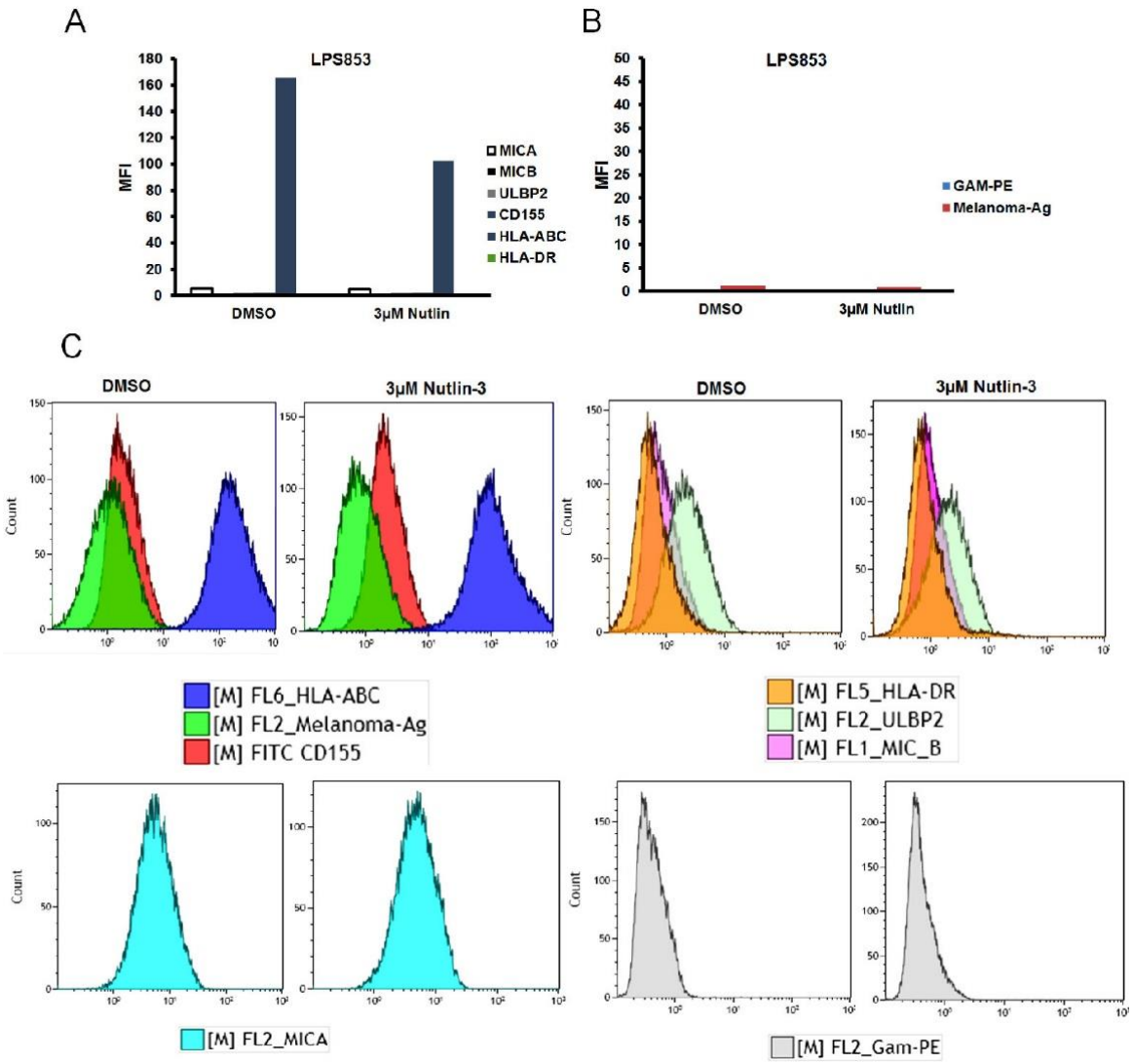

Figure S 11.6: **Delineation of NKG2D ligands in response to MDM2 inhibition in liposarcoma (LPS853). (A)** Bar graphs represent MFI (mean fluorescent intensity) of panel of markers/ligands: MICA, MICB, ULBP2, CD155, HLA-ABC, HLA-DR and **(B)** MFI of GAM-PE, Melanoma antigen in vehicle treated and MDM2i treated cells. **(C)** Corresponding histograms representing the expression of the ligands in LPS853**.**

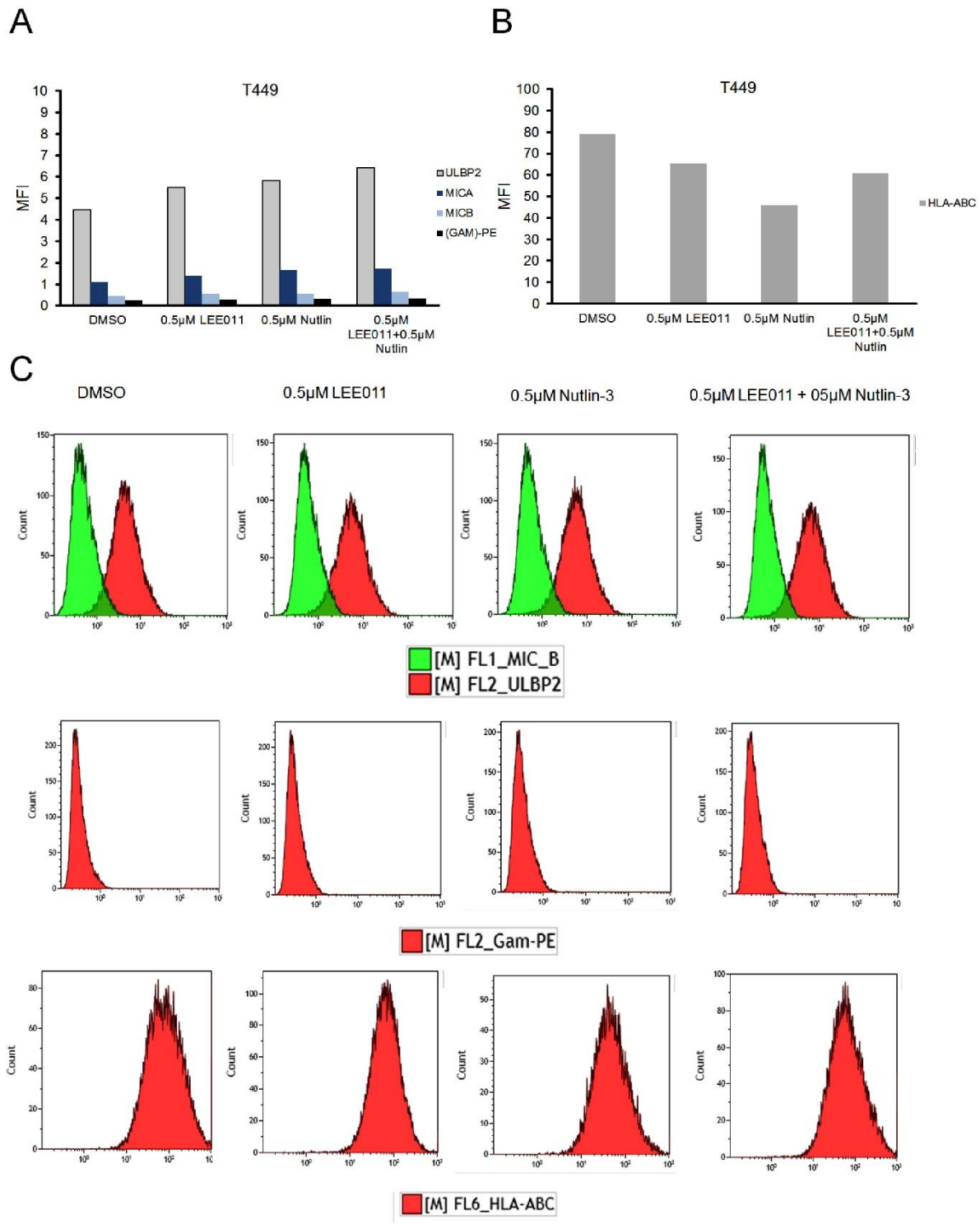

Figure S 11.7: **Delineation of NKG2D ligands in response to lower doses of MDM2 inhibitor (0.5μM) and CDK4 inhibitor (0.5μM) in liposarcoma cell line T449. (A)** Bar graphs represent MFI (mean fluorescent intensity) of panel of markers/ligands: MICA, MICB, ULBP2, GAM-PE and **(B)** MFI of HLA-ABC. **(C)** Corresponding histograms representing the expression of the ligands in T449.

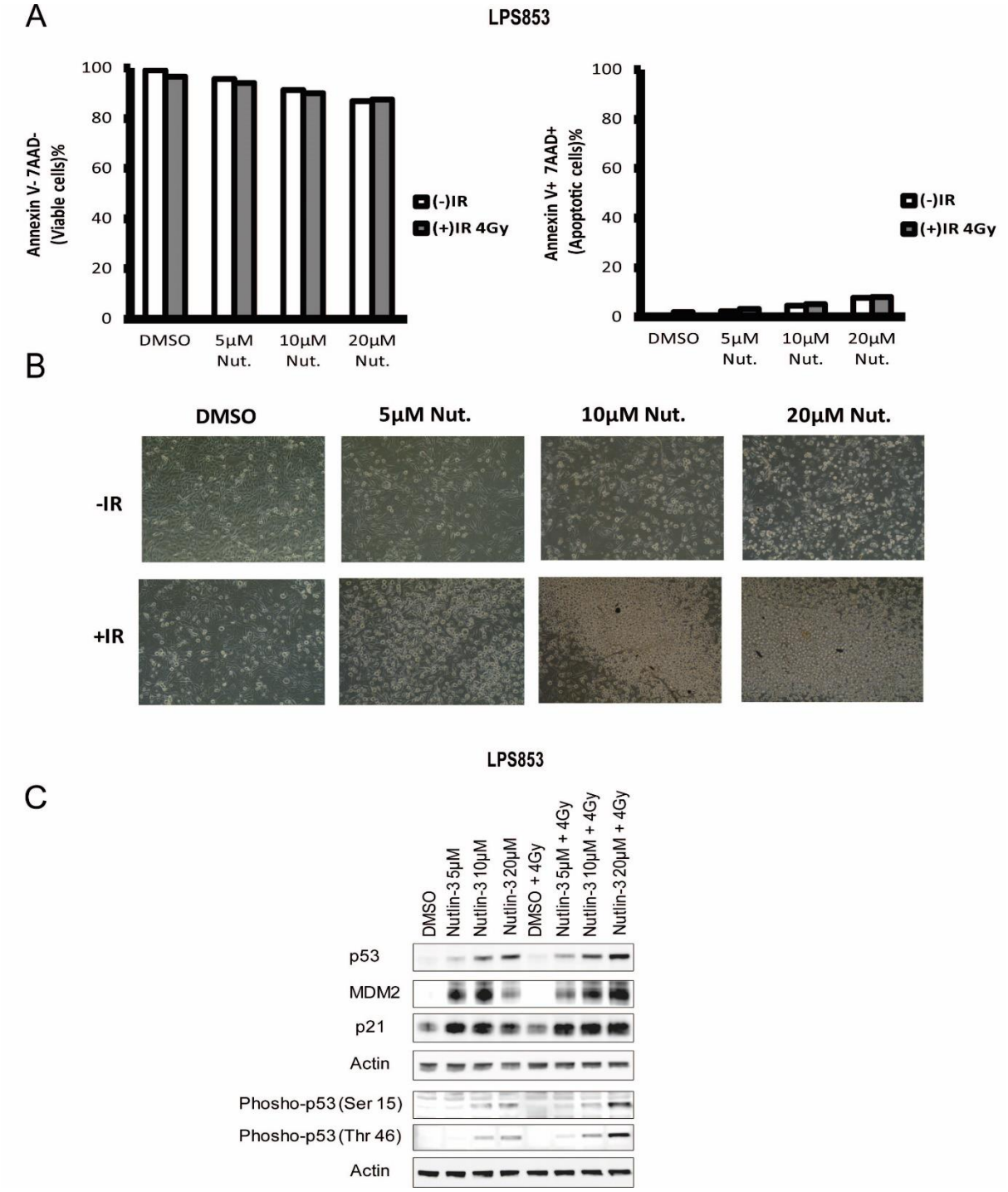

Figure S 11.8: **Higher dose of Nutlin-3 and RT did not exert additive effect in LPS853**. **(A)** Bar graphs represent viable (-Annexin V/-7AAD) and apoptotic (+Annexin V /+7AAD) cells following treatment with increasing doses of nutlin-3 (5µM, 10µM and 20µM) with constant dose of RT (4 Gy) in LPS853. **(B)** Representative bright field images taken from the centre of the 6-well plates following treatment. **(C)** Immunoblot of p53, MDM2, p21, phospho-p53 (Ser-15), phospho-p53 (Thr-46) following treatment with increasing doses of Nutlin-3 and RT. Actin was used as loading control.

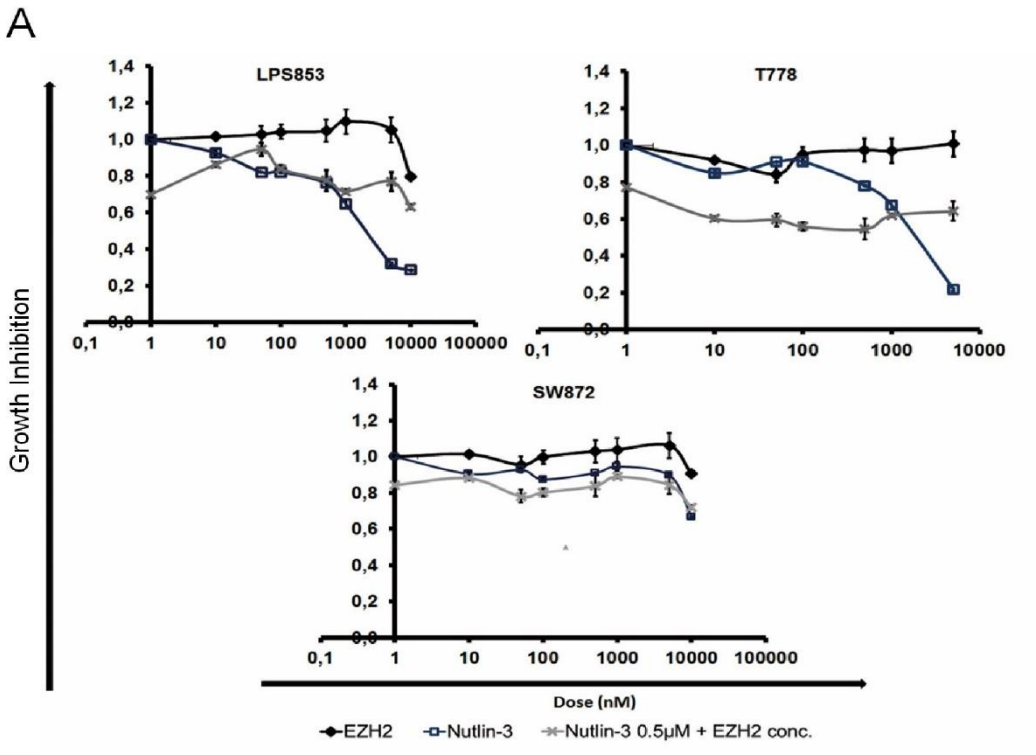

Figure S 11.9: **Co-targeting p53-dependent and p53-independent axis in liposarcoma (LPS853, T778 and SW872)**. **(A)** SRB assay graphs displaying growth inhibition in response to combination treatment to a concentration starting from 1nM to 10µM of MDM2 inhibitor (Nutlin-3) alone, 1nM to 10µM of EZH2 inhibitor alone, and fixed concentration (0.5µM) of MDM2 inhibitor and increasing concentration of EZH2 inhibitor.

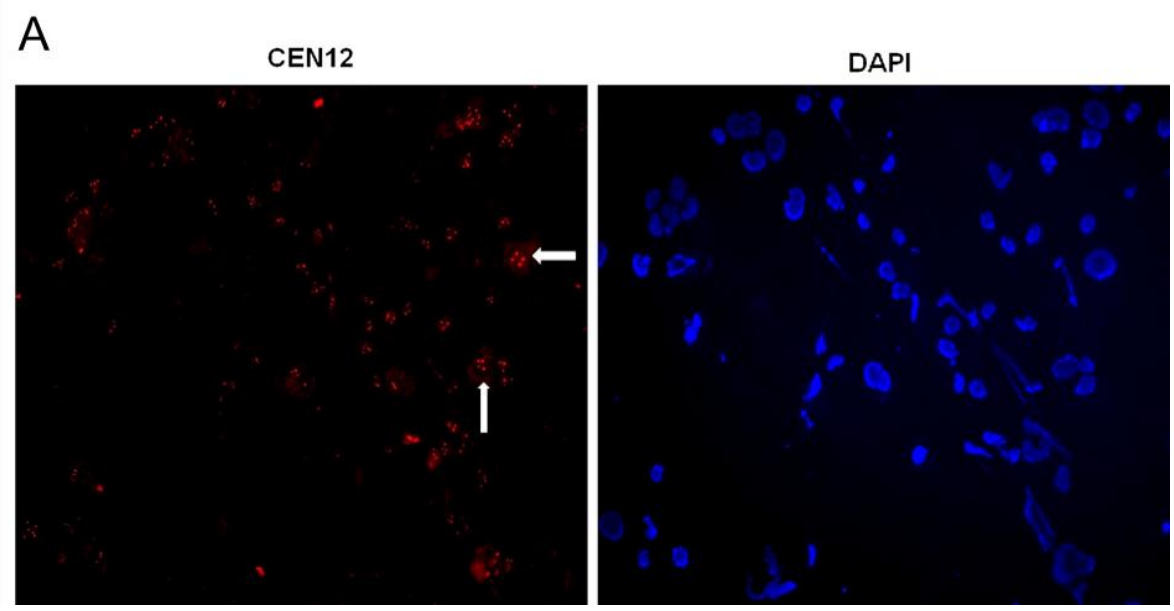

Figure S 11.10: **Existence of intrinsic polyploid cells in liposarcoma. (A)** FISH (Fluorescence *in situ* hybridization) staining of CEN12 and DAPI stain of interphase cells of T778.

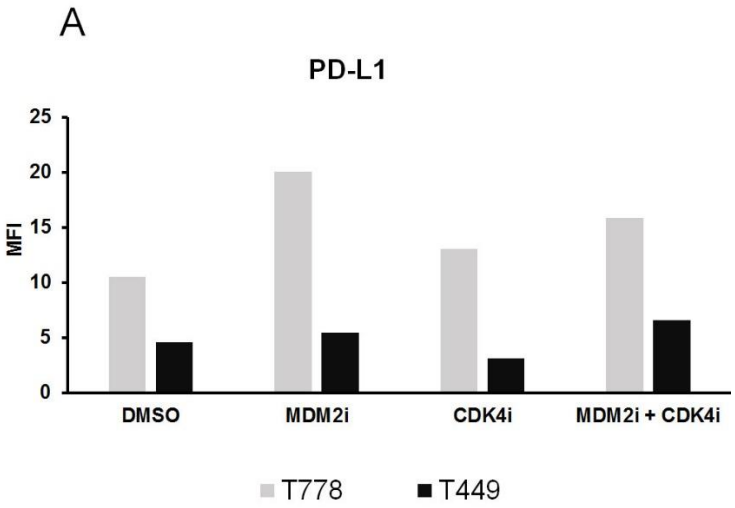

Figure S 11.11: **Modulation of PD-L1 in liposarcoma following targeted therapy. (A)** Bar graphs represent the MFI (mean fluorescent intensity) of PD-L1 in T778, LPS141 and T449 as measured by multicolor flow cytometry in response to different treatment and combinations after 72h.

11.2 **Abbreviations**

7-AAD	7-aminoactinomycin D
A. dest	Aqua destillata
Amp	Amplification
APC	allophycocyanin
ATM	Ataxia telangiectasia mutated
ATR	ATM and Rad3-related
BSA	Bovine serum albumin
CD155	Cluster of differentiation 155
CD56	Cluster of differentiation 56
CDK4	Cyclin-dependent kinase 4
CDK4i	Cyclin-dependent kinase 4 inhibitor
DAPI	4',6-Diamidino-2-phenylindole
DDR	DNA damage response
DER	Dose enhancement ratio
DMEM	Dulbecco's modified Eagle's medium
DMSO	Dimethylsulfoxide
DPBS	Dulbecco's phosphate-buffered saline
DSB	Double strand break
EDTA	Ethylendiaminetetraacetic acid
FACS	Fluorescence-activated cell sorting
FBS	Fetal bovine serum
FITC	Fluorescein isothiocyanate
Gy	Gray
H2AX	Histone H2AX
HLA	Human leukocyte antigen
HR	Homologous recombination
LPS	Liposarcoma
MAP3K5	Mitogen-Activated Protein Kinase Kinase Kinase 5
MDM2	Mouse double minute 2 homolog

MDM2i	Mouse double minute 2 homolog inhibitor
MICA	MHC class I polypeptide-related sequence A
MICB	MHC class I polypeptide-related sequence B
MFI	Mean Fluorescent intensity
MTT	3-(4,5-Dimethylthiazol-2-yl)-2,5-Diphenyltetrazolium Bromide
Mut	Mutated
NHEJ	Non-homologous end-joining
NK cells	Natural killer cells
NKG2D	Natural killer group 2D
P16	Cyclin-dependent kinase inhibitor 2A
P21	Cyclin-dependent kinase inhibitor 1 or CDK-interacting protein 1
P53	Tumor protein 53
PARP-1	Poly-(ADPribose)-polymerase
PE	R-phycoerythrin
PFA	Paraformaldehyde
PI	Propidium iodide
Rb	Retinoblastoma protein
RPMI	Roswell Park Memorial Institute medium
RT	Radiation treatment
SD	Standard Deviation
SDS	Sodium dodecyl sulfate
SER	Sensitization Enhancement Ratio
Ser	Serine
SRB	Sulforhodamine B
TGI	Total growth inhibition
ULBP2	UL16 binding protein 2
WT	Wild-type
ZBTB1	Zinc finger and BTB domain containing 1

11.3 **Figure index**

11.4 **Table index**

11.5 **Acknowledgement**

I would like to sincerely thank PD. Dr. Jürgen Thomale for being my formal supervisor and for his advice, corrections and solving my queries. I have benefitted a lot from several discussions with him.

I would like to convey my sincere thanks to Prof. Georg Iliakis. He provided many valuable suggestions to my radiotherapy part of the thesis. My sincere thanks to him for providing me with the opportunity to conduct my radiation experiments in Institute of Medical radiation.

Further thanks go to Prof. Sebastian Bauer for providing me lab space, sarcoma cell lines and resources to conduct my experiments for my PhD.

I would also like to thank to Prof Bastian Schilling for providing me the guidance in my immunotherapy experiments.

I would like to thank Prof Ralf Küppers who has helped me a lot as the chairperson of doctoral committee of Faculty of Biology to arrive at the stage of thesis submission.

Many thanks to the all the members associated with ``Tumor and Signaling´´, Biome core. It was a great learning experience from all the seminars, talks and retreats. Special thanks go to Delia Cosgrove for all her help.

Finally, I would like to thank all my friends and family for all their love and care, for their faith in me and support on all of my pursuits during my PhD.

11.6 Curriculum vitae

"Der Lebenslauf ist in der Online-Version aus Gründen des Datenschutzes nicht enthalten" .

"Der Lebenslauf ist in der Online-Version aus Gründen des Datenschutzes nicht enthalten" .

"Der Lebenslauf ist in der Online-Version aus Gründen des Datenschutzes nicht enthalten" .

Erklärung:

Hiermit erkläre ich, gem. § 6 Abs. (2) g) der Promotionsordnung der Fakultät für Biologie zur Erlangung der Dr. rer. nat., dass ich das Arbeitsgebiet, dem das Thema ***„Targeting liposarcoma by various therapeutic approaches with concurrent exploitation of genetic aberrations“*** zuzuordnen ist, in Forschung und Lehre vertrete und den Antrag von ***Samayita Das*** befürworte und die Betreuung auch im Falle eines Weggangs, wenn nicht wichtige Gründe dem entgegenstehen, weiterführen werde.

Essen, den _____ _____

Unterschrift eines Mitglieds der Universität Duisburg-Essen

Erklärung:

Hiermit erkläre ich, gem. § 7 Abs. (2) d) + f) der Promotionsordnung der Fakultät für Biologie zur Erlangung des Dr. rer. nat., dass ich die vorliegende Dissertation selbständig verfasst und mich keiner anderen als der angegebenen Hilfsmittel bedient, bei der Abfassung der Dissertation nur die angegeben Hilfsmittel benutzt und alle wörtlich oder inhaltlich übernommenen Stellen als solche gekennzeichnet habe.

Essen, den _____ _____

Unterschrift des/r Doktoranden/in

Erklärung:

Hiermit erkläre ich, gem. § 7 Abs. (2) e) + g) der Promotionsordnung der Fakultät für Biologie zur Erlangung des Dr. rer. nat., dass ich keine anderen Promotionen bzw. Promotionsversuche in der Vergangenheit durchgeführt habe und dass diese Arbeit von keiner anderen Fakultät/Fachbereich abgelehnt worden ist.

Essen, den _____ _____

Unterschrift des Doktoranden